BENEFICIAL EFFECTS OF CAFFEINE CONSUMPTION ON DIABETES-INDUCED ALTERATIONS IN THE HIPPOCAMPUS

João Miguel das Neves Duarte

Faculdade de Ciências e Tecnologia da Universidade de Coimbra

Coimbra 2008

Dissertação apresentada à Faculdade de Ciências e Tecnologia da Universidade de Coimbra, para prestação de provas de doutoramento em Bioquímica, na especialidade de Bioquímica.

O trabalho exeprimental que constitui a presente tese foi realizado em Coimbra, Departamento de Bioquímica da Faculdade de Ciências e Tecnologia da Universidade de Coimbra e no Centro de Neurociências e Biologia Celular, e em Lausanne, no Centre d'Imagerie BioMédicale.

ERRATA

João Miguel das Neves Duarte PhD Thesis

These are the typos and errors that should be corrected in the thesis:

Page	Paragraph	Line	Reads	Should be
Front page	5	2	"…especialidade de Bioquímica."	"…especialidade de Bioenergética."
xiii	1	8	"…compensação osmotica…"	"…compensação osmótica…"
5	1	3	"Lunetta *et al,*. 1994"	"Lunetta *et al.*, 1994"
5	1	5	"Gradmann *et al*, 1993"	"Gradmann *et al.*, 1993"
45	3	5	"…in ethanol ethanol solutions…"	"…in ethanol solutions…"
122	2	9	"…crossing and reading events…	"…crossing and rearing events…
126	1	9	"…(figures 4.39C)."	"…(figure 4.39C)."
138	2	7	"…and that it has…"	"…and it has…"
145	2	5	"…must by related…"	"…must be related…"
148	1	6	"(P>0.05, n=4, Figure 4.52D)"	"(P>0.05, n=4, Figure 4.53D)"
149	1	5	"…showed a increase…"	"…showed an increase…"
150	Caption of Figure 4.55	9	"…immunoreactivity ehich was…"	"…immunoreactivity, which was…"

Figures 4.52 to 4.55 lack reference to the amount of protein applied in the SDS-PAGE gel. It was applied 45 µg of protein in total or nerve terminal membranes for the Western blot analysis of adenosine A_1 receptor, and 25 µg for synaptic proteins, GFAP and vimentin.

On page 139, Figure 4.46A is:

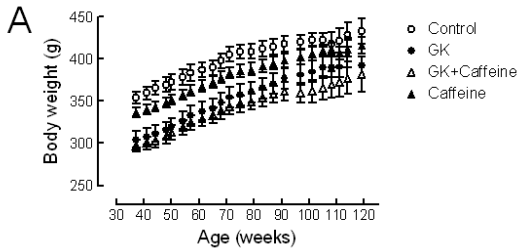

should be:

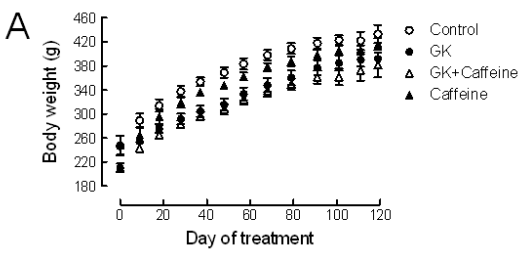

None of these errors affect the conclusions of the thesis.

Table of contents

Agradecimentos/Acknowledgments

Uma reflexão cuidada sobre o percurso desenvolvido nos útimos quatro anos, permitiu que percebesse o valor fundamental do contributo colectivo, acrescido à vontade individual, na realização deste trabalho. Por me ser impossível agradecer a todos aqueles que cruzaram este caminho, ajudando na sua construção e colaborando no processo de aprendizagem e enriquecimento pessoal e científico daí resultante, dirijo especiais agradecimentos:

Aos meus orientadores, Professor Doutor Rui Carvalho e Professor Doutor Rodrigo Cunha, pelo apoio e incentivo permanentes, pelos conhecimentos e entusiasmo transmitidos na forma de «fazer ciência», pela confiança em mim depositada.

A todos os membros do grupo *Purines at CNC* (Centro de Neurociências e Biologia Celular de Coimbra), destacando os colegas e amigos Paula Canas, Nelson Rebola e Ricardo Rodrigues, que me receberam, foram exemplo e sempre prestaram a ajuda necessária no laboratório; a eles, devo um profundo agradecimento pelo companheirismo.

À Patrícia Nunes, pela reconhecida amizade, por toda a sua espontaneidade e disponibilidade. À Francisca Soares e Teresa Delgado, pela boa disposição e alegrias partilhadas.

Aos Doutores John G. Jones, Attila Köfalvi e Jean Oses, agradeço todos os bons momentos, as frutíferas discussões científicas e a ajuda nas mais variadas situações.

À Professora Doutora Catarina Oliveira, por me conceder a excelente oportunidade de trabalho no CNC.

Ao Professor Doutor Carlos Geraldes, por permitir a utilização do Laboratório de Ressonância Magnética Nuclear da Faculdade de Ciências e Tecnologia da Universidade de Coimbra, imprescindível na concretização do projecto.

To Professor Rolf Gruetter, who supervised part of the project carried out in the *Centre d'Imagerie BioMédicale* (CIBM), for his permanent help and for sharing with me his optimism and enthusiasm.

I am also grateful to all the members of the CIBM for the technical help and scientific advices that were crucial for the development of my work. A special thank to Kai, Ruud, Tobias, Cristina, Nicolas, Vladimir, Hanne, Lijing and Hongxia, for making my stay in Lausanne so pleasant.

Aos meus amigos, pelo incentivo e pela partilha deste percurso.

À minha família, em particular aos meus pais e irmão, dedico o meu carinho e gratidão. A eles agradeço o esforço, incentivo, apoio e paciência. Tudo lhes devo.

À Daniela, pelo seu amor e ternura... e pelos sonhos que partilhamos.

My work was supported by Fundação para a Ciência e a Tecnologia from 2004 to 2008 (PhD fellowship SFRH/BD/17795/2004). The project was financed by Fundação para a Ciência e a Tecnologia (grant POCTI/SAU-NEU/56098/2004) and by Fundo Fundação Oriente/Johnson & Johnson Para a Saúde.

Abbreviation list

2-AG, 2-arachidonoylglycerol

4AP, 4-aminopyridine

5'NT, endo-5'-nucleotidase (E.C. 3.1.3.5)

A_1R, adenosine A_1 receptor

A_{2A}R, adenosine A_{2A} receptor

ACS, acyl-CoA synthetase

ADA, adenosine deaminase (E.C. 3.5.4.4)

ADP, adenosine 5'-diphosphate

AK, adenosine kinase (E.C. 2.7.1.20)

Ala, alanine

αKG, α-ketoglutarate

AM or AM251, *N*-(piperidin-1-yl)-5-(4-iodophenyl)-1-(2,4-dichlorophenyl)-4-methyl-1H-pyrazole-3-carboxamide

AMP, adenosine 5'-monophosphate

AMPA, alpha-amino-3-hydroxy-5-methyl-4-isoxazolepropionic acid

ANOVA, analysis of variance

Asc, ascorbate

Asp, aspartate

ATP, adenosine 5'-triphosphate

ATT, alanine aminotransferase (E.C. 2.6.1.2)

βHB, β-hydroxybutyrate

BB/Wor, Biobreeding/Worcester

BBB, blood-brain-barrier

BDNF, Brain-derived neurotrophic factor

BSA, bovine serum albumin

CA, *cornu Ammonis*

cAMP, cyclic AMP

CB1R, cannabinoid receptor type 1

cDNA, complementary deoxyribonucleic acid

CGS 21680, 2-[4-(2-*p*-carboxyethyl)-phenethylamino]-5'- *N*-ethylcarboxamidoadenosine

CMR_{gluc}, cerebral metabolic rate of glucose consumption

CNS, central nervous system

CoA, coenzyme A

Cr, creatine

CRLB, Cramér-Rao lower bound

CSF, cerebrospinal fluid

Δ^9-THC, Δ^9-tetrahydrocannabinol

DMSO, dimethyl sulfoxide

DPCPX, 1,3-dipropyl-8-cyclopentylxanthine

E.C., Enzyme Comission

e.g., from Latin "*exempli gratia*", meaning "for the sake of example"

EC, energy charge

EDTA, ethylenediaminetetraacetic acid

ELISA, enzyme-linked immunosorbent assay

et al., from Latin "*et alii*" or "*et aliae*", meaning "and others"

$FADH_2$, flavin adenine dinucleotide (reduced form)

Fc0, fractional contribution of unlabelled sources for glutamate ^{13}C labelling

Fc12, fractional contribution of [U-^{13}C]glucose for glutamate ^{13}C labelling

Fc2, fractional contribution of [2-^{13}C]acetate for glutamate ^{13}C labelling

fMRI, functional magnetic resonance imaging

GABA, γ-aminobutiric acid

GAD, glutamate decarboxylase (E.C. 4.1.1.15)

Gase, glutaminase (E.C. 3.5.1.2)

gf, Gaussian filter

GFAP, glial fibrillary acidic protein

GK, Goto-Kakizaki

Glc , glucose

Gln, glutamine

Glu, glutamate

GLUT, glucose transporter

GPC, glycerophosphorylcholine

GS, glutamine synthetase (E.C. 6.3.1.2)

gsf, shifted Gaussian filter

GSH, glutathione

HEPES, 4-(2-hydroxyethyl)-1-piperazineethanesulfonic acid

HMIT1, H^+-*myo*-inositol co-transorter

HPLC, high-performance liquid chromatography (or high pressure liquid chromatography)

i.e., from Latin "*id est*", meaning "that is"

i.p., intra-peritoneal

i.v., intra-venous

Ins, *myo*-inositol

IP3, inositol 1,4,5-trisphosphate

Lac, lactate

LDH, lactate dehydrogenase (E.C. 1.1.1.27)

LTD, long-term depression

LTP, long-term potentiation

MAP2, microtubule-associated protein type 2

MAPK, mitogen-activated protein kinases

mGluR, metabotropic glutamate receptor

MRI, magnetic resonance imaging

mRNA, messenger ribonucleic acid

NAA, *N*-acetylaspartate

NAAG, *N*-acetylaspartylglutamate

NADH, nicotinamide adenine dinucleotide (reduced form)

NMDA, *N*-methyl-D-aspartate

NMR, nuclear magnetic resonance

NOD, non-obese diabetes

OAA, oxaloacetate

P1, type 1 purine receptors, i.e. adenosine receptors

P2, type 2 purine receptors, i.e. nucleotide receptors

P2X, ionotropic ATP receptors

P2Y, metabotropic nucleotide receptors

P_aCO_2, arterial pressure of CO_2

P_aO_2, arterial pressure of O_2

PBS, phosphate-buffered saline

PC, pyruvate carboxylase (E.C. 6.4.1.1)

PCA, perchloric acid

PCho, phosphorylcholine

PCr, phosphocreatine

PCR, polymerase chain reaction

PDH, pyruvate dehydrogenase complex (E.C. 1.2.4.1)

PE, phosphorylehtanolamine

PET, positron emission tomography

PKA, protein kinase A (E.C. 2.7.11.11)

PSD95, postsynaptic density protein of 95 kDa

Pyr, pyruvate

SAH, S-adenosyl-homocystein

SCH 58261, 7-(2-phenylethyl)-5-amino-2-(2-furyl)-pyrazolo-[4,3-e]-1,2,4-triazolo[1,5-c]pyrimidine

Scyllo, *scyllo*-inositol

SDS-PAGE, sodium dodecyl sulfate polyacrylamide gel electrophoresis

SEM, standard error of the mean

SLC2, solute carrier family 2

SNAP25, synaptosome-associated protein of 25 kDa

STZ, streptozotocin or 2-deoxy-2-(3-(methyl-3-nitrosoureido)-D-glucopyranose

Tau , taurine

TBS-T, trizma buffered saline with Tween-20

TCA cycle, tricarboxylic acid cycle

vGAT, vesicular GABA transporter

vGluT, vesicular glutamate transporter

VOI, volume of interest

WIN or WIN55212-2, (R)-(+)-[2,3-dihydro-5-methyl-3-(4-morpholinylmethyl)pyrrolo[1,2,3-de]-1,4-benzoxazin-6-yl]-1-naphthalenylmethanone mesylate

XAC, 8-{4-[(2-aminoethyl)amino]carbonylmethyl-oxyphenyl}xanthine

Y, anaplerotic flux.

Resumo

O declínio cognitivo é uma consequência normal do envelhecimento e é acentuado por doenças neurodegenerativas, como seja a doença de Alzheimer, que leva à deterioração progressiva de processos de aprendizagem e memória, atenção e concentração, uso da linguagem e outras funções mentais.

Do mesmo modo, o avanço da idade também reduz a regulação da glicémia, conduzindo à instalação de um quadro de diabetes *mellitus* que contribui para a incidência de disfunção cognitiva. De facto, a diabetes e a resistência à insulina estão associadas a modificações da morfologia e plasticidade do hipocampo, uma estrutura do cérebro envolvida no processamento da aprendizagem e da memória. Nomeadamente, a diabetes induz uma modificação da síntese e da libertação de neurotransmissores, da potenciação de longa duração (que é um paradigma electrofisiológico de formação e armazenamento de memória), da conectividade sináptica e da viabilidade neuronial. A deterioração cerebral pela diabetes foi chamada encefalopatia diabética.

O trabalho experimental que dá forma à presente tese de doutoramento teve como objectivo compreender que modificações moleculares e metabólicas ocorrem no hippocampo que possam contribuir para a demência diabética. Três modelos animais de diabetes *mellitus* foram estudados: um modelo de diabetes tipo 1 que consiste no tratamento de ratos com estreptozotocina (STZ), um fármaco que destrói as células β, cessando a produção de insulina; ratos Goto-Kakizaki (GK) que são espontaneamente resistentes à insulina; e ratinhos NONcNZO10/LtJ alimentados com uma dieta rica em gordura (11%) que constituem um modelo de diabetes tipo 2 associada à obesidade, assemelhando-se o seu fenótipo à diabetes tipo 2 humana. Tal como ocorre em doentes diabéticos, estes modelos animais de diabetes apresentam um défice mnemónico dependente do hippocampo, sugerido pela redução da alternação espontânea num labirinto em Y (*Y-maze*).

Os processos de aprendizagem e memória envolvem eventos sinápticos, e consistentemente, foram observadas alterações sinápticas no hipocampo destes modelos animais de diabetes, nomeadamente degeneração sináptica caracterizada por uma redução na densidade de proteínas envolvidas na neurotransmição como a sintaxina, a sinaptofisina ou a SNAP25. Juntamente com a degeneração sináptica, a diabetes induziu uma astrogliose no hipocampo, avaliada por imuno-histoquímica e análise de Western blot da proteína acídica fibrilhar da glia (GFAP) e da vimentina.

Estudos da cinética do transporte de glucose no hipocampo revelaram que o transorte de glucose através da barreira hemato-encefálica não estava alterado em ratos tratados com STZ e ratos

GK. No entanto, descobriu-se que a diabetes altera o metabolismo da [1-^{13}C]glucose no hipocampo sugerindo, em particular, que existe um rearranjo de vias metabólicas intermediárias no hipocampo diabético para lidar com elevadas concentrações de glucose (observadas no hipocampo destes animais diabéticos). Mais ainda, por resonância magética nuclear (NMR) de protão *in vivo* foi mostrado que, em comparação com animais controlo, ratos diabéticos tiveram alterações do perfil neuroquímico do hipocampo, que se relacionam com a regulação osmótica e não com o metabolismo energético. Então, uma situação de diabetes não controlada, caracterizada por hiperglicémia crónica, induz mecanismos de compensação osmotica e uma adaptação de vias metabólicas intermediárias, possivelmente no compartimento glial, para contrabalançar a elevada concentração de glucose e para manter o balanço energético necessário à homeostase celular e à neurotransmissão. Uma vez que os mecanismos de transporte de glucose na barreira hemato-encefálica não são alterados numa condição de diabetes, a hiperglicémia crónica induz uma permanente elevada concentração de glucose no hipocampo, levando a neurotoxicidade e degeneração, que se observou ter início a nível sináptico.

Sistemas de neuromodulação operados pela adenosina, ATP e endocanabinóides, são capazes de controlar quer a transmissão sináptica quer o metabolismo intermediário. Observou-se que estes sistemas são afectados pela diabetes, nomeadamente no hipocampo. Assim, a hiperglicémia crónica alterou estes três sistemas de modulação ao nível da sinapse, onde modulam processos de neurotransmissão, e principalmente em membranas totais do hipocampo, que incluem membranas do corpo celular neuronial e de células da glia, onde podem controlar o metabolismo, homeostase celular, proliferação glial e neuroinflamação.

No caso particular do sistema adenosinérgico, a diabetes causou uma redução da densidade de receptores inibitórios A_1 e um aumento da densidade de receptores facilitatórios A_{2A} no hipocampo. O antagonismo de receptores A_{2A} tem sido referido como tendo propriedades neuprototectoras no sistema nervoso central sujeito a insultos crónicos como sejam doenças neurodegenerativas. Por isso, administrou-se cafeína a animais diabéticos (1 g/L na água de beber). A cafeína é a substância psico-activa de maior consumo e é um antagonista não selectivo de receptores de adenosina, actuando principalmente em receptores A_1 e A_{2A}. Por um lado, a cafeína melhora o desempenho em testes de aprendizagem e memória; por outro, ela estimula o metabolismo periférico, o gasto energético e a perda de peso, reduzindo o risco de desenvolvimento de complicações diabéticas. A hipótese de que o consumo de cafeína poderia prevenir alterações no hipocampo causadas pela diabetes foi testada e os resultados obtidos mostraram que a cafeina pode ter efeitos benéficos perante a encefalopatia diabética. O consumo crónico de cafeína preveniu ou

atenuou a maioria das alterações moleculares e metabólicas induzidas pela diabetes no hipocampo, assim como a redução da memória espacial dependente do hipocampo.

Em suma, no presente trabalho foram encontradas diversas alterações induzidas por condições de diabetes no hipocampo, que poderão contribuir para o declínio na aprendizagem e memória dependentes do hipocampo, nomeadamente a degeneração sináptica. O consumo habitual de cafeína mostrou-se efectivamente benéfico na sua prevenção.

Abstract

The decline in memory and cognitive function is a normal consequence of aging and is accentuated by neurodegenerative pathologies, such as Alzheimer's disease, which cause progressive deterioration of learning and memory, attention and concentration, use of language, and other mental functions.

Also peripheral glucose regulation decreases with age, leading to diabetes *mellitus* that contributes to the incidence of cognitive dysfunction. In fact, diabetes and insulin resistance are associated with modifications of morphology and plasticity in the hippocampus, a brain structure involved in learning and memory processing. Namely, there is a modification of neurotransmitter synthesis and release, long-term potentiation (which is an electrophysiological paradigm for memory formation and storage), synaptic connectivity and neuronal viability. The affection of the brain by diabetes has been called diabetic encephalopathy.

The experimental work leading to the present doctoral thesis aimed at understanding which molecular and metabolic modifications occur in the hippocampus that may contribute to the dementia observed in diabetic patients. Different animal models of diabetes *mellitus* were studied: a model of type 1 diabetes that consisted on the treatment of rats with streptozotocin (STZ), a drug that destroys pancreatic β-cells, ceasing insulin production; Goto-Kakizaki (GK) rats that are spontaneously insulin resistant; and NONcNZO10/LtJ mice fed on 11% fat diet that constitute a model for type 2 diabetes associated with obesity, displaying a phenotype very similar to the human type 2 diabetes. As occurs with human diabetic patients, these animal models of diabetes display hippocampal-dependent memory impairment, suggested by reduced spontaneous alternation in a Y-maze.

Learning and memory processes involve synaptic events and, accordingly, the different diabetic animal models displayed synaptic alterations in the hippocampus, namely synaptic degeneration characterized by a reduction of the density of proteins involved in neurotransmission such as syntaxin, synaptophysin or SNAP25. Along with synaptic degeneration, diabetes induced the occurrence of astrogliosis in the hippocampus, evaluated by both immunohistochemistry and Western blot analysis of glial fibrillary acidic protein (GFAP) and vimentin.

The study of the kinetics of glucose transport in the hippocampus revealed that the transport of glucose across the blood-brain-barrier (BBB) is not altered in STZ-induced and GK diabetic rats. However, diabetes was found to alter the metabolism of [1-^{13}C]glucose in the hippocampus, in

particular suggesting that pathways of intermediary metabolism are rearranged in the diabetic hippocampus to deal with high glucose concentration (found in the hippocampus of these animals). Furthermore, *in vivo* ^{1}H nuclear magnetic resonance (NMR) spectroscopy showed that, in comparison to controls, diabetic rats have alterations of the neurochemical profile of the hippocampus, which are related to osmolarity regulation rather than energy metabolism. Thus, uncontrolled diabetes characterised by chronic hyperglycaemia triggers mechanisms of osmotic compensation and induce an adaptation of intermediary metabolic pathways, possibly in the astrocytic compartment, in order to counteract the high glucose concentration and to maintain proper energetic balance for cellular homeostasis and neurotransmission. Since the mechanism of glucose transport across the BBB is not altered upon diabetes, chronic hyperglycaemia causes a permanent increase of glucose concentration in the hippocampus, leading to neurotoxicity and degeneration, which was observed to begin at the level of the synapse.

Neuromodulation systems that are able to control both synaptic transmission and intermediary metabolism, namely those operated by adenosine, ATP and endocannabinoids, were found to be affected by diabetes, in particular in the hippocampus. Thus, chronic hyperglycaemia was observed to alter these three modulation systems in membranes from the synapse, where such systems modulate neurotransmission, and principally in membranes from the whole hippocampus that include membrane from neuronal cell bodies and glial cells, where they can be involved in the control of metabolism, cellular homeostasis, glial proliferation and neuroinflammation.

In the particular case of the adenosinergic system, diabetes caused both down-regulation of inhibitory A_1 receptors and up-regulation of facilitatory A_{2A} receptors in the hippocampus. The antagonism of adenosine A_{2A} receptors has been referred as having neuroprotective properties in the central nervous system subjected to chronic insults such as neurodegenerative pathologies. Thus it was tested the ability of caffeine (1 g/L in the drinking water), the most widely consumed psycho-active drug that acts as a non-selective antagonist of adenosine receptors, to counteract the hippocampal modifications found in the animal models of diabetes. The results obtained showed that caffeine may have beneficial effects on the management of diabetic encephalopathy. Thus, chronic caffeine consumption was able to prevent or attenuate most of the diabetes-induced molecular and metabolic alterations in the hippocampus, as well as the impairment of hippocampal-dependent spatial memory.

In conclusion, the present work found several alterations induced by diabetic conditions to the hippocampus. Such alterations, in particular the synaptic degeneration, can contribute to the impairment of hippocampal-dependent learning and memory. Habitual caffeine intake was found to prevent or ameliorate these hippocampal alterations, as well as the memory deficits.

Publication list

The scientific content of the present thesis has been included in the following original articles in peer-reviewed international scientific journals and in other manuscripts in preparation:

Duarte JMN, Oliveira CR, Ambrósio AF, Cunha RA (2006) Modification of adenosine A_1 and A_{2A} receptor density in the hippocampus of streptozotocin-induced diabetic rats, Neurochemistry International 48(2), 144-150.

Duarte JMN, Cunha RA, Carvalho RA (2007) Different metabolism of glutamatergic and GABAergic compartments in superfused hippocampal slices characterized by nuclear magnetic resonance spectroscopy. Neuroscience 144(4), 1305-1313.

Duarte JMN, Nogueira C, Mackie K, Oliveira CR, Cunha RA, Köfalvi A (2007) Increase of cannabinoid CB1 receptor density in the hippocampus of streptozotocin-induced diabetic rats. Experimental Neurology 204(1), 479-484.

Duarte JMN, Oses JP, Rodrigues RJ, Cunha RA (2007) Modification of purinergic signalling in the hippocampus of streptozotocin-induced diabetic rats. Neuroscience 149(2), 382-391.

Duarte JMN, Cunha RA, Carvalho RA, Adenosine A_1 receptors control the recovery of hippocampal metabolism after hypoxia. In preparation.

Duarte JMN, Carvalho RA, Cunha RA, Köfalvi A, Effect of CB1 receptor activation on the intermediary metabolism of rat hippocampal slices. In preparation.

Duarte JMN, Carvalho RA, Cunha RA, Chronic caffeine consumption prevents diabetes-induced alterations in the hippocampus of NONcNZO10/LtJ mice. In preparation.

Duarte JMN, Carvalho RA, Cunha RA, Gruetter R, Glucose transport and neurochemical profile in the hippocampus of streptozotocin-induced diabetic rats - effect of caffeine consumption. In preparation.

Duarte JMN, Carvalho RA, Cunha RA, Gruetter R, Glucose transport and neurochemical profile in the hippocampus of Goto-Kakizaki diabetic rats - effect of caffeine consumption. In preparation.

Duarte JMN, Carvalho RA, Cunha RA, Caffeine consumption prevents diabetes-induced spatial memory impairment, synaptic degeneration and astrogliosis in the hippocampus of Goto-Kakizaki rats. In preparation.

1. Introduction

1.1. Introduction to diabetes *mellitus*

The increase of glucose concentration in the blood stream, *e.g.* after a meal, triggers the release of insulin, a pancreatic hormone, which stimulates cells, namely from muscle, fat and liver, to clear blood glucose, decreasing it to normal levels. In diabetic individuals, blood sugar levels (glycaemia) remain high because insulin is not produced, is insufficient, or is ineffective. Therefore, diabetes *mellitus* is defined as a chronic metabolic disorder characterized by hyperglycaemia, resulting from inappropriate insulin secretion and/or action (World Health Organization, 1999).

The vast majority of the diabetes cases are included in two main categories, classified according to the underlying cause, which are type 1 diabetes or insulin-dependent diabetes, generally caused by an autoimmune reaction to antigens of pancreatic β-cells leading to impaired insulin production, and type 2 diabetes or insulin-resistant diabetes, characterised by inefficiency of insulin action. While type 1 diabetes is mainly observed in children and adolescents, type 2 diabetes is more common among adults, accounting for more than 90% of the diabetes cases worldwide. The rapid rising of the prevalence of diabetes and impaired glucose tolerance achieved now epidemic proportions, accounting respectively to 5.9% and 7.5% of the world population (International Diabetes Federation, 2006), and is a leading cause of dead (the 10th for men and 5th for women) within the European Union (Eurostat, 2007). In Portugal, diabetes *mellitus* is the 7th cause of dead contributing to 4.8% of the deaths in 2005 (Instituto Nacional de Estatística, 2007). The main contributor for the high prevalence of diabetes is the rise of obesity, related to the combination of ample food availability and a sedentary lifestyle, contrasting to less abundant food supplies and higher physical activity observed until a century ago (International Diabetes Federation, 2006).

1.1.1. Overview of glycaemia regulation

The regulation of metabolic processes in the organism starts with the control of substrate availability in the blood stream. Carbohydrates like glucose are the main substrate feeding the majority of the organs and its homeostasis was described in several textbooks on mammalian physiology (*e.g.* Kacsoh, 2000). The endocrine regulation of carbohydrate metabolism is complex and involves several pancreatic and non-pancreatic hormones. These hormones can be grouped in hypoglycaemic or hyperglycaemic if they reduce or increase plasma glucose levels, respectively.

Physiologically, insulin is the only important hypoglycaemic agent, while practically all the other hormones are hyperglycaemic (*e.g.* glucagon, cortisol or adrenaline). Due to this redundancy in antagonists of insulin, their deficiencies are usually compensated and masked; in contrast, deficiency of insulin signalling is manifested as diabetes *mellitus*. Insulin is produced in the pancreas, in cellular clusters called islets of Langerhans, which include α-cells and β-cells that secrete glucagon and insulin respectively (Kacsoh, 2000). Both cell types are highly sensitive to small changes in blood glucose concentration and can regulate hormone secretion adequately (Kacsoh, 2000). Briefly, insulin is released upon increased glycaemia and restores glucose homeostasis by stimulating glucose uptake principally into the liver, muscle and adipose tissue, which are the main target organs of glycaemia regulation (Kacsoh, 2000). In addition, insulin inhibits hepatic gluconeogenesis and glucose secretion, stimulates glucose storage in the form of glycogen or lipid, and promotes glucose oxidation for energy production and formation of carbohydrate intermediates to be used in other metabolic pathways. With an action opposite to that of insulin, glucagon is released upon low glycaemia (*e.g.* during exercise or fasting) triggering glycogen breakdown and switching the body to use energy stores, namely glycogen, lipids and proteins (Kacsoh, 2000).

1.1.2. Diabetic encephalopathy

Diabetes *mellitus* is associated with the occurrence of well described microvascular complications that affect different organs, leading most commonly to retinopathy, nephropathy and peripheral neuropathy, which development is dependent on the duration of the disease and glycaemia control (Malecki, 2004). The concept that diabetes affects the central nervous system (CNS) was recognised in 1922, when evidences appeared for diabetes-induced cognitive dysfunction (Miles and Root, 1922), and the term "diabetic encephalopathy" was introduced in 1950 to describe the complication of diabetes resulting on brain dysfunction and leading to cognitive impairment (De Jong, 1950).

Several clinical studies reported lowered performance on several cognitive domains in type 1 diabetic patients, when compared to the general healthy population, including notably learning and memory impairment (*e.g.* Brands *et al.*, 2005; Holmes and Richman, 1985; Ryan and Williams, 1993; Ryan *et al.*, 1993; Ryan, 1988). The magnitude of these cognitive deficits is mild in most cases but severe cases can occur (Deary *et al.*, 1993; Gold *et al.*, 1994). Along with these deficits on brain function, diabetes can also induce structural alterations, neuronal loss, demyelination and gliosis

(De Jong, 1977). Accordingly, magnetic resonance imaging (MRI) and computed tomography showed general brain atrophy and increased occurrence of white mater hyper-intensities that are thought to result from small infarcts (Araki *et al*., 1994; Lunetta *et al*,. 1994; Perros *et al*., 1997). In type 2 diabetic patients, impaired cognitive function was observed in particular when solving complex cognitive tasks (*e.g.* Gradman *et al*, 1993; Perlmuter *et al*., 1984; Reaven *et al*., 1990; Ryan and Geckle, 2000; Strachan *et al*., 1997; Worrall *et al*., 1993). Cognitive dysfunction is further accentuated in elderly type 2 diabetic patients with reduced diabetes control (Sinclair *et al*., 2000; Tun *et al*., 1990). In summary, diabetes causes cognitive dysfunction that is moderated at younger age but can be accentuated in elderly diabetic patients and hampers daily functioning, reducing the quality of life. The mechanisms underlying the development of diabetes-associated cognitive decline are poorly understood. Animal experimentation has begun aiming to understand processes leading to diabetic encephalopathy, but greater efforts must still be taken to achieve this goal.

Different animal models of diabetes *mellitus* have been shown to mimic human diabetic phenotypes including cerebral dysfunction. Structural alterations were reported in the blood-brain-barrier (BBB) of diabetic animals (reviewed in Mooradian, 1997), consistent with increased BBB permeability observed in type 2 diabetic individuals (Starr *et al*., 2003), suggesting that loss of BBB integrity may de involved in CNS dysfunction in diabetes. Compared to non-diabetic control rats, neuronal loss was observed in STZ-induced diabetic rats (Jakobsen *et al*., 1987) and BB/Wor diabetic rats (Li *et al*., 2002a), and synaptic alterations were observed in the brain of both diabetic Chinese hamster (Luse, 1970) and STZ-induced diabetic rats (Nita *et al*., 2002; Malone *et al*., 2006). In comparison to controls, reduced hippocampal neurogenesis was reported to occur in two models of type 1 diabetes, the non-obese diabetic (NOD) mice (Beauquis *et al*., 2008) and the STZ-induced diabetic rats (Beauquis *et al*., 2006; Stranahan *et al*., 2008). The concentration of neurotransmitters appears to be altered in diabetic brains. In particular, the content of dopamine, norepinephrine and serotonin was reported to be altered in certain brain regions in alloxan-induced (Kulikov *et al*., 1986) and STZ-induced (Trulson *et al*., 1986; Barber *et al*., 2003) diabetic rats, which may be prevented by insulin treatment (Barber *et al*., 2003), suggesting that the monoaminergic system is affected by diabetes.

The latencies of auditory and visual potentials were found to be prolonged in STZ-induced diabetic rats (Biessels *et al*., 1999; Rubini *et al*., 1992) and type 1 BB/Wor diabetic rats (Chakrabarti *et al*., 1991; Sima *et al*., 1992) in relation to controls. Likewise, in hippocampal slices from STZ-induced diabetic rats, long-term potentiation (LTP) is impaired, whereas long-term depression (LTD) is enhanced compared with control rats (Biessels *et al*., 1996, 1998; Kamal *et al*., 1999, 2000), indicating that altered hippocampal synaptic transmission and plasticity occurs in type 1 diabetic rats. This

altered plasticity was associated with reduced spatial learning and memory (*e.g.* Gispen and Biessels, 2000; Kamal *et al*., 2000) and was prevented by insulin treatment (Biessels *et al*., 1998). Impaired spatial learning and memory have been demonstrated in different animal models of diabetes using the Morris water maze (Flood *et al*., 1990; Biessels *et al*., 1996; Kamal *et al*., 2000; Luesse *et al*., 2001; Li *et al*., 2002b) and the Y-maze (Nitta *et al*., 2002).

Diabetes *mellitus* is characterised by hyperglycaemia and its treatment with insulin frequently results in hypoglycaemia episodes. It remains controversial whether the major responsible for CNS injury is diabetes itself or the occurrence of recurrent hypoglycaemia episodes due to treatment. Several studies suggested that cognitive performance may be altered during experimentally induced hypoglycaemia (Cox *et al*., 1993; Deary *et al*., 2003; Draelos *et al*., 1995; Gold *et al*., 1995; Maran *et al*., 1995; McAulay *et al*., 2001; Sommerfield *et al*., 2003). Furthermore, some studies in patients with type 1 diabetes suggest an association between recurrent hypoglycaemia and cognitive impairment (Deary *et al*., 1993; Fanelli *et al*., 1998a; Langan *et al*., 1991; Lincoln *et al*., 1996; Perros *et al*., 1997; Wredling *et al*., 1990). Despite cognitive decline in diabetic patients treated with insulin has so far largely been attributed to recurrent episodes of hypoglycaemia rather than to hyperglycaemia, some observations do not support this notion (Deary and Frier, 1996; Austin and Deary, 1999). Moreover, patients with type 1 diabetes without hypoglycaemia episodes also displayed a decline in cognitive function (Kramer *et al*., 1998; Schoenle *et al*., 2002).

1.1.3. Glucose homeostasis and cognitive performance

Glucose metabolism is the major pathway of energy production in the mature brain and increases in glucose metabolism during brain activation have been used for functional mapping by 2-deoxyglucose autoradiography (Sokoloff *et al*., 1977; Schwartz *et al*., 1979) and positron-emission tomography (Phelps *et al*., 1982), and indirectly influence signal changes observed with functional MRI (DeYoe *et al*., 1994). In fact, brain glucose oxidation was suggested to be stoichiometricaly linked to the glutamine-glutamate cycling between astrocytes and neurons, resulting from glutamatergic neurotransmission (Sibson *et al*., 1998). Furthermore, it was shown that extracellular glucose decreased in the hippocampus during a hippocampal-dependent spatial memory test that depends on this structure (McNay *et al*., 2000), and that blockade of brain glucose transport or astrocytic glucose metabolism inhibits memory consolidation (see Gibbs *et al*., 2008 and references therein). Thus, alterations on brain glucose homeostasis may compromise learning processes and

memory consolidation, and this could possibly be the link between diabetes and brain alterations leading to diabetic encephalopathy.

1.2. Overview of brain metabolism

Cerebral function depends on the coordinated interaction of distinct cell types, such as neurons, astrocytes, oligodendrocytes or microglial cells, and relies on a high metabolic activity supported by the continuous and adequate supply of glucose and oxygen from the blood stream. The high metabolic rate of the brain is used to provide energy for the generation and propagation of action potentials, and for neurotransmitter clearance from the synaptic cleft. Neuronal action potentials mainly result from Na^+ influx and K^+ efflux through the neuronal membrane, and increased extracellular K^+ and intracellular Na^+ concentrations stimulate Na^+,K^+-ATPase activity (E.C. 3.6.1.3) to restore ionic gradients to their normal resting levels, with high energy demand (Shinohara *et al*., 1979). Action potentials are associated with neurotransmitter release from nerve terminals, such as glutamate that must be cleared from the synaptic cleft to avoid neurotoxicity. Through Na^+-dependent glutamate transporters, astrocytes reuptake glutamate together with Na^+ into the cell, and the rise of intracellular Na^+ activate astrocytic Na^+,K^+-ATPase activity and energy metabolism (Takahashi *et al*., 1995). In addition, astrocytes convert glutamate to glutamine, also consuming energy. Astrocytes surround the blood vessels and uptake glucose which is believed to be mainly oxidized to pyruvate/lactate that are then shuttled to neurons (Pellerin and Magistretti, 1994). The molecules of ATP produced in astrocytic glycolysis are mainly used for processing glutamate, and the ATP formed from the oxidation of pyruvate is consumed to restore ionic gradients and action potentials (Sokoloff, 2004). In general, metabolism in the brain tissue starts with the transport of glucose or monocarboxylate precursors (*e.g.* lactate, pyruvate, acetate) across the BBB and the plasma membrane of both glial and neuronal cells. After transport, follows the cytosolic production of pyruvate and reducing equivalents (through the glycolytic pathway if from glucose) and subsequent transport to the mitochondrial matrix, and finally the oxidation of pyruvate in the mitochondrial tricarboxylic acid (TCA) cycle.

1.2.1. Brain glucose transport

The brain has the ability to consume several types of substrates but cerebral energy metabolism mostly relies on glucose provided from the blood flow to sustain neural activity both in the basal and activated states (Sokoloff, 2004). The rate of cerebral blood flow is directly related to

cerebral oxygen consumption (Sokoloff *et al*., 1977), and glucose transport and metabolism namely through glycolysis and TCA cycle make the link between the two. In mammalian cells, the transport of glucose and other hexoses across the plasma membrane is mediated by the Solute Carrier Family 2 (SLC2) family of 13 transport proteins, which include glucose trnasporters (GLUT1 to GLUT12) and the *myo*-inositol transporter HMIT1 (summarised in Joost *et al*., 2002). Most of these transporters are present in the brain but many of them are either unable to transport glucose (GLUT5, -6, and -11, and HMIT1 have low affinity for glucose), or have limited localization and densities (GLUT2 and -4), or their location or ability to transport glucose is not known (GLUT8 and -10) (reviewed in Simpson *et al*., 2007). Excluding these, the predominant cerebral transporters involved in cerebral glucose utilization are GLUT1 and GLUT3. GLUT1 is present in all brain cells (with low density in neurons) including the endothelial cells of the capillaries, existing in two forms with different degree of glycosylation, leading to apparent molecular masses of 55 and 45 kDa. While the 55 kDa form is essentially localised in brain microvessels, the 45 kDa protein is widely present in brain cells and particularly abundant in astrocytes (reviewed in Maher *et al*., 1994). GLUT3 localisation is almost restricted to neurons (*e.g.* Maher *et al*., 1992, 1996; McCall *et al*., 1994; Nagamatsu *et al*., 1993). Thus, GLUT1 is the main responsible for the facilitative transport of glucose across the BBB. With the exception of the HMIT1 which is proton-driven, the GLUTs are facilitative transporters (see Simpson *et al*., 2007), mediating energy-independent transport that leads to glucose equilibration. On the other hand, these transporters catalyze bi-directional fluxes, and the presence of intracellular and extracellular glucose affects the kinetics of transport both in and out of the cell (*e.g.* Gjedde, 1980; Gruetter *et al*., 1998; Qutub and Hunt, 2005). The transport across the BBB is usually described by a classical Michaelis-Menten kinetics and several types of transport models were considered for this system (*e.g.* Gruetter *et al*., 1998; Lund-Andersen, 1979).

1.2.2. Brain energy metabolism

Astrocytes are the metabolically most active glial cells in brain, participating in several processes, such as provision of nutrients and energy to neurons, uptake and recycling of neurotransmitters, and removal of toxic compounds (reviewed in Zwingmann and Leibfritz, 2003). However, the specific activity of TCA cycle enzymes is higher in neuronal cells leading to increased oxidative capacity relative to glia (Hertz and Hertz, 2003; Hertz, 2004; Stewart *et al*., 1998). Thus, different cellular functions originate at least two distinct metabolic compartments in the brain,

neurons and glia, with kinetically different TCA cycles that are connected by the exchange of metabolites.

Glucose crosses the BBB through the endothelial cells and is metabolized mainly in neurons. However, a predominant neuronal oxidative metabolism does not necessarily imply that the majority of glucose is taken up by neurons. In fact, it is assumed that due to their contact with the endothelial cells, astrocytes uptake glucose that is metabolized to produce lactate or other products of glucose metabolism that are then provided to neurons (Pellerin and Magistretti, 1994). Thus, astrocytes play a pivotal role in cerebral metabolism as a shuttle for the metabolic feeding of neurons, and in the coupling of different cellular compartments. In any case, once glucose is in the intracellular milieu, it is taken by the glycolytic pathway and converted to two molecules of pyruvate with formation of two ATP and two NADH. Pyruvate is then transaminated to alanine or reduced to lactate, or can enter into the mitochondria, where it is decarboxylated to acetyl-CoA, in a reaction mediated by pyruvate dehydrogenase complex (PDH, E.C. 1.2.4.1) forming NADH and releasing CO_2 (Patel and Korotchkina, 2001). Molecules of acetyl-CoA condensate with oxaloacetate entering the TCA cycle, which constitutes the ultimate oxidation pathway for carbohydrates, fatty acids and amino acids. For each acetyl-CoA condensed with oxaloacetate, the TCA cycle produces three NADH, one $FADH_2$ and one GTP molecules. Considering that every $FADH_2$ and NADH molecule yield respectively three and two ATP molecules when oxidised in the mitochondrial respiratory chain, the complete oxidation of one glucose molecule generates 38 or 36 ATP, if the glucose-generated NADH is transported via the malate-aspartate or the glycerol 3-phosphate mitochondrial shuttles (Voet and Voet, 1995).

The aerobic oxidation of substrates through the TCA cycle is crucial to provide not only the energy needed to maintain cerebral functions (Hertz and Dienel, 2002), but also carbohydrate intermediates for biosynthetic processes including neurotransmitter synthesis (see Gruetter, 2002 and references therein). Likewise, in neurons there is a continuous drain of α-ketoglutarate for glutamate production, the major excitatory neurotransmitter, and therefore neurons need an anaplerotic oxaloacetate formation to condense with acetyl-CoA. Thus, in the brain, oxaloacetate synthesis must occur by pyruvate carboxylation (Gamberino *et al*., 1997), catalysed by pyruvate carboxylase (PC, E.C. 6.4.1.1), that is an exclusively glial enzyme (*e.g.* Hassel, 2000; Zwingmann and Leibfritz, 2003; Waagepetersen *et al*., 2001). The transference of oxaloacetate from glia to the neuronal compartment probably occurs via aspartate exchange (Cruz and Cerdán, 1999).

To ensure proper brain function, astrocytes rapidly remove neurotransmitters released to the synaptic cleft. In the case of glutamate, it is mainly taken by astrocytic glutamate transporters, maintaining a low extracellular glutamate concentration to avoid excitotoxicity (*e.g.* reviewed in

Gruetter, 2002). Glutamate is converted to glutamine by glutamine synthetase (GS, E.C. 6.3.1.2), another specific glial enzyme, and then glutamine is transported to neurons where it is hydrolysed to glutamate by glutaminase (Gase, E.C. 3.5.1.2), completing the glutamine-glutamate cycle (Shen *et al*., 1999; Zwingmann and Leibfritz, 2003). This cycle has the principal function of replenishing glutamate losses in the neuron due to neurotransmission and is probably complemented by the transport of NH_4^+ between both compartments, carried out by lactate-alanine shuttle (Zwingmann *et al*., 2000, 2001) or other amino acid shuttles (Sibson *et al*., 2001; reviewed in Zwingmann and Leibfritz, 2003).

The maintenance of glutamate synthesis from α-ketoglutarate requires a permanent flow through the TCA cycle. In conditions of low acetyl-CoA availability, this metabolite can be formed by pyruvate recycling that may occur in astrocytes and to a less extent in neurons (Olstad *et al*., 2007; Cruz *et al*., 1998; Waagepetersen *et al*., 2002; Sonnewald *et al*., 1996). Beside the catabolism of energetic substrates, two other metabolic pathways converge to the production of pyruvate from TCA cycle intermediates: the malic enzyme (E.C. 1.1.1.40) converting malate to pyruvate (Bakken *et al*., 1997; Bernstine *et al*., 1979; Cruz *et al*., 1998), and the combined action of phophoenolpyruvate carboxykinase (E.C. 4.1.1.32) and pyruvate kinase (E.C. 2.7.1.4) returning oxaloacetate to phosphoenolpyruvate and pyruvate (Cruz *et al*., 1998). Then pyruvate can form lactate or alanine, or be re-introduced into the TCA cycle via acetyl-CoA to complete the pyruvate recycling pathway.

The inhibitory neurotransmitter γ-aminobutiric acid (GABA) is mainly produced in the cytosol of GABAergic neurons from glutamate, via glutamate decarboxylase (GAD, L-glutamate-1-carboxy-lyase, E.C. 4.1.1.15) (Martin and Rimvall, 1993). After being released, GABA is taken from the synaptic cleft mainly by astrocytes through specific GABA transporters and introduced in the astrocytic TCA cycle in the form of succinate, after the sequential actions of GABA-transaminase (E.C. 2.6.1.19) and succinic semialdehyde dehydrogenase (E.C. 1.2.1.24) (Balázs *et al*., 1970). In this pathway, α-ketoglutarate is transaminated to glutamate that can be provided to the neurons in the form of glutamine for neurotransmitter re-synthesis.

Figure 1.1 depicts the principal metabolic pathways for glucose oxidation within neurons and glia, leading to the generation of GABA and glutamate that are the main inhibitory and excitatory neurotransmitters, respectively. However, other substrates are involved in brain metabolism though pathways interacting and regulating glucose oxidation that are coupled to neurotransmission. Another metabolic pathway that coexists in the brain, supporting the use of other carbohydrate sources than glucose is, for instance, fatty acid oxidative metabolism through β-oxidation (Kuge *et al*., 1995, 2002), which can contribute up to 20% of the whole cerebral oxidative metabolism *in vivo* (Ebert *et al*., 2003). Also monocarboxylates are taken from blood stream to feed

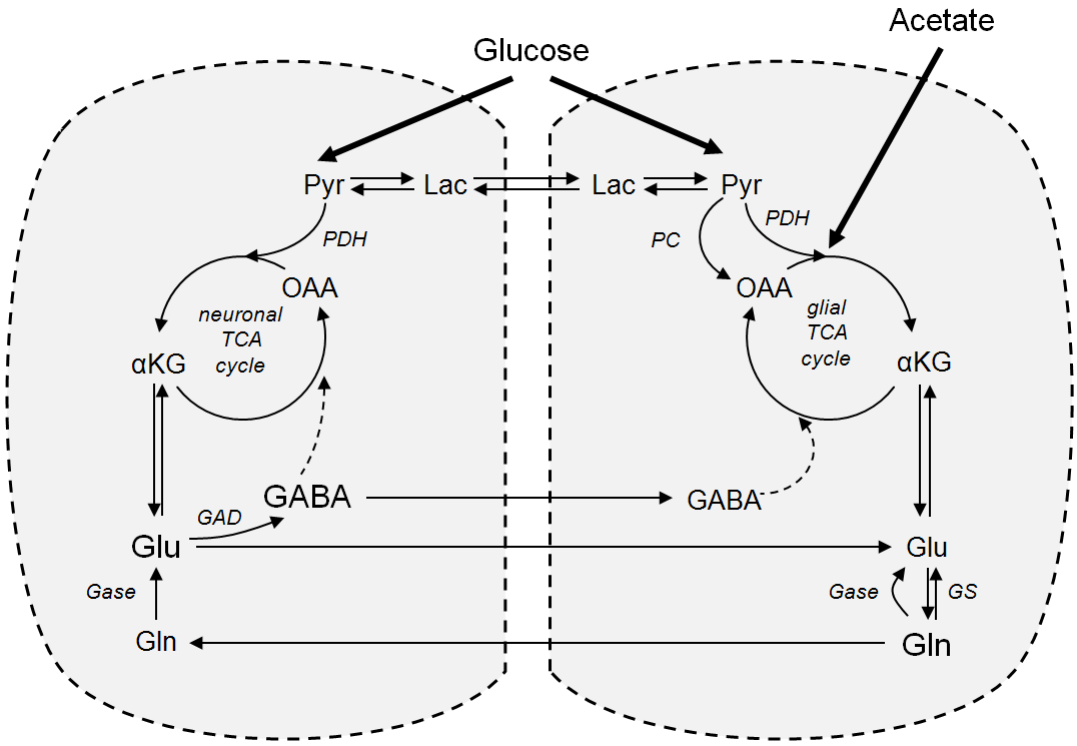

Figure 1.1. Schematic model of compartmentalised brain metabolism with special enphasis to coupling of glucose oxidation and neurotransmission, and metabolic interactions between neurons and astrocytes. Glucose is taken by both neurons and glial cells and metabolised as described. Acetate metabolism was included in the figure since it may be used as specific substrate for the study of the glial compartment. αKG, α-ketoglutarate; GABA, γ-aminobutiric acid; GAD, glutamate decarboxylase; Gase, glutaminase; Gln, glutamine; Glu, glutamate; GS, glutamine synthetase; Lac, lactate; OAA, oxaloacetate; PC, pyruvate carboxylase; PDH, pyruvate dehydrogenase complex; Pyr, pyruvate.

neuronal and glial TCA cycles, namely lactate (Bouzier *et al*., 2000), β-hydroxybutyrate (Künnecke *et al*., 1993), acetate (Badar-Goffer *et al*., 1990; Cerdán *et al*., 1990) and acetoacetate (Ito and Quastel 1970), and these substrates may become important in conditions of reduced substrate availability like hypoglycaemia.

Lactate and pyruvate are two important monocarboxylates since they are involved in the so called astrocyte to neuron lactate shuttle (reviewed in Pellerin *et al*., 2007), in which glutamate released by neurons stimulates astrocytic glycolysis. Briefly, during cerebral activation, glutamatergic neurons release glutamate into the synaptic cleft that is taken up by the surrounding astrocytes co-transported with Na^+ that must return to the extracellular milieu through Na^+,K^+-ATPase, consuming one molecule of ATP. Once in the astrocyte, glutamate is converted to glutamine by glutamine synthetase at the expense of an additional ATP molecule. These two molecules of ATP used to clear glutamate are thought to be derived from the glycolytic pathway with formation of two molecules of pyruvate that are reduced to lactate. Astrocytic lactate and glutamine are then shuttled to neurons for oxidation in the neuronal TCA cycle (leading to energy

production) and glutamate regeneration, respectively, both required for maintenance of neurotransmission.

Glycogen is present in significant amounts in brain (Choi *et al*., 1999). It constitutes an important source of glucose equivalents, and mainly acts as buffer upon reduced substrate availability from the blood stream or strong functional activation (Gruetter, 2003). Brain glycogen metabolism is affected by hormones, neurotransmitters and second messengers, and the regulation of its content is dependent on glucose availability and on a putative gluconeogenic pathway. Actually, production of glucose and glycogen from three-carbon compounds may occur in the brain, probably in astroglial cells (Bernard-Hélary *et al*., 2002; Dringen *et al*., 1993; Phillips and Coxon, 1975; Schmoll *et al*., 1995a), suggesting that the brain can provide endogenous sources of glucose. In fact, all the specific enzymatic machinery necessary for the occurrence of such gluconeogenic pathway is present in the brain, namely glucose-6-phosphatase (E.C. 3.1.3.9) (Anchors *et al*. 1975; Dodd *et al*., 1971, 1972; Ghosh *et al*. 2005), fructose-1,6-bisphosphatase (D-fructose-1,6-bisphosphate 1-phosphohydrolase; E.C. 3.1.3.11) (Cloix *et al*., 1997; Löffler *et al*., 2001; Majumder and Eisenberg, 1977; Vergé *et al*., 1995; Schmoll *et al*., 1995b), and phosphoenolpyruvate carboxykinase (PEPCK, E.C. 4.1.1.32) (Cheng and Cheng, 1972; Sharma and Patnaik, 1983). Since cerebral gluconeogenesis rate is considered negligible compared to the flux of glycolysis (*e.g.* Gruetter, 2002), these enzymatic activities may possibly function as regulators of metabolic fluxes.

1.2.3. Study of brain metabolism

Initial studies of cerebral metabolism used radioactive isotopes or optical methods which required the preparation of homogenates and extracts, or isolation and purification of the enzymes or transport systems involved to investigate their *in vitro* kinetics (*e.g.* Siesjo 1982; Sokoloff 1989). This reductionist approach provided fundamental information on metabolic processes of the CNS, but the development of non-invasive methodologies over the last decades allowed studying the mammalian brain *in vivo*, enhancing the possibility to investigate and understand regulation of brain function. Positron Emission Tomography (PET) was the first technique used to non-invasively investigate glucose uptake in animals and man with acceptable resolution (Wienhard, 2002). Similarly, functional MRI (fMRI) allowed investigation of changes in the local hemodynamics and blood oxygenation, resulting from alterations in neuronal activity associated with for example sensory or motor stimulation (Heeger and Ress, 2002). Thus, PET and fMRI provided information on the coupling between neuronal activity and metabolism but without investigating metabolic

pathways underlying these cerebral processes. The development of novel strategies based on tracers detectable by NMR spectroscopy allowed to overcome many of the limitations of the traditional approaches. In particular, the use of ^{13}C labelled tracers provided the quantitative assessment of transport mechanisms, metabolic fluxes, and cellular and sub-cellular compartmentation of metabolic pathways like glycolysis, pyruvate recycling and TCA cycle in a plethora of systems (reviewed in Gruetter *et al*., 2003; Shulman *et al*., 2004) ranging from *in vitro* primary cell cultures or tissue preparations (*e.g.* Fonseca *et al*., 2005) to the intact rodent or human brain (*e.g.* Behar *et al*., 1986; Henry *et al*., 2003; Patel *et al*., 2005).

Concerning the investigation of the regulation of brain metabolism, basically four types of methodologies are now becoming important, namely autoradiography, PET, dual photon fluorescence confocal microscopy, and NMR. The radioactivity-based autoradiography and PET uses glucose analogs labelled with ^{14}C or ^{18}F for the determination of cerebral metabolic rates of glucose consumption (CMR_{gluc}) (Herholz and Heiss, 2004; Wienhard, 2002), or $^{15}O_2$ to quantify blood volume, blood flow and oxygen consumption rates in the brain (Hatazawa *et al*., 1995). Dual photon fluorescence confocal microscopy is particularly interesting for the *in vivo* measurement and mapping of NADH fluorescence (Chance, 2004), which basically depends on NADH producing and consuming pathways, namely the balanced fluxes through glycolysis and TCA cycle (NADH fluorescence increases with increased glycolytic activity and decreases with augmented TCA cycle flux). Finally, NMR spectroscopy methods can be used to access brain metabolism *in vivo* by detecting chemical species that are relevant to certain brain processes (*e.g.* Ross and Sachdev, 2004).

NMR is based on the magnetic properties of nuclei and can be used in different modalities for the most diverse purposes, including the study of brain metabolism (de Graaf, 1998). ^{1}H NMR takes advantage of the most sensitive nucleus for magnetic resonance in terms of intrinsic sensitivity and natural abundance. However ^{1}H NMR has a number of challenges, including the high concentration of water in the tissue (several orders of magnitude more concentrated than metabolites) that originates an enormous resonance in the proton spectra, the narrow chemical shift[1] range (5 ppm) that causes several metabolite resonances to overlap, and the low sensitivity of the NMR phenomena that compromises the detection of low concentrated metabolites. In any case, with the appropriate calibration of the parameters for the NMR scanning, ^{1}H NMR spectroscopy can provide reliable quantification of metabolite concentrations. ^{31}P NMR spectroscopy relies on the relatively high sensitivity of the ^{31}P nucleus (7% of ^{1}H), the 100% natural abundance and the large dispersion of phosphate resonances in the spectrum (over 30 ppm). Despite the limited number of

[1] The chemical shift describes the dependence of nuclear magnetic energy levels on the electronic environment, and is represented in terms of variations of nuclear magnetic resonance frequencies.

detectable resonances, ^{31}P NMR spectroscopy is useful for the detection of phosphate-containing metabolites related to energy metabolism. *In vivo* ^{31}P NMR can also provide other indirect relevant parameters such as intracellular pH and Mg^{2+} concentration. Like protons, almost all metabolites contain carbon atoms. NMR detects the stable isotope ^{13}C with a chemical shift spanning of about 200 ppm. However, ^{13}C has a natural abundance of 1.1% and a magnetogyric ratio one fourth of the proton, and moreover the strong heteronuclear scalar coupling complicates the spectra and reduces the sensitivity, so that additional hardware is needed for decoupling. Nevertheless, the low natural abundance of ^{13}C may be converted to an advantage when using specific ^{13}C-enriched substrates that are infused to follow incorporation into metabolites and study a variety of metabolic pathways. By applying ^{13}C NMR and ^{13}C tracers to the *in vivo* and *in vitro* study of brain metabolism and associating this strategy with adequate mathematical models, it has been possible in the last couple of decades to detail specificities of regional metabolism in different brain areas, cellular interactions and their alteration in pathological situations (Gruetter, 2002; Gruetter *et al*., 2003).

1.3. Modulation systems in the brain

Processes of learning and memory are associated to synaptic events, namely neurotransmission that is tightly coupled to brain energy metabolism. Therefore, modulators of synaptic activity may directly or indirectly influence energy metabolism, by balancing the cellular energy charge, regulating metabolic pathways or controlling substrate uptake from the blood stream.

Diabetes-induced dysfunction of synaptic plasticity is likely to be due to a perturbed efficiency of the release of neurotransmitters, as gauged by the reduction of neurotransmitter release (Guyot *et al*., 2001; Yamato *et al*., 2004) and possible change in pre-synaptic proteins associated with vesicular release of neurotransmitters upon diabetes (Grillo *et al*., 2005; Nitta *et al*., 2002). Thus, one possible strategy to correct this diabetes-induced modification of synaptic efficiency might be to target neuromodulation systems, in particular at the level of the nerve terminal.

1.3.1. Purinergic signalling systems

Adenosine 5´-triphosphate (ATP) is the main adenine nucleotide accumulated and stored in synaptic vesicles, at the presynaptic terminal (Sperlagh and Vizi, 1996). Therefore, ATP is released from nerve terminals upon stimulation via exocytosis (Pankratov *et al*., 2006) in a frequency dependent-manner (Wieraszko *et al*., 1989; Cunha *et al*., 1996). Other brain compartments, such as glial cells (*e.g.* Caciagli *et al*., 1988; Coco *et al*., 2003; Queiroz *et al*., 1997) and postsynaptic structures (Hammann *et al*., 1996; Inoue *et al*., 1995) may also contribute to ATP release. Once in the extracellular milieu, ATP acts directly through the activation of P2 receptors (Ralevic and Burnstock, 1998), and additionally it can act as a substrate for ecto-protein kinases (Wierasko and Enrlich, 1994) or be converted through ecto-nucleotidases into adenosine (Zimmermann, 2000), with subsequent activation of adenosine (P1) receptors (Fredholm *et al*., 2005).

This division of purine receptors in P1 receptors that have adenosine as the main natural ligand, and P2 receptors recognizing principally ATP and adenosine 5´-diphosphate (ADP) is based on the relative potencies and affinities of adenine nucleotides and adenosine, and according to their distinct molecular structures and pharmacological profiles (Ralevic and Burnstock, 1998).

The ATP molecule is used by virtually all cells as intracellular energy transfer in the most diverse metabolic pathways modulating the cellular metabolic state. ATP is a nucleotide composed by adenine (a purine) bound to ribose (a pentose), constituting adenosine, which is attached to three phosphate moieties (Figure 1.2). Moreover, ATP/adenosine also constitutes nucleic acids, the genetic material of the cell. Along with these pivotal roles of intracellular ATP, it is also released to the extracellular milieu where it acts as signalling molecule in several biological systems and as neuromodulator in the nervous system (reviewed in Burnstock, 2006). Like ATP, besides its metabolic involvement, adenosine exerts several biological effects including a role as neuromodulator in the nervous system controlling neurotransmission and other cellular functions (reviewed in Cunha, 2001).

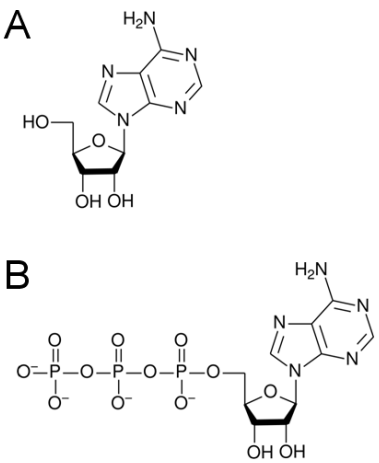

Figure 1.2. The chemical structures of adenosine (A) and ATP (B).

1.3.1.1. Metabolism of adenosine and adenine nucleotides

ATP and adenosine are metabolised both intra- and extracellularly in the CNS (Figure 1.3). The intracellular levels of adenosine result from the balance between its anabolism and catabolism. This nucleoside is formed from degradation of adenosine 5'-monophosphate (AMP) by action of the cytosolic 5´-nucleotidase (5'-ribonucleotide phosphohydrolase, 5'-NT, E.C. 3.1.3.5), and from hydrolysis of S-adenosyl-homocystein (SAH) by S-adenosyl-L-homocystein hydrolase (E.C. 3.3.1.1) (Latini *et al*., 1996; Latini and Pedata, 2001). Adenosine may be phosphorylated to AMP by adenosine kinase (ATP:adenosine 5'-phosphotransferase, E.C. 2.7.1.20), deaminated to inosine by adenosine deaminase (adenosine aminohydrolase, E.C. 3.5.4.4), or converted to SAH by reaction with L-homocystein (reviewed in Latini and Pedata, 2001).

The intracellular concentration of ATP is tightly controlled and only changes upon profound metabolic imbalance (Doolette, 1997; Stumpe and Schrader, 1997). ATP and AMP concentrations are in the milimolar and the nanomolar range, respectively. Thus, under metabolic stress or increased metabolic rate, only minor changes in the ATP catabolism induce large increase in the AMP concentration (discussed in Cunha, 2001). The substrate cycle between AMP and adenosine, with the enzymatic activities of 5´-nucleotidase and adenosine kinase, allows the translation of the modification of ATP concentration in a profound modification of adenosine concentration (Decking

et al., 1997; Kroll *et al.*, 1993), which has the capacity of being transported to the extracellular medium, unlike AMP, through non-concentrative bi-directional adenosine transporters (Cass *et al.*, 1998). Thus, once formed, intracellular adenosine must be transported out of the cell in order to exert its effects upon cell surface P1 receptors.

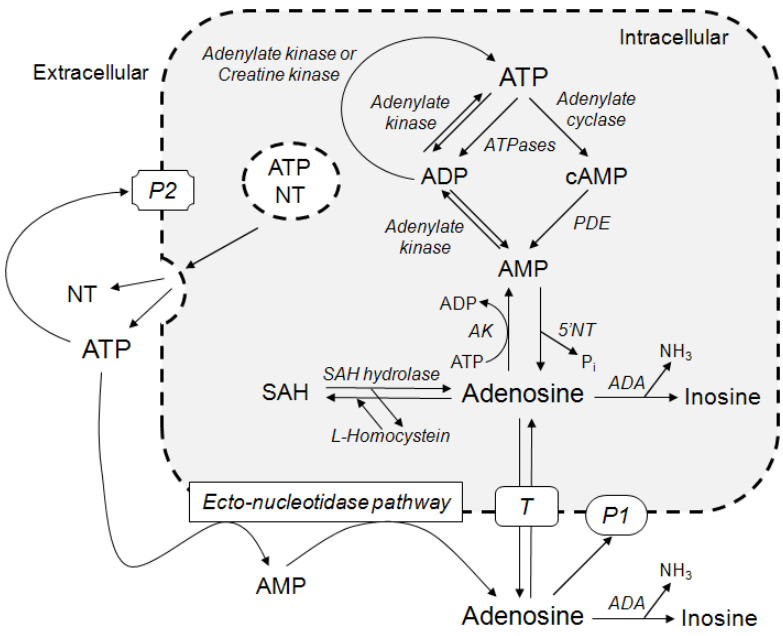

Figure 1.3. Main intra- and extracellular pathways of ATP and adenosine metabolism. ADA, adenosine deaminase; AK, adenosine kinase; 5'NT, endo-5'-nucleotidase; NT, neurotransmitters; SAH, S-adenosyl-homocystein; T, adenosine transporters.

While ATP is ubiquitously distributed in the intracellular milieu with concentrations in the millimolar range, extracellular ATP concentrations range from nanomolar to micromolar (Agteresch *et al.*, 1999; Schwiebert, 2000), and thus there is a concentration gradient for ATP efflux, transport or secretion out of the cells. ATP is co-released to the extracellular medium with neurotransmitters from synaptic vesicles by Ca^{2+}-dependent membrane-vesicle fusion, but it can also be directly released from the cytosol through membrane channels or transporters, or leak via the damaged cell membranes (reviewed in Zimmermann, 1996). ATP transporters at the plasma membrane include connexin hemichannels (Cotrina *et al.*, 2000), osmotic transporters linked to anion channels (Abdipranoto *et al.*, 2003; Darby *et al.*, 2003), or ATP-binding cassette transporters (Schwiebert, 1999; Ballerini *et al.*, 2002).

The extracellular ATP controls neuronal activity directly through adenine nucleotide receptor (P2 receptors), or indirectly after being hydrolysed by the ecto-nucleotidase pathway. Ecto-nucleotidases are membrane-bound enzymes with their catalytic site facing the extracellular medium, and also include cleaved and soluble isoforms. Several activities which constitute the ecto-nucleotidase pathway are involved in the extracellular catabolism of ATP (for review see Zimmermann, 1996), converting it to AMP: ecto-ATPase (E.C. 3.6.1.3), ecto-ADPase (E.C. 3.6.1.6), ecto-ATP-diphosphohydrolase (E.C. 3.6.1.5), ecto-adenylate kinase (E.C. 2.7.4.3) and ecto-ATP-pyrophosphatase (E.C. 3.6.1.8). Finally, the ecto-5'-nucleotidase activity (E.C. 3.1.3.5) converts AMP to adenosine. The ecto-alkaline phosphatase activity (E.C. 3.1.3.1) is able to convert ATP to adenosine directly. Beside ATP, other nucleotides can be released, and may constitute a source of

extracellular adenosine if they are substrates for ecto-nucleotidases (Latini and Pedata, 2001; Miras-Portugal *et al*., 1999).

The adenosine in the extracellular medium has two origins: either the release from cells through non-concentrative bi-directional adenosine transporters or the dephosphorylation of adenine nucleotides by the ecto-nucleotidase pathway, which appears to be the main source of adenosine at the synaptic level (discussed in Cunha, 2001). Adenosine can be removed from the extracellular medium by uptake into the cytosol via adenosine transporters or by action of the extracellular adenosine deaminase activity (Franco *et al*., 1997). Adenosine is deaminated to inosine which may be a substrate for purine-nucleoside phosphorylase (purine-nucleoside:phosphate ribosyltransferase, E.C. 2.4.2.1), xanthine dehydrogenase (xanthine:NAD+ oxidoreductase, E.C. 1.1.1.204) and xanthine oxidase (xanthine:oxygen oxidoreductase, E.C. 1.1.3.22), which catalyse the oxidation of inosine leading to the formation of uric acid (Barsotti *et al*., 2003; Moriwaki *et al*., 1993; Wajner and Harkness, 1989).

1.3.1.2. ATP receptors

Purinergic P2 receptors are classified in two main families, ionotropic P2X and metabotropic P2Y receptors, based on protein structure and signal transduction mechanisms, being both robustly expressed in the CNS (reviewed in Ralevic and Burnstock, 1998).

Seven mammalian P2X receptor subunits ($P2X_{1\text{-}7}$) have been cloned (Ralevic and Burnstock, 1998). They are ligand-gated cation channels that, upon activation by the principal endogenous ligand ATP mediate opening of a non-selective cation pore, permeable to Na^+, K^+ and Ca^{2+} (North, 2002). P2X receptor subunits are composed by two transmembrane domains and have both N- and C-terminal regions lying on the intracellular milieu. The C-terminus binds to protein kinases responsible for the kinetics, permeation and desensitization of the channels, while the extracellular loop contains the ATP binding sites and sites for antagonists and modulators (Khakh, 2001). Functional and biochemical data established several functional homomultimers and heteromultimers of P2X receptors (Brown *et al*., 2002; King *et al*., 2000; Lê *et al*., 1998, 1999; Nicke *et al*., 2005; North and Surprenant, 2000; Radford *et al*., 1997).

In contrast to P2X receptors, P2Y receptors not only bind to ATP, but also ADP and the pyrimidine nucleotides. Metabotropic P2Y receptors are G protein coupled receptors with seven transmembranar domains, an extracelullar N-terminus and an intracellular C-terminus. Eight different mammalian P2Y receptors subtypes ($P2Y_{1,2,4,6,11,12,13,14}$) have been cloned so far (Abbracchio

et al., 2006). The intracellular loops and the C-terminus are structurally diverse among the P2Y receptor subtypes, conditioning the interaction with different G proteins (Abbracchio *et al*., 2006). Each P2Y receptor binds to a single heterotrimeric G protein, tipically $G_{q/11}$, stimulating phospholipase C (E.C. 3.1.4.3), resulting in the formation of inositol-(1,4,5)-triphosphate (IP3) and diacylglycerol, with subsequent mobilization of Ca^{2+} from intracelullar stores (Abbracchio *et al*., 2006). However $P2Y_{11}$ can couple to both $G_{q/11}$ and G_s, stimulating adenylate cyclase, and $P2Y_{12,13,14}$ couple to G_i inhibiting adenylate cyclase (Abbracchio *et al*., 2006). In addition, P2Y receptors may activate other second messengers like phospholipases A2 and D, mitogen-activated protein kinases (MAPK), tyrosine kinase and the serine-threonine kinase Akt (reviewed in Lazarowski *et al*., 2003).

The conjugation of several experimental techniques identified the presence of P2X and P2Y receptors in different regions of the CNS, including the hippocampus (*e.g.* Rodrigues *et al*., 2005a; Rubio and Soto, 2001), located in either neurons (reviewed in Illes and Ribeiro, 2004) or glial cells (Abbracchio and Verderio, 2006). The existence of multiple sources of extracellular ATP and the localization of distinct P2 receptors in the CNS suggests several possible roles for extracellular ATP. In glial elements, P2 receptors are involved in glia-glia and glia-neuron communication (Fields and Burnstock, 2006), astrocyte proliferation (Neary *et al*., 2006), chemotaxis and control of microglia reactivity (Farber and Kettenman, 2006). In neurons, P2 receptors constitute a neuromodulatory system (Cunha and Ribeiro, 2000), controlling for example excitatory glutamate release (Rodrigues *et al*., 2005a).

As described above, ATP is co-released with other neurotransmitters, such as glutamate, GABA (Pankratov *et al*., 2006) and acetylcholine (Richardson and Brown, 1987), placing ATP in distinct synaptic populations. ATP is not only released by the presynaptic terminal, but can be released postsynaptically or from non-neuronal cells (Volonté *et al*., 2003) and, moreover, each of the products of ATP hydrolysis can activate different receptors (P2 receptors bind ATP and ADP and P1 receptors bind adenosine). These features expand the possibility of ATP as a ubiquitous neuromodulator in the CNS. Furthermore, P2X receptors can interact with different ionotropic receptors, like $GABA_A$ receptors (Boue-Grabot *et al*., 2004; Sokolova *et al*., 2001), nicotinic acetylcholine receptors (Rodrigues *et al*., 2006), serotonin receptors (Boue-Grabot *et al*., 2003), and eventually NMDA (Pankratov *et al*., 2002; Peoples and Li, 1998) and AMPA/kainate receptors (Zona *et al*., 2000). This interesting feature of P2X receptors reinforces the possible neuromodulatory role operated by these receptors and suggests that ATP signalling via activation of P2 receptors may also control other modulatory systems.

Functional studies following the release of neurotransmitters in different brain regions, suggest that the neuromodulation role of P2 receptors involves a dual action controlling synaptic

events operated by inhibitory P2Y and facilitatory P2X receptors (reviewed in Cunha and Ribeiro, 2000; Hussl and Boehm, 2006). On the other hand, not only there is a direct involvement of presynaptic P2 receptor on synaptic function, but there are also astrocyte-mediated effects that may lead to modulation of synaptic function. In particular, the activation of astrocytic $P2X_7$ receptors modulates the release of glutamate (Duan *et al*., 2003) and GABA (Sperlágh *et al*., 2002). Moreover, P2X receptors may also control postsynaptic events (Khakh and Henderson, 1998). In the particular case of the hippocampus, it was reported a facilitatory effect mediated by presynaptic $P2X_2$ receptors controlling excitatory transmission (Khakh *et al*., 2003), activation of presynaptic $P2X_7$ receptors depresses synaptic transmission (Armstrong *et al*., 2002), and $P2Y_1$ receptor activation increases synaptic inhibition of hippocampal circuits (Bowser and Khakh, 2004).

1.3.1.3. Adenosine receptors

Adenosine exerts its effects through the activation of specific membrane receptors (P1 receptors) identified in all types of cells studied (reviewed in Ralevic and Burnstock, 1998). The P1 receptor family comprises A_1, A_{2A}, A_{2B} and A_3 adenosine receptors, identified by convergent molecular, biochemical and pharmacological data. In the CNS, activation of adenosine A_1 receptors is associated with inhibitory effects on neurotransmission, and activation of adenosine A_{2A} and A_{2B} is linked to facilitatory events (reviewed in Fredholm *et al*., 2005). The lack of good pharmacological tools has delayed the knowledge about the function of A_{2B} and A_3 in the nervous system.

All adenosine receptors couple to G proteins and, in common with other G protein-coupled receptors, they have seven putative transmembrane domains, the N-terminal lying on the extracellular side and the C-terminal on the cytoplasmic side of the membrane. In general, while A_1 and A_3 are negatively coupled to adenylate cyclase via G_i protein, A_{2A} and A_{2B} are positively coupled to adenylate cyclase via G_s protein (Fredholm *et al*., 2001). However, all adenosine receptors may be coupled to other G proteins and operate through different signal transducing pathways (see Cunha, 2005).

The A_1 receptor, with an apparent molecular mass of 34-38 kDa (Nakata, 1992; Stiles *et al*., 1985), is widely distributed in the CNS, with particular abundance in the hippocampus, cerebral cortex, cerebellum, and in certain thalamic nuclei (Ochiishi *et al*., 1999), and is specially enriched in synapses (Rebola *et al*., 2003a; Tetzlaff *et al*., 1987). A_1 receptors couple to G_i/G_o proteins (Nanoff *et al*., 1995) and, upon activation, can inhibit adenylate cyclase, activate potassium channels, inactivate calcium channels and activate phospholipase C, modulating both pre- and postsynaptic

mechanisms that summed will cause decreased neuronal excitability (reviewed in Ralevic and Burnstock, 1998). This control of neuronal excitability is important for normal brain function (see for example, Brambilla *et al*., 2005; Pascual *et al*., 2005) and is particularly relevant in pathological conditions where excessive stimulation of neurons may eventually lead to neuronal death (Dodd, 2002). In glial cells, A_1 receptors modulate calcium signals (Alloisio, *et al*., 2004; Cormier *et al*., 2001), cAMP accumulation (Peakman and Hill, 1996) and phospholipase C activation (Biber *et al*., 1997). A_1 receptors were also reported to modulate oligodendrocyte migration (Othman *et al*., 2003). However, and besides all these evidences for the presence of functional A_1 receptors in glia cells, their role to brain function needs further clarification.

The A_{2A} receptor has an apparent molecular mass of 45 kDa (Barrington *et al*., 1989) and, in the brain, is mainly localized in the striatum, nucleus accumbens and olfactory bulb (Peterfreund *et al*., 1996; Rosin *et al*., 1998). It is also present in the hippocampus, but at much lower density (Cunha *et al*., 1994a; Peterfreund *et al*., 1996), and here it is particularly enriched in synapses (Rebola *et al*., 2005a). In the brain, the A_{2A} receptor may couple to different G proteins in different regions (discussed in Fredholm *et al*., 2003), including coupling to G_s (Marala and Mustafa, 1993; Olah, 1997; Cunha *et al*., 1999) and to G_{olf} (Kull *et al*., 2000) proteins, increasing cAMP levels, and activating protein kinase A and MAPK. Neuronal A_{2A} receptors were suggested to control neurotransmitter release by controlling protein kinase C activity independently of cAMP levels (Gubitz *et al*., 1996; Norenberg *et al*., 1998; Cunha and Ribeiro, 2000b; Queiroz *et al*., 2003; Rebola *et al*., 2003b). Other signalling pathways that may be recruited by the A_{2A} receptor include coupling to G_{12}/G_{13} (Sexl *et al*., 1997) and $G_{15/16}$ (Offermanns and Simon, 1995) proteins. Presynaptically, A_{2A} receptors control the release of neurotransmitters, namely GABA (Cunha and Ribeiro, 2000c; Shindou *et al*., 2002), acetylcholine (Rebola *et al*., 2002), glutamate (Lopes *et al*., 2002) and serotonin (Okada *et al*., 2001), which appears to be mostly due to the control of the conductance of calcium channels (Gonçalves *et al*., 1997; Cunha and Ribeiro, 2000). A_{2A} receptor activation has been reported to increase neuronal excitability (Sebastião and Ribeiro, 1992), synaptic transmission (Cunha *et al*., 1997) and long-term potentiation (d'Alcantara *et al*., 2001; de Mendonça and Ribeiro, 1994; Rebola *et al*., 2008). The A_{2A} receptor is also present in glial cells and was suggested to modulate glutamate release and calcium transients in astrocytes (Nishizaki *et al*., 2002; Alloisio *et al*., 2004), astroglyosis (Brambilla *et al*., 2003), and microglia activation (Fiebich *et al*., 1996b; Saura *et al*., 2005).

In the brain, the A_{2B} receptor has a low density but is globally distributed (Dixon *et al*., 1996). It can couple to different signalling pathways, such as activation of adenylate cyclase, activation of phospholipase C through coupling to G_q/G_{11}, and increase in intracellular calcium concentrations through IP3 production (reviewed in Ravelic and Burnstock 1998) and MAPK activation (Schulte

and Fredholm, 2003). These receptors seem to have a low affinity for adenosine compared to the other adenosine receptors, which indicates a role in pathologic conditions in the CNS (Fredholm *et al*., 2001). A_{2B} receptors in the brain are mainly restricted to glia cells where they were reported to control important cellular processes like cAMP accumulation (Peakman and Hill, 1994), interleukin secretion (*e.g.* Fiebich *et al*., 1996; Schwaninger *et al*., 1997), ATP-induced calcium transients (Jiménez *et al*., 1999), or glycogen turnover (Allaman *et al*., 2003).

The A_3 receptor is abundant in peripheral tissues (Ravelic and Burnstock 1998) and the presence of its mRNA was observed in several brain regions including the hippocampus (Dixon *et al*., 1996). Among several transducing pathways (Gessi *et al*., 2008), the A_3 receptor couples to G_i protein inhibiting adenylate cyclase activity, and to G_q protein activating phospholipase C, increasing IP3 levels and intracellular calcium concentration. The functions of this receptor are poorly understood but it was also found to be present and functional in cultured microglia cells (Hammarberg *et al*., 2003; Lee *et al*., 2006), to promote cytoskeleton reorganization in human astrocytoma cells (Abbracchio *et al*., 1997), and to induce apoptosis in cultured astrocytes (Appel *et al*., 2001).

The effects of adenosine on synaptic transmission are mostly mediated by A_1 receptor activation, causing inhibition of excitatory neurotransmission and decrease of neuronal excitability (Dunwiddie and Masino, 2001), that mainly results from inhibition of glutamate release (Ambrósio *et al*., 1997; Gundlfinger *et al*., 2007). A_1 receptors can also modulate GABA release (Cunha and Ribeiro, 2000c; Yang *et al*., 2004) that seems to be important in the hippocampus of immature animals (Jeong *et al*., 2003), and may act at the postsynaptic level by increasing potassium currents (Proctor and Dunwiddie, 1987) and by decreasing NMDA receptor function (de Mendonça *et al*., 1995) and voltage sensitive calcium channels function (Mogul *et al*., 1993). A_1 receptor activation was reported to oppositely decrease (de Mendonça and Ribeiro, 1994) or stimulate long-term potentiation (LTP) (Pascual *et al*., 2005). This receptor has been observed to be involved in inducing heterosynaptic depression of glutamatergic synaptic transmission in CA1 area of the hippocampus (Zhang *et al*., 2003). As mentioned above, A_1 receptors are also present in astrocytes, which may have an important role in modulating synaptic transmission (Haydon and Carmignoto, 2006).

Contrasting with A_1 receptors, A_{2A} receptors have mainly been described to stimulate neurotransmitter release (Cunha, 2001). A_{2A} receptor activation has been reported to modulate the release of GABA (Cunha and Ribeiro, 2000c; Shindou *et al*., 2002), acetylcholine (Rebola *et al*., 2002), glutamate (Lopes *et al*., 2002) and serotonin (Okada *et al*., 2001). In the hippocampus, it increases LTP amplitude (de Mendonça and Ribeiro, 1994; Fujii *et al*., 2000), stimulates excitatory synaptic transmission by a mechanism dependent on A_1 receptor activation (Lopes *et al*., 2002), and

modulates postsynaptic NMDA responses (Rebola *et al*., 2008). The modulation of inhibitory synaptic transmission by A_{2A} receptors is controversial, being reported its inhibition (Mori *et al*., 1996) and stimulation (Shindou *et al*., 2002).

In the hippocampus, A_3 receptor activation was shown to decrease synaptic transmission (Brand *et al*., 2001; Hentschel *et al*., 2003), to modulate synaptic plasticity (Costenla *et al*., 2001) and to control metabotropic glutamate receptor (mGluR) functions (Macek *et al*., 1998; Huang *et al*., 2007). Nonetheless, the effect of A_3 receptor activation on neuronal activity is still mostly unknown, as well as A_{2B} receptor functions.

Like ATP, adenosine acts also as a modulator of other modulator systems allowing a fine-tuning of synaptic activity. For example, A_{2A} receptor activation modulates the roles of some peptides like calcitonin gene related peptide (Correia-de-Sá and Ribeiro, 1994) and brain-derived neurotrophic factor (BDNF) (Diógenes *et al*., 2004), and thus may also indirectly affect hippocampal neurotransmission. Moreover, adenosine receptors were described to form hetero-oligomers with other receptors. The A_1 receptor has been shown to form heteromers with dopamine D1 (Gines *et al*., 2000), purinergic $P2Y_1$ (Tonazzini *et al*., 2007; Yoshioka *et al*., 2001), glutamate mGluR1 (Ciruela *et al*., 2001) and A_{2A} (Ciruela *et al*., 2006) receptors. The A_{2A} receptor may form functional heteromers with mGluR5 (Ferre *et al*., 2002) and CB1 (Carriba *et al*., 2007) receptors. In the striatum, the A_{2A} receptor may heteromerize with the dopamine D2 receptor in the GABAergic neurons (reviewed in Svenningsson *et al*., 1999), forming a functional entity that has been explored as a potential therapeutic for the treatment of Parkinsons disease (Diaz-Cabiale *et al*., 2001; Ikeda *et al*., 2002; Ferré *et al*., 1991).

1.3.2. Endocanabinoid system

The research on the endocannabinoid system was boosted after the characterization of the chemical structure of Δ^9-tetrahydrocannabinol (Δ^9-THC), the main component of marijuana, and recently much importance was attributed to it due to the involvement in the control of metabolic functions on peripheral tissues (reviewed in Pagotto *et al*., 2006). The endocannabinoid system is constituted by cannabinoid receptors, endogenous cannabinoids (endocannabinoids), and enzymes that produce and degrade endocannabinoids. Although endocannabinoids can be transported by transporter proteins, they are very lipophilic and easily cross cellular membranes, so that their actions must be regulated at the level of synthesis and degradation (Piomelli, 2003). This system is involved in many physiological functions, and in the brain it has neuromodulation functions

(reviewed in Marsicano and Lutz, 2006), regulates certain processes of learning and memory (*e.g.* Marsicano *et al*., 2002a; Varvel and Lichtman, 2002; Wotjak, 2005) and may afford neuroprotection against injuries and degeneration (*e.g.* Jackson *et al*., 2005; Marsicano *et al*., 2002b, 2003; Panikashvili *et al*., 2001, 2005), indicating the possible use of endocannabinoid system as therapeutic target (Mackie, 2006).

Up to now, two cannabinoid receptors have been identified and molecularly characterised: the cannabinoid receptors type 1 (CB1 receptor) (Matsuda *et al*., 1990) and type 2 (CB2 receptor) (Munro *et al*., 1993). Pharmacological studies suggest the existence of other cannabinoid receptors (Köfalvi, 2008) but they were not cloned yet. CB1 receptors, which are considered the most abundant metabotropic receptors in the brain, are activated by Δ^9-THC, the main psychoactive constituent of marijuana, as well as by certain endocannabinoids such as 2-arachidonoylglycerol (2-AG) and anandamide (see Irving *et al*., 2008). While the CB1 receptor is present at much lower density in glia than neurons (*e.g.* Molina-Holgado *et al*., 2002; Ramirez *et al*., 2005), the brain CB2 receptor is thought to mainly mediate glial functions, in particular controlling immune responses. However, they were also suggested to occur in neuronal cells (van Sickle *et al*., 2005). Both CB1 and CB2 receptors can modulate multiple second messenger effectors depending on the cell type or experimental conditions but generally couple to inhibitory $G_{i/o}$ proteins and its activation will then inhibit adenilate cyclases, depleting intracellular cAMP levels and inactivating the protein kinase A, and stimulate MAPK pathway (Irving *et al*., 2008). These receptors are also able to modulate phosphoinositide 3-kinases, glycogen synthase kinase 3 β, and nitric oxide synthase activities, through which they afford neuroprotection (Campbell and Downer, 2008).

The CB1 receptor is particularly highly abundant in the human and the rodent hippocampus (Katona *et al*., 1999, 2000; Degroot *et al*., 2006) that is known to be a crucial area involved in learning and memory processes (Agranoff *et al*., 1999). The prominent pre-synaptic localisation of CB1 receptors and their capacity of inhibiting Ca^{2+} and activate K^+ channels suggest a role in modulating neurotransmission and neuronal excitability (for review see Gerdeman and Lovinger 2003). In fact, activation of hippocampal CB1 receptors reduces neurotransmitter release, namely the release of GABA (Katona *et al*., 1999, 2000), glutamate (Kawamura *et al*., 2006), dopamine and acetylcholine (Degroot *et al*., 2006), which will be reflected on the control of cognition and memory consolidation (for review see Hampson and Deadwyler, 1999). The inhibition of synaptic transmission can be transient, occurring by depolarization-induced suppression of inhibition or excitation that relies on endocannabinoid production after intracellular Ca^{2+} increase, or it can result on modulation of long-term depression (LTD) that is a synaptic plasticity form that can occur from hours to weeks (Gerdeman and Lovinger 2003).

CB1 receptors may occur in different splice variants or isoforms and homodimerize, generating functional diversity (Irving *et al*., 2008). Furthermore, CB1 receptors might form functional heterodimers with different receptors, such as with dopamine D2 receptors (Kearn *et al*., 2005), adenosine A_1 receptors (Carriba *et al*., 2007), type 1 orexin receptors (Hilairet *et al*., 2003) and 5-HT serotonin receptors (Devlin and Christopoulos, 2002).

1.3.3. Neuroprotection by modulation systems

The CNS has mechanisms to protect its cells, namely neurons, from degeneration upon injury. Stressful conditions, for example ischemia, induce adenosine release to the extracellular space, which acts predominantly as a neuroprotective factor (Fredhom *et al*., 2005). Manipulations of extracellular adenosine levels with pharmacological or genetic tools were observed to control the degree of injury upon noxious stimuli, suggesting an important role of adenosine in neuroprotection (Andine *et al*., 1990; Park and Rudolphi, 1994; Tatlisumak *et al*., 1998; Pignataro *et al*., 2007). In fact, many effects of adenosine in the CNS are compatible with neuroprotective properties, for example the ability to decrease excitatory amino acid release, hyperpolarize neurons, restrain the activation of *N*-methyl-D-aspartate (NMDA) receptors, limit calcium influx, inhibit free radical formation, and exert other modulatory effects in astrocytes and microglia (de Mendonça *et al*., 2000), most of these effects being mediated by A_1 receptor activation (Cunha, 2001). Corroborating this hypothesis, A_1 receptor agonists decreased injury whereas A_1 receptor antagonists aggravated damage in adult animals (de Mendonça *et al*., 2000). A_1 receptor activation is protective against brain ischemia in adult animals (*e.g.* Rudolphi *et al*., 1992a, 1992b; von Lubitz *et al*., 1994a, 1994b, 1995), and in excitotoxicity models induced by kainate or quinolinic acid (MacGregor *et al*., 1993, 1997), or by 3-nitopropionic acid (Blum *et al*., 2002). A_1 receptor activation in microglia cells also attenuates neuroinflammation and demyelination in an animal model of multiple sclerosis (Tsutsui *et al*., 2004).

Oppositely, under some circumstances adenosine may contribute to neurotoxicity (de Mendonça *et al*., 2000), caused by activation of other adenosine receptors, namely the A_{2A} receptor (reviewed by Fredholm *et al*., 2005). Despite its low abundance in areas of the CNS others than the basal ganglia (Cunha, 2001), pharmacological or genetic blockade of A_{2A} receptors results in a decrease of the injured cortical tissue area after cerebral-induced ischemia in rodents (*e.g.* Monopoli *et al*., 1998; Chen *et al*., 1999). Blocking A_{2A} receptors also proved efficacious in other models of

neurodegeneration (*e.g.* Chen *et al*., 2001; Ikeda *et al*., 2002; Popoli *et al*., 2002), suggesting that this might be a general neuroprotective strategy.

Compared to the A_1 and the A_{2A} receptor much less is known about the participation of the A_{2B} and the A_3 receptor activation concerning neuroprotection, but the A_3 receptor activation was suggested to be neuroprotective against ischemia and hypoxia (Chen *et al*., 2006; Von Lubitz *et al*., 1994c; Fedorova *et al*., 2003).

Extracellular ATP is used as a danger signal in the CNS, and was suggested to control neurodegeneration. ATP can activate $P2X_7$ receptors in astrocytes to release glutamate and GABA, and can also regulate the excitability of neurons in certain pathological conditions. The interference with the ATP-induced excitatory responses may provide neuroprotection and possible therapeutic consequences (Majumder *et al*., 2007). $P2X_7$ receptors mediated neuroprotection may also be related to control of microglia reactivity (Melani *et al*., 2006; Choi *et al*., 2007; Yanagisawa *et al*., 2008). Pharmacological blockade or genetic deletion of $P2Y_1$ receptors prevented memory impairment, as well as hippocampal synaptotoxicity, dendritic atrophy and neuronal dead caused by glutamate excitotoxicity and amyloid-β, suggesting that $P2Y_1$ receptor blockade can be protective upon Alzheimer's disease (Cunha *et al*., 2006a).

Evidence accumulated over the last few years indicates that the endocannabinoid system is potentially useful to reduce the effects of neurodegeneration (Campbell and Downer, 2008). In fact, neuronal damage can increase the production of endocannabinoids (Stella *et al*., 1997; Marsicano *et al*., 2003), and cells lacking CB1 receptors are more vulnerable to damage (Marsicano *et al*., 2003). Cannabinoid receptors may be useful targets for the management of neurodegeneration for example in Alzheimer's disease (Campbell and Gowran, 2007), multiple sclerosis (*e.g.* Baker *et al*., 2007), Hungtinton's disease (*e.g.* Lastres-Becker *et al*., 2003), or ischemia (*e.g.* Louw *et al*., 2000), through mechanisms that involve the control of excytotoxicity, calcium influx, oxidative stress, neuroinflamation, expression of transcription factors and neurotrophins, and other events (Campbell and Downer, 2008). CB1 receptor activation can also promote adult hippocampal neurogenesis (Jiang *et al*., 2005) and regulate interneuron migration and specification (Berghuis *et al*., 2005), which could counteract impairment of hippocampal neurogenesis in neurodegenerative pathologies like diabetes (Beauquis *et al*., 2006; Stranahan *et al*., 2008).

2. Aim

The fundamental purpose of this doctoral research was to evaluate the existence of molecular and metabolic alterations in the hippocampus of animal models of diabetes that could contribute to learning and memory impairment, and identify if such alterations could be prevented or corrected by manipulating modulation systems in order to try to overcome the cognitive deficits. To accomplish these main goals, the following tasks were established:

1. Identification of neuromodulation systems able to control intermediary metabolism in the hippocampus, since learning and memory processes are synaptic events and diabetes is a metabolic disease.
2. Understand the effect of diabetes on hippocampal neuromodulation systems, which could control not only synaptic phenomena but also metabolic events.
3. Investigate hippocampal alterations induced by diabetes at molecular, metabolic and behavioural levels.
4. Test the use of caffeine as a mean for prevention or amelioration of diabetes-induced hippocampal alterations and cognitive deficits.

The experimental work performed to accomplish the four objectives stated above is described in chapter 3, and resulted in the observations described in chapter 4, which is divided in different sections pertinently discussed: the first three sections match the first three objectives described above and the last section comprises the last 2 objectives since caffeine consumption studies also covered diabetes-induced alterations not studied before.

All the studies were conducted in the hippocampus for the following reasons. Elderly-associated mild memory and cognitive impairment and Alzheimer's disease are accompanied by atrophy of hippocampal formation (Convit *et al*., 1997; de la Monte, 1989; de Leon *et al*., 1997; Pennanen *et al*., 2004). When compared to healthy subjects, individuals with type 2 diabetes display deficits in hippocampal-based memory performance with preservation of other cognitive domains, and also show reduction of hippocampal volume but not other brain areas (Gold *et al*., 2007). Cognitive dysfunctions during diabetes are therefore associated with significant changes in the integrity of the hippocampus, a brain region considered to mediate memory formation in animals (Biessels *et al*., 2002; Trudeau *et al*., 2004), and electrophysiological analysis indicate that diabetes induces defects on LTP in hippocampal slices, a form of synaptic plasticity considered to reflect learning and memory processes in mammals (Biessels *et al*., 2002). These evidences drove us to perform the majority of the studies focusing on the hippocampus.

3. Materials and methods

3.1. Animals

All rats and mice used thorough the experimental work here described were handled according with the EU guidelines for the use of experimental animals (86/609/EEC), with particular care to minimize both animal suffering and the number of animals used in each study. Unless otherwise stated, the experiments were performed using male Wistar rats (8 weeks old, obtained from Harlan Ibérica, Barcelona, Spain), being animals sacrificed by decapitation under halothane anaesthesia.

3.1.1. Experimental models of diabetes

We used a well studied and validated model of type 1 diabetes *mellitus*, which is based on the administration of 2-deoxy-2-(3-(methyl-3-nitrosoureido)-D-glucopyranose (streptozotocin or STZ) that acts on β-cells impairing insulin secretion (Szkudelski, 2001; Rees and Alcolado, 2005). Male Wistar rats were used for the induction of type 1 diabetes, except for the *in vivo* NMR studies that were performed in male Sprague-Dawley rats (8-weeks old, obtained from Charles River Laboratoires, France). STZ (65 mg/kg, prepared in sodium citrate buffer 10 mM, pH 4.5) was administered by intra-peritoneal (i.p.) injection and induced sustained levels of blood glucose above 250 mg/dL after 3 days, as measured by the glucose oxidase method using a glucometer (OneTouch Ultra, LifeScan, Portugal). After injected, the rats were maintained with food and water *ad libitum* and all the analysis were carried out 7, 30 or 90 days after STZ treatment. Control rats were age-matched untreated or vehicle injected rats maintained in the same conditions. STZ is specifically taken by GLUT2 transporters which are particularly abundant in pancreatic β-cells (Junod *et al*., 1969), and is not known to cross the BBB having to be injected into the brain to cause direct effects in the brain parenchyma (*e.g.* Lester-Coll *et al*., 2006). Thus, it is assumed that the modifications caused by STZ mainly result from its ability to induce a type 1 diabetic state characterised by chronic hyperglycaemia (*e.g.* Rees and Alcolado, 2005).

As model for type 2 diabetes *mellitus* we used male Goto-Kakizaki (GK) rats (obtained from Taconic, Lille Skensved, Denmark) that spontaneously develop insulin resistance, *i.e.* non-insulin-dependent diabetes, without obesity. The GK rat was produced by repeated selective breeding of

originally non-diabetic Wistar rats (Goto and Kakizaki, 1981) and therefore we used age-matched Wistar-Hannover-Galas rats (also from Taconic) as controls for this model of diabetes.

For the study of obesity-induced type 2 diabetes, we used the recombinant congenic strain NONcNZO10/LtJ developed at The Jackson Laboratory (Bar Harbor, Maine, USA). The NONcNZO10/LtJ mouse strain develops type 2 diabetes characterized by maturity onset obesity, hyperglycaemia and insulin resistance, among other organ-specific diabetes phenotypes common to the human diabetes (Cho *et al*., 2007). Diabetic NONcNZO10/LtJ mice and control NON/LtJ mice were acquired from The Jackson Laboratory with 6 months of age and maintained in identical housing conditions, under an 11% fat diet (Labdiet 5K20, from International Product Supplies, UK).

3.1.2. Caffeine treatment

During the present studies, all the animals were housed at room temperature (20 to 25 ^{o}C) with food and water *ad libitum*.

Caffeine was administered in the drinking water at 1g/L. Due to polydipsia, STZ-induced diabetic rats received a variable caffeine dose (depending on fluid volume intake) to achieve caffeine consumption levels similar to controls. STZ-treated rats and respective controls were exposed to caffeine from 2 weeks before STZ administration until the day of the experiment. GK rats and respective controls received caffeine for 14 weeks starting on 8 weeks of age. NONcNZO10/LtJ and NON/LtJ mice were treated with caffeine from 7 to 11 months of age.

During treatment, weight and caffeine consumption were monitored each second day, and preprandial glycaemia was measured from tail blood, using a glucometer based on the glucose oxidase method (OneTouch Ultra, LifeScan, Portugal; or Ascencia Contour, Bayer, Switzerland). For insulin and caffeine quantification, blood samples were collected, allowed clotting, and the serum was separated by centrifugation.

3.2. Behavioural tasks

3.2.1. Open field

Exploratory behaviour and locomotor activity of mice were evaluated over 5 minutes in the dark, using a squared open field arena, being the animals placed in the central area of the arena. For

mice, the arena measured 30x30 cm and 25 cm high, and was divided in 9 squares of 10x10 cm. For rats, the arena was 34x34 cm and 30 cm high, and was divided in 4 squares of 17x17 cm. The number of crossings of these squares and the number of rearing movements with forepaws were quantified as horizontal and vertical activities, respectively. Rearing with the forepaws pressed against the walls was not considered.

3.2.2. Y-maze

The Y-maze is a gross test for spatial memory (*e.g*. Lalonde, 2002; Myhrer, 2003). It tests if the animal remembers the arm it has just explored and will therefore enter one of the other arms of the maze. This spontaneous alternation was observed in a Y-maze constructed in black Plexiglas, with three arms converging to an equal angle. For mice, each arm was 30 cm long, 5 cm wide and 25 cm height. For rats, the arms measured 35 cm long, 9 cm wide and 30 cm height. The animals were placed at the bottom of one arm in the Y-maze and allowed to explore freely all three arms for a single 8 minute session in the dark. The measured spontaneous alternation behaviour was used to access hippocampal-dependent spatial memory (*e.g*. Lalonde, 2002). If the mouse remembers the arm it has just explored, will therefore enter one of the other arms of the maze. Complete spontaneous alternation was defined as successive entries into the three arms and expressed as fraction of the possible alternations in the respective test. Additionally to the open field test, the number of entries in the arms of the maze also allowed to access locomotor activity and exploratory behaviour of the rodents in test.

3.3. Biological preparations

3.3.1. Nerve terminal preparations (synaptosomes)

Modulation systems are able to fine-tune basic cell functions to maintain cellular homeostasis, and synaptic events to regulate neurotransmission. To study diabetes-induced synaptic alterations, we used purified nerve terminals, *i.e.* synaptosomes (Cunha, 1998). The homogenization of nervous tissue allows separating the nerve terminal from the respective axon and, once separated from the axon, the membrane of the nerve terminal re-seals forming isolated synaptosomes, which are free of their integration in the neuronal networks (Gray and Whittaker,

1962). Synaptosomes are biochemically and metabolically autonomous (Marchbanks, 1967) and maintain viable neurotransmission systems (Scott and Nicholls, 1980), being useful for studies of bioenergetics or neurotransmitter release, as well as their modulation. Due to the low contamination with glial components the synaptosomal preparation can also be used to study the presence and density of synaptic proteins (Cunha, 1998).

3.3.1.1. Nerve terminals purified by 45% Percoll gradient

For the generality of the experiments, hippocampal and cortical nerve terminals were prepared using a protocol previously described (Lopes *et al*., 2002). After decapitation under halothane anaesthesia, the brain was rapidly removed and the hippocampus and/or cortex were dissected. The brain tissue samples from one rat or mouse was homogenized at 4 ºC in sucrose-HEPES buffer, containing 0.32 M sucrose, 1 mM EDTA, 10 mM HEPES, 1 mg/mL bovine serum albumin (BSA), pH 7.4. The resulting homogenate was centrifuged at 3,000 *g* for 10 min at 4 ºC, the supernatant collected and centrifuged at 14,000 *g* for 12 min at 4 ºC. The pellet was re-suspended in 1 mL of a 45% (v/v) Percoll solution made up in Krebs-HEPES solution (composition in mM: 140 NaCl, 5 KCl, 10 HEPES, 1 EDTA, 5 glucose, pH 7.4). After centrifugation at 21,000 *g* for 2 min at 4 ºC, the top layer (synaptosomal fraction) was removed, washed and re-suspended in Krebs-HEPES solution. Protein content was quantified by the bicinchoninic acid method (Smith *et al*., 1985) using a kit from Pierce Biotechnology (Rockford, USA).

3.3.1.2. Nerve terminals purified by discontinuous Percoll gradient

For immunochemical analysis of mouse hippocampal nerve terminals, synaptosomes were obtained through a discontinuous Percoll gradient as previously described (Dunkley *et al*., 1988; Rodrigues *et al*., 2005). Mice were decapitated under halothane anaesthesia and the hippocampi readily dissected and homogenized in a medium containing 0.25 M sucrose and 10 mM HEPES (pH 7.4) at 4 ºC. The homogenate was centrifuged at 2,000 *g* for 3 min at 4 ºC and the supernatant centrifuged again at 9,500 *g* for 13 min. Then, the pellets were re-suspended in 2 mL of 0.25 M sucrose and 10 mM HEPES (pH 7.4) and were placed onto 3 mL of Percoll discontinuous gradients containing 0.32 M sucrose, 1 mM EDTA, 0.25 mM dithiothreitol and 3, 10, or 23% (v/v) Percoll, pH 7.4. The gradients were centrifuged at 25,000 *g* for 11 min at 4 ºC. Synaptosomes were collected

between the 10 and 23% (v/v) Percoll phases and diluted in 15 mL of HEPES buffered medium (140 mM NaCl, 5 mM KCl, 5 mM $NaHCO_3$, 1.2 mM NaH_2PO_4, 1 mM $MgCl_2$, 10 mM glucose, and 10 mM HEPES, pH 7.4). After centrifugation at 22,000 *g* for 11 min at 4 ºC, the pellet constitutes the synaptosomal fraction.

3.3.2. Total membrane preparation

For total membrane preparation, the brain tissue was homogenized at 4 ºC in sucrose-HEPES buffer. The homogenate was centrifuged at 3,000 *g* for 10 min at 4 ºC. The supernatant was then re-suspended in a solution of 50 mM Tris and 10 mM $MgCl_2$ (pH 7.4), centrifuged at 28,000 *g* for 20 min at 4 ºC, and the resulting pellet re-suspended in a Krebs-HEPES solution. An aliquot of each membrane preparation was saved for protein quantification by the bicinchoninic acid method (Smith *et al*., 1985) using a commercial kit (Pierce Biotechnology, Rockford, USA).

3.3.3. Hippocampal slices - preparation and superfusion

The hippocampus, located near the thalamus deep in the temporal lobe (one in each hemisphere), plays a key role in some forms of learning and memory, especially in the processing of complex spatial and temporal patterns, and it is involved in many neurological disorders (Purves *et al*., 2004). It was divided into two regions (regio inferior and regio superior) by Ramon y Cajal in 1911, and later (in 1934) into four *cornu Ammonis* (CA) regions from CA1 to CA4, being CA1 and CA3 the biggest and the most clearly distinguished parts by Lorente de Nó (see El-Falougy and Benuska, 2006). In addition to CA regions, the hippocampal formation consists of the dentate gyrus, the subiculum and the entorhinal cortex. The neuronal organization of the hippocampus is well defined, with a main excitatory circuit that can be preserved in transversal slices (see Lopes da Silva and Arnolds, 1978). The well known cyto-architecture of the hippocampus makes it very suitable for physiological and pharmacological investigations isolated from the nervous system. The hippocampal slice preparation is also used because it constitutes an excellent electrophysiology model for learning and memory, due to the functional plasticity of its circuits. Acutely dissociated hippocampal slices were now used to study the modulation of intermediary metabolism.

The brain was rapidly removed and the isolated hippocampi were transversely cut in 400 µm slices using a McIlwain tissue chopper. Hippocampal slices were allowed to recover in a

modified Krebs solution (115 mM NaCl, 25 mM $NaHCO_3$, 3 mM KCl, 1.2 mM KH_2PO_4, 2 mM $CaCl_2$, 1.2 mM $MgSO_4$, 5.5 mM glucose and 2 mM sodium acetate, previously and continuously gassed with 95% O_2 and 5% CO_2 mixture, pH 7.4), at room temperature and during 45 minutes. Hippocampal slices were transferred to a submerged chamber and superfused (3 mL/min) with the same gassed solution at 37 ºC. After 60 minutes to allow recovery and stabilization (Fredholm *et al*., 1984), hippocampal slices were superfused with different experimental protocols that are detailed when necessary. For the study of intermediary metabolism, glucose and acetate from the perfusate were replaced by [U-^{13}C]glucose and [2-^{13}C]acetate (both from Isotec, Miamisburg, USA). In some experiments, slices were superfused in the presence of 4-aminopyridine (4AP; from Alomone Labs, Jerusalem, Israel) to allow intermittent burst-like stimulation (Tibbs *et al*., 1989). To challenge the slices with hypoxia, the superfusion solution was gassed with a gas mixture of 95% N_2 + 5% CO_2 (Gasin, Coimbra, Portugal). During superfusion, perfusate samples were collected, lyophilized and stored at 4 ºC for measurement of lactate production and release from hippocampal slices.

At the end of the superfusion protocol, hippocampal slices were transferred to liquid nitrogen and the water-soluble metabolites were extracted with 7% (v/v) perchloric acid (PCA). The grinded tissue mixed with PCA (300 µL for each hippocampus) was centrifuged at 21,000 *g* during 15 minutes, at 4 ºC. The supernatant was neutralized with KOH, lyophilised, and stored for high-performance liquid chromatography (HPLC) and/or NMR spectroscopy. The pellet from the extraction was re-dissolved in a 6 M urea solution containing 5% of sodium dodecyl sulphate, and the protein content was determined by the bicinchoninic acid method (Smith *et al*., 1985) using a kit from Pierce (Rockford, USA).

3.4. Western blot analysis

Western blot analysis was used for the determination of the density of proteins in synaptosomal and total membrane preparations. Each sample was diluted with five volumes of SDS-PAGE buffer containing 30% (v/v) glycerol, 0.6 M dithiothreitol, 10% (w/v) sodium dodecyl sulphate and 375 mM Tris-HCl pH 6.8, and boiled at 95 ºC for 5 min. These diluted samples were separated by SDS-PAGE (7.5% separation gel with a 4% concentrating gel in the top) under reducing conditions, together with pre-stained molecular weight markers (Biorad, USA), and then electro-transferred to polyvinylidene difluoride membranes (0.45 mm, from Amersham Biosciences, UK). After blocking for 1 h at room temperature with 5% milk in Tris-buffered saline (Tris 20 mM, NaCl 140 mM, pH 7.6), containing 0.1% Tween 20 (TBS-T), the membranes were incubated

overnight at 4 ºC with the primary antibodies against the respective proteins (Table 3.1). After three 15 min washing periods with TBS-T containing 0.5% milk, the membranes were incubated with the alkaline phosphatase-conjugated anti-rabbit IgG (Amersham Biosciences, Carnaxide, Portugal), anti-mouse IgG (Amersham Biosciences) or anti-goat IgG (Santa Cruz Biotechnology, Frilabo, Portugal) secondary antibody (dilution 1:10,000) in TBS-T containing 1% milk during 90 min at room temperature. After three 20 min-washes in TBS-T with 0.5% milk the membranes were incubated with enhanced chemi-fluorescent substrate (Amersham Biosciences), and then immunoreactivity was analysed with a VersaDoc 3000 system and the Quantity One software (Biorad, USA).

The membranes were then re-probed and tested for α-tubulin or β-actin immunoreactivity to confirm that similar amounts of protein were applied to the gels. Briefly, the membranes were incubated at room temperature for 30 min with 40% (v/v) methanol and 1 h with a stripping buffer [containing 0.1 M glycine, 0.1% (w/v) SDS, 1% (v/v) Tween 20, pH 2.2], and then blocked as previously described before incubation with mouse anti-α-tubulin or anti-β-actin antibodies (dilution 1:10,000) for 2 h at room temperature. The membranes were then washed, incubated with

Table 3.1. Primary antibodies used in Western blot analysis.

Primary antibodies	Supplier	Host	Dilution
A_1 receptor	Affinity Bioreagents	Rabbit	1:600
CB1 receptor	Kindly provided by Dr. Ken Mackie	Rabbit	1:500
$P2X_1$ receptor	Alomone Labs	Rabbit	1:500
$P2X_2$ receptor	Santa Cruz Biotechnology	Goat	1:500
$P2X_3$ receptor	Alomone Labs	Goat	1:1,000
$P2X_4$ receptor	Alomone Labs	Rabbit	1:500
$P2X_5$ receptor	Santa Cruz Biotechnology	Goat	1:200
$P2X_6$ receptor	Santa Cruz Biotechnology	Goat	1:200
$P2X_7$ receptor	Alomone Labs	Rabbit	1:5,000
$P2Y_1$ receptor	Santa Cruz Biotechnology	Goat	1:500
$P2Y_2$ receptor	Alomone Labs	Rabbit	1:500
$P2Y_4$ receptor	Alomone Labs	Rabbit	1:1,000
$P2Y_6$ receptor	Santa Cruz Biotechnology	Goat	1:500
$P2Y_{11}$ receptor	Zymed	Rabbit	1:500
β-actin	Sigma	Mouse	1:10,000
α-tubulin	Sigma	Mouse	1:10,000
Synaptophysin	Sigma	Mouse	1:10,000
SNAP-25	Sigma	Mouse	1:5,000
Syntaxin	Chemicon	Mouse	1:5,000
PSD-95	Chemicon	Mouse	1:20,000
MAP2	Santa Cruz Biotechnology	Rabbit	1:1,000
Vimentin	Sigma	Mouse	1:1,000
GFAP	Sigma	Rabbit	1:5,000

an anti-mouse IgG alkaline phosphatase-conjugated secondary antibody and analysed as described above.

3.5. Binding assay

Hippocampal (either total or synaptosomal) membranes were first incubated with 2 U/ml adenosine deaminase for 30 min at 37°C, to remove endogenous adenosine. The mixture was then centrifuged at 14,000 *g* for 10 min at 4°C and the pellets re-suspended in the incubation buffer, containing 50 mM Tris-HCl and 10 mM $MgCl_2$ (for [^{3}H]SCH 58261 experiments) or 2 mM $MgCl_2$ (for [^{3}H]DPCPX experiments) at pH 7.4. Binding of a saturating but selective concentration (10 nM) of the A_1 receptor antagonist [^{3}H]DPCPX (specific activity 109.0 Ci/mmol; from DuPont NEN, Anagene, Portugal) (Lopes *et al*., 2004) was for 2 hours at room temperature (23-35ºC) with 92-251 µg of protein in a final volume of 200 µl in the incubation solution containing 2 U/ml adenosine deaminase, as previously described (Rebola *et al*., 2003a). Binding of a saturating but selective concentration (6 nM) of the A_{2A} receptor antagonist [^{3}H]SCH 58261 (specific activity 77.0 Ci/mmol; prepared by Amersham, Buckinghamshire, UK) (Lopes *et al*., 2004) was for 1 h at room temperature with 92-251 µg of protein in a final volume of 200 µl in the incubation solution containing 4 U/ml adenosine deaminase, as previously described (Rebola *et al*., 2005a). Specific binding was determined by subtraction of the non-specific binding, which was measured in the presence of 1 µM 8-{4-[(2-aminoethyl)amino]carbonylmethyl-oxyphenyl}xanthine (XAC), a mixed A_1 and A_2 receptor antagonist. All binding assays were performed in duplicate. The binding reactions were stopped by vacuum filtration through glass fibre filters (GF/C filters, from Whatman) using a 24 wells Brandel harvester. The filters were then placed in scintillation vials and 4 ml of scintillation liquid (Ready Safe, Pharmacia-Portugal) added. Radioactivity was determined after at least 12 hours with a counting efficiency of 55-60%. To ensure an error lower than 5% of counts, the samples were counted for 10 min.

For CB1 receptors, radioligand binding assays were performed identically to a previous study (Thomas *et al*., 1998). Briefly, hippocampal (either total or nerve terminal-enriched) membranes were resuspended in the incubation buffer (50 mM Tris, 2 mM $MgCl_2$, 1 mM EGTA, pH 7.4). A saturation curve was constructed using 5 different concentrations (0.25–10 nM) of the CB1 receptor antagonist [^{3}H]SR141716A (Amersham, specific activity 42.0 Ci/mmol). Binding was carried out for 1 h at room temperature (23–25 °C) with 32–51 µg of protein in a final volume of 200 µl of the incubation buffer. Specific binding was determined by subtraction of the non-specific

binding, which was measured in the presence of 10 μM *N*-(piperidin-1-yl)-5-(4-iodophenyl)-1-(2,4-dichlorophenyl)-4-methyl-1H-pyrazole-3-carboxamide (AM251), another selective CB1 receptor antagonist. All binding assays were performed in duplicate. The binding reactions were stopped by rapid vacuum filtration through glass fibre filters (GF/C filters) using a 24-well Brandel harvester, followed by washing with 5 ml of incubation buffer containing 0.5% (w/v) BSA. The filters were then placed in scintillation vials with 4 ml of scintillation liquid (Packard Ultima Gold). The specific binding derived from these saturation experiments was fitted by non-linear regression to a one binding site equation, using the Raphson–Newton method, performed with a commercial software (GraphPad Prism), to determine the binding parameters (dissociation constant K_D, and maximal number of binding sites B_{max}).

3.6. Real-time PCR

The rat brain was rapidly removed and the hippocampus and cortex isolated and immediately frozen in liquid N_2. Total RNA was extracted from these tissue samples with MagNA Lyser Instrument and MagNA Pure Compact RNA Isolation kit (Roche, Portugal) according to the manufacturer's instructions. Reverse transcription for first-strand cDNA synthesis from each sample was performed using random hexamer primer with the Transcriptor First Strand cDNA Synthesis kit (Roche) according to manufacturer's instructions. Resulting cDNAs were used as template for real-time PCR, which was carried out on LightCycler instrument using the FastStart DNA Master SYBR Green I kit (Roche) and the primers (Tib MolBiol, Germany) listed in Table 3.2.

Quantification of mRNA in the samples was carried out on the basis of standard curves run simultaneously. The cDNA standards for the calibration curve were generated by conventional PCR amplification (Table 3.3). The PCR products were run in a 3% agarose gel electrophoresis to verify

Table 3.2. Primers used in the real-time PCR analysis.

	Acession number	Primer sequence		Expected product size (bp)
CB1 receptor (Hansson *et al*., 2006)	NM_012784	F	5′- AGA CCT CCT CTA CGT GGG CTC G -3′	314
		R	5′- GTA CAG CGA TGG CCA GCT GCT G -3′	
β-actin (Peinnequin *et al*., 2004)	V01217	F	5′- AAG TCC CTC ACC CTC CCA AAA G -3′	97
		R	5′- AAG CAA TGC TGT CAC CTT CCC -3′	
A_1 receptor (Grenz *et al*., 2006)	NM_017155	F	5′- CTC CAT TCT GGC TCT GCT CG -3′	207
		R	5′- ACA CTG CCG TTG GCT CTC C -3′	
A_{2A} receptor (Pawelczyk *et al*., 2005)	NM_053294	F	5′ CAT CTT CTC CCA CAG CAA CTC 3′	420
		R	5′ GGG GCA AAC TCT GAA GAC CAT G 3′	

fragment size and the absence of other contaminant fragments, quantified by absorbance at 260 nm, and serially diluted to produce the standard curve (10^0 to 10^8 copies/μL). Each real-time PCR reaction was run in triplicate and contained 2 μL of cDNA template, 0.3 μM each primer, and 3 or 3.5 mM $MgCl_2$ (see Table 3.3), in a reaction volume of 20 μL. Cycling parameters are described in Table 3.3. Melting curves analysis was performed to ensure that only a single product was amplified. The expression of mRNA was calculated relative to β-actin mRNA expression.

Table 3.3. Cycling parameters for real-time and conventional PCR analysis.

Real time PCR

	$MgCl_2$ (mM)	Initial denaturation	Amplification				Melting curve analysis
			Denaturation	Anealing	Extension	Cycles	
CB1 receptor	3	95 °C, 10 min	95 °C, 10 s	62 °C, 10 s	72 °C, 14 s	40	
β-actin	3.5	95 °C, 10 min	95 °C, 10 s	61 °C, 5 s	72 °C, 4 s	45	
A_1 receptor	3	95 °C, 10 min	95 °C, 10 s	64 °C, 10 s	72 °C, 8 s	45	
A_{2A} receptor	3	95 °C, 30 s	95 °C, 1 s	64 °C, 5 s	72 °C, 21 s	40	

Conventional PCR

	$MgCl_2$ (mM)	Initial denaturation	Amplification				Elongation
			Denaturation	Anealing	Extension	Cycles	
CB1 receptor	1.5	95 °C, 5 min	95 °C, 1 min	59 °C, 1 min	72 °C, 1 min	45	72 °C, 4 min
β-actin				56 °C, 1 min			
A_1 receptor				64 °C, 1 min			
A_{2A} receptor				64 °C, 30 s			

3.7. Immunocytochemical analysis in hippocampal nerve terminals

Hippocampal synaptosomes purified by discontinuous Percoll gradient were resuspended in HEPES buffered medium and placed onto poly-L-lisine-coated cover-slips, fixed with 4% paraformaldehyde for 15 min and washed twice with phosphate-buffered saline (PBS) medium (140 mM NaCl, 3 mM KCl, 20 mM NaH_2PO_4, 15 mM KH_2PO_4, pH 7.4). The synaptosomes were permeabilized in PBS containing 0.2% Triton X-100 for 10 min and then blocked for 1 h in PBS with 3% (w/v) BSA and 5% (v/v) normal rat serum. The synaptosomes were then washed twice with PBS and incubated for 1 h at room temperature with the following combinations of antibodies (in PBS with 3% BSA): mouse anti-synaptophysin (dilution 1:200; from Sigma), rabbit anti-A_1R (1:200; from Affinity Bioreagents) or goat anti-A_{2A}R (1:200; from Santa Cruz Biotechnology), and guinea pig anti-vGAT (1:1,000; from Calbiochem) or guinea pig anti-vGluT1 (1:1,000; from Chemicon) plus guinea pig anti-vGluT2 (1:1,000; from Chemicon). It should be emphasized that the antibodies anti-vesicular glutamate transporters type 1 and type 2 (anti-vGluT1 and anti-vGluT2) were applied

together to identify the population of hippocampal glutamatergic nerve terminals, being hereafter designated as vGluT1/2. The synaptosomes were then washed three times with PBS with 3% (w/v) BSA and incubated for 1 h at room temperature with secondary antibodies (in PBS with 3% BSA; dilution 1:200): goat anti-mouse, donkey anti-rabbit or donkey anti-goat conjugated with AlexaFluor-488 (Invitogen, Barceona, Spain), and goat anti-guinea pig conjugated with AlexaFluor-598 (Invitogen). After washing and mounting onto slides with Prolong Gold Antifading (Invitrogen), the preparations were visualized in a Zeiss Axioscope fluorescence microscope (Hitec, Lisbon, Portugal).

3.8. Mouse brain histochemistry

The preparation of brain sections was carried out as previously described (Cunha *et al*., 2006). Mice were anesthetized with pentobarbital (60 mg/kg), the heart was exposed and, after clamping the descending aorta, a catheter was inserted in the ascending aorta. The animal was then perfused with 20 mL of saline [0.9% (w/v) NaCl solution] while opening the right atria to allow the outflow of the perfusate. Mice were then perfused with 20 mL of 4% (w/v) paraformaldehyde prepared in saline solution. After its fixation, the brain was removed, maintained for 12 h in the same paraformaldehyde solution and subsequently for 48 h in PBS containing 30% sucrose at 4 °C. The brain was then frozen and sliced in 20 µm coronal sections using a cryostat (Leica Microsistemas, Lisboa, Portugal). The sections were stored in PBS containing 0.01% sodium azide at 4 °C until mounting in slides coated with 2% gelatine with chromium and potassium sulphate. After drying at room temperature, the mounted sections were stored at -20 °C. Consecutive sections from each animal were used to carry out the histochemical procedures described below. The resulting brain slices were then visualized and examined under a Zeiss Axioscope fluorescence microscope (Hitec, Lisbon, Portugal). Microscope photographs were processed and analysed with the software ImageJ 1.37v (National Institutes of Health, USA).

Cresyl violet staining of Nissl bodies: The general neuronal morphology in hippocampal sections was evaluated by using a Cresyl violet staining of Nissl bodies. Briefly, the sections were dried at room temperature and stained for 10 min with 0.5% (w/v) Cresyl violet solution prepared in acetate buffer (200 mM, pH 4). The sections were then rinsed twice with acetate buffer, dehydrated by rinsing sequentially in ethanol ethanol solutions [75%, 95% and 100%(v/v)], and cleared in xylene (during 2 to 3 minutes) before being mounted with H-5000 Vectamount medium

(Vecta Laboratories, Burlingame, CA, USA). Nissl staining was evaluated qualitatively by particular inspection of the pyramidal cell layer in optical microscopy photographs.

FluoroJade-C staining: To evaluate recent neuronal dead and degeneration, sections were stained with FluoroJade-C (Schmued *et al*., 2005). The brain sections were immersed in 0.1% (w/v) NaOH in 80% (v/v) ethanol for 5 min, rinsed for 2 min in 70% (v/v) ethanol and then for 2 min in distilled water. The slides were then transferred to a solution of 0.06% (w/v) potassium permanganate for 10 min and were gently shaken on a rotating platform. The slides were then rinsed for 2 min in distilled water and incubated with a 10 ppm FluoroJade solution in 0.1% (v/v) acetate, being gently shaken for 10 min. The sections were then rinsed three times for 1 min with distilled water, dried and immersed in xylene and then cover slipped with DPX Mountant medium (from Sigma).

Nerve terminal immunohistochemistry: The detection of nerve terminals was carried out as previously described (Cunha *et al*., 2006) using an immunohistochemical detection of synaptophysin, a protein located in synaptic vesicles. Mouse brain sections were first rinsed for 30 minutes in Tris buffer saline (TBS: 0.05 M Tris base buffer containing 150 mM of NaCl, pH 7.4) at room temperature. After permeabilization for 1 h in TBS containing 1% (v/v) Triton X-100, the brain sections were blocked with 10% (v/v) calf serum in TBS during 1 h, and then incubated for 24 h at 4 °C in the presence of the mouse anti-synaptophysin antibody (dilution 1:500, from Sigma), prepared in TBS containing 10% (v/v) calf serum. Sections were rinsed three times for 15 min in TBS and subsequently incubated for 2 h at room temperature, in the dark, with goat anti-mouse secondary antibody conjugated with the fluorophore AlexaFluor 488 (dilution 1:200; from Invitrogen), prepared in TBS containing 10% (v/v) calf serum. After rinsing three times for 15 min in TBS, the sections were dehydrated in ethanol and passed through xylol before mounting with Vectashield H-1400 mounting medium (Vecta Laboratories). The intensity of synaptophysin immunoreactivity in the hippocampus was quantified in the acquired photographs with the software ImageJ 1.37v. For this quantification, the total intensity was measured in different regions of the pictures from CA1, CA3 and DG, excluding the nuclei of the pyramidal cell layer. Immunoreactivity was then expressed as percentage of the average for the corresponding pictures of control animals.

Astrocyte immunodetection: The population of astrocytes in the hippocampus was evaluated by immunohistochemical detection of glial fibrillary acidic protein (GFAP). The brain sections were permeabilized and blocked as described above and then incubated overnight with Cy3-tagged anti-GFAP antibody (dilution 1:1000, from Sigma) at 4 ^{o}C. After rinsing three times for 15 min in TBS, the sections were dehydrated and cleared in xylol before mounting with Vectashield H-1400.

Dendritic immunodetection: Dendritic processes were evaluated by detection of microtubule-associated protein 2 (MAP2) immunoreactivity. The brain sections were permeabilized and blocked as described above and then incubated overnight with rabbit anti-MAP-2 antibody (dilution 1:500, from Santa Cruz Biotechnology) at 4 ^{o}C. After rinsing three times for 15 min in TBS, slides were incubated with donkey anti-rabbit secondary antibody conjugated with the fluorophore AlexaFluor-488 (dilution 1:200), rinsed again, dehydrated and cleared in xylol before mounting.

3.9. ATP quantification in the cerebrospinal fluid

Rats were anesthetized with sodium thiopental (40 mg/kg, i.p.) and the cerebrospinal fluid (CSF) was drawn (40-60 µL per rat) by direct puncture of the cisterna magna with a tuberculin syringe (27 gauge x 13 mm length), and immediately stored at -80 ^{o}C until ATP quantification. These samples and standard solutions of ATP (10^{-9} to 10^{-12} M) were placed in wells of a white 96-well microplate to determine ATP levels using the luciferin-luciferase luminometric assay (Cunha *et al*., 1996). Briefly, 50 µL of luciferin-luciferase solution (FLAAM kit from Sigma, re-suspended in 5 mL) were added to 25 µL of sample (diluted 1/5) and the luminescence produced was quantified in an LMax II384 luminometer (Molecular Devices, Union City, USA).

3.10. ATP release from hippocampal nerve terminals

The measurement of ATP release from synaptosomes was adapted from a previous study (Cunha *et al*., 1996). Synaptosomes were re-suspended in calcium containing Krebs-HEPES solution (composition in mM: 124 NaCl, 3 KCl, 1.25 NaH_2PO_4, 1 $MgSO_4$, 2 $CaCl_2$, 26 HEPES, 10 glucose, pH 7.4). Aliquots of 240 µL of synaptosomes (0.21-0.36 mg of protein) were placed in wells of a white 96-well microplate to which 50 µL of luciferin-luciferase solution (FLAAM kit from Sigma, prepared in 5 mL of water) were added. The mixture was placed in the luminometer at 37 ^{o}C and the electrical signal generated by the photomultiplier recorded. After obtaining a stable baseline, 10 µL of Krebs/HEPES solution with concentrated KCl (to attain a final concentration of 20 mM) were automatically injected and the plate shacked for 2 s. The measurement of the photomultiplier signal restarted after 4 s, and the variation in signal recorded was used to estimate the evoked release of ATP by interpolation in a calibration curve of ATP standards. Mechanical stimulation of the nerve

terminals also triggered an outflow of ATP, but this displayed a slower time course and had amplitude considerably lower than the K^+-evoked release of ATP.

3.11. ATP catabolism in hippocampal nerve terminals

Synaptosomes (0.32 to 0.43 mg of protein) were re-suspended in 500 µL of Krebs-HEPES solution and incubated at 37 ºC for at least 5 min of stabilization. At time zero, ATP (made up in Krebs-HEPES solution) was added to a final concentration of 10 µM and samples (75 µL) were collected every minute during the next 5 min of incubation. Each sample was spun down, and the supernatant immediately frozen in liquid N_2 and then at -80 ºC until HPLC analysis of adenine nucleotides as described bellow.

3.12. Analysis of adenine nucleotides by HPLC

Separation of adenine nucleotides was performed at room temperature as previously described (Cunha *et al*., 2001), using a reverse-phase column [LiChroCART 125x4mm LiChrospher 100 RP-18 (5 µm) cartridge fitted into a ManuCART holder (Merck Darmstadt, Germany)], using a GOLDTM system (Beckman, UK) equipped with a UV detector set at 254 nm. The eluent was a 100 mM KH_2PO_4 (BDH, UK) solution with 1.2% methanol (from Riedel-de Haën, Sigma-Aldrich, Sintra Portugal), at pH 6.5, with a flow rate of 1.2 mL/min. The identification of the peaks was performed by comparison of relative retention times with standards and their quantification achieved by calculating the peak areas then converted to concentration values by calibration with known standards (0.1-100 µM).

Adenylate energy charge (EC) of the tissue was determined with nucleotide concentrations and the following equation (Atkinson, 1968): EC = ([ATP] + ½[ADP]) / ([AMP] + [ADP] + [ATP]).

3.13. High-resolution NMR spectroscopy

Lyophilised extracts were re-dissolved in 600 µL ^2H_2O and the p^{2}H was re-adjusted to 7.0 with ^{2}HCl or NaO^{2}H solutions (both from Sigma-Aldrich, Sintra, Portugal). Sodium fumarate (2 mM) was used as an internal standard for quantification by ^{1}H NMR spectroscopy. NMR spectra were acquired at 25 ºC on an 11.7 T Varian Unity-500 spectrometer (Varian, Palo Alto, USA), using a

5 mm broadband probe. Solvent-suppressed ^{1}H NMR spectra were acquired with 8 kHz sweep width, using 14 s delay for allowing total proton relaxation, 3 s water pre-saturation, 70º pulse angle, 3 s acquisition time, and at least 200 scans per tissue extract (or 10 scans for perfusate samples). Proton decoupled ^{13}C NMR spectra were acquired using 30 kHz sweep width, 45º pulse angle, 1.5 s acquisition time and a 1.5 s relaxation delay. The total repetition time (3 s) allowed full relaxation of the aliphatic carbons. To achieve adequate signal to noise ratio, the number of scans recorded was at least 10,000. Proton decoupled ^{31}P NMR spectra were acquired with a 32 kHz sweep width, 45º pulse angle and a 2.2 s acquisition time, followed by 3 s delay. For each ^{31}P spectrum at least 6,000 scans were acquired. In both ^{13}C and ^{31}P NMR spectra, ^{1}H broadband decoupling was achieved using a WALTZ-16 decoupling sequence.

All the acquired spectra were processed using the NUTS software (Acorn NMR, Fremont, USA). Free induction decays were baseline corrected, zero-filled and multiplied by an exponential function (0.5 Hz for ^{1}H and ^{13}C spectra; 10 Hz for ^{31}P spectra), prior to Fourier transformation. The areas of relevant signals in the spectra were quantified by curve fitting. The concentrations of metabolites were determined by measuring the peak areas in the ^{1}H NMR spectra, using sodium fumarate as internal standard, and normalized to total creatine content. The ^{13}C isotopomer populations were determined from the analysis of ^{13}C NMR spectra by deconvolution of the multiplets present in the resonance of each carbon, and each multiplet area was reported as a fraction of the total area for that specific carbon resonance. PCre/ATP and ATP/ADP ratios were calculated from the ^{31}P NMR spectra, averaging the signal areas of the 3 ATP and the 2 ADP resonances.

3.13.1. Metabolic modelling of ^{13}C NMR spectra

Multiplets from glutamate (C2, C3 and C4), GABA (C2, C3) and aspartate (C2 and C3) resonances in the ^{13}C NMR spectra were used in the estimation of relative fluxes feeding the TCA cycle using tcaCALC[1] (Malloy *et al*., 1988; Fonseca *et al*., 2005). Glutamate and GABA isotopomer data were used in separated fittings and in combination with aspartate isotopomer data. The model used to fit the ^{13}C data is presented in Figure 3.1 and includes the following parameters: fraction of acetyl-CoA derived from [2-^{13}C]acetate (Fc2); fraction of acetyl-CoA derived from the oxidation of

[1] The metabolic program tcaCALC was kindly provided by Professor Mark Jeffrey from the Rogers Magnetic Resonance Center at the University of Texas Southwestern Medical Center. It consists in an input-output metabolic model which uses both ^{13}C fractional enrichment and ^{13}C isotopomer data to determine acetyl-CoA fractional enrichments (Fc0, Fc1, Fc2 and Fc12) and fluxes associated with the tricarboxylic acid (TCA) cycle including fluxes through pyruvate dehydrogenase (PDH), pyruvate carboxylase (PC), phosphoenolpyruvate carboxykinase (PEPCK) (Malloy *et al*., 1988).

[U-^{13}C]glucose (Fc12) via pyruvate dehydrogenase (PDH); fraction of acetyl-CoA formed from unlabelled precursors (Fc0) through acyl-CoA synthetase (ACS); combined anaplerotic flux from all sources (Y); flux through pyruvate carboxylase (PC); flux through lactate dehydrogenase (LDH). The estimated flux parameters are relative to the TCA cycle flux, arbitrarily set to 1.

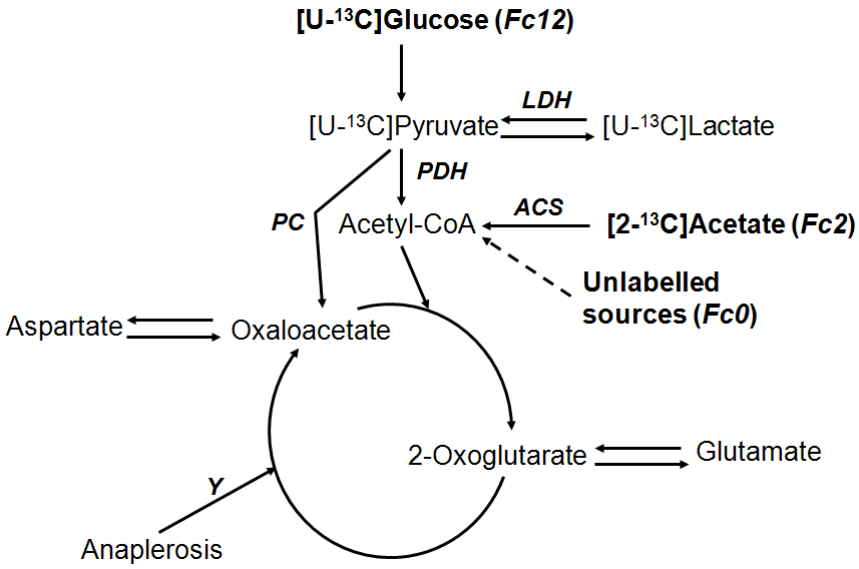

Figure 3.1. Metabolic model used to fit the ^{13}C isotopomer data in the tcaCALC program. Fc0 corresponds to the contribution of unlabeled acetyl-CoA from unlabeled endogenous substrates; Fc2 and Fc12 show the fraction of acetyl-CoA labeled in C2 (originated from [2-^{13}C]acetate) and both C1 and C2 (originated from [U-^{13}C]glucose), respectively. Fluxes depicted in these model: PDH, pyruvate dehydrogenase; ACS, acyl-CoA synthetase; Y, combined anaplerotic flux; PC, pyruvate carboxylase; LDH lactate dehydrogenase.

3.14. Brain neurochemistry by *in vivo* localised ^{1}H NMR spectroscopy

3.14.1. Animal preparation

Animals were anaesthetized using 2% isoflurane (Attane, Minrad, USA) in oxygen gas for surgery (PanGas, Ecublens, Switzerland), and then intubated and ventilated with a pressure-driven ventilator (MRI-1, CWE incorporated, PA, USA). Catheters were inserted into the femoral artery for monitoring blood gases, glucose, lactate and arterial blood pressure, and into the femoral vein for intravenous (i.v.) infusion of α-chloralose (Acros Organics, Geel, Belgium), D-glucose (Sigma-Aldrich, Switzerland) and insulin (Humulin Normal, Eli Lilly, Switzerland). After surgery, a blood sample (200 µL) was collected and the serum was separated by centrifugation and stored for quantification of insulin and caffeine. Animals were placed in a home-built holder with a bite bar and two ear inserts to provide a fixed position of the skull, which ensures stability of the

experimental set-up for extended measuring times. Body temperature was maintained around 37.5 °C with a warm water circulation system based on a feedback obtained from a rectal temperature probe. Arterial blood pressure, heart rate and respiratory rate were continuously monitored with an animal monitoring system (SA Instruments, NY, USA). Before inserting the animal in the bore of the magnet, the anaesthesia was switched to α-chloralose (i.v. bolus of 80 mg/kg and infusion of 25 mg/kg/h). Insulin (0.5 U/mL solution) and D-glucose [20% (w/v) solution] were infused at a rate adjusted based on the concomitantly measured arterial plasma glucose concentrations to achieve stable targeted glycaemia levels. NMR measurements were performed after each glucose level had been stable for more than 15 minutes. Arterial pH and pressures of O_2 and CO_2 were measured using a blood gas analyser (AVL Compact 3, Diamond Diagnostics, MA, USA). Plasma glucose and lactate concentrations were quantified with the glucose oxidase and lactate oxidase methods, respectively, using 2 multi-assay analysers (GW7 Micro-Stat, Analox Instruments, UK).

3.14.2. Localized ^{1}H NMR spectroscopy

All experiments were carried out on a Varian INOVA spectrometer (Varian, Palo Alto, CA, USA) interfaced to an actively-shielded 9.4 T magnet with a 31 cm horizontal bore (Magnex Scientific, Abingdon, UK) using a homebuilt 10 mm ^{1}H quadrature surface coil. The rat brain was positioned in the isocentre of the magnet and located with fast-spin-echo images. Shimming was performed with FAST(EST)MAP (Gruetter, 1993; Gruetter and Tkác, 2000), and ^{1}H NMR spectra were acquired from a volume of interest (VOI) of 18 μL placed in the left hippocampus using SPECIAL spectroscopy (Mlynárik *et al*., 2006), with echo time of 2.8 ms and repetition time of 4 s. The spectral analysis was carried out using LCModel (Provencher, 1993) including a macromolecule spectrum in the database, as in previous studies (Mlynárik *et al*., 2006; Tkáč *et al*., 1999). The unsuppressed water signal measured from the same VOI was used as an internal reference (assuming the existence of 80% of water in the brain tissue) for the quantification of the following metabolites that constitute the neurochemical profile: glucose (Glc), ascorbate (Asc), phosphorylehtanolamine (PE), creatine (Cr), phosphocreatine (PCr), *myo*-inositol (Ins), taurine (Tau), *N*-acetylaspartate (NAA), aspartate (Asp), glutamate (Glu), glutamine (Gln), γ-aminobutyrate (GABA), alanine (Ala), lactate (Lac), β-hydroxybutyrate (βHB), glycerophosphorylcholine (GPC) phosphorylcholine (PCho), glutathione (GSH), *N*-acetylaspartylglutamate (NAAG), *scyllo*-inositol (scyllo). The Cramér-Rao lower bound (CRLB) was provided by LCModel as a measure of the reliability of the apparent metabolite concentration quantification.

3.14.3. Determination of glucose transport kinetics

^{1}H NMR spectra were acquired at different glycaemia states, and the quantification of hippocampal glucose as function of plasma glucose can provide the insight on the kinetics of glucose transport across the BBB.

The predominant transporter protein involved in the facilitative transport of glucose across the BBB is GLUT1. The model of glucose transport across the BBB was simplified to consider a 3 compartment system (Lund-Andersen, 1979, Gruetter *et al.*, 1998): the BBB separates the blood circulation compartment from the brain aqueous phase, which is virtually separated from the metabolic pool where glucose is consumed. In this model, the physical distribution space of glucose at steady-state was assumed to equal the brain water phase, which implies that glucose is evenly distributed in the intra and extracellular spaces. The BBB was considered to behave as a single membrane, which is a considerable approximation but valid at steady-state. The transport across the BBB was described using a classical Michaelis-Menten kinetics with unidirectional fluxes and symmetric kinetic constants for influx and efflux, and non-specific permeability of the BBB to glucose was excluded. With a blood volume of 3% in the brain and a dry weight of 20%, the size of the entire aqueous phase (V_d) was considered 77% of brain's volume. Cerebral glucose consumption rate was considered invariable at euglycaemia and above. Under the steady-state condition, the model of glucose transport is represented by the following mathematical equation:

$$\frac{dG_{hipp}}{dt} = T_{influx} - T_{efflux} - CMR_{gluc} = 0 \qquad (1).$$

In this equation, G_{hipp} is the glucose in the hippocampus (in μmol.g^{-1}), T is the rate of glucose influx or efflux across the BBB (in μmol.g^{-1}min^{-1}), and CMR_{gluc} is the cerebral metabolic rate for glucose consumption (in μmol.g^{-1}min^{-1}).

Two types of enzymatic mechanism were considered for the glucose transporter. First, the standard Michaelis-Menten model (Figure 3.2A) uses the unidirectional mechanism given by:

$$G_{plasma} + GT \rightleftharpoons GT\text{-}G \rightarrow G_{hipp} + GT \qquad (2).$$

G_{plasma} denotes plasma glucose and GT denotes the glucose transporter protein present at the BBB. The following expression is obtained for the relation of hippocampal glucose to plasma glucose, as derived in several reports (see Gruetter *et al.*, 1998 and references therein):

$$G_{hipp} = V_d K_t \frac{\left(\frac{T_{max}}{CMR_{gluc}} - 1\right) G_{plasma} - K_t}{\left(\frac{T_{max}}{CMR_{gluc}} + 1\right) K_t + G_{plasma}} \qquad (3).$$

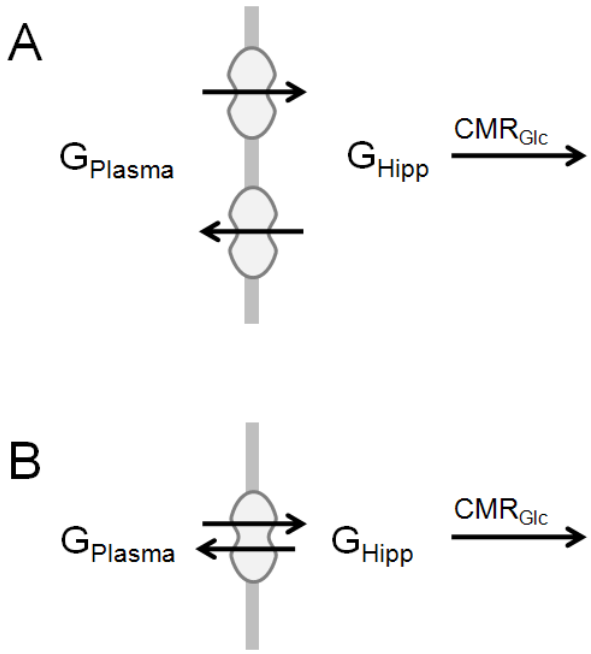

Figure 3.2. Scheme of the standard Michaelis–Menten model of glucose transport (A), that assumes that product formation for glucose transport in both directions of the BBB is independent of the respective product concentration, *i.e.* transported glucose has no effect on the transport mechanism, and of reversible Michaelis–Menten kinetics of glucose transport (B) showing a representation of bidirectional fluxes in the glucose transporter at steady state. G_{plasma} and G_{hipp} denote plasma and hippocampal glucose (in µmol.g^{-1}), and CMR_{gluc} is the cerebral metabolic rate for glucose consumption (in µmol.g^{-1}min^{-1}).

T_{max} denotes the apparent maximal transport rate across the BBB (µmol.g^{-1}min^{-1}), K_t denotes the apparent Michaelis-Menten (mM), V_d is the volume of the physical distribution space of glucose in the brain (0.77 mL/g).

Second, since at hyperglycemia the hippocampal glucose concentration approaches or even exceeds the K_t obtained with the standard Michaelis-Menten model, was used a reversible Michaelis-Menten kinetics of glucose transport (Figure 3.2B) that assumes that the product formation, *i.e.* the transport of glucose into the brain, is not unidirectional:

$G_{plasma} + GT \rightleftharpoons GT\text{-}G_{plasma} \rightleftharpoons GT\text{-}G_{hipp} \rightleftharpoons G_{hipp} + GT$ (4).

Using this model at steady state, the following equation expresses brain glucose concentrations as function of plasma glucose (Gruetter *et al.*, 1998):

$$G_{hipp} = V_d \frac{\left(\frac{T_{max}}{CMR_{gluc}} - 1\right) G_{plasma} - K_t}{\frac{T_{max}}{CMR_{gluc}} + 1} \qquad (5).$$

Assuming the existence of a single membrane at the BBB, the reversible Michaelis-Menten model suggests a linear relation of hippocampal glucose to plasma glucose as previously described (Gruetter *et al.*, 1998).

3.15. Intermediary metabolism by *ex vivo* ^{13}C NMR spectroscopy

Diabetic GK and control Wistar rats (6 months of age) were anaesthetized with i.p. injection of a mixture of ketamine hydrochloride (84 mg/kg; Ketalar from Pfizer, Porto Salvo, Portugal) and chlorpromazine hydrochloride (8.4 mg/kg; Largactil from Laboratórios Vitória, Amadora, Portugal), and cannulated in the left femural vein and artery for [1-^{13}C]glucose 20%(w/v) infusion and blood collection, respectively. Body temperature was monitored using a rectal probe and maintained at 37.5˚C. A bolus of [1-^{13}C]glucose was infused i.v. at an exponentially decaying rate over 5 min, followed by a continuous infusion with rate adjustable to animal glycaemia (Henry *et al*,. 2003). Arterial blood glucose was measured every 10-20 min and maintained constant at 320-370 mg/dL for controls and at 450-500 for GK rats. This protocol result in a rapid rise of glucose ^{13}C isotopic enrichment from natural abundance to 70% or 40% for controls and GK rats respectively (see results section). Arterial blood samples were analysed with a GEM Premier 3000 instrument (Instrumentation Laboratory, MA, USA) for pH, gas pressures (CO_2 and O_2), and electrolytes. At the end of each infusion protocol, rats were decapitated and the head immediately frozen in liquid N_2. Perchloric acid extracts of the hippocampal tissue were lyophilized and saved for NMR spectroscopy. ^{1}H and ^{13}C NMR spectra were acquired on a Bruker 600 NMR spectrometer with a 14.1 T UltraShield magnet (Bruker, Germany) and were analysed with MestReC software (Mestrelab Research, Santiago de Compostela, Spain). The signal of ^{13}C labelled CH_3 lactate in ^{1}H spectra was used as reference for ^{13}C NMR signal quantification.

3.16. Insulin quantification

Insulin concentration was quantified by enzyme-linked immunosorbent assay (ELISA) using the Mercodia Ultrasensitive Mouse Insulin ELISA kit (Mercodia, Uppsala, Sweden) according to manufacturer's instructions. Briefly, this ELISA for insulin determination was a solid phase two-site enzyme immunoassay, based on the direct sandwich technique in which two monoclonal antibodies were directed against separate antigenic determinants on the insulin molecule. During 2 hours of incubation, insulin in the samples (25 µL) and standards (0.025 to 6.4 µg/L) reacts with peroxidase-conjugated anti-insulin antibody and anti-insulin antibody immobilised in a 96 well-microplate. Unbound enzyme-labelled antibody was removed by washing and the bound conjugate was detected by reaction with 3,3',5,5'-tetramethylbenzidine. The reaction was stopped with H_2SO_4, and

the colorimetric endpoint measured in a SpectraMax Plus384 spectrometer (Molecular Devices, Union City, USA).

3.17. Caffeine quantification

For caffeine measurement, serum samples from each mouse were added to equal volume of methanol-acetone (4:1), mixed for 15 minutes, centrifuged at 3,000 *g* for 15 minutes, and the supernatant saved for caffeine quantification. Samples (20 µL) were separated at room temperature using a reverse-phase column [LiChroCART 125x4mm LiChrospher 100 RP-18 (5 µm) cartridge fitted into a ManuCART holder (Merck Darmstadt, Germany)], using a Gilson system equipped with a UV detector set at 274 nm. In our experimental conditions, the maximum peak in the absorption spectra of caffeine was confirmed in a 100 µM caffeine solution prepared in water-methanol (10:1), using a SpectraMax Plus384 spectrometer. The eluent was 40% (v/v) methanol with a flow rate of 0.8 mL/min. The identification of the caffeine peak was performed by comparison of relative retention time with standard samples prepared in water-methanol-acetone (5:4:1) and its quantification achieved by calculating the peak areas then converted to concentration values by calibration with known standards ranging from 1 to 100 µM.

3.18. Reagents

Here I refer the origin of the reagents used in the experimental work that were not directly stated in the description of the methods. [U-^{13}C]glucose (99%), sodium [2-^{13}C]acetate (99%) and $^{2}H_2O$ (99.9%) were purchased from Isotec (Miamisburg, USA). Carbogen (gas mixture of 95% O_2 + 5% CO_2) was purchased to Linde Sogás (Lisbon, Portugal). FluoroJade-C was obtained from HistoChem (Jefferson, AR, USA). H-5000 Vectamount and Vectashield H-1400 mounting mediums from Vector Laboratories were purchased to Batista Marques (Lisbon, Portugal). The CB1 receptor agonist (R)-(+)-[2,3-dihydro-5-methyl-3-(4-morpholinylmethyl)pyrrolo[1,2,3-de]-1,4-benzoxazin-6-yl]-1-naphthalenylmethanone mesylate (WIN55212-2 or WIN), the CB1 receptor antagonist *N*-(piperidin-1-yl)-5-(4-iodophenyl)-1-(2,4-dichlorophenyl)-4-methyl-1H-pyrazole-3-carboxamide (AM251 or AM), 8-{4-[(2-aminoethyl)amino]carbonylmethyl-oxyphenyl}xanthine (XAC), and the adenosine antagonist 1,3-dipropyl-8-cyclopentylxanthine (DPCPX) were purchased from Tocris (Bristol, UK). Solutions of ^{2}HCl (20% w/w) and NaO^{2}H (40% w/w), streptozotocin (STZ; chemical

name: 2-deoxy-2-(3-(methyl-3-nitrosoureido)-D-glucopyranose), DPX Mountant, Caffeine, Cresyl violet and other common-use reagents were purchased to Sigma-Aldrich (Sintra, Portugal).

3.19. Data presentation and statistics

All the data obtained from the present experimental work was analysed with the software GraphPad Prism 4. Results are presented as mean±SEM values of n experiments and significant group differences were considered at $P<0.05$ in the statistical test. Generally, Student's *t* test was used to compare two data sets, and one-way ANOVA test followed by Bonferroni's or Newman-Keuls' post-tests was used to compare the data from several experimental groups. For the comparison of time dependent data measured during the caffeine treatment period, namely body weight, caffeine intake and glycaemia, as well as results from behavioural studies performed before and after treatment, we used the two-way ANOVA test followed by the Bonferroni's post-test.

4. Results

4.1. Neuromodulation systems controlling intermediary metabolism in rat hippocampal slices

Neuromodulation systems not only control synaptic events that lead to regulation of neurotransmission, but can also regulate metabolic pathways that may be important when the cerebral tissue faces metabolic challenges, neurotoxic conditions, or even neurodegenerative disorders. To understand the involvement of modulation systems on intermediary metabolism acutely dissociated hippocampal slices were used. They were superfused under different conditions and in the presence of different drugs to study their metabolic profile, energy charge, and relative metabolic fluxes using NMR spectroscopy and HPLC. The first aim was to characterize the metabolic status of the hippocampal slice preparation, in order to establish the basis for studies of metabolic control by neuromodulation systems.

4.1.1. Characterization of the superfused hippocampal slice preparation for metabolic studies by NMR spectroscopy - different metabolism of glutamatergic and GABAergic compartments

^{13}C NMR spectroscopy is a powerful tool to investigate intermediary metabolism since it is able to simultaneously detect ^{13}C incorporation into molecules and the positions of ^{13}C incorporation within the same molecule (isotopomers). It has been used for studies of brain intermediary metabolism both *in vitro* and *in vivo* (*e.g.* Cerdán *et al*., 1990; Ebert *et al*., 2003; García-Espinosa *et al*., 2004; Gruetter, 2002; Künnecke *et al*., 1993; Zwingmann and Leibfritz, 2003), allowing to follow the fate of labelling from ^{13}C-enriched substrates through particular metabolic pathways. This has allowed demonstrating that glucose is the main metabolic fuel although the energy requirements of cerebral tissue can be satisfied by the oxidation of other substrates such as ketone bodies (Badar-Goffer *et al*., 1990; Cerdán *et al*., 1990; Künnecke *et al*., 1993; Melo *et al*., 2006), lactate (Bouzier *et al*., 2000; Hassel and Brathe 2000; Tyson *et al*., 2003) and even fatty acids (Ebert *et al*., 2003; Kuge *et al*., 1995).

Brain metabolism has been mainly investigated in the brain or in cultured brain cells, but scarcely in hippocampal slices (Ben-Yoseph *et al*., 1993; Bradler *et al*., 1991; Cohen *et al*., 1984; Schurr *et al*., 1999; Whittingham *et al*., 1984), which are the golden standard for electrophysiological studies

since slices preserve the anatomy of neuronal circuits and synaptic properties of excitability and plasticity (Bahr *et al.*, 1995). However, the physiological performance of hippocampal slices ultimately depends on its metabolic status, which has been poorly studied. As would be expected from its ability to endure prolonged periods of electrical activity, it has already been shown that hippocampal slices are metabolically competent (*e.g.* Whittingham *et al.*, 1984; Schurr *et al.*, 1999), but no detailed characterization of the intermediary metabolism of this preparation has yet been carried out. Therefore, to set the basis for studies of metabolism regulation, the present work intended to characterize the metabolic status of the superfused hippocampal slice preparation by ^{13}C NMR isotopomer analysis after labelling with [U-^{13}C]glucose and [2-^{13}C]acetate, to evaluate both neuronal and astrocytic metabolic compartments (Cerdán *et al.*, 1990; Melo *et al.*, 2006).

4.1.1.1. Metabolic status and stability over time of superfused hippocampal slices

Figure 4.1 shows typical ^{1}H NMR spectra from perchloric extracts of hippocampal slices superfused in the presence of unlabelled acetate and glucose for a period of 3 hours in the absence and in the presence of 4AP (50 µM) to trigger intermittent burst-like neuronal activity. The stimulation of the slices with 4AP induced a different metabolic status, namely an increase in amino

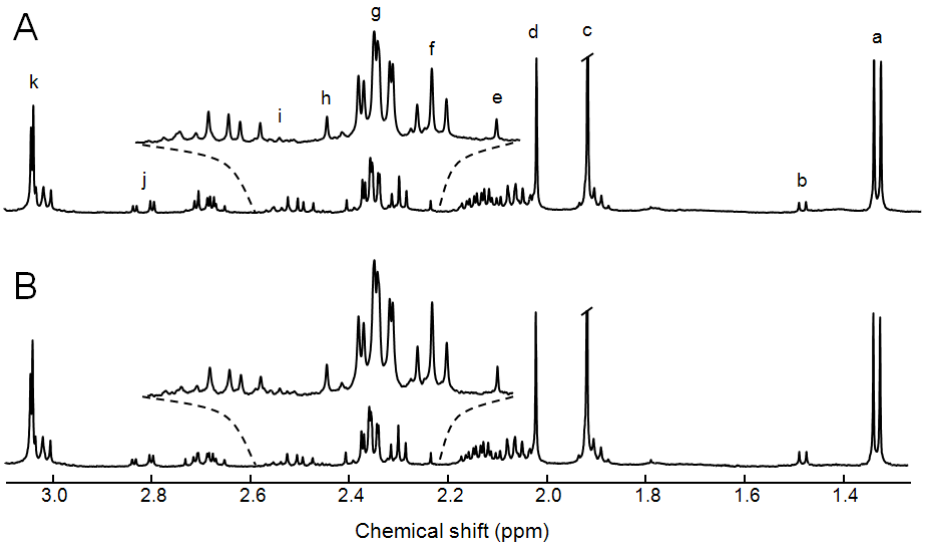

Figure 4.1. Typical ^{1}H NMR spectra of neutralized PCA extracts from hippocampal slices superfused for 3 hours with unlabelled acetate and glucose, in the absence (A) or presence (B) of 4AP. The height of the spectra was normalized to *N*-acetyl-aspartate singlet at 2.02 ppm. The signal assignment was based on the study of Govindaraju et al. (2000): a, lactate-CH_3; b, alanine-CH_3; c, acetate-CH_3; d, *N*-acetyl-aspartate2-CH_3 (from acetyl group); e, acetoacetate-CH_3; f, GABA4-CH_2; g, glutamate4-CH_2; h, pyruvate-CH_3; i, glutamine4-CH_2; j, aspartate3-CH_2 (half of the resonance); k, creatine and phosphocreatine N(CH_3).

Table 4.1. Metabolite levels in PCA extracts from hippocampal slices superfused during 3 hours in the absence or presence of 4AP, and from hippocampal tissue. Values were normalized relative to total creatine, and are presented as mean±SEM. One-tailed ANOVA followed by the Newman-Keuls multiple comparison test was used to compare the three groups. * P<0.05 compared to hippocampus; $ P<0.05 compared to hippocampal slices superfused in the absence of 4AP.

	Hippocampal Slices (n=6)	Hippocampal Slices + 4AP (n=6)	Hippocampus (n=3)
Lactate	1.61±0.14 *	1.43±0.17 *	0.92±0.05
Alanine	0.10±0.01	0.13±0.01 *	0.08±0.01
Glutamate	1.02±0.11	2.66±0.14 *, $	1.26±0.02
Glutamine	0.07±0.01 *	0.10±0.01 *	0.43±0.03
GABA	0.24±0.02	0.67±0.05 *, $	0.18±0.01
NAA	0.84±0.04	0.74±0.03	0.71±0.01
Aspartate	0.33±0.04	0.68±0.05 *, $	0.21±0.01
Pyruvate	0.03±0.01 *	0.05±0.01 *	0.08±0.01
myo-Inositol	0.48±0.05 *	0.48±0.03 *	0.81±0.01

acids such as glutamate, aspartate and GABA, which are quantified in Table 4.1. The profile in the proton spectra recorded after 3 hours of superfusion in the presence of unlabeled acetate and glucose was maintained from 1.5 up to 7.5 hours (spectra not shown). Figures 4.2 and 4.3 confirm the stability over time of superfused hippocampal slices. Alanine and lactate concentrations, which reflect the redox status (Ben-Yoseph *et al*., 1993), the neuronal marker NAA (Klunk *et al*., 1992; Sager *et al*., 1995), and the metabolic energy indicators PCre/Cre, PCre/ATP and ATP/ADP, were essentially constant during the tested superfusion period, both in the absence and in the presence of 4AP.

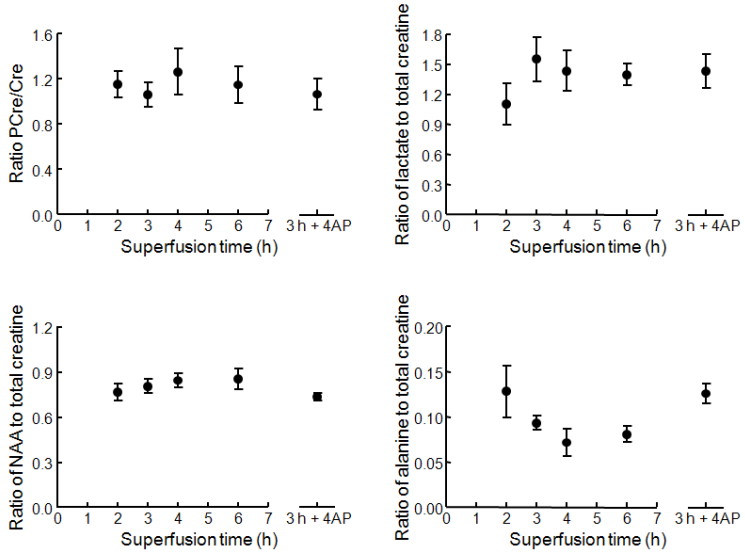

Figure 4.2. Evolution of the ratios of specific metabolites in extracts of hippocampal slices as a function of the suprefusion time. No particular changes in such ratios occur for superfusion periods up to 6 hours but some tissue deterioration seems to be taking place at longer superfusions. Results are presented as mean±SEM of 4 experiments.

Although these results confirmed the metabolic viability and stability over time of the superfused slice preparation (*e.g.* Whittingham *et al*., 1984), it was also noted that there were some metabolic differences between hippocampal slices and hippocampal tissue (Table 4.1). The most

notable difference was the profound depletion of the content of glutamine in hippocampal slices compared to hippocampal tissue.

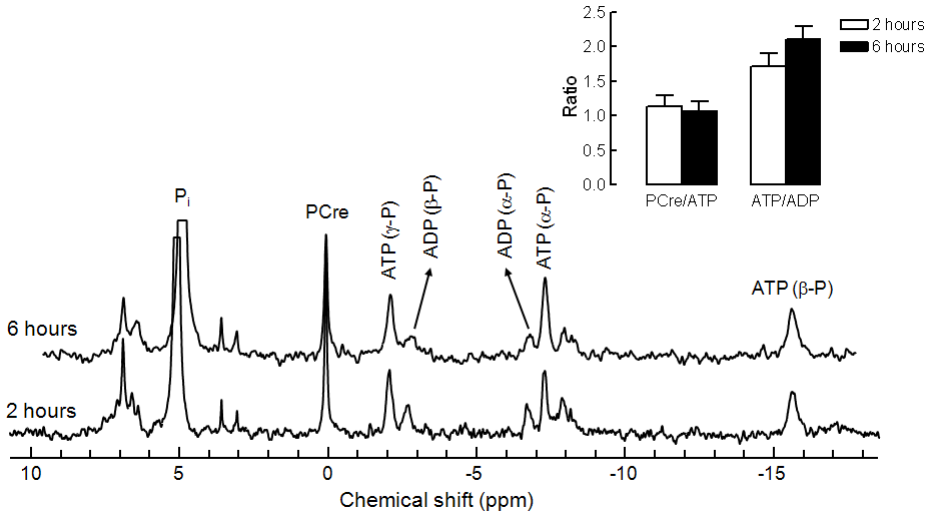

Figure 4.3. ^{31}P NMR spectrum of PCA extracts from hippocampal slices superfused for 2 (bottom) and 6 hours (top). The inserted histogram shows the PCre/ATP and ATP/ADP ratios as measured by deconvolution of the ^{31}P NMR spectra acquired for each superfusion period. The values in the inserted graph are presented as mean±SEM of 4 experiments.

4.1.1.2. Incorporation of [U-^{13}C]glucose and [2-^{13}C]acetate into intermediary metabolites

The metabolic fate of the provided ^{13}C labelled precursors is summarised in Figure 4.4 (see also Figure 3.1). [U-^{13}C]glucose is metabolized to [U-^{13}C]pyruvate that exchanges with [U-^{13}C]alanine and [U-^{13}C]lactate, or is converted to [1,2-^{13}C]acetyl-CoA entering the TCA cycle. [4,5-^{13}C]α-ketoglutarate is produced in the TCA cycle and exchanges with glutamate that subsequently

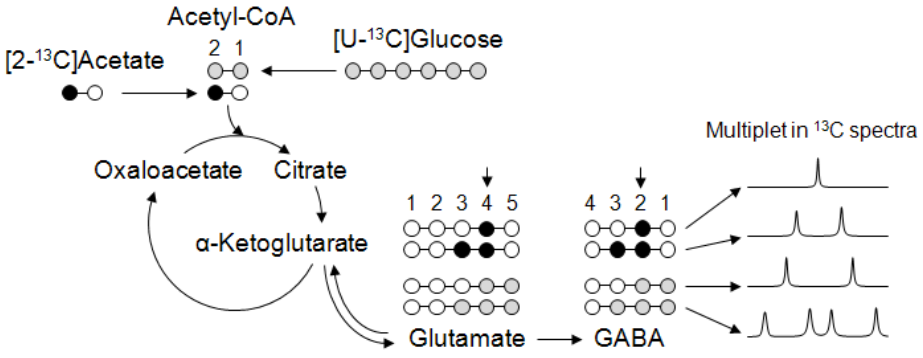

Figure 4.4. Schematic model of the fate of ^{13}C labelling in atoms of glutamate and GABA upon metabolism [U-^{13}C]glucose and [2-^{13}C]acetate. [2-^{13}C]acetate yields [2-^{13}C]acetyl-CoA and [U-^{13}C]glucose originates [1,2-^{13}C]acetyl-CoA. Both acetyl-CoA molecules enter the TCA cycle by condensation with oxaloacetate, leading to the formation of glutamate enriched in the carbons 4 and 4 + 5, respectively. In the next turns of the TCA cycle, when oxaloacetate becomes enriched, molecules of glutamate labelled in the carbons 3 + 4 and 3 + 4 + 5 are produced. This scheme was simplified to highlight the source of the labelling pattern observed in glutamate C4 and GABA C2.

can be decarboxylated to [1,2-^{13}C]GABA. If the labelling from [4,5-^{13}C]α-ketoglutarate remains in the TCA cycle, other intermediates will be ^{13}C enriched and other glutamate and GABA isotopomers, namely [3,4,5-^{13}C]glutamate and [1,2,3-^{13}C]GABA, will be produced in subsequent turns of the cycle. In the astrocytes, [U-^{13}C]pyruvate can also enter the TCA cycle if converted to [1,2,3-^{13}C]oxaloacetate by pyruvate carboxylase (PC), producing multilabelled isotopomers of glutamate and GABA. In contrast, [2-^{13}C]acetate is activated to [2-^{13}C]acetyl-CoA that preferentially enters the astrocytic TCA cycle (Waniewski *et al.*, 1998) producing [4-^{13}C]2-oxoglutarate and then [4-^{13}C]glutamate and [2-^{13}C]GABA. If the labelling from [4-^{13}C]2-oxoglutarate follows the TCA cycle, a second turn will produce namely [3,4-^{13}C]glutamate and [2,3-^{13}C]GABA.

A typical ^{13}C NMR spectrum of a perchloric acid extract of hippocampal slices, superfused during 3 hours in the presence of [U-^{13}C]glucose and [2-^{13}C]acetate, is shown in Figure 4.5 (top spectrum). Carbons of several metabolic intermediates, namely glutamate, glutamine, GABA, aspartate, lactate and alanine, become enriched by incorporation of ^{13}C derived from each substrate. The expansions of the spectrum show several enriched carbons from the various metabolites present in the extract, including the resonances of glutamate C4 and GABA C2 centred at 34.2 and 35.1 ppm, respectively. These two resonances are constituted by 9 lines that can be grouped in 4

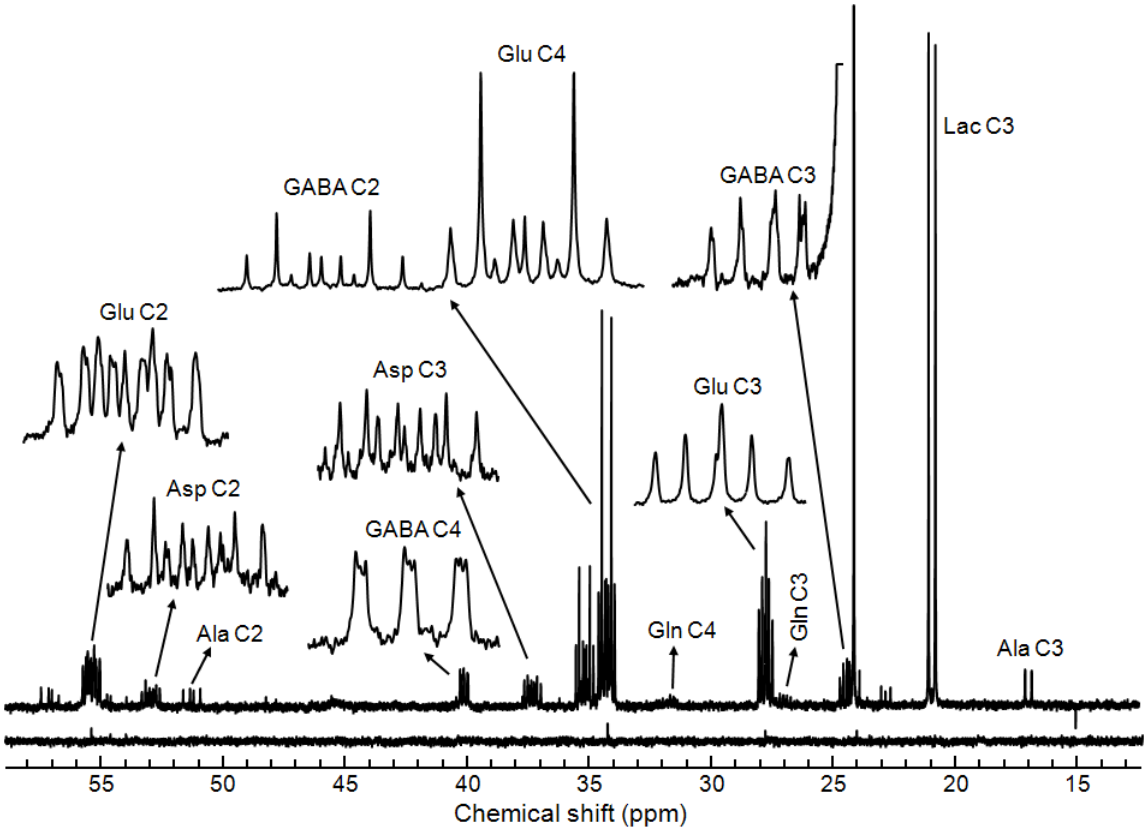

Figure 4.5. Representative ^{13}C-NMR spectra of PCA extracts from hippocampal slices superfused for 3 hours with unenriched acetate and glucose (bottom) or enriched [2-^{13}C]acetate and [U-^{13}C]glucose (top). Resonance assignment was as follows: Ala, Alanine; Lac, lactate; GABA, γ-aminobutyric acid; Glu, glutamate; Gln, glutamine; Asp, aspartate.

sets, based on the ^{13}C labelling patterns of the adjacent carbons. Glutamate C4 resonance allows distinguishing C4S (C3 and C5 are unenriched), C4D34 (C3 is enriched but C5 is not), C4D45 (C5 is enriched but C3 is not) and C4Q (C3 and C5 are both enriched). GABA C2 resonance, which originates from glutamate C4, shows a labelling pattern almost identical to that described for glutamate but now the C1 of GABA behaves as the C5 of glutamate. The multiplets C2S, C2D23, C2D12 and C2Q refer to isotopomers having both C1 and C3 unenriched, C3 enriched but not C1, C1 enriched but not C3 and C1 and C3 both enriched, respectively.

The present ^{13}C isotopomer analysis was mostly centred in glutamate and GABA ^{13}C isotopomers because these two metabolites are the most abundant neurotransmitters and are related to the TCA cycle intermediate α-ketoglutarate. Nevertheless, as it can be appreciated from the expansions, other metabolites such as aspartate become enriched and can also be used in the metabolic analysis.

4.1.1.3. Evaluation of steady-state condition

In the present experimental setup, both [U-^{13}C]glucose and [2-^{13}C]acetate are enriched in ^{13}C by 98±1% (n=4) in the superfusion medium, as quantified by ^{1}H NMR spectroscopy of superfusate samples collected after superfusing the hippocampal slices.

As mentioned above, when [U-^{13}C]glucose and [2-^{13}C]acetate are oxidized, glutamate C4 becomes enriched in the first turn of the TCA cycle and its C3 and C2 isotopomers become enriched in the following TCA turns. Thus, the glutamate C3/C4 enrichment ratio is frequently used to evaluate metabolic steady-state, which was found to be reached at 7.5 hours of superfusion in the absence of 4AP (Figure 4.6). A similar period was required to reach isotopic steady-state of GABA, which enrichment is slower than glutamate (Figure 4.6). Stimulation of the slices with 4AP (50 µM) decreased the time required to reach the isotopic steady-state of both glutamate and GABA (Figure 4.6). In fact, glutamate C3/C4 (0.71±0.04, n=4) and GABA C3/C2 (0.76±0.02, n=4) ratios obtained after 3 hours in the presence of 4AP were close to

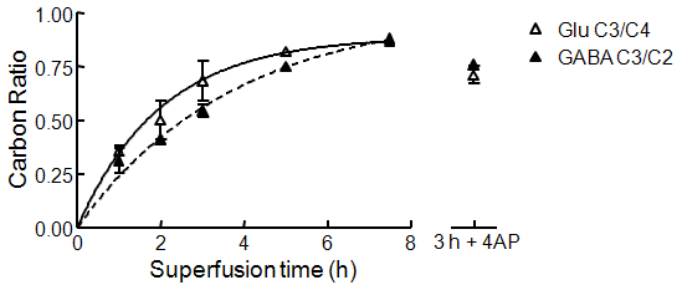

Figure 4.6. Evaluation of the isotopic steady-state in hippocampal slices based on the glutamate C3/C4 and GABA C3/C2 ratios during superfusion with [U-^{13}C]glucose and [2-^{13}C]acetate. With the increase in superfusion time both ratios increase and reach a "plateau" value for periods of 6-7.5 hours. In the presence of 4AP (50 µM) similar ratios are reached for approximately half of the superfusion time. Results are presented as mean±SEM of 4 experiments.

these obtained for 7.5 hours superfusion in the absence of 4AP.

4.1.1.4. Direct analysis of glutamate C4 and GABA C2

Ratios of multiplets of specific carbon resonances in the ^{13}C NMR spectra can be used for a direct evaluation of the metabolic status in non-steady-state metabolic conditions provided that the labelling patterns of competing oxidative substrates are carefully chosen (Malloy *et al*., 1990). [U-^{13}C]glucose yields [1,2-^{13}C]acetyl-CoA, which leads to the formation of [4,5-^{13}C]glutamate in a first turn of the TCA cycle and to the labelling of the other carbons of glutamate in following turns. On the other hand, [2-^{13}C]acetate yields [2-^{13}C]acetyl-CoA, which labels only carbon 4 of glutamate on the first turn of the TCA cycle and other carbons of glutamate (including C3, C2 and C1) in following turns. Independently of the labelling patterns of oxaloacetate, the labelling pattern at carbon 4 of glutamate will always be determined by the labelling pattern of the acetyl-CoA unit that enters the cycle and for that reason the glutamate C4 multiplets will always possess the information required to evaluate both the relative contributions of each oxidative substrate and the relative flux of the TCA cycle. Thus, the ratios of glutamate C4Q to C4D45 (GluC4Q/D45) and glutamate C4D34 to C4S (GluC4D34/S) indicate the flux into the TCA cycle(s) oxidizing [U-^{13}C]glucose and [2-^{13}C]acetate, respectively. Multiplets in GABA C2, since it derives directly from glutamate C4, can also be used in this direct isotopomer analysis. Thus, the ratios GABA C2Q to C2D12 (GABAC2Q/D12) and GABA C2D23 to C2S (GABAC2D23/S) also reflect the TCA cycle flux oxidizing [U-^{13}C]glucose and [2-^{13}C]acetate, respectively. This allows inferring glial TCA cycle flux by evaluating glutamate isotopomer populations originated by labelled acetate, based on the assumption that that glucose is oxidized in both neurons and glia while acetate is preferentially transported into glial cells (Waniewski and Martin, 1998).

As shown in Table 4.2, similar multiplet ratios were obtained for either glutamate C4 or GABA C2 in the absence of 4AP. However, the presence of 4AP increased GluC4D34/S compared

Table 4.2. Multiplet ratios calculated from glutamate C4 and GABA C2 resonances in ^{13}C NMR spectra acquired in extracts from hippocampal slices superfused with 5.5 mM [U-^{13}C]glucose and 2 mM [2-^{13}C]acetate in the absence or presence of 50 μM 4AP. Results are mean±SEM of 4 experiments and Student's *t* test used for comparison: * different from absence of 4AP ($P<0.01$), $ different from GluC4D34/S ($P<0.01$).

	Absence of 4AP	Presence of 4AP
GluC4D34/S	1.19±0.03	1.34±0.01 *
GluC4Q/D45	1.18±0.07	1.09±0.05 $
GABAC2D23/S	0.95±0.14	0.97±0.07 $
GABAC2Q/D12	1.17±0.09	1.00±0.04

to the absence of 4AP, which represents an increment of [2-^{13}C]acetate oxidation. This was not observed for GluC4Q/D45, equivalent to [U-^{13}C]glucose oxidation, neither for GABAC2D23/S which arises directly from GluC4D34/S by decarboxylation. These results suggest that the stimulation of the slices with 4AP causes a flux increase of the TCA cycle in the astrocytic compartment mainly exchanging with glutamatergic rather than GABAergic neurons.

4.1.1.5. Determination of relative metabolic fluxes

The obtained ^{13}C isotopomer data (relative peak areas from glutamate, GABA and aspartate resonances as well as the multiplet ratios GluC3/C4, GluC2/C4 and GABAC3/C2) were fitted to the metabolic model shown in Figure 3.1 using the program tcaCALC to calculate the fractional contributions to acetyl-CoA in both steady-state (Malloy *et al*., 1988) and non-steady-state conditions (Malloy *et al*., 1990) in superfused hippocampal slices. The results presented in Table 4.3 indicate that the major modification observed corresponds to the greater contribution of glucose oxidation as a source of acetyl-CoA upon stimulation with 4AP, as evaluated by the consistent increase of Fc12 (contribution of [U-^{13}C]glucose) compared to Fc2 (contribution of [2-^{13}C]acetate) and Fc0 (contribution of unlabelled sources). Furthermore, in accordance with the longer period to reach steady-state of the GABAergic compared to glutamatergic pool, there was also a greater contribution of non-labelled sources for GABA-related acetyl-CoA under resting conditions in the non-steady-state analysis (Table 4.3).

Further analysis of the relative fluxes related to the TCA cycle (figure 3.1) revealed additional differences between the metabolic organization of the glutamatergic and GABAergic

Table 4.3. Fractional contributions to acetyl-CoA in hippocampal slices after superfusion with 5.5 mM [U-^{13}C]glucose and 2 mM [2-^{13}C]acetate for 3 hours, in the absence and presence of 4AP (n=4). Fc0 corresponds to the contribution of unlabeled acetyl-CoA from unlabeled endogenous substrates; Fc2 and Fc12 show the fraction of acetyl-CoA labeled in C2 and both C1 and C2, respectively. Results are presented as mean±SEM of 4 experiments. $ different from glutamate (P<0.05), # different from non-steady-state (P<0.05), * different from absence of 4AP (P<0.05), Student's *t* test used for comparison.

	Absence of 4AP		Presence of 4AP	
	Glutamate	GABA	Glutamate	GABA
Non-steady-state:				
Fc0	0.16±0.01	0.26±0.02 $	0.14±0.02	0.25±0.04 $
Fc2	0.12±0.01	0.13±0.01	0.10±0.01 *	0.09±0.02 *
Fc12	0.72±0.01	0.62±0.02 $	0.76±0.02 *	0.66±0.03 $, *
Steady-state:				
Fc0	0.21±0.01 #	0.20±0.02	0.17±0.01 *	0.20±0.03
Fc2	0.12±0.01	0.14±0.01	0.12±0.01	0.11±0.02 *
Fc12	0.67±0.01 #	0.67±0.02	0.71±0.02 #, *	0.70±0.02

Table 4.4. Relative metabolic fluxes in hippocampal slices after a 3 hour superfusion period with 5.5 mM [U-^{13}C]glucose and 2 mM [2-^{13}C]acetate in the absence or presence of 50 µM 4AP. Flux parameters were estimated under steady-state assumptions from either glutamate or GABA multiplets. Results are presented as mean±SEM of 4 experiments, and Student's *t* test was used for comparison: * different from absence of 4AP ($P<0.05$), $ different from glutamate ($P<0.05$). The fitting results do not include aspartate multiplets since their inclusion did not affect the flux estimation (not shown).

	Absence of 4AP		Presence of 4AP	
	Glutamate	GABA	Glutamate	GABA
ACS	0.26±0.01	0.27±0.02	0.25±0.01	0.18±0.04 *, $
LDH	1.00±0.01	0.93±0.04 $	0.93±0.01 *	1.04±0.11
PC	0.25±0.01	0.20±0.02 $	0.17±0.01 *	0.22±0.07
Y	0.48±0.03	0.44±0.05	0.47±0.02	0.37±0.05 $
PDH	0.75±0.01	0.73±0.02	0.75±0.01	0.82±0.04 *, $

compartments (Table 4.4). Lower LDH flux estimated from GABA suggests a lower importance of the astrocyte-neuron lactate shuttle (Pellerin *et al.*, 1998) for GABAergic than for glutamatergic neurons. This is re-enforced by the observed lower flux through astrocytic PC estimated from GABA isotopomer populations, also consistent with a decreased requirement of astrocytes to replenish oxaloacetate in the TCA cycle, since the clearance of GABA by astrocytes leads to its conversion into succinate that enters the TCA cycle (*e.g.* Patel *et al.*, 2005). Likewise, the 4AP-induced decrease in LDH flux estimated from glutamate multiplets suggests an increased autonomy of neurons, *i.e.* lower dependency from the astrocytic compartment in terms of glucose oxidation. The decrease in astrocytic PC flux relatively to TCA cycle flux upon 4AP stimulation is consistent with the increase in the astrocytic TCA cycle flux inferred from the direct multiplet analysis. To sustain this increase, PDH, ACS and Y fluxes in astrocytic compartment increased in parallel with the increased flux of the TCA cycle. It was again confirmed that there is a greater contribution of glucose to feed the TCA cycle upon 4AP stimulation, which is far greater in GABAergic neurons, as concluded from the parallel increased relative flux of PDH and decreased relative flux of ACS. The decrease of the anapletoric flux Y estimated from GABA multiplets upon 4AP stimulation is consistent with the increased oxidative fluxes caused by the 4AP-induced higher metabolic demand. These results suggest that the metabolic network in GABAergic and glutamatergic compartments in superfused hippocampal slices has a different design and reacts differently to the stimulation by the presence of 4AP.

4.1.1.6. Discussion

The present results provide evidence that detailed metabolic studies of intermediary metabolism can be carried out in superfused hippocampal slices, which opens novel possibilities of

combining metabolic analysis with electrophysiological recordings in the most widely used brain preparation. This was now identified by showing different metabolic re-arragements of the glutamatergic and GABAergic compartments after stimulation of the slices with 4AP.

As occurs for the maintenance of synaptic transmission, excitability and ability to undergo plastic changes over extended periods of time, it was now confirmed that superfused hippocampal slices also displayed a robust and stable metabolic profile (Whittingham *et al*., 1984). Thus, there was no change in the amounts of different reporter metabolites within a 6 hours period of superfusion. Namely, key metabolic parameters such as PCre/Cre and ATP/ADP ratios display robust and constant values for periods of superfusion up to 6 hours, which indicates that superfused hippocampal slices remain metabolically competent over time. Most importantly, this robustness and stability of metabolic parameters in superfused hippocampal slices was maintained in conditions of continuous neuronal firing triggered by the presence of 4AP. This constitutes a re-assuring observation for more prolonged physiological studies carried out in brain slices, since it provides direct evidence that there is no long-term metabolic adaptation in this preparation to sustain electrical activity over prolonged periods *in vitro*. Instead, the metabolic status of superfused slices is maintained over extended periods, which guarantees that treatments of this preparation hours apart are comparable from the metabolic point of view.

This metabolic robustness and stability prompted the use of ^{13}C tracers combined with ^{13}C isotopomer analysis to characterise some basic features of intermediary metabolism in superfused hippocampal slices. The tested ^{13}C-enriched tracers allowed labelling different metabolites observed in the ^{13}C NMR spectrum of hippocampal extracts, out of which attention was focused mainly in glutamate and GABA isotopomers because of their abundance and physiological relevance. In fact, the combined analysis of glutamate and GABA isotopomers potentially allows distinguishing between putative glutamatergic and GABAergic metabolic compartments. Furthermore, a combination of ^{13}C-enriched tracers was selected to attempt distinguishing between neuronal and astrocytic metabolic compartments. Thus, [U-^{13}C]glucose is expected to be metabolised both in neurons and in astrocytes whereas [2-^{13}C]acetate is largely taken up by astrocytes (Waniewski and Martin, 1998) where it is metabolised (Cerdán *et al*., 1990). Finally, it was verified that a period of 3 hours under intermittent burst-like stimulation triggered by 4AP was required to reach steady-state metabolic conditions, the conditions allowing the most faithful estimates of the contribution of different metabolic sources for metabolism (*e.g.* Malloy *et al*., 1988). However, given the awareness that several potential relevant questions amenable for combined electrophysiological and metabolic studies in hippocampal slices occur in shorter time periods, mathematical tools to estimate

modifications of relative metabolic fluxes in non-steady-state conditions were also successfully applied (Malloy *et al*., 1990).

In accordance with expectations, the combined GABA and glutamate ^{13}C isotopomer analysis with the two different tracers ([U-^{13}C]glucose and [2-^{13}C]acetate) provided estimates of metabolic fluxes of the different targeted compartments, namely astrocytes, GABAergic and glutamatergic neurons. Initial characterization of the effect of intermittent burst-like neuronal firing caused by 4AP indicated that there was a different enhancement of the flux of the TCA cycle in the different compartments. In fact, the direct analysis of glutamate C4 and GABA C2 multiplet ratios revealed that 4AP induces an increase on the TCA cycle flux in astrocytes but not in glutamatergic or GABAergic neurons. This is in agreement with expectations both from the anatomical and functional point of views: in fact, there are larger numbers of astrocytes in the hippocampus and it is expected that continuous intermittent neuronal depolarization would demand a greater metabolic effort of astrocytes to control an excessive and potentially neurotoxic effect of enhanced and uncontrolled neuronal activity (Volterra and Steinhauser, 2004). This difference between the metabolic adaptations of the different studied compartments to 4AP-induced stimulation was confirmed and further detailed by mathematical fitting of the ^{13}C-isotopomer data. This indicated that the metabolism of glutamate and GABA use a different carbon source and adapt differently to conditions of increased metabolic demand. Thus, in resting conditions, there was a greater contribution of glucose oxidation to feed the TCA cycle associated with glutamate than with GABA metabolism. Stimulation with 4AP lead to a greater relative contribution of glucose oxidation to feed the TCA cycle associated with the production of GABA than with glutamate. Also GABAergic neurons seem to have more autonomy from astrocytic glucose oxidation than glutamatergic neurons, which also become more autonomous upon 4AP stimulation. These differences are relevant to understand the different potential susceptibility to failure of the GABAergic and glutamatergic systems in prolonged stressful conditions associated with lower glucose availability and increase dependency on the use of alternative carbon sources to feed the TCA cycle.

In spite of its usefulness to evaluate metabolic adaptations under different experimental conditions, the present study also indicates that there are some differences in the metabolic status of hippocampal slices when compared with hippocampal tissue. This situation is similar to that found in electrophysiological studies where differences between some parameters are also found between hippocampal slices and tissue (Bahr *et al*., 1995). The main metabolic differences found in hippocampal slices were decreased *myo*-inositol levels, which can be related to osmotic modifications (*e.g.* Lien *et al*., 1990, 1991), increased lactate levels and decreased pyruvate levels, which indicate a modification of the redox state, and decreased glutamine levels, suggesting a lower

metabolic trafficking from the astrocytic TCA cycle to neurons (Chateil *et al*., 2001; Müller *et al*., 1994). The later presented the greatest difference between hippocampal slices and tissue, which could limit the usefulness of hippocampal slices in studying astrocyte-to-neuron metabolic communication through the glutamate-glutamine cycle. However, this does not mean that this cycle is not operative in hippocampal slices since it was found an enrichment of glutamine in the ^{13}C NMR spectra.

In summary, the present study provides the first extensive metabolic analysis of superfused hippocampal slices using combined ^{1}H NMR spectroscopy and ^{13}C isotopomer analysis using different tracers. The results obtained indicate differences in metabolic recruitment of astrocytes, GABAergic and glutamatergic neurons on activation with 4AP and a different basic set-up and adaptability of the metabolism of GABAergic and glutamatergic compartment to stimulation. This provides a tool for probing intermediary metabolism in restricted brain regions using a well-defined preparation, offering the novel opportunity for parallel studies of electrophysiology and metabolism or metabolic injuries and pathologies affecting the central nervous system such as diabetes *mellitus*, hypoxia or ischemia.

4.1.2. Effect of CB1 receptor activation on intermediary metabolism in rat hippocampal slices

The CB1 receptor modulates brain function and affords neuroprotection (Jackson *et al*., 2005). It is highly abundant in the hippocampus (Degroot *et al*., 2006; Katona *et al*., 1999, 2000), and activation of hippocampal CB1 receptors reduces the release of several neurotransmitters, including GABA (Katona *et al*., 1999, 2000), glutamate (Kawamura *et al*., 2006), dopamine and acetylcholine (Degroot *et al*., 2006), which will be reflected on the control of synaptic plasticity and cognition and memory consolidation (for review see Hampson and Deadwyler, 1999).

CB1 receptor activation has been shown to modulate glucose uptake *in vivo*, in several brain areas (Freedland *et al*., 2002; Pontieri *et al*., 1999; Whitlow *et al*., 2002), and was suggested to control glucose oxidation to CO_2 and glucose incorporation into glycogen and phospholipids in cultured astrocytes and C6 glioma cells (Sánchez *et al*., 1997, 1998). Opposing the effect on other brain structures, activation of CB1 receptors was shown to reduce glucose uptake in the hippocampal tissue (Freedland *et al*., 2002; Pontieri *et al*., 1999; Whitlow *et al*., 2002), even after chronic cannabinoid exposure (Whitlow *et al*., 2003). Furthermore, cannabinoids were suggested to reduce regional blood flow in the hippocampus (Bloom *et al*., 1997; Stein *et al*., 1998). Up to now, the

reported results indicate that activation CB1 receptors has functional consequences in the hippocampus that require the modulation of substrate provided trough the blood flow, but is unknown if such receptors can control intermediary metabolism.

We now investigated the effect of selective CB1 receptor activation on hippocampal intermediary metabolism, using ^{13}C NMR isotopomer analysis of hippocampal slices superfused with ^{13}C enriched substrates. Briefly, hippocampal slices were superfused as described in the methods during an initial 60-minute period of stabilization, followed by the superfusion (for 3 hours, necessary to reach isotopic steady-state in these experimental conditions) in the presence of the ^{13}C-tracers [U-^{13}C]glucose and sodium [2-^{13}C]acetate (equimolar concentration of 5.5 mM), and 50 µM 4AP to allow intermittent burst-like stimulation (Tibbs *et al*., 1989). In this superfusion period ligands of the CB1 receptor were tested: the CB1 receptor agonist (R)-(+)-[2,3-dihydro-5-methyl-3-(4-morpholinylmethyl)pyrrolo[1,2,3-de]-1,4-benzoxazin-6-yl]-1-naphthalenylmethanone mesylate (WIN55212-2 or WIN, at 1 µM) and the CB1 receptor antagonist *N*-(piperidin-1-yl)-5-(4-iodophenyl)-1-(2,4-dichlorophenyl)-4-methyl-1H-pyrazole-3-carboxamide (AM251 or AM, at 0.5 µM), both obtained from Tocris (Bristol, UK). WIN and AM stock solutions were prepared in DMSO and the same volume of DMSO was included in the respective paired control experiments.

4.1.2.1. [U-^{13}C]glucose and [2-^{13}C]acetate metabolism upon CB1 receptor activation

As in previous experiments, in the present experimental design, the ^{13}C enrichment of both [U-^{13}C]glucose and [2-^{13}C]acetate was always 98±1% (n=5) in the superfusion medium, as measured in ^{1}H NMR spectra of superfusate samples collected after superfusing the hippocampal slices. The metabolism of [U-^{13}C]glucose trough glycolysis lead to the enrichment of lactate and alanine and, as shown in Figure 4.7, this enrichment was not changed by the pharmacological manipulation of CB1 receptors. WIN55212-2 and AM251 also failed to alter lactate and alanine concentration in hippocampal slices (Table 4.5). The concentration of the neuronal marker NAA and the metabolic energy indicator

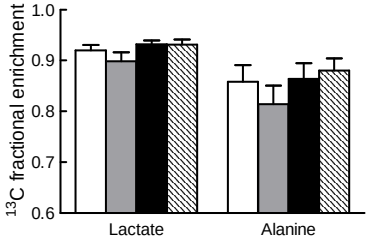

Figure 4.7. Fractional enrichment of lactate and alanine as calculated from ^{1}H NMR spectra from hippocampal slice extracts after a 3 hour superfusion period with 5.5 mM [U-^{13}C]glucose and 5.5 mM [2-^{13}C]acetate in the presence of 50 µM 4AP and CB1 receptor ligands (concentrations of agonist WIN55212-2 and antagonist AM251 were 1 and 0.5 µM, respectively). White, gray, black and striped bars represent control, WIN, WIN+AM and AM conditions. Results are presented as mean±SEM of 5 experiments.

Table 4.5. Metabolite concentrations are not significantly affected by pharmacological manipulation of the CB1 receptor. The concentrations of agonist WIN55212-2and antagonist AM were 1 and 0.5 µM, respectively, and the effect of these CB1 receptor ligands is reported in relation to the respective control condition (in the presence of DMSO). Values are mean±SEM of 5 experiments.

	Control (µmol/g protein)	**WIN55212-2** (% of control)	**WIN55212-2 + AM251** (% of control)	**AM251** (% of control)
NAA	16.7 ± 1.9	-0.7 ± 5.3	-5.7 ± 3.3	10.6 ± 5.7
PCre/Cre	0.63 ± 0.05	-6.3 ± 7.1	1.3 ± 6.6	-4.4 ± 6.9
Lactate	75.6 ± 9.7	-2.1 ± 9.2	7.3 ± 7.7	2.7 ± 7.9
Alanine	4.0 ± 0.4	9.0 ± 27.6	5.8 ± 8.3	-14.4 ± 7.0

PCre/Cre remained unaltered upon CB1 receptors activation or blockade (Table 4.5).

The metabolism of [U-^{13}C]glucose and [2-^{13}C]acetate in hippocampal slices (Figure 4.4) leads to the enrichment of intermediary metabolites that are related to the TCA cycle in neurons and glia. In particular, as described above, the incorporation of ^{13}C atoms into glutamate and GABA allowed inferring about neuronal and astrocytic TCA cycles. As shown in Figure 4.8, selective activation of CB1 receptors with 1 µM WIN55212-2 during the superfusion of the hippocampal slices with the ^{13}C-tracers decreased the ratios GluC4Q/D45 and GABAC2Q/D12 in the ^{13}C NMR spectra, suggesting a reduction of [U-^{13}C]glucose oxidation in the TCA cycles that contribute to the formation of both glutamate and GABA. The presence of the agonist WIN55212-2 in the superfusion medium also inhibited the oxidation of [2-^{13}C]acetate but only in the TCA cycle contributing to glutamate production, as suggested by the decreased ratio GABAC2D23/S. The presence of 0.5 µM AM251, which did not have effect by itself, prevented the effects of WIN55212-2 on the metabolism of [U-^{13}C]glucose and [2-^{13}C]acetate.

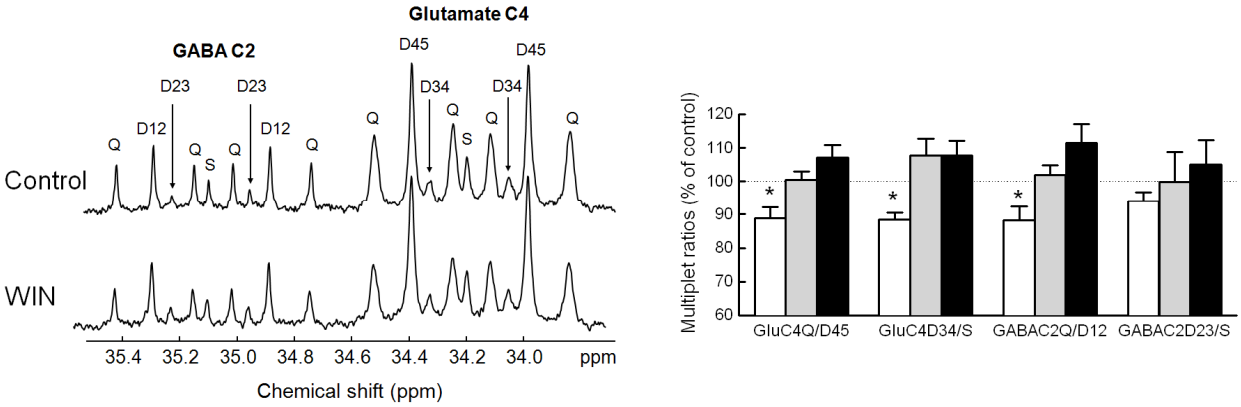

Figure 4.8. Representative resonances of glutamate C4 and GABA C2 in the ^{13}C NMR spectra (left panel) and multiplet ratios calculated from these resonances (panel on the right). ^{13}C NMR spectra were acquired from extracts from hippocampal slices superfused with 5.5 mM [U-^{13}C]glucose and 5.5 mM [2-^{13}C]acetate in the presence of 50 µM 4AP and CB1 receptor ligands WIN55212-2 (1 µM) and AM251 (0.5 µM). White, gray and black bars represent WIN, WIN+AM and AM conditions. All the experiments are paired experiments with a test condition (drug) versus control (containing DMSO), considered 100%. Results in the histogram are mean±SEM of 5 experiments, comparison was made with the Student's *t* test: * P<0.05, different from control.

4.1.2.2. Discussion

The present results show that selective CB1 receptor activation with WIN55212-2 decreases the global rate of oxidative metabolism in rat hippocampal slices, which is prevented by the presence of the antagonist AM251. The relative incorporation of ^{13}C atoms from [U-^{13}C]glucose and [2-^{13}C]acetate into the carbon position 3 of glutamate and GABA suggests a reduction in the flux through the TCA cycle of both neuronal and astrocytic compartments. CB1 activation inhibited TCA cycle flux in neurons participating in both glutamatergic and GABAergic neurotransmission, as indicated by reduced ^{13}C label incorporation from [U-^{13}C]glucose into glutamate and GABA C3, compared to glutamate C4 and GABA C2, respectively. However, the incorporation of labelling from [2-^{13}C]acetate was only reduced in glutamate and not in GABA, suggesting that metabolism in the astrocytic compartment supporting and feeding GABAergic neurons is not significantly affected by CB1 receptor modulation.

These data do not exclude the possibility of increased anaplerotic fluxes upon CB1 receptor activation. However, previous studies with [^{14}C]2-deoxyglucose autoradiography indicated that both WIN55212-2 and Δ^9-THC decrease rates of glucose uptake in the hippocampal tissue (Freedland *et al*., 2002; Pontieri *et al*., 1999; Whitlow *et al*., 2002), and these results are in agreement with decreased oxidative fluxes upon CB1 receptor activation. It was also reported that CB1 receptor activation stimulates glucose utilization in other brain regions (Freedland *et al*., 2002; Pontieri *et al*., 1999; Whitlow *et al*., 2002), and that Δ^9-THC increases glucose oxidation to CO_2 and glucose incorporation into glycogen and phospholipids in primary cultures of cortical and hippocampal astrocytes (Sánchez *et al*., 1998) and C6 glioma cells (Sánchez *et al*., 1997), which was suggested to occur through activation of MAPK (Guzmán and Sánchez, 1999). Moreover, the effect of CB1 receptor activation on the uptake of glucose derivatives was shown to be biphasic and dose-dependent (Margulies and Hammer, 1991), which could explain different results obtained by different authors. Together with these glucose uptake studies, reported decreases in cerebral blood flow by cannabinoids (*e.g.* Bloom *et al*., 1997; Stein *et al*., 1998) are in agreement with reductions in hippocampal intermediary metabolism.

It was reported that cannabinoids can modulate glucose uptake in the hippocampus (Freedland *et al*., 2002; Pontieri *et al*., 1999; Whitlow *et al*., 2002). However, in the present study, the fractional enrichments of lactate and alanine, as well as their concentrations, remained unchanged upon the manipulation of CB1 receptors. Since the concentration of glucose in the brain at

normoglycaemia is around 1 mM (*e.g.* Gruetter *et al*., 1998), the lack of effect of CB1 receptors on these glycolytic-related measures in superfused hippocampal slices may result from a certain degree of saturation of the glycolytic pathway by the amount of glucose provided in the superfusion medium (5.5 mM).

In the hippocampus, activation of CB1 receptors was shown to reduce glucose utilization (Freedland *et al*., 2002; Pontieri *et al*., 1999; Whitlow *et al*., 2002) and metabolism through the neuronal and glial TCA cycles (in the current study). This observations are in agreement with the role of CB1 receptors in controlling neurotransmission in the hippocampus, in particular reducing the release of neurotransmitters such as GABA (Katona *et al*., 1999, 2000), glutamate (Kawamura *et al*., 2006), dopamine and acetylcholine (Degroot *et al*., 2006).

It should be emphasized that astrocytes are expected to be involved in the uptake of glucose from the blood stream that is metabolized to lactate and shuttled to neurons (Magistretti and Pellerin, 1999), and since the superfusion of hippocampal slices provides substrates without using the vascular system, there is a metabolic component in astrocytic metabolism that may be modulated by CB1 receptor activation that is absent in our experimental system. In any case this does not affect the main conclusion of this study because all the cellular elements have access to the provided substrates. Thus these results directly show that the global effect of CB1 activation in hippocampal slices results in a reduction of neuronal and glial metabolism through the TCA cycle.

4.1.3. Adenosine A_1 receptors control the recovery of hippocampal metabolism after hypoxia

Adenosine is a neuromodulator predominantly inhibiting excitatory neurotransmission through activation of adenosine A_1 receptors (Dunwiddie and Masino, 2001), which afford neuroprotection upon acute neuronal injury. Thus, at the onset of brain injury, such as hypoxia and/or hypoglycaemia, both adenosine and A_1 receptor agonists attenuate cell loss and degeneration, whereas A_1 receptor antagonists exacerbate damage (de Mendonça *et al*., 2000). This A_1 receptor-mediated neuroprotection is thought to result from the activation of presynaptic A_1 receptors, which control the depression of excitatory transmission during hypoxia (*e.g.* Fowler, 1989, 1993; Gribkoff *et al*., 1990). In fact, hypoxia depresses excitatory synaptic transmission, which is fully reversible by re-oxygenation, but blockade or deletion of adenosine A_1 receptors decreases the hypoxia-induced depression of synaptic transmission and hampers its recovery after the insult (Arrigoni *et al*., 2005; Johansson *et al*., 2001; Sebastião *et al*., 2001).

Besides acting as a neuromodulator, adenosine also fulfils a general homeostatic role controlling intermediary metabolism, which is considered the basis of the non-brain tissue protective effects afforded by extracellular adenosine (reviewed in Cunha, 2001). For instance the cardioprotective effect of adenosine is related to the ability of A_1 receptor activation to control glucose and glycogen metabolism (Finegan *et al*., 1996; Fraser *et al*., 1999; Gao *et al*., 1997; Wyatt *et al*., 1989). Since adenosine also affects brain intermediary metabolism (Allaman *et al*., 2003; Blood *et al*., 2003; Håberg *et al*., 2000; Hammer *et al*., 2001; Magistretti *et al*., 1986), this ability of adenosine to control the metabolism of neurons and astrocytes could be an alternative mechanism by which adenosine affords neuroprotection. Thus, the present study was designed to investigate if the activation of the adenosine A_1 receptors controls the recovery of the hippocampal intermediary metabolism after hypoxia, using hippocampal slices superfused with ^{13}C enriched substrates, namely glucose and acetate that allow gaining insight on the metabolism in both glial and neuronal compartments, as previously described.

In this particular group of experiments, hippocampal slices were submitted to hypoxic (solution gassed with 95% N_2 + 5% CO_2 mixture) or normoxic conditions during 90 minutes, in the presence of unlabelled glucose and acetate, followed by 3 hours of superfusion in normoxic conditions in the presence of either unlabelled glucose (5.5 mM) and sodium acetate (2 mM) or [U-^{13}C]glucose and sodium [2-^{13}C]acetate. These experiments were repeated in the presence of 100 nM 1,3-dipropyl-8-cyclopentylxanthine (DPCPX, purchased from Tocris, Northpoint, UK) that is a selective antagonist of the adenosine A_1 receptor at this concentration (Sebastião *et al*., 2000). DPCPX stock solution was prepared in 99% DMSO and 1% NaOH 1 M at a concentration of 5 mM and diluted directly into the superfusion medium since amounts of DMSO below 0.01% are devoid of effects on intermediary metabolism. 50 μM 4AP was included in the superfusion medium to allow intermittent burst-like stimulation (Tibbs *et al*., 1989), which is essential to allow a build-up of sufficient extracellular adenosine to impact on synaptic transmission and hypoxia-induced modification of hippocampal function (*e.g*. Sebastião *et al*., 2001).

4.1.3.1. Metabolic status of hippocampal slices submitted to hypoxia and re-oxygenation

It was first characterized the effect of hypoxia and re-oxygenation in the levels of different key metabolites in hippocampal slices. For that purpose, metabolic pools and EC were quantified from PCA extracts of the tissue either after the 90 min of hypoxia or after 3 hours of re-oxygenation

(Table 4.6), using either ^{1}H NMR spectroscopy (Figure 4.9) or HPLC. The concentration of metabolites quantified in hippocampal slice preparations under normoxia (Table 4.6) is in general agreement with those reported by others (*e.g*. Whittingham *et al*., 1984).

In hippocampal slices submitted to 90 min of hypoxia, there was not only an increase in the concentration of lactate (Ben-Yoseph *et al*., 1993; Kauppinen and Williams, 1990; Müller *et al*., 1994;

Table 4.6. Effect of hypoxia (data on the top) or hypoxia plus re-oxygenation (bottom data) on metabolite concentrations (µmol/g protein), PCre/Cre, Glu/Gln and energy charge (EC), in the absence or presence of the selective A_1 receptor antagonist DPCPX (100 nM). Values are presented as mean±SEM (n=4-8). Data was compared using one-way ANOVA followed by Newman-Keuls test: * P<0.05, ** P<0.01, *** P<0.001, different from control; # P<0.05, ## P<0.01, ### P<0.001, different from control + DPCPX; $ P<0.05, $$ P<0.01, $$$ P<0.001, different from hypoxia or hypoxia plus re-oxygenation.

	Control (n=8)	**Hypoxia** (n=6)	**Control + DPCPX** (n=4)	**Hypoxia + DPCPX** (n=4)
Lac	33.8±4.0	57.7±11.6 *	42.7±5.7	70.2±3.0 ***, ##
Pyr	1.1±0.1	1.9±0.3 **	1.5±0.3	2.1±0.2 ***#
Ala	3.0±0.3	5.0±0.8 **	4.4±0.3 *	7.3±0.3 ***, ###, $$$
Glu	62.8±4.3	69.3±6.1	83.8±4.8 **	84.6±4.4 **, $
Gln	2.7±0.4	1.4±0.1 ***	2.6±0.2	1.7±0.2 **, ##
Glu/Gln	27.8±2.7	51.4±4.2 ***	33.3±3.4	50.3±3.0 ***, ###
Asp	15.8±0.9	14.0±1.0	19.6±1.0 **	19.4±0.8 **, $$$
GABA	15.8±1.3	18.9±2.3	19.3±1.5	25.4±1.7 ***, ##, $$
NAA	17.5±1.2	17.5±1.9	22.7±0.9 **	23.0±1.0 **, $$
Cr	11.9±1.0	14.9±1.2 *	16.7±1.2 **	21.5±1.3 ***, ##, $$$
PCr	11.9±1.3	8.1±1.7	14.5±1.4	9.9±2.2
Cr+PCr	23.8±1.5	22.9±2.6	31.2±1.3 **	31.4±1.2 **, $$
PCr/Cr	1.07±0.14	0.53±0.10 **	0.90±0.12	0.49±0.13 **, #
Ins	11.5±1.1	11.8±0.7	16.3±0.8 ***	16.2±0.8 ***, $$
EC	0.74±0.04	0.59±0.03 *	0.73±0.03	0.77±0.03 $

	Control (n=5)	**Hypoxia + Re-Oxygenation** (n=5)	**Control + DPCPX** (n=5)	**Hypoxia + Re-Oxygenation + DPCPX** (n=5)
Lac	35.4±3.0	29.3±3.5	35.6±3.8	36.8±2.4
Pyr	1.1±0.1	0.7±0.1	1.1±0.1	1.1±0.1
Ala	1.9±0.3	1.5±0.1	2.1±0.3	2.3±0.2
Glu	64.9±2.4	63.3±0.6	61.8±2.6	62.6±1.4
Gln	1.74±0.10	1.64±0.17	1.29±0.15	1.11±0.08 *, $
Glu/Gln	38.2±1.8	41.4±3.9	52.0±6.0	61.4±6.1 *, $
Asp	13.9±0.7	15.1±0.4	13.9±0.3	16.1±0.7 *, #
GABA	13.6±1.0	13.2±0.5	13.5±1.3	13.0±0.6
NAA	18.6±0.7	18.5±0.6	19.1±0.8	18.9±1.0
Cr	10.1±0.9	8.8±0.6	10.8±1.2	10.1±0.8
PCr	13.5±1.3	12.3±0.2	12.3±0.8	11.2±1.6
Cr+PCr	23.6±1.2	21.1±0.8	23.1±2.0	21.3±2.3
PCr/Cr	1.4±0.2	1.4±0.1	1.2±0.1	1.1±0.1
Ins	10.8±1.1	9.6±1.1	10.0±1.4	9.7±1.3
EC	0.78±0.03	0.80±0.01	0.73±0.02	0.65±0.04 *, $$

Sonnewald *et al.*, 1994) but also of alanine and pyruvate, three end-products of the glycolytic pathway. In accordance with the hypoxia-induced increase of the flux through the glycolytic pathway, it was observed an increase of lactate release from the superfused hippocampal slices (Figure 4.10). Hypoxia reduced the content of glutamine and increased the ratio glutamate/glutamine, suggesting a modification in glutamine-glutamate cycle between neurons and glia (Müller *et al.*, 1994). The chemical equilibrium between creatine and phosphocreatine, a buffer system to compensate for lack of oxygen or glucose and maintain ATP levels (reviewed in Balestrino *et al.*, 2002), was altered by hypoxia. As reported by others, hypoxia decreased not only the ratio PCre/Cre (Balestrino *et al.*, 2002; Brooks *et al.*, 1989; Kauppinen and Williams, 1990) but also the EC in hippocampal slices (Ikeda *et al.*, 1988; Müller *et al.*, 1994). These metabolic modifications are characteristic features of hypoxia and are globally consistent with an inhibition of the TCA cycle and an increased glycolytic flux, a situation characteristic of metabolic deterioration.

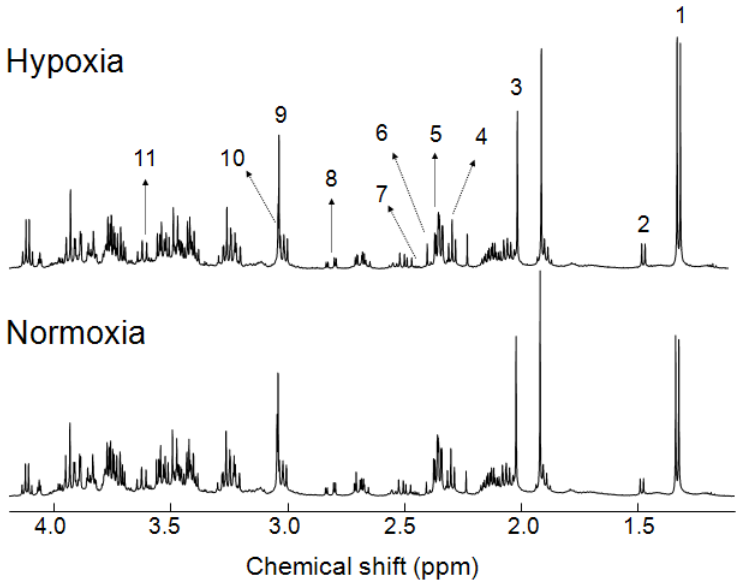

Figure 4.9. Typical ^{1}H NMR spectra of PCA extracts from hippocampal slices superfused with unlabelled acetate and glucose in hypoxic or normoxic conditions during 90 minutes. The signals used to estimate metabolite concentrations are number-tagged: lactate $^{3}CH_3$ (1), alanine $^{3}CH_3$ (2), NAA $^{2}CH_3$ from acetyl group (3), GABA $^{4}CH_2$ (4), glutamate $^{4}CH_2$ (5), pyruvate $^{3}CH_3$ (6), glutamine $^{4}CH_2$ (7), half resonance from aspartate $^{3}CH_2$ (8), creatine N(CH_3) (9), phosphocreatine N(CH_3) (10), *myo*-inositol ^{4}CH + ^{6}CH (11).

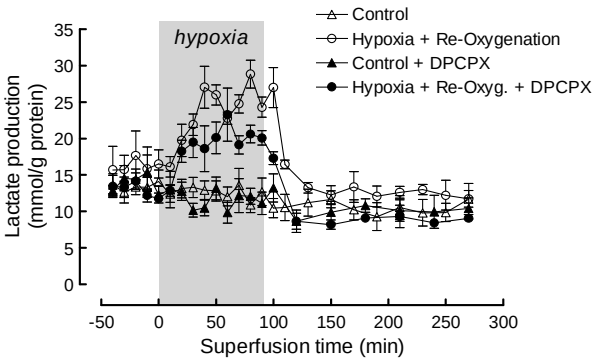

Figure 4.10. Release of lactate from superfused hippocampal slices. Lactate was quantified in superfusate samples by ^{1}H NMR spectroscopy. Data are presented as mean±SEM from 4 experiments.

Upon re-oxygenation (3 hours) there was a complete recovery of the metabolic modifications observed after 90 min of hypoxia (Table 4.6, Figure 4.10), as reported by others in cortical slices (Kauppinen and Williams, 1990) as well as in cell cultures (Sonnewald *et al.*, 1994) or *in vivo* studies (Ikeda *et al.*, 1988).

4.1.3.2. Role of A_1 receptors on hypoxia-induced metabolic modifications

The selective blockade of adenosine A_1 receptors with DPCPX (100 nM) caused an acute modification of the metabolic status of superfused hippocampal slices under normoxic conditions after 90 min of superfusion (Table 4.6). The presence of DPCPX for 90 min increased glutamate and aspartate concentrations, two excitatory amino acids, as well as the content of alanine, NAA, creatine plus phosphocreatine and *myo*-inositol, a major osmolyte in the brain. The simultaneous increase of the total creatine, NAA and *myo*-inositol levels might be related to osmolarity modification, which was reported to occur, for example, in the normal aging brain (Chang *et al*., 1996) and in the hippocampus of diabetic rats (van der Graaf *et al*., 2004). However, this effect of DPCPX under normoxia was transient, since the metabolic status of the hippocampal slices recovered to control conditions after 4.5 hours of superfusion in the presence of 100 nM DPCPX (Table 4.6)

As shown in Table 4.6, the main effect of DPCPX (100 nM) was its ability to affect several of the hypoxia-induced metabolic modifications. Namely, the hypoxia-induced increase of lactate, alanine and pyruvate was exacerbated in the presence of DPCPX. In contrast, neither the hypoxia-induced modification of glutamine content nor the ratios of glutamate to glutamine and phosphocreatine to creatine nor EC were significantly altered in the presence of 100 nM DPCPX. Notably, the concentration of GABA was particularly increased after hypoxia in the presence of DPCPX.

A complete recovery of hypoxia-induced metabolic changes was observed after re-oxygenation. However, this was prevented by the presence of 100 nM DPCPX (Table 4.6). Most notably, whereas the EC recovered to control values on re-oxygenation after hypoxia, this did not occur in the presence of DPCPX. DPCPX also prevented the recovery of glutamine concentration and Glu/Gln ratio, as well as aspartate levels in the re-oxygenated hippocampal slices. Interestingly, DPCPX failed to modify the levels of metabolites related with glycolysis (pyruvate, alanine or lactate; see Table 4.6), as well as the release of lactate (Figure 4.10) upon re-oxygenation. This suggests that the metabolic impairment caused by A_1 receptor blockade upon re-oxygenation might result from a modification of the TCA cycle and glutamate-glutamine cycle rather than of glycolysis.

4.1.3.3. Modification of the flux through the TCA cycle in hipocampal slices

In order to detail the putative effect of A_1 receptor blockade on the recovery from hypoxia of TCA cycle fluxes in hippocampal slices, it was carried out a ^{13}C isotopomer analysis (see Figure 4.4) after replacement of glucose and acetate in the superfusion medium by [U-^{13}C]glucose and [2-^{13}C]acetate during the 3 hour re-oxygenation period. Expansions of glutamate C4 and GABA C2 resonances from representative ^{13}C NMR spectra are shown in Figure 4.11A, and average ratios between the multiplet areas of these resonances are presented in Figure 4.11B. Hippocampal slices submitted to hypoxia followed by re-oxygenation displayed multiplet ratios similar to the control situation (*i.e.* normoxia). However, the presence of DPCPX during hypoxia plus re-oxygenation induced a significant increase (P=0.045) in glutamate C4Q/D45 (Figure 4.11B), indicating that the oxidation of glucose through the TCA cycle is indeed modified upon blockade of A_1 receptors. The values calculated for GABA C2Q/D12 show a trend similar to those obtained in glutamate C4Q/D45 (P=0.027). The amount of glutamate C4D34/S and of GABA C2D23/S reflect the metabolism of [2-^{13}C]acetate in the TCA cycle presumably in the astrocytic compartment. It is worth mentioning that their modification upon hypoxia and re-oxygenation in the presence of DPCPX displayed an opposite qualitative variation in contrast to the isotopomer populations of glutamate and GABA that reflect glucose oxidation (Figure 4.11B). This suggests that in the specific case of the putative astrocytic compartment, A_1 receptors may differentially regulate the formation of

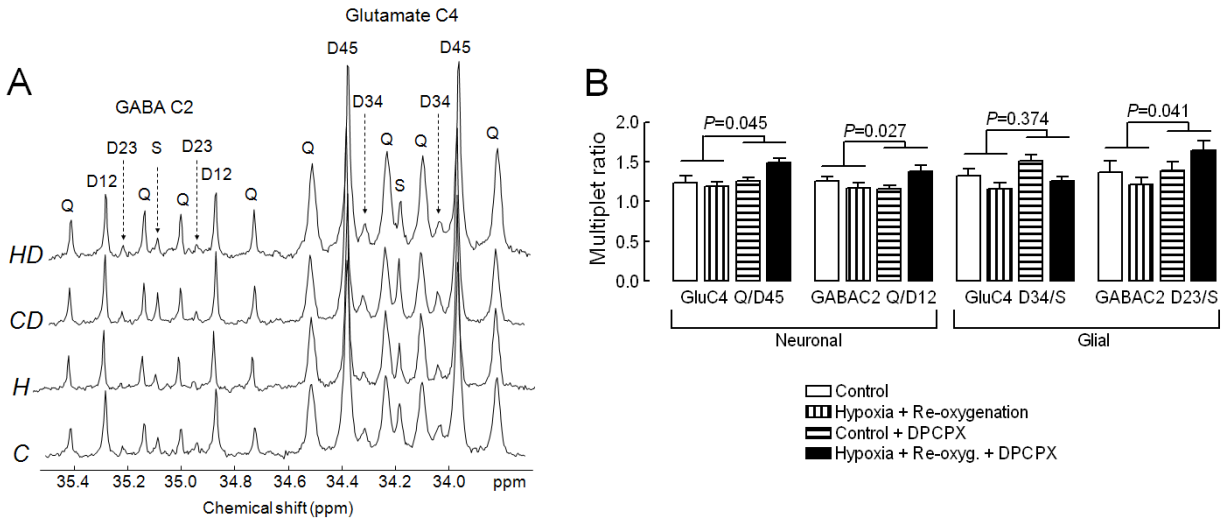

Figure 4.11. Panel A shows expansions of glutamate C4 and GABA C2 resonances from representative ^{13}C NMR spectra obtained from PCA extracts of hippocampal slices superfused as described before, for the 4 experimental conditions: normoxia (C), hypoxia plus re-oxygenation (H), normoxia plus DPCPX (CD), hypoxia plus re-oxygenation plus DPCPX (HD). In panel B shows calculated multiplet ratios from GluC4 and GABAC2 resonances. Values presented as mean±SEM (n=5-6). Student's *t* test was used to compare the effect of the presence and absence of DPCPX on the variation of multiplet ratios induced by hypoxia and re-oxygenation.

glutamate and GABA upon hypoxia followed by re-oxygenation.

4.1.3.4. Discussion

The present work provides the first direct demonstration that the tonic activation of adenosine A_1 receptors plays an important role in the recovery on re-oxygenation of the metabolic alterations caused by transient hypoxia in rat hippocampal slices. This complements previous work showing that the hypoxia-induced adenosine release from both neuronal and astrocytic sources (Frenguelli *et al*., 2003, Martin *et al*., 2007) contributes for the hypoxia-induced depression of excitatory synaptic transmission through activation of A_1 receptors (*e.g.* Fowler *et al*., 1989, 1993; Gribkoff *et al*., 1990), an effect that is crucial to prevent the long-term impairment of neuronal circuits (Arrigoni *et al*., 2005; Johansson *et al*., 2001; Sebastião *et al*., 2001). Since metabolic modifications have a strong impact on the efficiency of synaptic transmission (Nicholls, 2003), the present results indicate that this ability of A_1 receptors to control neuronal metabolism may be a mechanism by which adenosine affords brain neuroprotection upon acute noxious brain insults, such as upon hypoxia.

The reduced availability of oxygen during hypoxia caused an expected reduction of the energetic status of the preparation, typified by a decreased energy charge and phosphocreatine/creatine ratio (see also Brooks *et al*., 1989; Ikeda *et al*., 1988; Kauppinen and Williams, 1990; Müller *et al*., 1994). This likely results from a decreased flow through the TCA cycle upon decreased regeneration of reducing equivalents by the mitochondrial O_2-driven respiratory chain (*e.g.* Chateil *et al*., 2001), in spite of the increased flow through the glycolytic pathway that is aimed at fulfilling the energetic requirements of the tissue. This was experimentally confirmed, as concluded from the increased levels of the end-products of anaerobic glycolysis (lactate, pyruvate and alanine) as well as an higher release of lactate, together with decreased levels of glutamine, which suggests either a lower metabolic trafficking from the astrocytic TCA cycle to neurons (Chateil *et al*., 2001; Müller *et al*., 1994) that leads to reduced synthesis of glutamate and GABA from glutamine, or reduced glutamate and GABA turnover in neurons (Chateil *et al*., 2001). The blockade of A_1 receptors using the selective A_1 receptor antagonist DPCPX, caused an imbalance of this coordinated set of metabolic alterations triggered by hypoxia. Thus, the blockade of A_1 receptors during hypoxia aggravated the increase of the glycolytic flux, translated in a further increase of lactate, pyruvate and alanine. Concomitantly, the presence of DPCPX during hypoxia increased the levels of excitatory amino acids (glutamate and aspartate) and increased GABA levels, which might

be explained by an adaptation of the cells that release these inhibitory transmitter to compensate the lack of inhibitory modulation operated by the adenosinergic system during hypoxia (see also Lucchi *et al*., 1996).

Finally, it is interesting to note that the blockade of A_1 receptors during hypoxia increased the levels of myo-inositol and of total creatine-containing compounds, which is in accordance with previous suggestions that adenosine might control osmo-adaptation in brain tissues (Saransaari and Oja, 2000) that are expected to occur upon hypoxia-induced ionic imbalance (Martin *et al*., 1994). The elevated NAA content upon blockade of A_1 receptors is in accordance with its roles in osmo-regulation and storage of aspartate, which was also elevated (Baslow, 2003).

As occur with hypoxia-induced decrease of synaptic transmission (see Arrigoni *et al*., 2005; Johansson *et al*., 2001; Sebastião *et al*., 2001), all the hypoxia-induced metabolic modifications recovered upon re-oxygenation, and this metabolic recovery was prevented by the blockade of A_1 receptors. The most prominent finding was that the energy charge of hippocampal slices, which decreased on hypoxia and was restored after re-oxygenation, failed to decrease on hypoxia and was decreased after re-oxygenation in the presence of DPCPX. This indicates that the hypoxia-induced modification of the energy charge and reducing equivalents of the tissue are under the control of A_1 receptors and are imbalanced by the blockade of the A_1 receptors during hypoxia and re-oxygenation. The metabolic analysis carried out in the present work provides further indications on some metabolic pathways modified by the blockade of A_1 receptors on hypoxia and re-oxygenation. Namely there was an increase in the concentration of end-products of the glycolytic pathway, in particular of alanine. Since the release of lactate during hypoxia in the presence of DPCPX was lower than during hypoxia alone (Figure 4.10), it is expected that the observed increase in the levels of lactate correspond to an accumulation of intracellular lactate that contribute to an acidification of the intracellular medium rather than to provide a metabolic source for neurons on re-oxygenation (Bouzier-Sore *et al*., 2003; Tyson *et al*., 2003; Westergaard *et al*., 1995). In parallel, the presence of DPCPX during hypoxia plus re-oxygenation caused a permanent non-recoverable modification of the levels of glutamine and aspartate as well as the ratio glutamate/glutamine, suggesting an impairment of the glutamate-glutamine cycle (Hertz *et al*., 1999; Westergaard *et al*., 1995). Furthermore, the blockade of A_1 receptors led to an increase in the flow rate of TCA cycle upon re-oxygenation, as evaluated in the ^{13}C isotopomer analysis after [U-^{13}C]glucose metabolization. The decrease of oxygen availability during hypoxia is expected to decrease the flow rate of the TCA cycle (*e.g.* Chateil *et al*., 2001) in an effort to reduce the amount of reducing equivalents that are a potential source of toxic free radicals when handled in the mitochondria respiratory chain, effect that is particularly problematic upon re-oxygenation when there is a full load of reducing

equivalents and oxygen becomes available. Control systems have been proposed to understand how the flow rate of the TCA cycle is contained on re-oxygenation to avoid excessive formation of free radicals (*e.g.* Tretter and Adam-Vizi, 2004), and the presently observed increase in the flow rate of the TCA cycle on re-oxygenation in the presence of DPCPX suggest that A_1 receptors constitute one possible system with the ability to restrain the burst in the flow rate of the TCA cycle on re-oxygenation. Furthermore, since [2-^{13}C]acetate metabolism was not significantly modified and considering that carbon atoms from [U-^{13}C]glucose oxidized in astrocytes are mainly transported into neurons in the form of lactate (reviewed in Magistretti and Pellerin, 1999; Pellerin, 2003), it can be inferred that it is the neuronal TCA cycle that is mainly affected by the blockade of A_1 receptors, which is in accordance with the greater abundance of A_1 receptors in neurons compared to astrocytes (reviewed in Fredholm *et al.*, 2005). Overall, the obtained results suggest that the activation of A_1 receptors by endogenous adenosine during re-oxygenation following hypoxia plays a key role in the control of neuronal intermediary metabolism.

One important aspect that should be highlighted is the potential differences in metabolism between superfused hippocampal slices and native hippocampal tissue. One experimental limitation of slices is that the metabolic substrates are added by superfusion rather than through the vascular system. This may explain why it was concluded that neuronal metabolism was more intense than its astrocytic counterpart in spite of astrocytes being the most abundant cell type in brain tissue. In fact, astrocytes play a key role in the uptake of substrates from blood vessels (Magistretti and Pellerin, 1999), a role that is not expected to occur in superfused slices. Furthermore, our ability to discriminate astrocytic from neuronal metabolism relies on the use of [2-^{13}C]acetate, which was used in a concentration lower than [U-^{13}C]glucose to avoid the possibility of metabolic modifications due to toxicity, and this may also contribute to hamper our ability to highlight the importance of astrocytic metabolism. However, in spite of these technical limitations, the present study provides the first direct evidence that the tonic activation of adenosine A_1 receptors controls the recovery of hippocampal intermediary metabolism from transient hypoxia, which may be the mechanistic basis for the neuroprotection afforded by adenosine upon acute hypoxic insults.

4.2. Diabetes-induced modification of neuromodulation systems

As previously introduced, diabetes is often accompanied by cognitive deficits and modifications of hippocampal function and plasticity. Since reduced cognitive performance results from impairment on synaptic events, and diabetes result on metabolic alterations that may affect hippocampal metabolism, it was now studied if diabetes affected neuromodulation systems in both synaptic and extra-synaptic compartments of the hippocampus.

4.2.1. Modification of adenosine A_1 and A_{2A} receptors in the hippocampus of streptozotocin-induced diabetic rats

Adenosine is a neuromodulator acting mainly through metabotropic A_1 and A_{2A} receptors in the brain (reviewed in Fredholm *et al*., 2005), which can control memory performance in rodents (*e.g.* Kopf *et al*., 1999; Prediger *et al*., 2005). Although the A_1 receptor is the predominant adenosine receptor in the limbic and neo-cortex, chronic noxious brain conditions trigger a down-regulation of these inhibitory receptors and cause a parallel up-regulation of facilitatory A_{2A} receptors (reviewed in Cunha, 2005). Interestingly, a previous study reported a change of adenosine sensitivity in the hippocampus of diabetic rats (Morrison *et al*., 1992), suggesting that diabetic conditions may also induce an adaptation of the density of adenosine receptors in the brain. To test if the implementation of a diabetic state triggers a long-term modification of the density of brain adenosine receptors, it was evaluated if the density of adenosine A_1 and A_{2A} receptors and the expression of their mRNA are modified in the hippocampus of STZ-induced diabetic rats, from 7 to 90 days after diabetes induction.

For this study Wistar rats (8 weeks old) were treated with STZ and maintained with food

Table 4.7. Body weight and glycaemia of the rats used in the experiments before and after the induction of diabetes (* P<0.01, different from control; **P<0.01, different from before treatment; n.d., not determined).

	Weight (g)		**Glycaemia (mg/dL)**	
	Control	STZ-treated	Control	STZ-treated
Before treatment (n=8)	203.9±7.4	209.1±6.3	97.8±5.6	97.8±5.3
3 days after treatment (n=8)	n.d.	n.d.	101.5±7.8	423.5±26.1 *,**
7 days after treatment (n=8)	213.3±14.6	216.1±3.3	99.8±6.7	453.1±21.3 *,**
30 days after treatment (n=8)	304.0±16.5 **	220.1±10.4 *	104.2±4.4	497.3±31.0 *,**
90 days after treatment (n=6)	415.6±14.6 **	267.0±11.8 *	102.1±5.2	506.1±18.5 *,**

and water *ad libitum* for 7, 30 and 90 days. After STZ administration, rats displayed sustained hyperglycaemia and failed to gain weight (Table 4.7).

4.2.1.1. Modification of A_1 receptor density in total hippocampal membranes

The specific binding of the selective A_1 receptor antagonist, [^{3}H]DPCPX (10 nM), to total hippocampal membranes was 629±28 fmol/mg protein (n=12). As illustrated in Figure 4.12A, there was a lower (P<0.05) density of binding of [^{3}H]DPCPX to hippocampal membranes derived from STZ-induced diabetic rats. Thus, the specific binding of ^{3}H-DPCPX (10 nM) to total hippocampal membranes derived from rats 7 days after STZ administration was 409±49 fmol/mg protein (n=4, P<0.05) and remained lower than control (P<0.05) in total hippocampal membranes 30 days (437±15 fmol/mg protein, n=4) and 90 days (451±36 fmol/mg protein, n=4) after STZ administration (Figure 4.12A).

This decreased density of hippocampal A_1 receptors was confirmed by Western blot analysis of A_1 receptor immunoreactivity. As shown in Figure 4.12B, the A_1 receptor immunoreactivity was

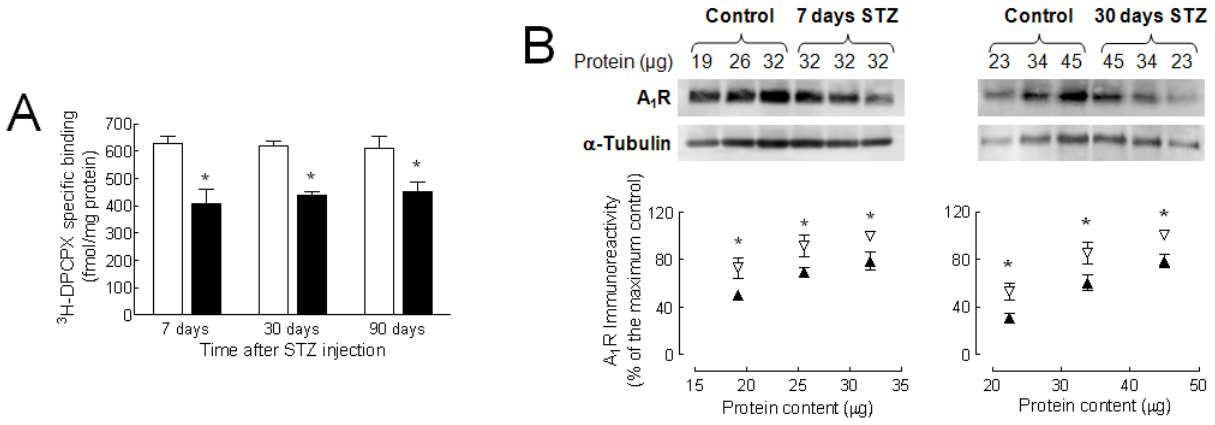

Figure 4.12. Decrease of the density of adenosine A_1 receptors in total hippocampal membranes from STZ-induced diabetic rats. Panel A shows the average specific binding of a saturating but selective concentration (10 nM) of the A_1 receptor antagonist [^{3}H]DPCPX to total membranes prepared from the hippocampus of control rats (open bars) or age-matched rats treated with STZ (filled bars) after different time periods, as indicated below each pair of bars. Results are mean±SEM of 4 experiments performed in duplicate. *P<0.05 between control and STZ-treated rats. Panel B shows a Western blot (representative of 4-5 similar blots from different groups of rats) comparing the A_1 receptor immunoreactivity, corresponding to the 37 kDa band, in total hippocampal membranes from control and STZ-treated rats after 7 days (left column) and after 30 days (right column), applied in different quantities to the SDS-PAGE gel as indicated above each lane. A re-probing of the membranes to detect α-tubulin is shown below each gel in each panel, and confirmed that similar concentrations of protein were added for each amount of total hippocampal membrane protein. The graphs below the gels show the average relative immunoreactivity of A_1 receptors in total hippocampal membranes from control rats (open symbols) and from STZ-treated rats (filled symbols) according to the amount of protein applied to gel in 4-5 different Western blot analysis using membranes from different groups of animals. *P<0.05 comparing A_1 receptor immunoreactivity between control and STZ-treated rats.

systematically less intense (21.9±4.2% lower, n=4, P<0.05) in total hippocampal membranes 7 days after STZ-induced diabetes. This decreased A_1 receptor immunoreactivity was maintained in total hippocampal membranes derived from rats sacrificed 30 days (21.4±4.6% lower, n=5, P<0.05) after STZ administration (Figure 4.12B). Western blot analysis was not performed to confirm the binding data obtained using membranes derived from rats maintained for 90 days in chronic hyperglycaemia after STZ injection because the higher mortality rate of this group limited the amount of biological material available.

4.2.1.2. Modification of A_{2A} receptor density in total hippocampal membranes

The effect of STZ-induced diabetes on the density of hippocampal A_{2A} receptors was the opposite of that observed for A_1 receptors. First, it is important to stress that the specific binding of the selective A_{2A} receptor antagonist, [^{3}H]SCH58261 (6 nM), to total hippocampal membranes was 26.1±4.1 fmol/mg protein (n=12), *i.e.* near 25-times lower than the binding of the A_1 receptor ligand (see above). However, whereas diabetes led to a decrease of A_1 receptors binding density (see Figure 4.12A), there was a higher (P<0.05) density of binding of [^{3}H]SCH58261 to hippocampal membranes derived from STZ diabetic rats (Figure 4.13). Thus, the specific binding of [^{3}H]SCH58261 (6 nM) to total hippocampal membranes derived from rats 7 days after STZ administration was 54.2±11.9 fmol/mg protein (n=4, P<0.05) and remained higher than control (P<0.05) in total hippocampal membranes 30 days (54.8±12.1 fmol/mg protein, n=4) and 90 days (41.6±6.3 fmol/mg protein, n=4) after STZ administration (Figure 4.13).

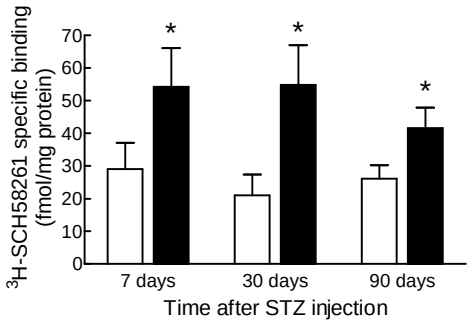

Figure 4.13. Increase of the binding density of A_{2A} receptors in total hippocampal membranes from STZ-induced diabetic rats. The ordinates represent the average specific binding of a saturating but selective concentration (6 nM) of the A_{2A} receptor antagonist, [^{3}H]SCH58261, to total membranes prepared from the hippocampus of control rats (open bars) or age-matched rats treated with STZ (filled bars) after different time periods, as indicated below each pair of bars. Results are mean±SEM of 4 experiments performed in duplicate. *P<0.05 between control and STZ-treated rats.

4.2.1.3. Modification of A_1 and A_{2A} receptor densities in hippocampal nerve terminals

In the hippocampus, both adenosine A_1 receptors (Rebola *et al*., 2003a) and A_{2A} receptors (Rebola *et al*., 2005a) are enriched in nerve terminals. Thus, it was next tested if the diabetes-induced modification of the density of A_1 and A_{2A} receptors was most evident in nerve terminals. The specific binding of [^{3}H]DPCPX (10 nM) to synaptosomal membranes was 985±78 fmol/mg protein, *i.e.* twice larger than that found in total membranes. Interestingly, as illustrated in Figure 4.14A, the

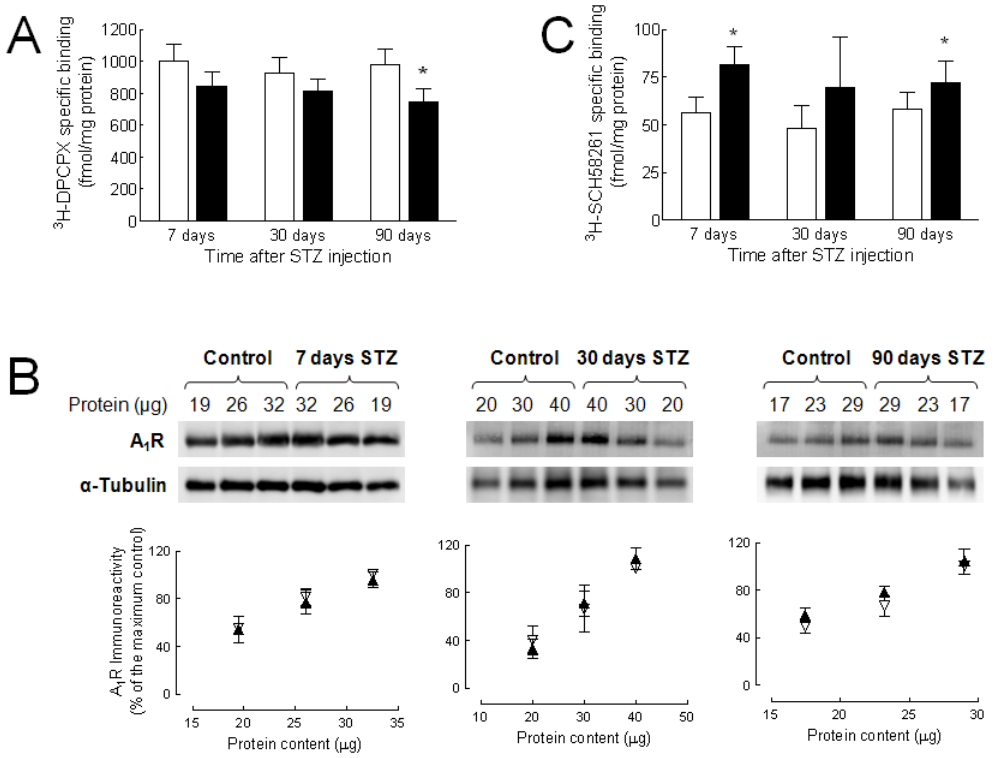

Figure 4.14. Absence of modification of the density of A_1 receptors and minor increase of the density of A_{2A} receptors in nerve terminals membranes from streptozotocin diabetic rats. Panel A shows the average specific binding of a saturating but selective concentration (10 nM) of the A_1 receptor antagonist, [^{3}H]DPCPX, to nerve terminals membranes prepared from the hippocampus of control rats (open bars) or age-matched rats treated with STZ (filled bars) after different time periods, as indicated below each pair of bars. Results are mean±SEM of 4 experiments performed in duplicate. *P<0.05 between control and STZ-treated rats. Panel B shows a Western blot (representative of 4-5 similar blots from different groups of rats) comparing the A_1 receptor immunoreactivity, corresponding to the 37 kDa band, in nerve terminal hippocampal membranes from control rats and from rats treated with STZ after 7 days (left column) and after 30 days (central column) and after 90 days (right column), applied in different quantities to the SDS-PAGE gel as indicated above each lane. A re-probing of the membranes with an anti-α-tubulin antibody, shown below each gel in each panel, confirmed that similar concentrations of protein were added for each amount of nerve terminal membranes. The graphs below the gels show the average relative immunoreactivity of A_1 receptors in nerve terminal hippocampal membranes from control rats (open symbols) and from STZ-induced diabetic mice (filled symbols) according to the amount of protein applied to gel in 4-5 different Western blot analysis using membranes from different groups of animals. *P<0.05 comparing A_1 receptor immunoreactivity in the two groups of animals. Panel C shows the average specific binding of a saturating but selective concentration (6 nM) of the A_{2A} receptor antagonist, [^{3}H]SCH58261, to nerve terminal membranes prepared from the hippocampus of control rats (open bars) or age-matched rats treated with STZ (filled bars) after different time periods, as indicated below each pair of bars. Results are mean±SEM of 4 experiments performed in duplicate. *P<0.05 between control and STZ-treated rats.

binding density of [^{3}H]DPCPX (10 nM) was not significantly (P>0.05) modified in synaptosomal membranes derived from STZ-treated rats (7-30 days). Likewise, the A_1 receptor immunoreactivity was similar (P>0.05) in synaptosomal membranes from control and STZ-treated rats (Figure 4.14B).

The average binding density of [^{3}H]SCH58261 (6 nM) to synaptosomal membranes (54.6±8.3 fmol/mg protein, n=12) was also twice larger than that observed in total hippocampal membranes. This binding density of A_{2A} receptors in synaptosomal membranes also tended to be larger upon STZ-induced diabetes, although with a lower amplitude than that observed to occur in total membranes. Thus, as illustrated in Figure 4.14C, the specific binding of [^{3}H]SCH58261 (6 nM) to synaptosomal hippocampal membranes derived from rats 7 days after STZ administration was 81.4±9.4 fmol/mg protein (n=4, P<0.05), there was a tendency for an increase that failed to reach statistical significance (P>0.05) after 30 days (69.8±26.4 fmol/mg protein, n=4) and it was again larger (P<0.05) than control after 90 days (72.2±11.3 fmol/mg protein, n=4).

This modified density of facilitatory A_{2A}, but not inhibitory A_1 receptors, in nerve terminals of STZ-induced diabetic rats might be related with changes in the efficiency of functioning of hippocampal synapses, typified by changes in the vesicular apparatus of hippocampal nerve terminals. In fact, the immunoreactivity of syntaxin, a protein located in synaptic vesicles, was decreased in synaptosomal membranes from the hippocampus of STZ-treated rats compared to controls (Figure 4.15). Thus, syntaxin immunoreactivity was 24.2±4.6% (n=5), 25.0±5.6% (n=6) and 20.9±4.1% (n=3) lower in hippocampal nerve terminal membranes from STZ-induced diabetic rats

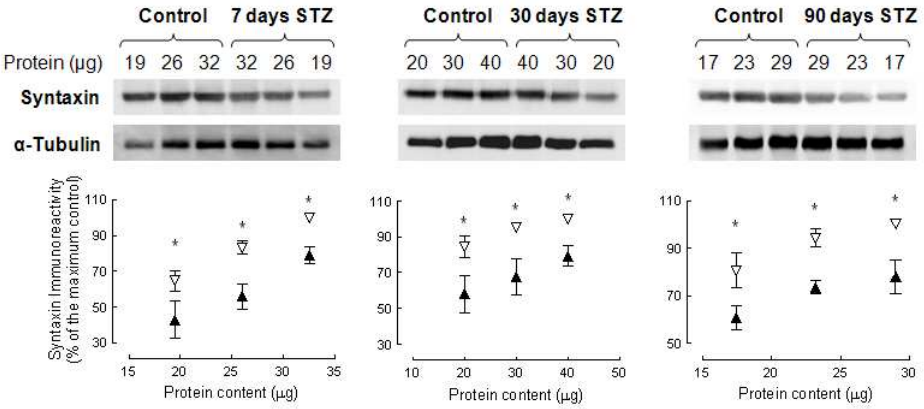

Figure 4.15. Decrease of syntaxin immunoreactivity in nerve terminal membranes from STZ-induced diabetic rats. The top gels correspond to a Western blot (representative of 4-5 similar blots from different groups of rats) comparing the syntaxin immunoreactivity, corresponding to the 37 kDa band, in nerve terminal membranes from the hippocampus of control rats and STZ-induced diabetic rats 7 (left column), 30 (central column) and 90 (right column) days after STZ administration. The membranes were applied in different quantities to the SDS-PAGE gel as indicated above each lane, and a re-probing of the membranes with anti-α-tubulin antibody, shown below each gel in each panel, confirmed that similar concentrations of protein were added for each amount of nerve terminal membranes. The graphs below the gels show the average relative immunoreactivity of syntaxin in nerve terminal hippocampal membranes from control rats (open symbols) and from STZ diabetic rats (filled symbols) according to the amount of protein applied to gel in 4-5 different Western blot analysis using membranes from different groups of animals. *P<0.05 comparing syntaxin immunoreactivity in the two groups of animals.

after 7 days, 30 days and 90 days, respectively, compared to their age-matched controls (see Figure 4.15).

4.2.1.4. Modification of A_1 and A_{2A} receptor mRNA expression in the hippocampus

To test whether modification of adenosine receptor density in the hippocampus of STZ-induced diabetic rats was caused by altered transcriptional processes, it was performed a quantitative analysis of mRNA expression by semi-quantitative real-time PCR. As shown in Figure 4.16A, the expression of A_1 receptor mRNA was significantly increased by 31.2±15.8% (n=7, P<0.05) in the hippocampus of STZ-treated rats 30 days after treatment, relative to control rats. On the contrary, STZ-induced diabetes failed to alter significantly the expression of A_{2A} receptor mRNA (Figure 4.16B). These results suggest that A_1 and A_{2A} receptor density is modified through mechanisms unrelated to the mRNA transcription.

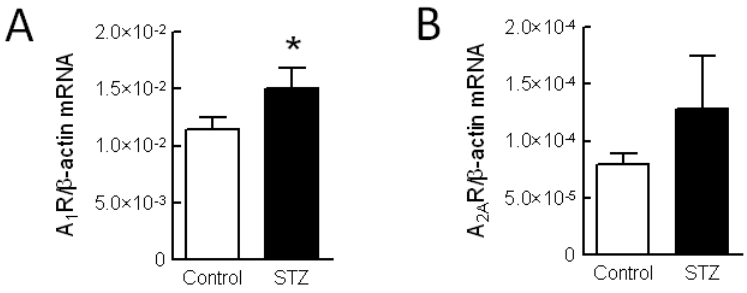

Figure 4.16. Expression of A_1 (panel A) and A_{2A} (panel B) receptor mRNA in the hippocampus of STZ-treated (black bars) and age-matched control (adjacent open bars) rats. Receptor mRNA expression was quantified by real-time PCR analysis and normalized to β-actin mRNA expression, and presented as mean±SEM of 7 experiments from different rats. Relative A_1 receptor mRNA expression was significantly increased in the hippocampus of STZ-treated rats when compared to controls (* P<0.05).

4.2.1.5. Discussion

The present results provide direct evidence that the density of adenosine A_1 and A_{2A} receptors is modified in the hippocampus of STZ-induced diabetic rats. In particular, there was a down-regulation of inhibitory A_1 receptors and an up-regulation of facilitatory A_{2A} receptors, indicating that the induction of diabetes is accompanied by an imbalance of the set-up of adenosine receptors in the rat hippocampus.

Diabetes can lead to several functional and morphological modifications in the central nervous system (reviewed in Artola *et al.*, 2002; Gispen and Biessels, 2000). Interestingly, the

observed modification of the density of adenosine receptors upon diabetes is in close agreement with the modification of the density of cortical adenosine receptors in other noxious brain conditions (reviewed in Cunha, 2005). In fact, the induction of epilepsy, either through kainate injection or electrical kindling (Rebola *et al*., 2005b), or sub-chronic restraint stress (Cunha *et al*., 2006) also led to a down-regulation of inhibitory A_1 receptors and an up-regulation of A_{2A} receptors in cortical regions, independently of neuronal loss. Likewise, independent studies by different groups have also concluded that ischemic and/or hypoxic insults lead to a long-term down-regulation of A_1 receptors (*e.g.* Lee *et al*., 1986; Nagasawa *et al*., 1994) and a parallel up-regulation of A_{2A} receptors (Kobayashi and Millhorn, 1999). Thus, there is a general trend for the occurrence of adaptative changes of the set-up of adenosine receptors upon prolonged noxious brain conditions, namely a decrease of inhibitory A_1 receptors and an increase of facilitatory A_{2A} receptors, which was now extended in the case of STZ-induced diabetes.

The mechanism by which STZ-induced diabetes leads to the observed modification of the density of hippocampal adenosine receptors still remains to be established. In other chronic noxious brain conditions, it has been proposed that the long-term down-regulation of A_1 receptors would be a consequence of their prolonged activation by endogenous adenosine. In fact, noxious insults to brain tissue trigger a sustained release of adenosine (reviewed in Latini and Pedata, 2001) and the prolonged activation of A_1 receptors leads to their down-regulation (*e.g.* Fernandez *et al*., 1996; Hettinger *et al*., 1998). However, it remains to be determined if STZ-induced diabetes enhances the extracellular levels of adenosine in the hippocampus. As for the up-regulation of A_{2A} receptors in noxious conditions, it is still awaiting for a candidate mechanism. But irrespective of the mechanism(s) underlying this opposite change of the density of hippocampal adenosine receptors upon implementation of a diabetic condition, the present results show that it is an early and sustained event. In fact, the up-regulation of A_{2A} receptors and down-regulation of A_1 receptors in the hippocampus is already present 7 days after STZ-induced diabetes, *i.e.* at a time when functional modifications of hippocampal circuit are not expected to be present (see Biessels *et al*., 1998 an references therein), and remains qualitatively constant up to 90 days after injection of STZ.

Cerebral cortical adenosine A_1 and A_{2A} receptors are enriched in synapses (Rebola *et al*., 2003a, 2005a) and their most widely recognized role is their ability to control synaptic transmission (reviewed in Fredholm *et al*., 2005). However, the changes of the density of adenosine receptors upon STZ-induced diabetes were most evident in total hippocampal membranes rather than in nerve terminal membranes, implying that it is extra-synaptic A_1 and A_{2A} receptors which are affected. This implies that the eventual role associated with the STZ-induced modification of the density of adenosine receptors is probably unrelated to the control of neurotransmitter release. Most

relevant for diabetes is the evidence that extracellular adenosine, operating through A_1 and A_{2A} receptors, acts as a regulator of brain metabolism (Blood *et al*., 2003; Håberg *et al*., 2000; Hammer *et al*., 2001; Magistretti *et al*., 1986), as is well documented to occur in different peripheral organs such as the heart (*e.g.* Wyatt *et al*., 1989). Given that diabetes is recognized as a metabolic disease, further work ought to be designed to investigate if adenosine receptors might control diabetes-induced metabolic modifications in the hippocampus (*e.g.* Biessels *et al*., 2001).

One of the prominent central modifications arising in diabetic patients is modified hippocampal morphology and function that is accompanied by a cognitive deterioration (see general introduction). This is particularly evident in young adult patients with type 1 diabetes (see Brands *et al*., 2005) and the encephalopathic modifications caused by diabetes resemble a condition of advanced aging, namely increasing the risk of dementia (reviewed in Artola *et al*., 2002). Interestingly, there is also an up-regulation and gain of function of hippocampal A_{2A} receptors upon aging (Rebola *et al*., 2003b) together with a down-regulation of A_1 receptors (Sebastião *et al*., 2000). Furthermore, adenosine A_{2A} receptors have recently been shown to be involved in the age-associated decline in memory performance in aged rats (Prediger *et al*., 2005). This raises the hypothesis that the blockade of adenosine A_{2A} receptors, which were now found to be up-regulated in the hippocampus of STZ-induced diabetic rats, might eventually counteract the cognitive deterioration associated with diabetes. Indirect support for this hypothesis is provided by the observation that the consumption of caffeine (an adenosine receptor antagonist, which mostly acts as an A_{2A} receptor antagonist when consumed chronically, see Quarta *et al*., 2004) is associated with a substantially lower risk of type 2 diabetes (*e.g.* van Dam and Hu, 2005; Salazar-Martinez *et al*., 2004). With respect to type 1 diabetes, caffeine intake may be a risk factor in childhood (Tuomilehto *et al*., 1990), probably because there is an ontogenic inversion of the role of brain adenosine receptors (Rebola *et al*., 2005c; reviewed in Cunha, 2005), whereas moderate caffeine consumption has been proposed as a useful adjuvant therapy for type 1 diabetic patients with hypoglycemia unawareness (*e.g.* Debrah *et al*., 1996).

Together with the protein density of adenosine receptors, it was evaluated the expression of A_1 and A_{2A} receptor mRNAs in the hippocampus of STZ-induced rats. Compared to controls, STZ-treated rats displayed increased hippocampal A_1 receptor mRNA expression (opposite to the change in A_1 receptor protein) without alteration in A_{2A} receptor mRNA levels. This observation suggests that the alteration on the density of membrane adenosine receptors may be caused by post-transcriptional events, affecting protein turnover for each of the studied receptors. The increased A_1 receptor mRNA expression may constitute a cellular adaptation to maintain the inhibitory function of the adenosinergic system, since the presence of inhibitory A_1 receptor protein in the membrane

may be required for the occurrence of A_{2A} facilitatory function (Lopes *et al*., 2002) which eventually depends on receptor heteromerization (Ciruela *et al*., 2006).

In summary, the present work provides the first direct demonstration that the set-up of adenosine receptors in the limbic cortex is modified in a rat model of diabetes. The observed up-regulation of A_{2A} receptors, together with the beneficial and protective effects afforded by A_{2A} receptor antagonists in different physio-pathological modifications of brain function (reviewed in Cunha, 2005), prompts the hypothesis that A_{2A} receptor antagonists might be considered as a novel candidate target to control the cognitive deficits associated with diabetes.

4.2.2. Modification of purinergic signalling in the hippocampus of streptozotocin-induced diabetic rats

One promising candidate to target and try to correct diabetes-induced deleterious effects on brain function is the ATP modulation system since it has the simultaneous potential to control neurotransmitter release (*e.g.* Rodrigues *et al*., 2005a) and synaptic plasticity (*e.g.* Pankratov *et al*., 2002), a purported neurophysiological trait of learning and memory (*e.g.* Lynch, 2004), and can also control glucose utilization (*e.g.* Solini *et al*., 2003) and insulin release (*e.g.* Léon *et al*., 2005).

ATP is released by most cells, namely from neurons in an exocytotic manner (North and Verkhratsky, 2006), and extracellular ATP regulates a variety of cellular processes through activation of P2 receptors, which include ionotropic P2X and metabotropic P2Y receptors (Abbracchio *et al*., 2006; Khakh and North, 2006). Extracellular ATP regulates key physiological functions such as neurotransmitter release (Rodrigues *et al*., 2005a), synaptic plasticity phenomena (*e.g.* Almeida *et al*., 2003) and glucose homeostasis, namely through the modulation of insulin secretion (*e.g.* Léon *et al*., 2005), hepatic glucose metabolism and release (Buxton *et al*., 1986; Haussinger *et al*., 1987), and glucose transport in several cell types (Fischer *et al*., 1999; Kim *et al*., 2002; Solini *et al*., 2003). However, extracellular ATP is a double-edge sword signalling system since it is also a danger signal (di Virgilio, 2000), and P2 receptor blockade was shown to afford neuroprotection against metabolic insults (Cavaliere *et al*., 2001a; 2001b), ischemic conditions (*e.g.* Lammer *et al*., 2006) and glutamate toxicity (reviewed in Franke *et al*., 2006).

Previous studies have already indicated diabetes-induced changes of the efficiency of P2 receptors in different peripheral tissues. Thus, the ATP-driven modulation of glucose transport, proposed to rely on P2Y receptor activation (Fischer *et al*., 1999; Kim *et al*., 2002), was found to be impaired in fibroblasts of type 2 diabetic individuals (Solini *et al*., 2003) and changes in pancreatic

P2 receptors were reported to occur in an experimental model of type 1 diabetes (Coutinho-Silva *et al*., 2003). Also, an enhanced $P2X_7$ receptor activity was associated with diabetes-induced vascular damage (Solini *et al*., 2004) and retinopathy (Sugiyama *et al*., 2004) and the $P2X_7$ receptor gene emerges as a candidate susceptibility gene for NOD diabetes (Elliott and Higgins, 2004). This prompts the hypothesis that diabetes may also cause modifications of the purinergic system in the brain, which may lead to an impairment of the physiological actions operated by ATP through the activation of P2 receptors, such as LTP, that may underlie diabetes-induced cognitive impairment. The present study was designed to investigate if the purinergic signalling, namely extracellular ATP homeostasis and the density of different P2 receptors, is altered in the hippocampus of STZ-treated rats, an animal model of type 1 diabetes, which displays learning deficits (*e.g.* Biessels *et al*., 1996).

In this study, male Wistar rats (8 weeks old) were injected with STZ and maintained for 30 days with food and water *ad libitum*. Table 4.8 summarises body weight and glycaemia of both control and diabetic rats.

Table 4.8. Body weight and glycaemia of the rats used in the experiments before and after the induction of diabetes (n=18 for each condition; * P<0.01, different from control; **P<0.01, different from before treatment; n.d., not determined).

	Weight (g)		**Glycaemia (mg/dL)**	
	Control	STZ-treated	Control	STZ-treated
Before treatment	254.7±13.2	245.1±8.0	93.0±6.1	100.5±4.3
3 days after treatment	n.d.	n.d.	108.5±7.8	471.6±24.6 *,**
30 days after treatment	345.7±14.8 **	225.0±5.6 *	105.2±6.4	491.3±16.6 *,**

4.2.2.1. Modification of extracellular ATP concentration and metabolism

It was first evaluated if the diabetic rats presented abnormal extracellular ATP levels in the brain. As shown in Figure 4.17A, one month after STZ-induction of diabetes, the concentration of ATP in the CSF was less than half of that in control rats. The synaptic levels of ATP were also decreased in diabetic rats, as gauged by the reduction of the K^+-induced evoked release of ATP from hippocampal nerve terminals (Figure 4.17B, C).

It was next investigated the rate of extracellular catabolism of ATP by following the hydrolysis of ATP after its addition to a synaptosomal suspension (see Cunha, 2001a). It was found that the rate of hydrolysis of extracellular ATP and the consequent formation of ADP was reduced in hippocampal nerve terminals derived from diabetic rats (Figure 4.18A, B). This indicates that diabetes induces a reduction in the activity of membrane-bound ecto-enzymes involved in ATP catabolism (Figure 4.18C). This global reduction of extracellular ATP homeostasis prompts the

hypothesis that P2 receptors in the brain of diabetic rats may face lower extracellular ATP levels than in control rats.

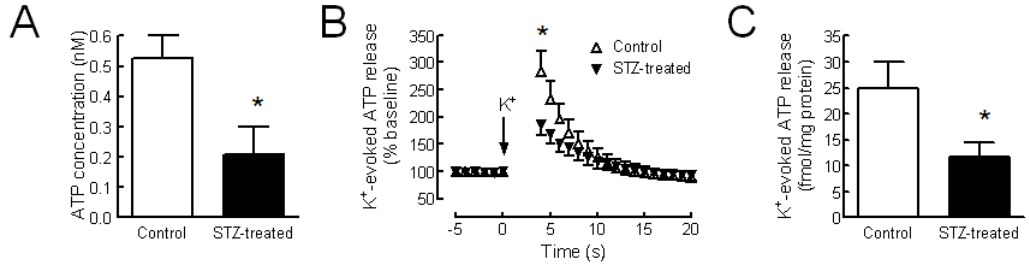

Figure 4.17. Extracellular ATP levels are modified in the brain of STZ-treated rats. Panel A shows ATP concentration in the CSF, measured with a luminometric assay, was lower in diabetic (filled bars) than control (open bars) rats (n=7, * P<0.05). Panel B presents the K^+-evoked release of ATP from hippocampal nerve terminals prepared from STZ-treated rats (filled symbols) was also lower when compared to controls (open symbols). In this experiment, KCl was added at time zero in a concentration of 20 mM, thus depolarising the nerve terminals and triggering a vesicular release of ATP, which was quantified by luminometry. In C are presented the average data showing that the initial evoked release of ATP (measured 4 s after KCl addition) from hippocampal nerve terminals of diabetic (filled bars) was nearly half of that observed in hippocampal nerve terminals of control (open bars) rats (n=4, * P<0.05).

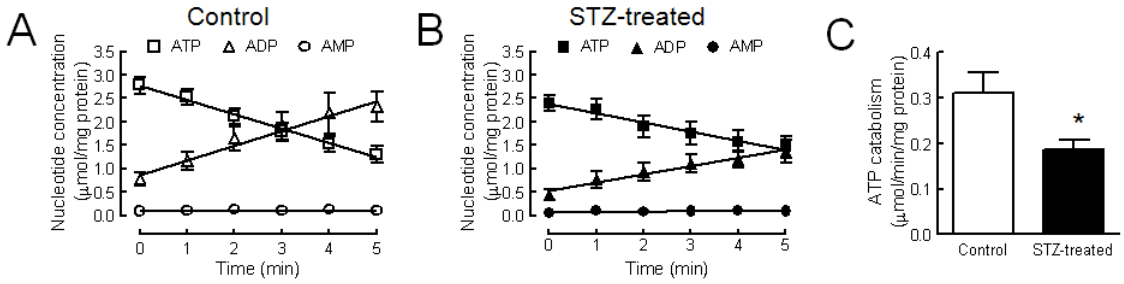

Figure 4.18. Diabetes reduced extracellular ATP hydrolysis activity in rat hippocampal nerve terminals. ATP (10 µM) was added at zero time to rat hippocampal nerve terminals (87-145 µg protein) and samples were collected from the bath at 0, 1, 2, 3, 4 and 5 min. Each collected sample was analysed by HPLC to separate and quantify ATP and its metabolites, ADP and AMP. Panel A and B show the average time-course kinetics of ATP (square symbols) catabolism and consequent formation of ADP (triangle symbols) and AMP (circle symbols) hippocampal nerve terminals in nerve terminals from either control (A) or rats treated one month before with STZ (B). The ordinates display the amount of each nucleotide in the bath at each time point, normalised by the amount of synaptosomal protein in the assay and each point is the mean±SEM of 7 experiments. Panel C displays the average rate of ATP catabolism (n=7, * P<0.05) found in control (open bars) and STZ-treated rats (filled bars). The activity of the ecto-enzymes responsible for the extracellular catabolism of ATP was defined as the rate of ATP degradation. The initial rates were calculated by fitting the initial decrease of ATP concentration normalised by the amount of protein in the assay.

4.2.2.2. Modification of the density of P2 receptors in hippocampal membranes

Since ATP simultaneously fulfils a role as a synaptic modulator (North and Verkhratsky, 2006) and as a non-synaptic role as a neuron-glia messenger (Fields and Burnstock, 2006), it was simultaneously evaluated if there was a modification of the density of P2 receptors in synaptic

membranes and in whole membranes of the hippocampus of diabetic rats. This was achieved with Western blot analysis using antibodies that were previously defined to be selective for hippocampal P2 receptors (Rodrigues *et al*., 2005a). Two or three different amounts of loaded protein (nerve terminals or whole membranes) from the hippocampus of control and diabetic rats were always evaluated in each gel to simultaneously gauge the sensitivity of the Western blot assay. This was attempted for all the P2X receptor subunits and most P2Y receptors and all results were then expressed as average percentage of modification (density found in diabetic relative to its respective control) and summarised in the Figure 4.19.

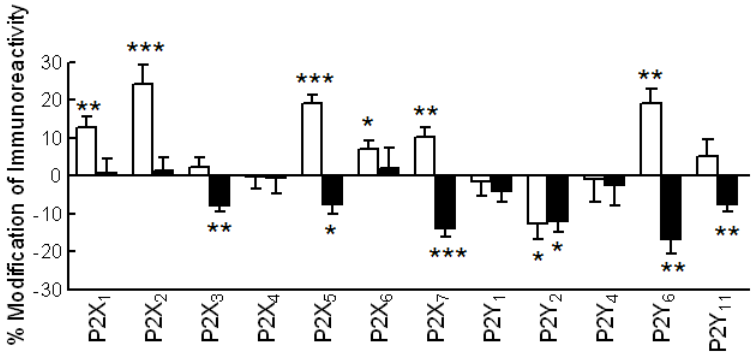

Figure 4.19. STZ-induced diabetes causes opposite modification of the density of P2Rs in nerve terminals (filled bars) and in total membranes (open bars) prepared from the hippocampus. Thus, whereas P2 receptor immunoreactivity tends to decrease in nerve terminal-enriched membranes, there is a global trend for the increase of P2 receptor immunoreactivity in whole membranes of STZ-treated rats relative to controls, as evaluated by Western blot analysis (n=3-8, * P<0.05, ** P<0.01, *** P<0.001).

In hippocampal nerve terminal membranes of diabetic rats one month after STZ-treatment, there was a global trend towards a decrease of the immunoreactivity of P2 receptors. The density of the ionotropic receptors $P2X_3$, $P2X_5$ and $P2X_7$ was decreased by 7.8±1.6% (n=6, P<0.005), 7.5±2.4% (n=6, P<0.03) and 13.7±2.3% (n=6, P<0.0001), respectively (Figure 4.20). Also the density of the metabotropic receptors $P2Y_2$, $P2Y_6$ and $P2Y_{11}$ was reduced by 12.0±3.0% (n=4, P<0.03), 16.7±3.8% (n=4, P<0.005) and 7.5±1.8% (n=3, P<0.005), respectively (Figure 4.21).

In contrast, in whole hippocampal membranes (which include both neurons and mainly glia) of diabetic rats one month after STZ-treatment, there was a global trend towards an increase of the immunoreactivity of P2 receptors. In fact, as illustrated in Figure 4.22, there was an increase of all ionotropic P2 receptors (with the exception of $P2X_3$ and $P2X_4$). There was an increased density of receptors $P2X_1$ (+12.8±3.0%, n=8, P<0.005), $P2X_2$ (+24.4±4.9%, n=8, P<0.0001), $P2X_5$ (+19.2±2.1%, n=5, P<0.0001), $P2X_6$ (+7.1±2.4%, n=5, P<0.03) and $P2X_7$ (+10.2±2.6%, n=6, P<0.001) in whole membranes derived from rats one month after STZ treatment. With respect to metabotropic P2Y receptors in whole hippocampal membranes of diabetic hippocampus, it was found that the density of $P2Y_6$

receptors was 19.3±3.7% larger than control (n=3, P<0.001). In contrast, the density of the other P2Y receptors was not significantly altered (P>0.05) compared to whole membranes from control rats, except for $P2Y_2$ receptors, which density was decreased by 14.1±4.7% (n=7, P<0.03) in diabetic rats (Figure 4.23).

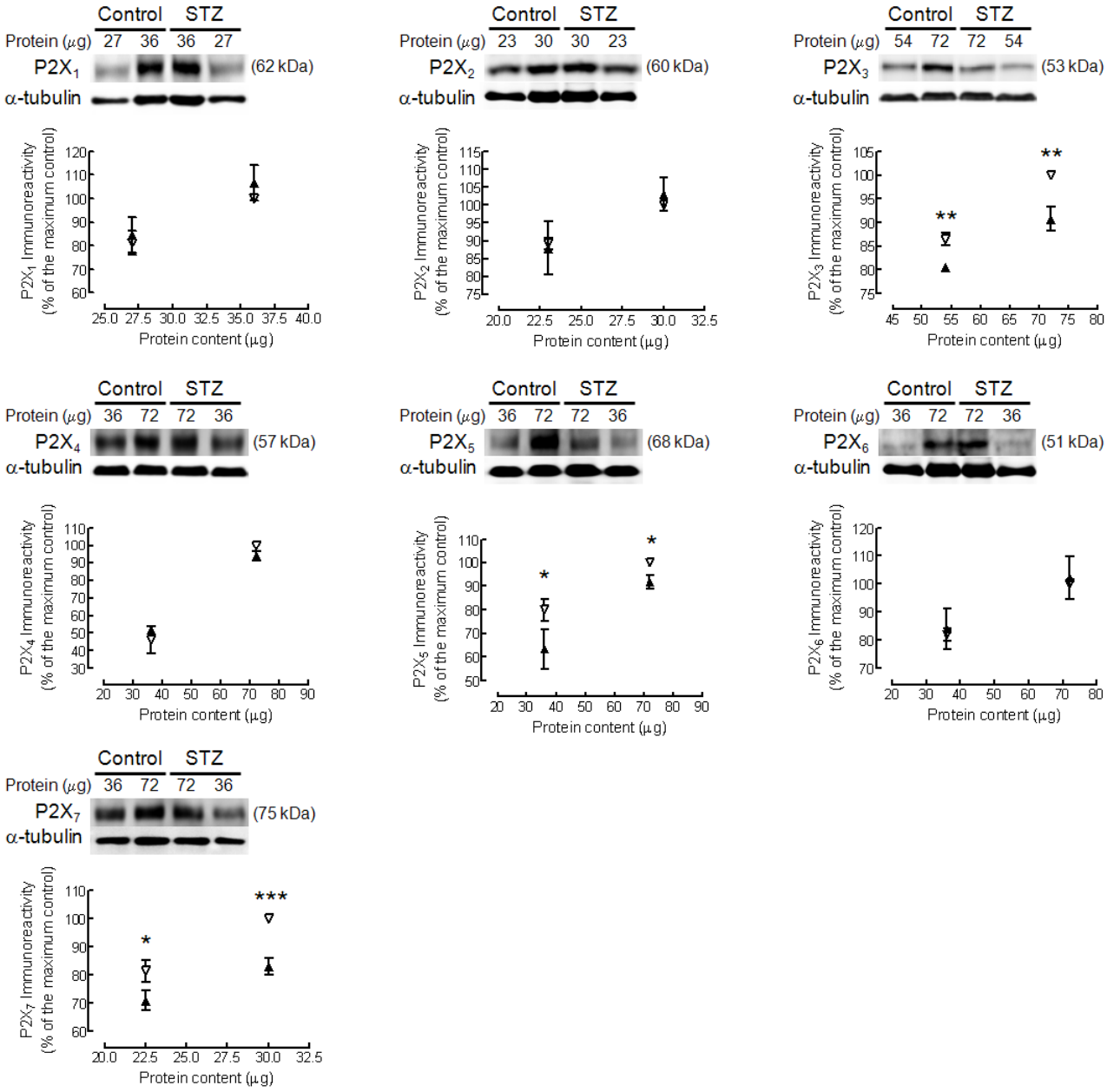

Figure 4.20. Representative Western blots comparing the P2X receptor immunoreactivity in nerve terminal-enriched membranes from the hippocampus of control rats and from rats treated with STZ, applied in different quantities to the SDS-PAGE gel as indicated above each lane. A re-probing of the membranes with an anti-α-tubulin antibody, shown below each gel in each panel, confirmed that similar amounts of protein were added for each concentration of hippocampal membranes. The graphs below the gels show the average relative immunoreactivity of in synaptosomal membranes from control rats (open symbols) and from STZ-treated rats (filled symbols) according to the amount of protein applied to gel in different Western blot analysis using membranes from different groups of rats (n=6 for $P2X_{1,2,3,5,7}$ and n=5 for $P2X_{4,6}$ receptors). * P<0.05, ** P<0.01, *** P<0.001 comparing the immunoreactivity in the two groups of animals.

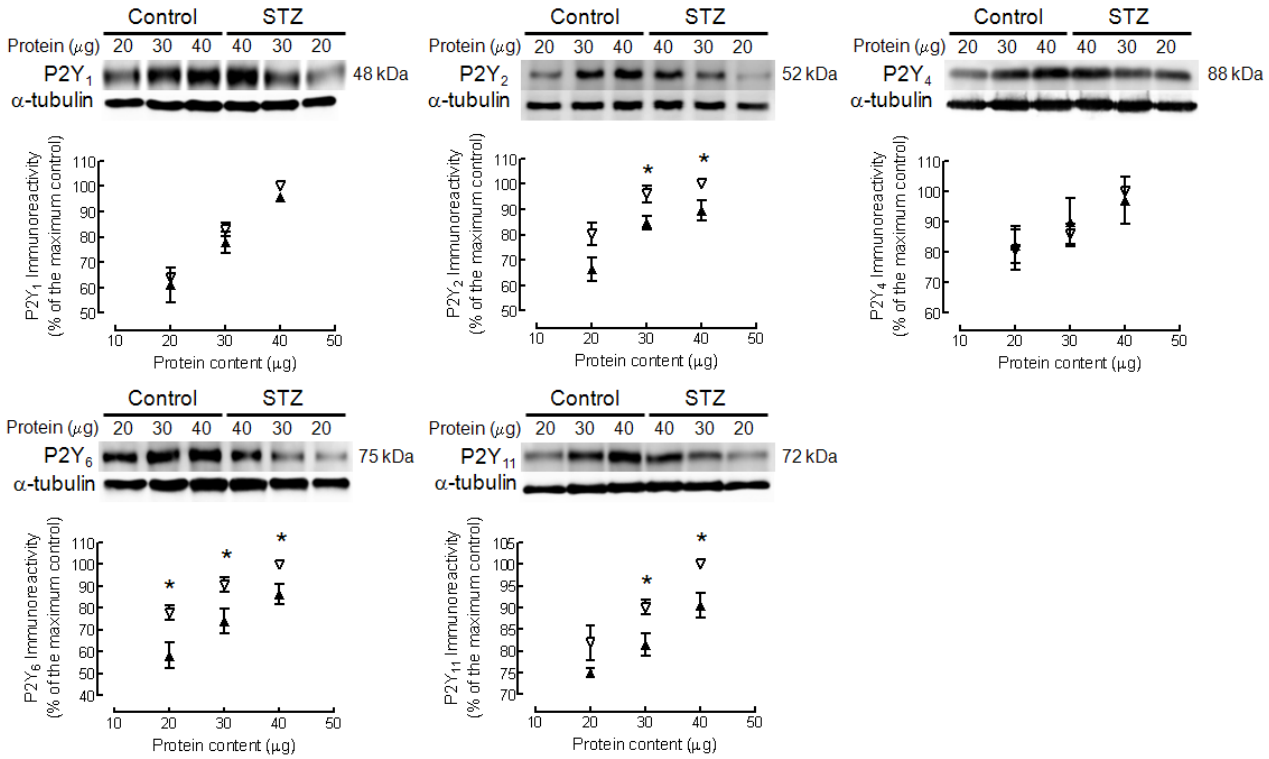

Figure 4.21. Representative Western blots comparing the P2Y receptor immunoreactivity in nerve terminal-enriched membranes from the hippocampus of control rats and from rats treated with STZ, applied in different quantities to the SDS-PAGE gel as indicated above each lane. A re-probing of the membranes with an anti-α-tubulin antibody, shown below each gel in each panel, confirmed that similar amounts of protein were added for each concentration of hippocampal membranes. The graphs below the gels show the average relative immunoreactivity of in synaptosomal membranes from control rats (open symbols) and from STZ-treated rats (filled symbols) according to the amount of protein applied to gel in different Western blot analysis using membranes from different groups of rats (n=3 for $P2Y_{1,11}$ and n=4 for $P2Y_{2,4,6}$ receptors). * $P<0.05$ comparing the immunoreactivity in the two groups of animals.

4.2.2.3. Discussion

The main conclusion of this study is that there is a deregulation of P2 receptor-mediated signalling in the hippocampus of STZ-induced type 1 diabetic rats. It was found that there was a decrease in the CSF levels of ATP in diabetic rats, together with a decrease of the evoked release of ATP in hippocampal nerve terminals, suggesting that P2 receptors may be facing lower concentration of extracellular ATP. Also the extracellular metabolism of ATP is reduced in nerve terminals from the diabetic hippocampus, possibly due to decreased activity of ecto-nucleotidases from the ecto-ATPase family (Zimmermann, 2000). Interestingly, it was found that there was an asymmetric global modification of the density of P2 receptors in synapses and outside synapses in the hippocampus, in accordance with the double role of ATP as a synaptic modulator (North and Verkhratsky, 2006; Cunha and Ribeiro, 2000) and as an extra-synaptic neuron-glia messenger (Fields

and Burnstock, 2006). In fact, in nerve terminal membranes, there was a global decrease of the density of P2 receptors, whereas in whole hippocampal membranes there was a global trend for an increased density of P2 receptors.

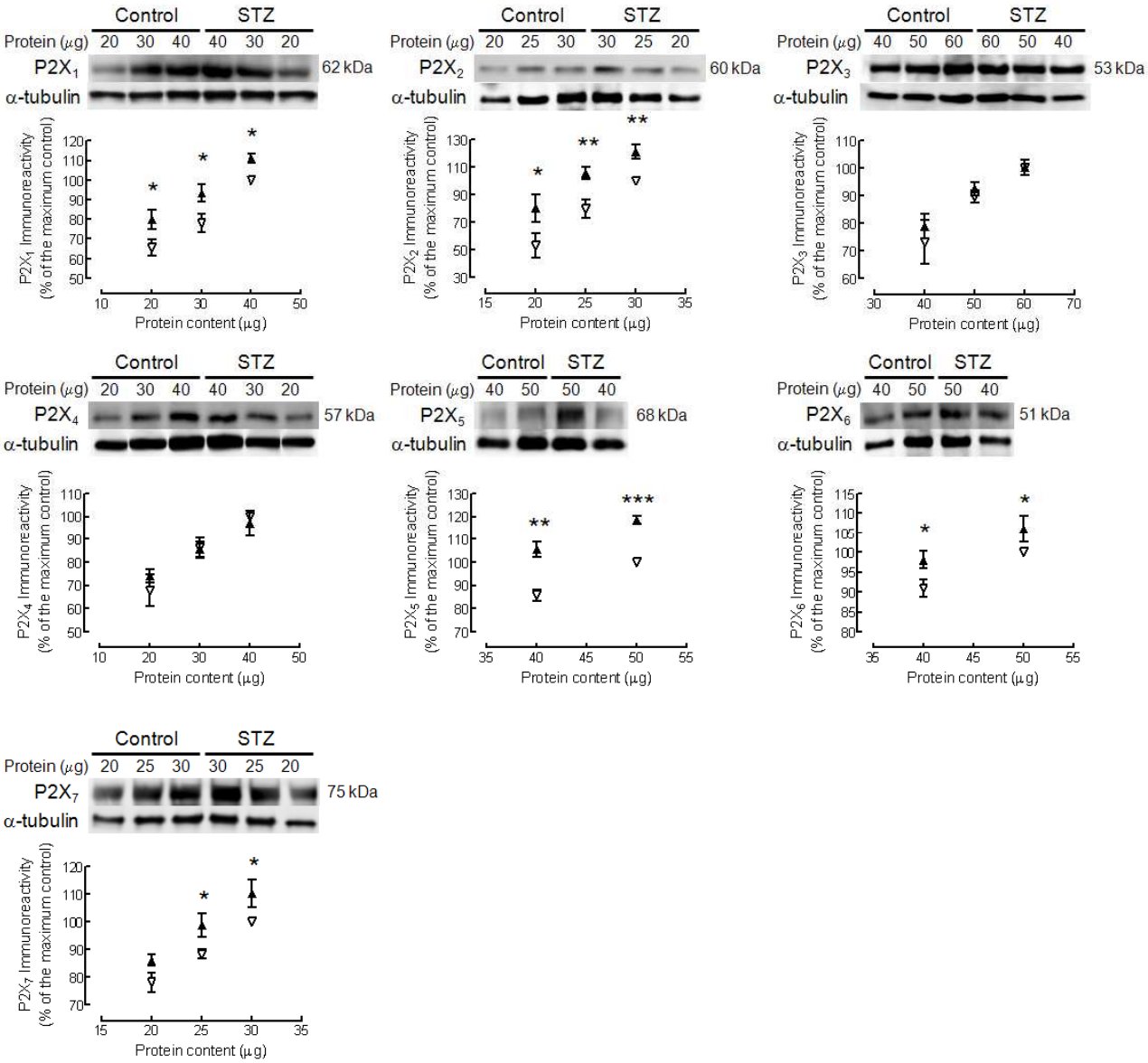

Figure 4.22. Representative Western blots comparing the P2X receptor immunoreactivity in total membranes from the hippocampus of control rats and from rats treated with STZ, applied in different quantities to the SDS-PAGE gel as indicated above each lane. A re-probing of the membranes with an anti-α-tubulin antibody, shown below each gel in each panel, confirmed that similar amounts of protein were added for each concentration of hippocampal membranes. The graphs below the gels show the average relative immunoreactivity of in total hippocampal membranes from control rats (open symbols) and from STZ-treated rats (filled symbols) according to the amount of protein applied to gel in different Western blot analysis using membranes from different groups of rats (n=8 for $P2X_{1,2,3}$, n=7 for $P2X_4$, n=5 for $P2X_{5,6}$ and n=6 for $P2X_7$ receptors). * P<0.05, ** P<0.01, *** P<0.001 comparing the immunoreactivity in the two groups of animals.

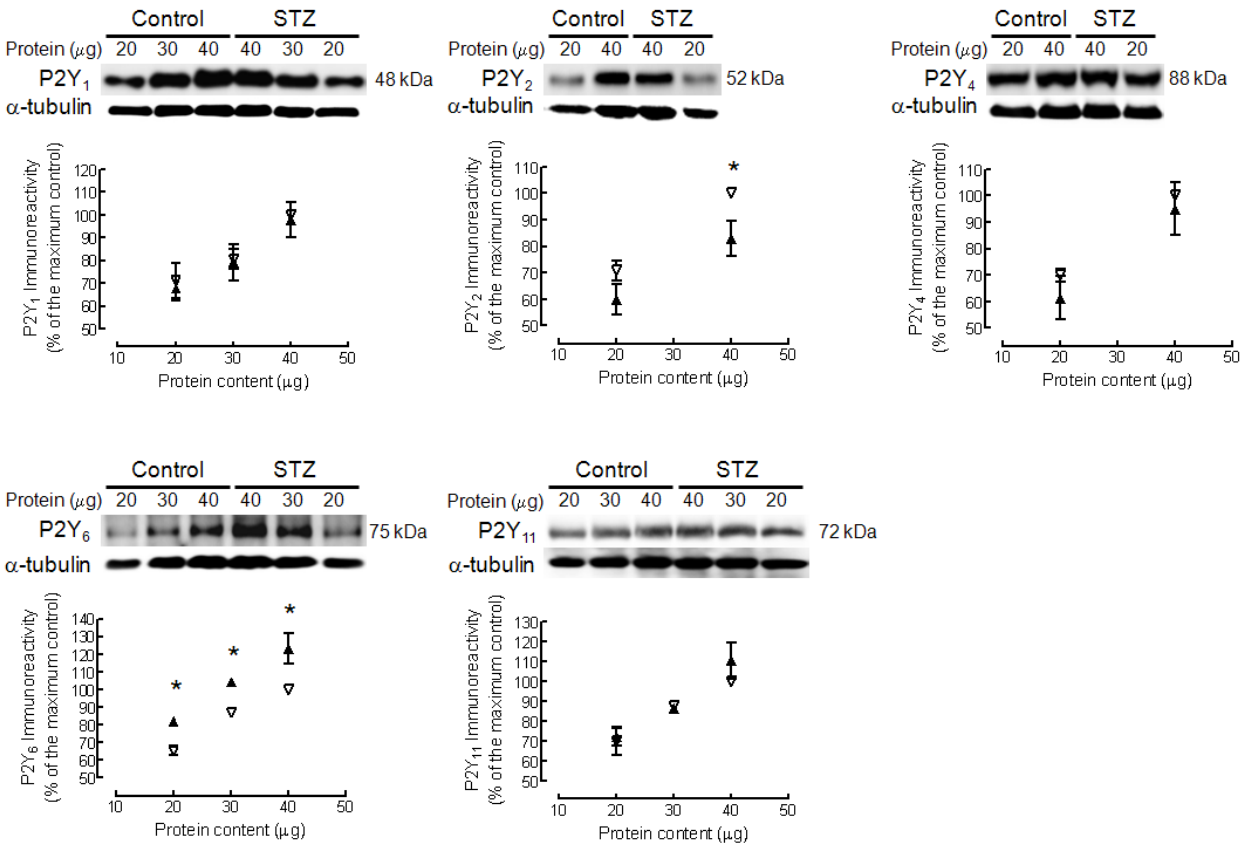

Figure 4.23.Representative Western blots comparing the P2Y receptor immunoreactivity in total membranes from the hippocampus of control rats and from rats treated with STZ, applied in different quantities to the SDS-PAGE gel as indicated above each lane. A re-probing of the membranes with an anti-α-tubulin antibody, shown below each gel in each panel, confirmed that similar amounts of protein were added for each concentration of hippocampal membranes. The graphs below the gels show the average relative immunoreactivity of in total hippocampal membranes from control rats (open symbols) and from STZ-treated rats (filled symbols) according to the amount of protein applied to gel in different Western blot analysis using membranes from different groups of rats (n=8 for $P2Y_1$, n=7 for $P2Y_2$, n=5 for $P2Y_4$, n=3 for $P2Y_6$ and n=4 for $P2Y_{11}$ receptors). * $P<0.05$ comparing the immunoreactivity in the two groups of animals.

It is well established that the development of a diabetic condition is accompanied by the increased incidence of neurological complications, in particular cognitive dysfunction (Cox *et al.*, 2005; Gispen and Biessels, 2000). The hippocampus is a brain region with a key role in the implementation of mnemonic traits, and deficits in hippocampal function prime cognitive dysfunction (Squire *et al.*, 2004). In particular, deficits in hippocampal synaptic plasticity phenomena, namely of LTP, are considered a neurophysiological trait of memory dysfunction (Lynch, 2004). Accordingly, there is a parallel deficit of the induction and maintenance of LTP as well as of the performance in memory-related tasks in STZ-induced diabetic rats (Biessels *et al.*, 1996). Interestingly, extracellular ATP, which is released in a frequency-dependent manner (Cunha *et al.*, 1996), plays a role in the development of LTP-like changes of synaptic efficiency through the activation of P2 receptors (*e.g.* Pankratov *et al.*, 2002; Almeida *et al.*, 2003). This might be due to combined effects of different P2Rs acting both presynaptically to control the release of glutamate

(Rodrigues *et al*., 2005a) and postsynaptically to facilitate the activation of ionotropic glutamate receptors, namely NMDA receptors (Kloda *et al*., 2004; Ortinau *et al*., 2003). Thus, the currently observed lower release of ATP together with the global down-regulation of synaptic P2 receptors in the hippocampus of diabetic rats raises the hypothesis that the deficit in synaptic ATP signalling may contribute for the memory dysfunction observed in diabetes.

This down-regulation of ATP signalling in hippocampal synapses may also be an adaptive response to preserve nerve terminals. In fact, type 1 diabetes is associated and constitutes a risk factor for neurological conditions associated with dysfunction of synaptic transmission, which can eventually lead to idiopathic generalised seizures (*e.g.* McCorry *et al*., 2006). Convulsive episodes are precipitated by hypoglycemic episodes (see Jones and Davis, 2003) and are effective triggers for synaptic and neuronal damage (Pitkänen and Sutula, 2002). These hypoglycemic episodes cause an acute release of ATP (Juranyi *et al*., 1999), which play a key role in triggering (*e.g.* Cavaliere *et al*., 2001a) and controlling the recovery (Aihara *et al*., 2002) of hypoglycemia-induced neuronal damage. Therefore, the decrease of synaptic ATP signalling can be viewed as an adaptive response to compensate increased risk of P2 receptor-mediated neurotoxicity in type 1 diabetes.

In contrast to what occurs in hippocampal synapses, it was observed that there was a trend for an increase of the density of P2 receptors in whole hippocampal membranes, which are mainly derived from extra-synaptic membranes given that synapses only represent <2 % of hippocampal volume (Rusakov *et al*., 1998). Apart from its synaptic role in the control of synaptic transmission and plasticity, extracellular ATP also fulfils important signalling roles outside synapses, mainly in the communication between neurons and glia, which may also contribute for non-synaptic-mediated neuromodulation (reviewed in Fields and Burnstock, 2006). In astrocytes, which are the most abundant cellular elements in the brain, there is evidence that P2 receptors can contribute to astrogliosis (Abbraccio and Verderio, 2006; Neary and Kang, 2005) and P2 receptors actually protect astrocytes from damage (Shinozaki *et al*., 2005). This is particularly relevant in diabetic conditions since astrocytes are expected to be the main cellular element able to metabolise and resolve the increased extracellular levels of glucose (Pellerin and Magistretti, 2004). Hence, it seems logical to expect maintenance of this astrocytic ATP signalling in a diabetic condition and the increased P2 receptor density in whole membranes may be an adaptive response to compensate for the decreased ATP levels faced by these extra-synaptic P2 receptors. Since it has been reported that there is an astrogliosis in type 1 diabetes (Saravia *et al*., 2002), it will be interesting to test if there will be an increased P2 receptor-mediated signalling in astrocytes in the diabetic brain and whether this may be related to an increased ability to handle extracellular glucose.

In conclusion, the present study provides evidence showing that the ATP signalling system is compromised in the hippocampus of STZ-treated rats, an experimental model of type 1 diabetes *mellitus*. These modifications could lead to alterations in the modulation of neurotransmission and gliotransmission, which may contribute to the diabetes-induced progressive cognitive impairment, although the direct impact of such alterations on both neuronal and glial functions remains to be determined. In particular, the diversity of P2 receptors and the currently observed different modification of the density of different receptors in this model of type 1 diabetes open the real possibility of selectively manipulating beneficial responses operated by particular P2 receptors without exacerbating noxious responses mediated by other P2 receptors.

4.2.3. Modification of cannabinoid CB1 receptor in the hippocampus of streptozotocin-induced diabetic rats

CB1 receptors are ubiquitously expressed in the brain, where they are mostly located presynaptically (although also located postsynaptically) in a wide range of neurons (for review see Marsicano and Kuner, 2007). In particular, they are highly abundant in the human and the rodent hippocampus (Katona *et al*., 1999, 2000; Degroot *et al*., 2006, and activation of presynaptic hippocampal CB1 receptors diminishes the release of GABA (Katona *et al*., 1999, 2000), glutamate (Kawamura *et al*.,2006), dopamine and acetylcholine (Degroot *et al*., 2006). These neurochemical findings may underlie the ability of CB1 receptor activation to control cognition and memory consolidation (Hampson and Deadwyler, 1999). Of particular interest is the finding that in several brain areas including the hippocampus, CB1 receptors have been shown to modulate glucose utilisation (*e.g.* Pontieri *et al*., 1999; Freedland *et al*., 2003). As described in the general introduction, CB1 receptors are involved in a wide spectrum of physiological and pathological mechanisms that are affected in diabetic encephalopathy. Thus, it was now tested whether the density and the expression of CB1 receptor is changed in the hippocampus of STZ-induced diabetic rats.

Table 4.9. Body weight and glycaemia of the rats used in the experiments before and after the induction of diabetes (n=6 for each condition). * P<0.01, different from before treatment; # P<0.01, different from control; n.d, not determined.

	Weight (g)		**Glycaemia (mg/dL)**	
	Control	STZ-treated	Control	STZ-treated
Before treatment	225 ± 14	231 ± 11	91 ± 4	96 ± 6
3 days after treatment	n.d.	221 ± 7	n.d.	460 ± 14 *
30 days after treatment	327 ± 21 *	208 ± 15 #	93 ± 1	448 ± 24 *, #

In this study, the animals were maintained for 30 days after STZ administration. STZ-treated rats developed sustained hyperglycaemia as measured 3 and 30 days following STZ treatment, and failed to gain body weight (see Table 4.9).

4.2.3.1. Increase of CB1 receptor density in hippocampal membranes and decrease of hippocampal CB1 mRNA expression

As shown in Figure 4.24A, the hippocampus of STZ-induced diabetic rats presented significantly increased CB1 receptor immunoreactivity in total membranes (13.0±2.5%, n=6, P<0.05),

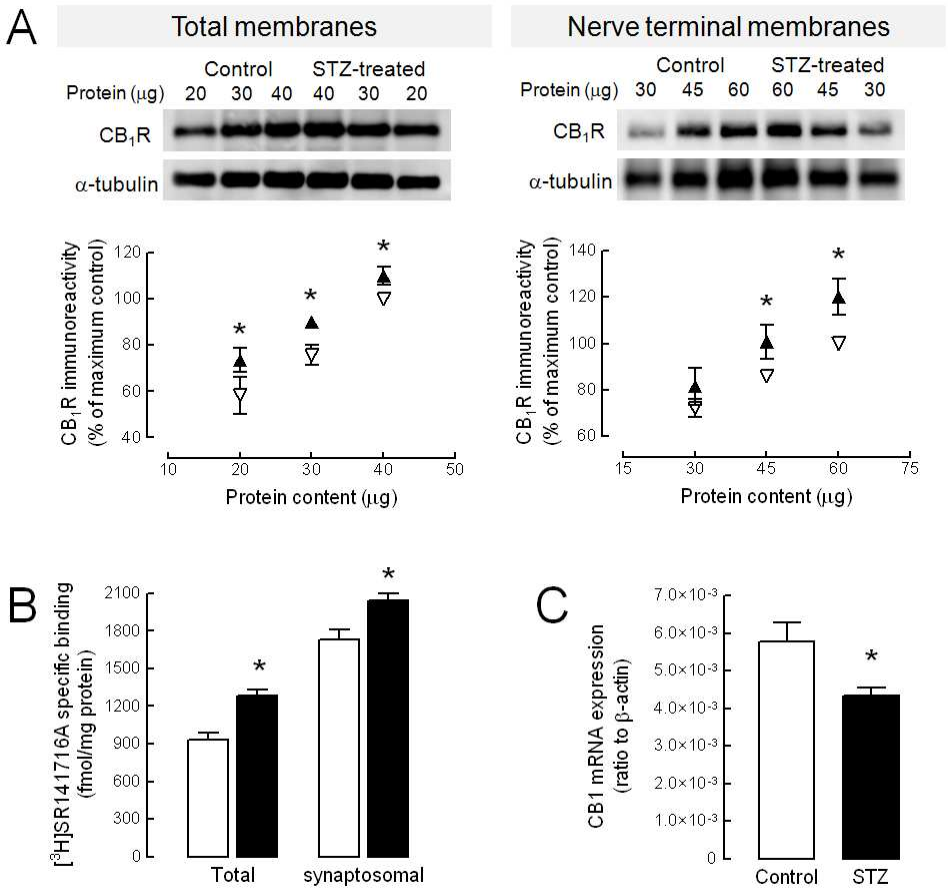

Figure 4.24. Panel A shows representative Western blots comparing the CB1 receptor immunoreactivity (53 kDa band) in total hippocampal membranes (left panel) and nerve terminal enriched membranes (right panel) from control and STZ-treated rats. In the graphs bellow, each data point represents the average of relative immunoreactivity from six different control rats (open symbols) and six STZ-treated rats (filled symbols), at three different protein loads. Below CB1 receptor bands, α-tubulin immunoreactivity is presented confirming that equal protein loadings in the SDS-PAGE gel. Panel B shows specific binding determined from saturation plots in total and synaptosomal (nerve terminal enriched) membranes from the hippocampus of control (open bars) and STZ-treated (filled bars) rats (n=4 for each data point). In panel C is presented the expression of the CB1 receptor (average from seven different rats for each group) that is significantly diminished in the hippocampus of STZ-treated animals (filled bar) compared to controls (open bar). Each CB1 receptor mRNA concentration value was normalized to β-actin. Results are mean±SEM and were compared with Student's *t* test. * P<0.05, comparing control and diabetic rats.

as well as in nerve terminal-enriched membranes (14.8±3.7%, n=6, P<0.05), compared to controls. This observation suggests augmented CB1 receptor density, which was confirmed by measuring CB1 receptor binding in total and nerve terminal-enriched membranes. It was found a 38% increase in the B_{max} of [^{3}H]SR141716A (a measure of the density of the receptor) in the total membranes of the hippocampus of the STZ-treated rats (n=4, P<0.05, Figure 4.24B), and an 18% increase in the nerve terminal-enriched membranes (n=4, P<0.05, Figure 4.24B). These different relative increases of CB1 receptor density might correspond to similar absolute amounts of CB1 receptors since the B_{max} of [^{3}H]SR141716A was 86% greater (P<0.05) in nerve terminal-enriched than in total hippocampal membranes (Figure 4.24B, black bars). In parallel, it was observed that the K_D values (a measure of the affinity of a ligand for a receptor) tend to increase upon STZ treatment, although this did not reach the level of significance (from 1.61 nM [95% confidence interval: 1.21–2.01 nM] to 2.71 nM [1.80–3.62 nM] in total membranes; and from 1.06 nM [0.89–1.24 nM] to 1.59 nM [1.10–2.08 nM] in nerve terminal-enriched membranes). To test if increased CB1 receptor density in hippocampal membranes of STZ-treated rats is due to an altered mRNA expression, it was performed quantitative real-time PCR in total hippocampal membranes obtained from vehicle-injected and STZ-treated rats, 30 days after injection. Melting curve analysis confirmed that one single product has been obtained. Intriguingly, the expression of CB1 receptor mRNA (normalized to β-actin from the same sample) is significantly decreased by 25% (n=7, P<0.05, Figure 4.24C) in the STZ-induced diabetic animals.

4.2.3.2. Discussion

The involvement of the CB1 receptors in metabolic disorders such as obesity and non-insulin-dependent diabetes has attracted much attention in the last decade. Deletion of CB1 receptors leads to leanness and resistance to diet-induced obesity (Cota *et al*., 2003), which anticipates a major role for CB1 receptors in controlling diabetes, given that obesity is a major risk factor for insulin-resistant (type 2) diabetes. CB1 receptors can also control insulin levels (Juan-Picó *et al*., 2006, Matias *et al*., 2006), and CB1 receptor blockade can decrease hyper-insulinemia in obese subjects (Gelfand and Cannon, 2006). Furthermore, individuals with obese and/or hyperglycaemic type 2 diabetes exhibit higher endocannabinoid concentrations in serum and visceral fat (Matias *et al*., 2006). Accordingly, therapy with the CB1 receptor antagonist SR141716A (introduced to the European market under the name of Acomplia) is associated with weight loss, favourable changes in serum lipid levels, improved glycemic control in pre-diabetic and type 2 diabetic patients, and

decreased hyper-insulinemia in obese subjects (Gelfand and Cannon, 2006; Matias *et al*., 2006). Not much is known about the role of CB1 receptors in insulin-dependent diabetes. In diabetes induced by STZ administration, it was now shown that there is an increase in the density of CB1 receptors in the hippocampus, in both total membranes and nerve terminals.

This increased density of synaptic CB1 receptors may reflect an elevated neuromodulator power for the CB1 receptor. In the hippocampus, endocannabinoids such as anandamide or 2-arachidonoyl glycerol, which are endogenous activators of the CB1 receptor, are released upon postsynaptic activation and then travel back to the pre-synaptic site to activate CB1 receptors, inhibiting transmitter release (for review see Freund *et al*., 2003). This so-called retrograde transmission participates in both short and long forms of synaptic plasticity thought to be key elements of cognitive behaviour. LTP is impaired in STZ-induced diabetic animals (Biessels *et al*., 1996), which also display an impairment of Ca^{2+}-dependent regulation of postsynaptic AMPA receptors (Chabot *et al*., 1997). Since endocannabinoids can facilitate the induction of LTP in the hippocampus via pre-synaptic blockade of GABAergic neurotransmission (Carlson *et al*., 2002) the upregulation of presynaptic CB1 receptors may contribute to restoring normal LTP functions. Alternatively, the increased density of CB1 receptors may be an adaptive response to counterbalance impaired postsynaptic Ca^{2+} level regulation and AMPA functions that result in a diminished endocannabinoid release. Opposing to these, CB1 receptor activation can restrict LTP via presynaptic CB1 receptor activation in glutamatergic terminals (Slanina *et al*., 2005). Clearly, further functional studies will be required to explore the modification of CB1 receptor signalling in GABAergic and glutamatergic synapses in the hippocampus of STZ-treated rats to pinpoint the exact functional relevance of this modified density of CB1 receptors.

The observed increase in CB1 receptor density in total membranes upon STZ-induced diabetes suggests that there is a broader modification of CB1 receptor function upon chronic hyperglycaemia, which is observed in uncontrolled type 1 diabetes. Elevated CB1 receptor density in membranes from the whole hippocampus of diabetic rats may reflect a compensatory role for CB1 receptors not only in synaptic plasticity but also in metabolic control, cell survival and neurogenesis. Indeed, CB1 receptors stimulate adult hippocampal neurogenesis (Jiang *et al*., 2005) that is impaired upon STZ-induced diabetes (Beauquis *et al*., 2006; Stranahan *et al*., 2008).

The level of phosphorylated (active) Akt is also increased in the STZ-induced diabetes, with a concomitant increase in levels of phosphorylated (inactive) glycogen synthase kinase 3β (GSK3β) (Clodfelder-Miller *et al*., 2005). Since CB1 receptors can activate the survival factor Akt (Gómez del Pulgar *et al*., 2002), and thus indirectly inhibit GSK3β, they can promote survival, as well as dendritic arborisation, which are normally controlled by the active form of GSK3β (for review see

Kalkman, 2006). Controlling glucose utilisation of hippocampal neurons (Freedland *et al*., 2002, 2003; Pontieri *et al*., 1999; Whitlow *et al*., 2002) is another aspect whereby CB1 receptors may affect hippocampal function, in particular upon a metabolic disorder like diabetes. CB1 receptors might control glia-related functions, such as neuroinflammation (Campbell and Downer, 2008), an this should not be excluded given that total membranes also include glial membranes. One striking aspect of our study was the observed disparity between changes in the expression and the density of CB1 receptors after STZ treatment. This suggests either a modification of protein translation, as was reported to occur in the hippocampus after traumatic brain injury (Chen *et al*., 2007), or alternatively a modification of the turnover of CB1 receptors that might be related to oxidative stress found in the hippocampus of STZ-induced diabetic rats (Ates *et al*., 2006a, 2006b).

In conclusion, the elevated density of the CB1 receptor in the hippocampus may represent a compensatory or a pathophysiological process. This change can either counteract or contribute to pathophysiological, structural and eventually, cognitive abnormalities, which involve synaptic deficits, hampered cell proliferation and apoptosis upon sustained hyperglycemia. Therefore, this study prompts the need to explore if the CB1 receptor antagonists would affect (worsen or improve) neuro-pathological consequences of diabetes.

4.2.4. Modification of neuromodulation systems in the cerebral cortex of streptozotocin-induced and Goto-Kakizaki diabetic rats

Hippocampal atrophy occur in patients with diabetes (Convit *et al*., 2003; Gold *et al*., 2007), and hippocampal function and hippocampal-dependent learning and memory were found to be impaired in animal models of diabetes (Biessels *et al*., 1996; Kamal *et al*., 1999; reviewed in Trudeau et a., 2004), and to be prevented by adequate control of glycaemia (Biessels *et al*., 1998). Along with hippocampal alterations, the cerebral cortex can also be affected by diabetes. Thus, cortical atrophy was observed in diabetic patients (Manschot *et al*., 2006, 2007), and several alterations were reported to occur in the cortex of diabetic rodents, such as morphological changes in neurons (*e.g.* Nitta *et al*., 2002; Malone *et al*., 2006) and glia (Baydas *et al*., 2003), increased oxidative stress (*e.g.* Ates *et al*., 2006a, 2006b) and modification of synaptic transmission (Gagné *et al*., 1997; Valastro *et al*., 2002).

It was previously shown that neuromodulation systems can be altered in the hippocampus of STZ-induced diabetic rats, particularly the adenosinergic and the endocannabinoid systems, which have not only a function in modulating synaptic activity but also intermediary metabolism. It was found that adenosine A_1 and A_{2A} receptors were respectively down- and up-regulated in the

hippocampus of STZ-treated rats maintained up to 3 months under chronic hyperglycaemia. It was also observed that the density of CB1 receptors increased in hippocampal membranes from STZ-treated rats, compared to controls. Since diabetes is being suggested to affect the cerebral cortex, it was now tested if the expression and density of cortical A_1 and A_{2A} as well as CB1 receptors are modified by diabetes, using STZ-induced diabetic rats and Goto-Kakizaki rats, which are models for type 1 and type 2 diabetes, respectively.

For the STZ-treated rats used in this study, body weight and glycaemia were measured before and after induction of diabetes, and at the time of experiment, *i.e.* 30 days after STZ administration. As shown in Table 4.10, when compared to controls, STZ-induced diabetic rats failed to gain weight and displayed sustained increase in blood glucose levels, indicating the establishment of chronic hyperglycaemia. At the time of experiment, GK rats (6 month old) presented decreased body weight (427.0±12.1 g *versus* 505.7±15.7 g of age-matched controls, P<0.01, n=8) and increased pre-prandial glycaemia (14.8±2.0 mM *versus* 4.9±0.3 mM in control rats, P<0.01, n=8).

Table 4.10. Body weight and glycaemia of STZ-treated rats and respective age-matched controls. Data are shown as mean±SEM of 7 rats, and compared with Student's *t* test. * P<0.01, different from control; ** P<0.01, different from before treatment.

	Weight (g)		**Glycaemia (mM)**	
	Control	STZ-treated	Control	STZ-treated
Before treatment	246.1±6.4	264.6±6.3	5.7±0.2	5.8±0.2
3 days after treatment	260.9±6.5	267.6±7.5	5.8±0.2	25.1±2.3 *,**
30 days after treatment	369.6±11.2 **	251.3±14.8 *	5.8±0.2	30.3±2.1 *,**

4.2.4.1. Modification of A_1 receptor density in total membranes without alteration of A_1 and A_{2A} mRNA expression

When studying the effect of STZ-induced diabetes on A_1 and A_{2A} receptors in the hippocampal formation, it was found that the modification in the density of these adenosine receptors was most evident in total membranes rather than in nerve terminal-enriched membranes. Thus, efforts were now focused on studying whole membranes prepared from the cerebral cortex. As illustrated in Figure 4.25, Western blot analysis revealed significantly reduced intensity of A_1 receptor immunoreactivity in membranes prepared from the cortex of either STZ-treated (Figure 4.25A) or GK (Figure 4.25B) rats, when compared to age-matched control rats. In relation to

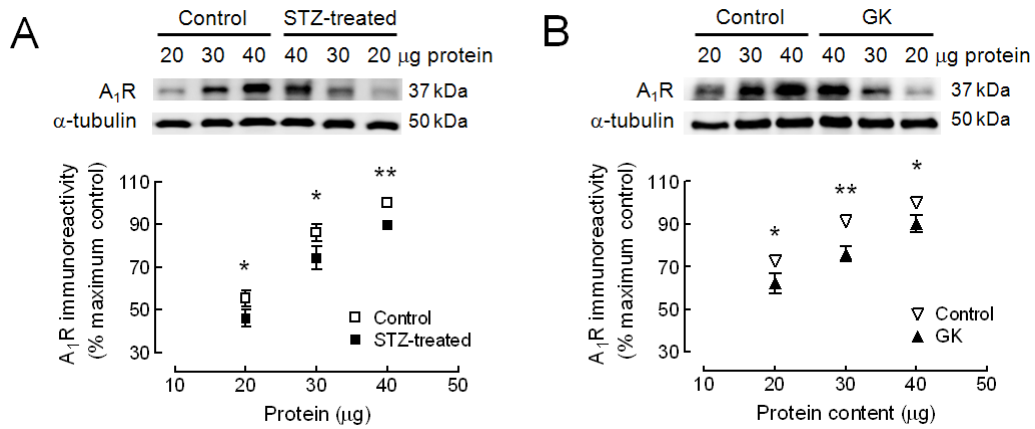

Figure 4.25. Decrease of A_1 receptor immunoreactivity in total membranes prepared from the cerebral cortex of STZ-treated (A) and GK (B) rats, analyzed by Western blot. The figure shows a Western blot (representative of experiments from different groups of rats, n=5 for STZ-treated rats and n=8 for GK rats), comparing A_1 receptor immunoreactivity corresponding to a 37 kDa band in cortical membranes. Membranes from age-matched control rats and STZ-treated (A) or GK (B) rats were applied in different concentrations to the SDS-PAGE gel, as indicated above each lane, to simultaneously access the sensibility of the assay. Reprobing of the Western blot membranes with anti-α-tubulin antibody (displayed under the A_1 receptor bands) confirmed that similar amounts of protein were added for each concentration of cortical membranes. The graphs bellow the western blots show the respective average relative immunoreactivity of A_1R in control rats (open symbols) and STZ-treated or GK rats (filled symbols), according to the amount of protein applied in the gel. Data are shown as mean±SEM and compared with Student's *t* test. * P<0.05, ** P<0.01, comparing immunoreactivity to controls.

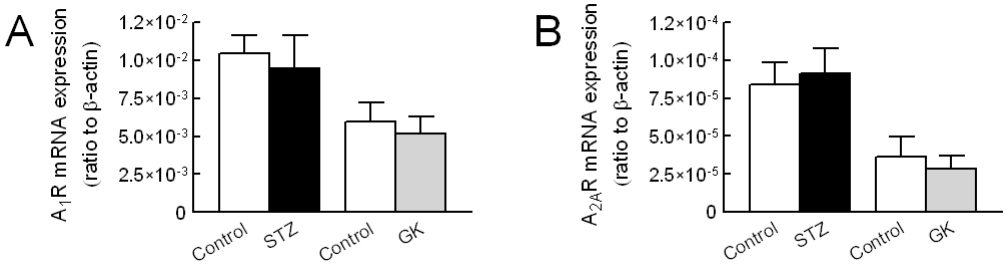

Figure 4.26. Expression of A_1 receptor (A) and A_{2A} receptor (B) mRNAs in the cerebral cortex of STZ-treated (black bars, n=7) and GK (gray bars, n=8) rats, compared to age-matched control rats (adjacent open bars). Receptor mRNA expression was quantified by real-time PCR analysis and normalized to β-actin mRNA expression, and results are presented as mean±SEM.

controls, A_1 receptor immunoreactivity was reduced by 9.8±1.9% (n=5, P<0.05) in the cortex of STZ-induced diabetic rats, and by 11.9±2.3% (n=8, P<0.01) in the cortex of GK diabetic rats.

To test whether modification of adenosine receptor density in the cortex of diabetic animals was caused by altered transcriptional processes, it was performed a quantitative analysis of mRNA expression relative to the constitutive expression of β-actin, by real-time PCR. When compared to the respective controls, neither STZ-induced diabetic rats nor GK rats displayed altered expression of A_1 receptor (Figure 4.26A) or A_{2A} receptor (Figure 4.26B) mRNAs in the cortex (P>0.05).

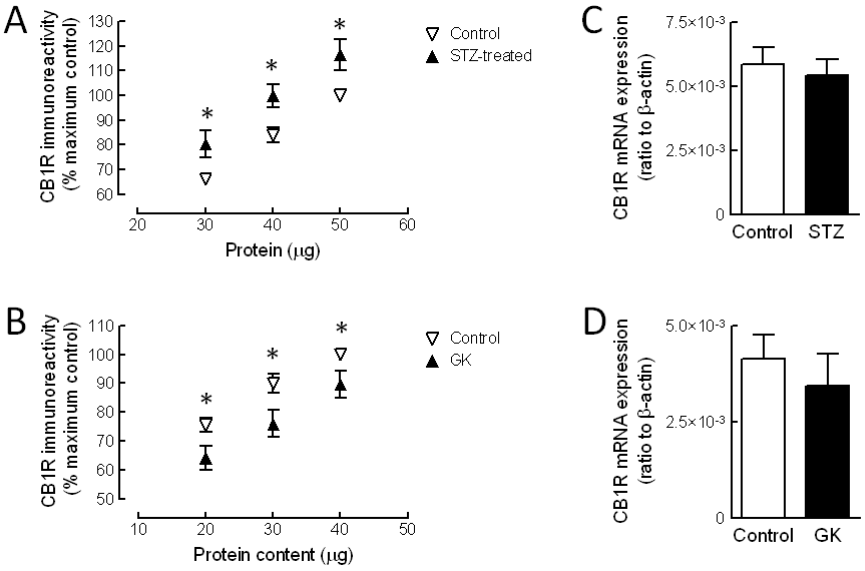

Figure 4.27. Modification of CB1 receptor immunoreactivity and expression of CB1 receptor mRNA in the cortex of STZ-treated (A, B) and GK (C, D) rats, analyzed by Western blot and quantitative real-time PCR, respectively. The figure shows the respective average relative immunoreactivity of CB1 receptor in control rats (open symbols) and STZ-treated (A) or GK (B) rats (filled symbols), according to the amount of protein applied in the gel. The expression of CB1 receptor mRNA in the cerebral cortex of STZ-treated (B) and GK (C) rats (black bars) was not modified in comparison to age-matched control rats (adjacent open bars). Receptor mRNA expression was quantified by real-time PCR analysis and normalized to β-actin mRNA expression. Results are shown as mean±SEM of n=8 and n=7 for Western blot and PCR analysis, respectively, and was compared with Student's *t* test. * P<0.05, comparing immunoreactivity to controls.

4.2.4.2. Modification of cannabinoid CB1 receptor in the cerebral cortex of streptozotocin-induced and Goto-Kakizaki diabetic rats

The immunoreactivity of the CB1 receptor in total membranes prepared from the cortex of STZ-induced diabetic rats (one month after STZ administration) was significantly increased by 16.1±4.5% (P<0.01, n=8, Figure 4.27A) in comparison to age-matched control rats. Oppositely, cortical membranes of insulin-resistant GK rats (6 months old) displayed a significant reduction of CB1 receptor immunoreactivity (-10.9±3.2%, P<0.01, n=8, Figure 4.27B). In the cortex of the same rats, the expression of CB1 receptor mRNA was quantified by real-time PCR analysis relatively to the constitutive expression of β-actin mRNA. When compared to the respective controls, neither STZ-induced (Figure 4.27C) nor GK (Figure 4.27D) rats showed significant alteration of CB1 receptor mRNA expression (P>0.05).

4.2.4.3. Discussion

The results obtained in the present work indicate that the adenosinergic modulation system is altered in the cortex of both insulin-dependent and insulin-resistant diabetic rats, when compared to controls. A reduction of about 10% was observed in the density of inhibitory A_1 receptors in cortical membranes of STZ-induced and GK diabetic rats.

It was previously found that A_{2A} receptors were up-regulated and A_1 receptors were down-regulated in membranes from the hippocampus of STZ-induced diabetic rats compared to controls. These alterations in receptor density were more evident in total membranes, suggesting that upon chronic hyperglycaemia the modification of the adenosinergic system may be related to other functions that the control of neurotransmission, such as the control of intermediary metabolism (Håberg *et al*., 2000; Hammer *et al*., 2001) or neuroinflamation (Tsutsui *et al*., 2004, 2008). In total membranes prepared from the cortex of both STZ-induced and GK diabetic rats, it was now found similar modification of the adenosine receptors, suggesting that diabetes induced changes of adenosinergic function are not restricted to the hippocampal formation. Together with the protein density of adenosine receptors, their mRNA expression was now also studied. Diabetes failed to alter the relative expression of either A_1 receptor or A_{2A} receptor mRNAs in the cortex of both STZ-induced rats and GK diabetic rats, suggesting that the alteration on the density of membrane adenosine receptors may be caused by post-transcriptional events, affecting protein turnover for each of the studied receptors.

In summary, as occurring in the diabetic hippocampus, also in the cerebral cortex there is a down-regulation of inhibitory A_1 receptors upon a diabetic condition, which is not supported by concomitant modification of mRNA expression. These results confirm the possibility of using A_{2A} receptor antagonists for the management of diabetes-associated brain dysfunction, as purposed for other neurodegenerative pathologies (Cunha, 2005).

Regarding the endocannabinoid system, and the CB1 receptor in particular, it was found an increased density of CB1 receptors in total membranes from the cortex of STZ-induced diabetic animals, which was of the same magnitude of the observed increase in the hippocampus. Conversely, in the cortex of GK rats, the density of CB1 receptors was decreased. Since it was observed that diabetes failed to induce alterations of CB1 receptor mRNA expression, like for adenosine receptors, it is also concluded that the modifications of CB1 receptor density in the cortex of diabetic animals are related to post-transcriptional events.

The present finding of an opposite change in insulin-dependent and insulin-resistant diabetic animals, suggests that CB1 receptor density in cortical membranes is inversely correlated

with the levels of circulating insulin. Together with reported observations of the ability of CB1 receptors to modulate brain glucose uptake (Freedland *et al*., 2002; Pontieri *et al*., 1999; Whitlow *et al*., 2002), the present results suggest that an interaction between the signalling pathways operated by CB1 receptor and insulin receptors may occur. Notably, insulin and CB1 receptors share the same signalling cascades: the PI3K-PKB/Akt pathway which can lead to glucose transporter up-regulation (Summers and Birnbaum, 1997; Plum *et al*., 2006), and the PKB/Akt-glycogen synthase kinase 3β pathway (Clodfelder-Miller *et al*., 2005). In fact, in CB1 receptor blockade was suggested to prevent insulin-induced MAPK activation (Boulaboula *et al*., 1997), and to modulate insulin sensitivity in adipocytes (Motaghedi and McGraw, 2008). Further work is needed to understand the relation between endocannabinoids and insulin in controlling the regulation of brain glucose transport and metabolism, and to explore this interaction as a possible therapeutic target in diabetic encephalopathy.

4.3. Diabetes-induced alterations of intermediary metabolism

Diabetes *mellitus* is a metabolic disorder resulting from inadequate insulin release or insulin resistance, leading to an inadequate utilization of glucose as a substrate that, as described in the general introduction, may have negative impacts on the CNS (*e.g.* Biessels *et al*., 2002; Trudeau *et al*., 2004; Manschot *et al*., 2006), and lead to increased risk of dementia (Biessels *et al*., 2006a) and Alzheimer's disease (Biessels *et al*., 2006b).

It is widely recognized that the brain requires glucose as the primary fuel to generate energy for cellular homeostasis and synaptic transmission. Uncontrolled diabetes was suggested not to affect brain glucose concentration (Seaquist *et al*., 2005). Also blood-to-brain glucose transport and cerebral glucose metabolism were found not to be reduced in type 1 diabetes (Fanelli *et al*., 1998b). However, subjects with type 1 diabetes and hypoglycemia unawareness display significantly higher brain glucose concentrations (Criego *et al*., 2005a), which does not occur in healthy subjects submitted to recurrent hypoglycaemia (Criego *et al*., 2005b). Other authors suggested that glucose metabolism in the brain is reduced by chronic hyperglycaemia (Garcia-Espinosa *et al*., 2003), which could affect neurotransmitter synthesis and release (Trudeau *et al*., 2004), and eventually cause alterations in synaptic connectivity and neuronal loss, mainly through apoptotic events (Sima *et al*., 2004). Apart from glucose, the brain is able to use other carbon sources to produce the energy required to sustain basic cellular functions and neurotransmission. Thus, the brain uses the glycogen stores present within astrocytes to acutely buffer glucose demand (Gruetter *et al*., 2003). Also lactate taken from the blood stream or produced in astrocytes, can be provided to neurons, playing a role in brain energy metabolism and sustaining glutamatergic neurotransmission (*e.g.* Pellerin, 2003). Ketone bodies can also be used to produce acetyl-CoA to enter the TCA cycle, and lipolysis and proteolysis may also serve as carbon source (McCall, 2004). The contribution of these alternative carbon sources for brain metabolism may eventually be altered upon diabetes. For example, the monocarboxylic acid transport and oxidative metabolism of acetate have been reported to be increased in type 1 diabetic subjects (Mason *et al*., 2006).

The lack of knowledge of the impact of a diabetic condition on the metabolic network in the brain, and in the hippocampus in particular, prompted the present study aiming at exploring changes of hippocampal metabolism in STZ-induced and GK diabetic rats.

4.3.1. Intermediary metabolism is not altered in superfused hippocampal slices from STZ-induced diabetic rats

Hippocampal slices are the gold standard for electrophysiology studies and, electrophysiological analysis indicate that diabetes affects synaptic plasticity in hippocampal slices, which is associated with learning and memory processes. In particular, impairment of LTP (*e.g.* Biessels *et al.*, 1996) and facilitation of LTD (Kamal *et al.*, 1999) were reported to occur in hippocampal slices prepared from STZ-induced diabetic rats. Likewise, it was now tested if intermediary metabolism is also altered in hippocampal slices prepared from rats submitted to chronic hyperglycaemia induced by STZ administration.

In this study, male Wistar rats (8 weeks old) were injected with STZ and maintained for 30 days with food and water *ad libitum*, as well as untreated control rats. Table 4.11 summarises body weight and glycaemia of both control and diabetic rats. After the 30 days of chronic hyperglycaemia, hippocampal slices were prepared and superfused with modified Krebs solution containing 5.5 mM [U-^{13}C]glucose and 5.5 mM [2-^{13}C]acetate, in the absence or presence of 50 μM 4AP.

HPLC analysis of adenine nucleotide concentrations in PCA extracts from superfused hippocampal slices revealed similar energy charge in slices from control and STZ-treated rats (Figure 4.28A), in the absence or presence of stimulation with 50 μM 4AP, suggesting that the global energy status is not affected by diabetes. PCA extracts of superfused hippocampal slices were then analysed by ^{1}H NMR spectroscopy for quantification of the fractional enrichment of lactate and alanine. Hippocampal slices from controls and STZ-induced diabetic rats showed equal incorporation of labelling from [U-^{13}C]glucose into lactate and alanine, in the absence or presence of 4AP (Figure 4.28B). The ^{13}C NMR spectra of metabolite extracts from hippocampal slices were used to analyse the multiplet patterns in the resonances of glutamate C4 and GABA C2, by performing a direct ^{13}C isotomoper analysis of the glutamate and GABA (Malloy *et al.*, 1990) as described in section 4.1.1.4. Briefly, the ratios of GluC4Q/D45 (or GABAC2Q/D12) and GluC4D34/S (or

Table 4.11. Body weight and glycaemia of STZ-treated rats and respective age-matched controls. Data are shown as mean±SEM of 18 rats, and compared with Student's *t* test. * P<0.01, different from control; ** P<0.01, different from before treatment; n.d., not determined.

	Weight (g)		**Glycaemia (mg/dL)**	
	Control	STZ-treated	Control	STZ-treated
Before treatment	222.3±7.5	224.8±7.8	92.7±4.2	92.3±4.1
3 days after treatment	n.d.	211.3±8.1	n.d.	452.1±12.3 *,**
30 days after treatment	318.9±9.0 **	209.3±8.2 *	92.1±1.2	458.0±15.1 *,**

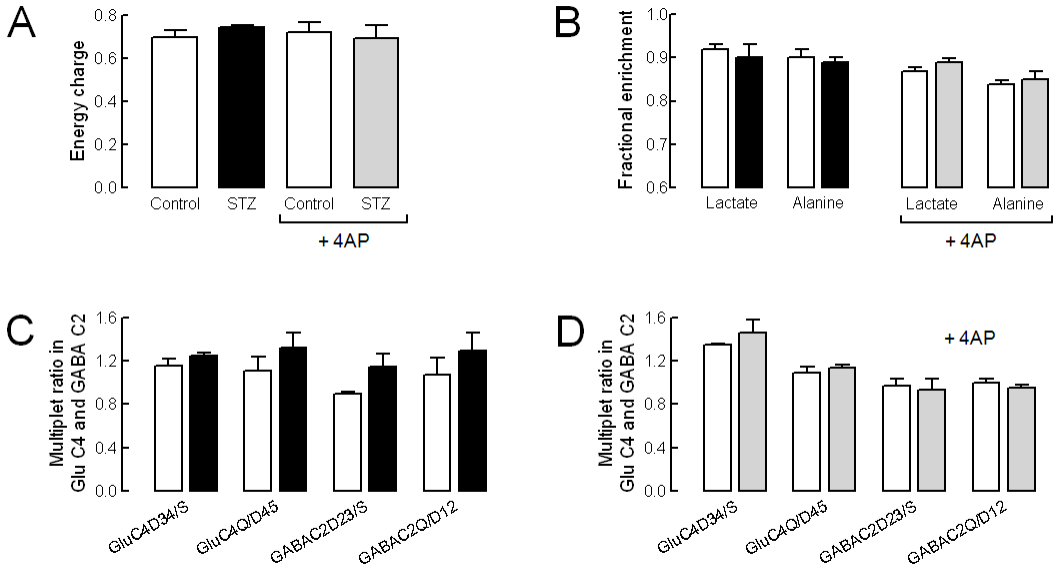

Figure 4.28. Intermediary metabolism in hippocampal slices from STZ-treated rats was similar to controls, both under resting conditions or stimulation with 4AP. Hippocampal slices prepared from both control (white bars) and STZ-induced diabetic rats (black/gray bars) were superfused with modified Krebs solution including 5.5 mM [U-^{13}C]glucose and 5.5 mM [2-^{13}C]acetate for 3 hours, in the absence (n=3, black bars) and presence (n=4, gray bars) of 50 µM 4AP. Panel A presents energy charge from the hippocampal sliced, determined by HPLC analysis. Panel B shows fractional enrichment of lactate and alanine in hippocampal slices from control and STZ-induced diabetic rats at the end of the superfusion period, calculated from ^{1}H NMR spectra. Panel C and D show the multiplet ratios directly calculated from both glutamate C4 and GABA C2 resonances in ^{13}C NMR spectra, in the absence (C) or presence (D) of 4AP.

GABAC2D23/S) indicate the flux into the TCA cycle(s) oxidizing [U-^{13}C]glucose and [2-^{13}C]acetate, respectively, and this allows inferring about neuronal and glial TCA cycles leading to glutamate and GABA synthesis. As illustrated in Figure 4.28C and D, hippocampal slices from STZ-induced diabetic rats showed multiplet ratios similar to controls, either calculated from glutamate C4 or GABA C2, in the absence or presence of stimulation with 4AP. Furthermore, when compared to controls, STZ-induced diabetes failed to alter the contribution of [U-^{13}C]glucose (Fc3) and [2-^{13}C]acetate (Fc2) to the pool of acetyl-CoA, either analysed from glutamate C4 or GABA C2 resonances (Figure 4.29).

4.3.1.1. Discussion

The present results show that hippocampal slices prepared from healthy controls or STZ-induced diabetic rats have identical metabolic behaviour at the level of the TCA cycle activity and anaplerotic fluxes, in resting conditions or upon stimulation with 4AP. Thus, it can be inferred that, despite the alterations to which the diabetic hippocampus is submitted *in vivo*, it can adapt and

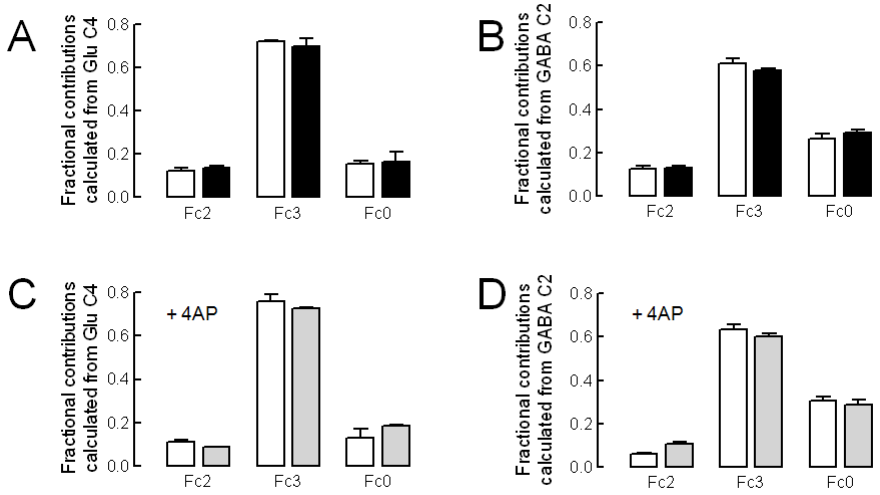

Figure 4.29. Identical intermediary metabolism of 5.5 mM [U-^{13}C]glucose and 5.5 mM [2-^{13}C]acetate for 3 hours in hippocampal slices from STZ-treated rats (black/gray bars) and controls (open bars), both under resting conditions (A and B) or stimulation with 4AP (C and D) lead to similar fractional contributions to acetyl-CoA estimated from glutamate C4 (A and C) and GABA C2 (B and D) with the program tcaCALC, using non-steady-state analysis.

perform metabolically identical to controls upon the same metabolic imposition, in this case provision of 5.5 mM glucose and 5.5 mM acetate.

Other functional changes have been recorded in hippocampal slices prepared from STZ-induced diabetic rats when compared to controls. In particular, when compared to controls, hippocampal slices from STZ-induced diabetic rats displayed altered long-term potentiation (LTP) and long-term depression (LTD) (Biessels *et al*., 1996, 1998; Kamal *et al*., 1999, 2000), indicating altered hippocampal synaptic transmission and plasticity, which was associated with reduced spatial learning and memory (*e.g.* Gispen and Biessels, 2000; Kamal *et al*., 2000). Furthermore, chronic hyperglycaemia may eventually lead to modification of NMDA receptor density, localization or function in the brain, therefore contributing to altered synaptic transmission and plasticity (reviewed in Trudeau *et al*., 2004). As shown above (section 4.1), the metabolic competence of hippocampal slices is preserved if substrates and oxygen are properly provided (*e.g.* Nichols, 2003). Moreover, the hippocampus of STZ-treated rats displayed structural changes, namely synaptic degeneration (see section 4.2.1.3) that can contribute to memory impairment. Thus, the reduction of syntaxin density in hippocampal nerve terminals seven days after STZ-administration, which was sustained for at least three months (Figure 4.15), suggests that STZ-treatment caused acute rather than chronic toxicity in the hippocampus. This toxicity causes a damage of the hippocampal tissue namely at the level of the synapse, possibly being preserved the rest of the tissue. Thus, STZ-induced chronic hyperglycaemia may cause synaptic deficits that are permanent and dramatically affect learning and memory, but does not lead to metabolic adaptations of the hippocampus that are maintained in superfused hippocampal slices.

Other metabolic changes may occur in the hippocampus of STZ-treated rats that unrelated to the metabolism of glucose and acetate. However, other substrates were not tested in the superfused hippocampal slices. For example, processing or presence of free fatty acids or ketone bodies in the hippocampus may negatively affect glucose metabolism in the tissue. In particular, ketone bodies like β-hydroxybutyrate were shown to by preferentially consumed in the diabetic hippocampus (Robinson and Williamson, 1980), and to inhibit glucose oxidation (*e.g.* Lapidot and Haber, 2001). Upon hyperglycaemia, this will further increase the availability of glucose in the hippocampus, contributing to neurotoxicity (Tomlinson and Gardiner, 2008). Furthermore, glial metabolism was suggested to have a greater contribution to the brain energy production in STZ-induced diabetic rats than in controls (Garcia-Espinosa *et al*., 2003), and acetate (mainly taken by glial cells) uptake and metabolism was suggested to be increased in type 1 diabetic subjects (Mason *et al*., 2006). However, the balance of neuronal and glial metabolism was not altered in superfused hippocampal slices, possibly because all the cellular elements in the slice have free access to the substrates in the superfusion medium and neurons do not depend on the metabolic support from astrocytes.

A deregulation of osmolarity may occur in the diabetic hippocampus subjected to hyperglycaemia, inducing a metabolic adaptation of the tissue (Lien *et al*., 1990, 1991). In fact, high concentration of osmolytes, such as *myo*-inositol, was also reported in the brain of diabetic patients (Geissler *et al*., 2003; Kreis and Ross, 1992), as well as in the hippocampus of Zucker diabetic fatty rats (van der Graaf *et al*., 2004). Such metabolic adaptation to osmotic modifications was not observed in hippocampal slices prepared from STZ-treated rats since they were superfused in the same conditions as controls, in particular in the presence of the same glucose concentration.

In summary, the results now obtained failed to find altered metabolic performance of superfused hippocampal slices from diabetic rats compared to controls, in opposition to altered synaptic plasticity (e.g. Biessels *et al*., 1996), suggesting that learning and memory impairment caused by diabetes is related to synaptic alterations rather than metabolic stress caused by chronic hyperglycaemia.

4.3.2. *In vivo* metabolism of [1-^{13}C]glucose in the hippocampus of Goto-Kakizaki diabetic rats

Since the hippocampus plays a crucial role in learning and memory processes that require high glucose supply, glucose metabolism was studied in the hippocampus of insulin-resistant GK diabetic rats using ^{13}C NMR spectroscopy upon *in vivo* infusion of enriched [1-^{13}C]glucose.

In this study, 6 months old GK rats were used and they displayed significantly increased glycaemia (233.4±23.7 mg/dL *versus* 84.1±11.4 mg/dL of controls, n=15, P<0.0001) and decreased body weight (424.6±28.1 g *versus* 524.7±13.0 g of controls, n=15, P<0.001). Diabetic GK and age-matched Wistar rats were infused i.v. with [1-^{13}C]glucose under ketamine-chlorpromazine anaesthesia at an exponentially decaying rate bolus over 5 min, followed by a continuous infusion with a rate adjustable to animal's glycaemia to maintain stable glucose levels in the blood (Figure 4.30A), which resulted in a rapid rise of glucose ^{13}C isotopic enrichment from natural abundance to 70% or 40% for controls and GK rats respectively. This was confirmed by ^{1}H NMR spectroscopy of blood samples and Figure 4.30B shows the concentration of [1-^{13}C]glucose in the blood of control and diabetic GK rats. At the end of each infusion protocol (for different periods), PCA extracts of the hippocampal tissue were prepared and analysed by ^{1}H and ^{13}C NMR spectroscopy. The ^{1}H spectra allowed quantifying hippocampal [1-^{13}C]glucose concentration (Figure 4.30C) that accompanies plasma glucose ^{13}C enrichment.

Figure 4.31 shows typical ^{13}C NMR spectra obtained from PCA extracts of the rat hippocampus after [1-^{13}C]glucose infusion, illustrating the ^{13}C label incorporation into intermediary metabolites including lactate, alanine, glutamate, glutamine, GABA and aspartate. After 90 minutes of [1-^{13}C]glucose infusion, one can appreciate doublet signals namely in glutamate resonances. This multiplets were not observable at lower infusion times, in particular in GK rats, and therefore were

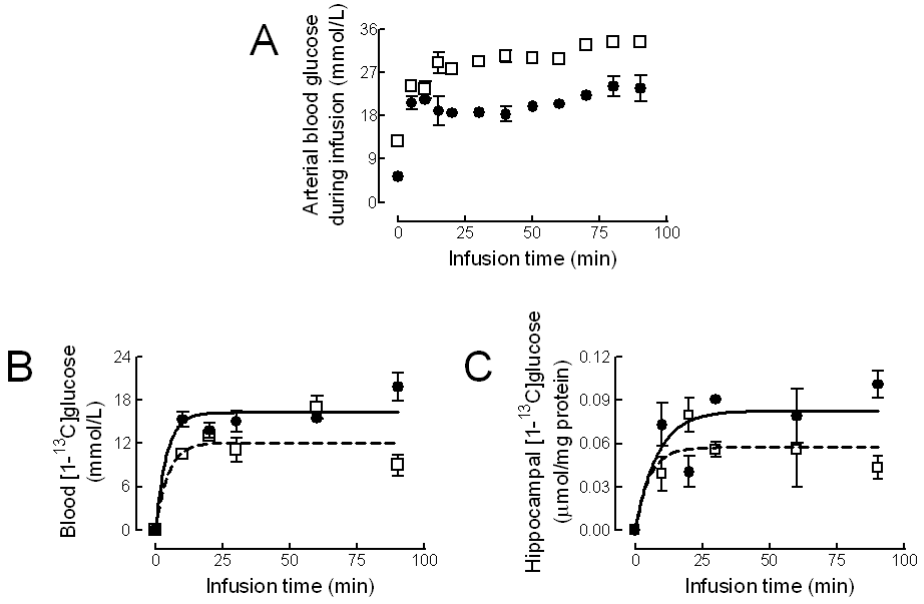

Figure 4.30. Glucose concentration in the arterial blood during [1-^{13}C]glucose infusion measured by glucose oxidase method(A), and concentration of [1-^{13}C]glucose in the blood (B) and in the hippocampus (C) of control (filled symbols) and GK rats (open symbols). As described in the methods, an exponential bolus of [1-^{13}C]glucose was given to rapidly achieve glucose levels of 320-370 mg/dL for controls and at 450-500 for GK rats, which were maintained constant through experiment. [1-^{13}C]glucose content in both blood and hippocampus was quantified by ^{1}H NMR spectroscopy of PCA extracts of the tissue at 500 and 600 MHz, respectively. Values are mean±SEM of 15 animals in each group.

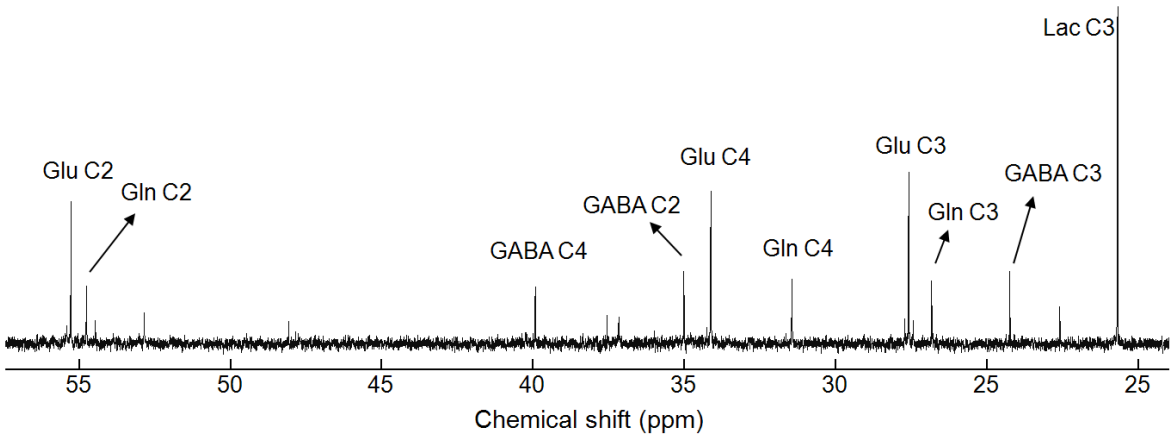

Figure 4.31. Representative ^{13}C NMR spectrum at 150.7 MHz (expansion from 18 to 58 ppm) of a PCA extract from the hippocampus of a control rat, after infusion of [1-^{13}C]glucose for a period of 90 min. [1-^{13}C]glucose was metabolised in the hippocampus leading to labelling of intermediary metabolites, in particular ^{13}C was incorporated in aliphatic carbons of glutamate, GABA and glutamine.

not analysed, being quantified the entire area of the resonance.

Figure 4.32 presents the ^{13}C enrichment of glutamate and glutamine C4 and C3, and GABA C2 and C3, which directly reflect the flux of labelling through the TCA cycle(s) in neurons and astrocytes and are involved in neurotransmission and cycling between neuronal and astrocytic compartments. Due to insulin resistance there was a much greater accumulation of glucose in the blood of GK rats than in controls (Figure 4.30A) and thus reduced infusion rate in GK rats compared to controls originated lower ^{13}C enrichment in blood glucose that, consequently, resulted in proportionally reduced ^{13}C incorporation into intermediary metabolites (Figure 4.32). This high labelling dilution observed in GK rats impairs the observation of alterations in metabolic fluxes. Alternatively, the ratios C3/C4 in glutamate and glutamine were calculated, since they are inversely proportional to the rate of the TCA cycle in neurons and astrocytes, respectively (Figure 4.33). When compared to controls, the hippocampus of diabetic GK rats displayed higher C3/C4 in both glutamate and glutamine, suggesting increased contributions of unlabelled carbon sources to the pool of acetyl-CoA or increased anaplerosis through pyruvate carboxylase (PC). PC activity directly labels carbon C2 of glutamate and glutamine from the C3 of pyruvate (*e.g.* Gruetter *et al.*, 2001). Methodological limitations of this study did not allow the proper quantification of labelling in glutamate and glutamine C2, but due to randomization of ^{13}C enrichment between C2 and C3 in the TCA cycle due to back scrambling at the level of fumarase, the analysis of labelling of C3 relative to C4 can be used for anaplerotic flux analysis.

In summary, the hippocampus of GK rats displayed a reduction in the ^{13}C enrichment of the carbons in glutamate, glutamine and GABA, as result of labelling dilution due to metabolism of unlabelled glucose and possibly other carbon sources. In this study, when compared to controls, the hippocampus of GK rats showed an increase of ^{13}C incorporation in C3 relative to C4 position in

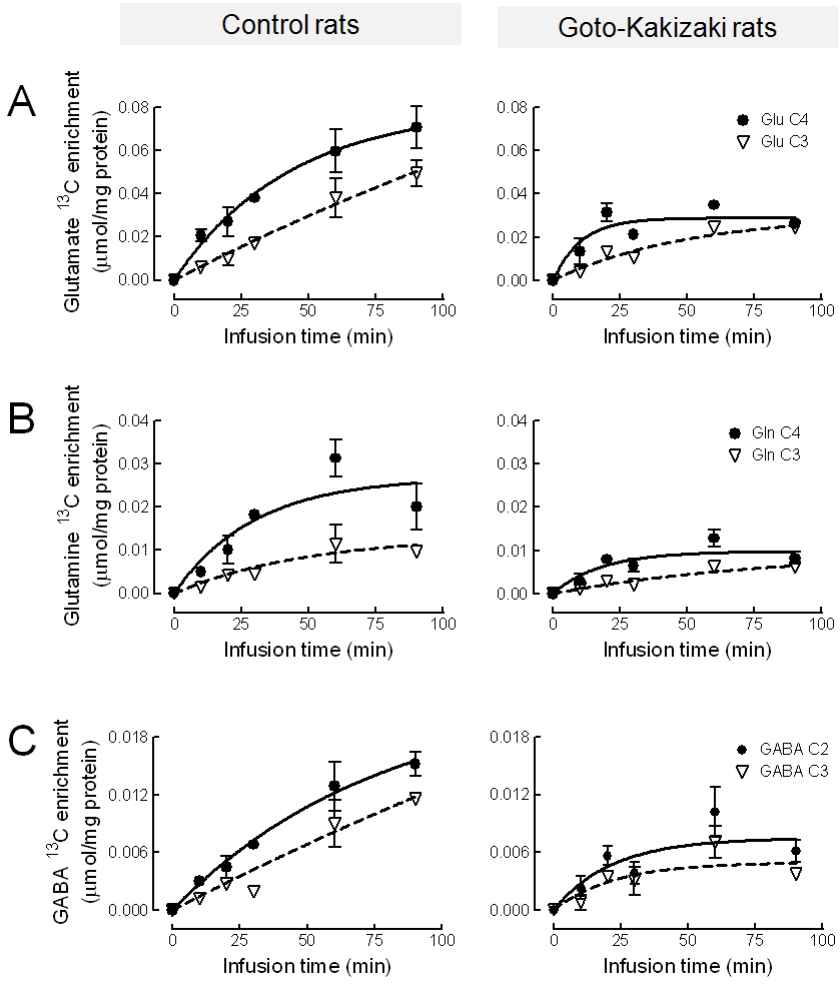

Figure 4.32. Enrichment of glutamate (A), glutamine (B) and GABA (C) in PCA extracts of the hippocampus of control (left column) and GK (right column) rats, upon infusion [1-^{13}C]glucose, as quantified by ^{13}C NMR spectroscopy at 150.7 MHz. Open symbols represent enrichment in C3 of glutamate, glutamine and GABA, while filled symbols represent C4 of glutamate and glutamine, and C2 of GABA. The labelling appears due to metabolism in the TCA cycle: the first turn of the TCA cycle produces labelling of Glu and Gln C4 and GABA C2, and if the labelling continues on a second turn of the cycle, will enrich the C3 positions of these metabolites. Values are mean±SEM of 3 rats in each data point (total of 15 animals in each group).

both glutamate and glutamine, suggesting increased contribution of carbon sources other than precursors of pyruvate to the hippocampal pool(s) of acetyl-CoA upon diabetes. Possibly, increased rate of anaplerosis through PC activity may also account for increased ^{13}C enrichment in C3 *versus* C4 mainly in molecules of glutamate and glutamine, in comparison to controls.

4.3.2.1. Discussion

The *in vivo* infusion of [1-^{13}C]glucose and the analysis of ^{13}C enrichment of hippocampal metabolites allowed to access the relative contribution of metabolic fluxes feeding hippocampal TCA cycle(s). The present study evaluated the metabolism of [1-^{13}C]glucose in the hippocampus of

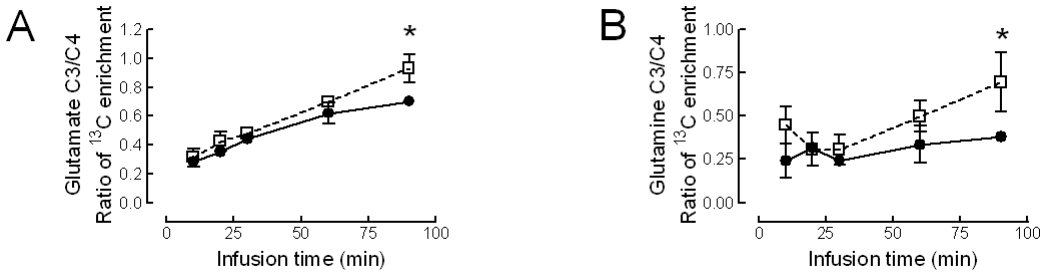

Figure 4.33. Glutamate and glutamine C3/C4 ratios tend to increase in the hippocampus of GK rats (filled symbols) compared to controls (open symbols). Values are mean±SEM of 3 rats in each data point (total of 15 animals in each group). * P<0.05, comparing control and diabetic rats.

GK diabetic rats in comparison to control rats, and was challenged by the high ^{13}C labelling dilution in diabetic GK rats by hyperglycaemia even after overnight fasting.

When compared to controls, the hippocampus of GK rats showed an increase of ^{13}C incorporation in C3 relative to C4 position in both glutamate and glutamine, suggesting increased contribution of carbon sources other than precursors of pyruvate to the hippocampal pool(s) of acetyl-CoA upon diabetes. In particular, ketone bodies like β-hydroxybutyrate may inhibit glucose oxidation (*e.g.* Lapidot and Haber, 2001) and be preferentially consumed in the diabetic hippocampus (Robinson and Williamson, 1980). Possibly, increased rate of anaplerosis, namely through pyruvate carboxylation by PC activity that takes place in astrocytes, may also account for the diabetes-induced increase in ^{13}C enrichment in C3 *versus* C4 mainly in glutamine, but also in glutamate by exchange in the glutamine-glutamate cycle between neurons and astrocytes. Furthermore, some intermediate metabolites of the TCA cycle can be produced from amino acids or be used to synthesize them (Voet and Voet, 1995), and the high glucose and pyruvate availability in the hippocampus submitted to a diabetic condition may inhibit the catabolism of amino acids, leading to reduced anaplerotic incorporation of unlabeled carbon atoms into glutamate and glutamine C1, C2 and C3 positions.

The present observation of increased anaplerotic fluxes through pyruvate carboxilation (relative to the TCA cycle activity) in the hippocampus upon diabetes is consistent with increased metabolic activity of glial cells relative to the neuronal populations. In fact, the brain of STZ-induced diabetic rats was suggested to display increased contribution of glial metabolism (Garcia-Espinosa *et al*., 2003), and acetate (mainly taken by glial cells) uptake and metabolism was reported to be increased in type 1 diabetic subjects (Mason *et al*., 2006), and this higher glial metabolic fluxes could be a form of compensation for probable altered glucose transport and metabolism. In agreement with higher metabolic support from astrocytes to neurons, the specific glial enzyme glutamine synthetase was increased in the diabetic rat brain (Bhardwaj *et al*., 1998). Likewise,

increased astrocyte metabolism in the diabetic hippocampus is consistent with the occurrence of astrogliosis, which was observed in animal models of diabetes, namely in STZ-treated rats and NOD mice (Baydas *et al*., 2003; Revsin *et al*., 2005; Saravia *et al*., 2002). Moreover, since astrocytes are considered the main cells involved in glycogen metabolism and storage (see Gruetter, 2003, and references therein), the glucose buffering capacity of the diabetic hippocampus is enhanced by the increased metabolic activity of astrocytes.

In conclusion, the results obtained in the present study suggest that the hippocampus submitted to a diabetic condition will rearrange the relative fluxes through intermediary metabolic pathways, possibly to counteract alterations of glucose transport and utilization as substrate. From the observations of this and previous studies on the brain metabolism upon diabetes (discussed above), it can be proposed that in the diabetic hippocampus there is an increased oxidation of acetyl-CoA precursors other than pyruvate (*e.g.* acetate, β-hydroxybutyrate, fatty acids) and pyruvate is then carboxylated to oxaloacetate to enter the TCA cycle.

4.4. Ability of caffeine consumption to counteract diabetes-induced alterations in the hippocampus

A decline in memory and cognitive function is considered to be a normal consequence of ageing. However, this age-related cognitive decline is accentuated by neurodegenerative pathologies, causing severe deterioration in memory and learning, attention and concentration, use of language, and other mental functions (*e.g.* Keller, 2006). One condition that exacerbates age-related memory deficits is diabetes (*e.g.* reviewed in Brayne *et al*., 2005; Convit, 2005), which are particularly associated with atrophy of the hippocampal formation that is involved in learning and memory processing (Convit *et al*., 2003; Gold *et al*., 2007; Lupien *et al*., 1998). However, the mechanisms underlying the development of diabetic encephalopathy and associated cognitive impairments remain unknown.

The prevention of neurodegeneration represents one of the critical goals of medical research today, and one candidate to manage diabetes-induced neurodegeneration is caffeine. Caffeine is the most widely consumed psycho-active substance and was suggested to improve performance in learning and memory tasks (discussed in Fredholm *et al*., 1999) in both humans (*e.g.* Johnson-Kozlow *et al*., 2002) and animals (*e.g.* Angelucci *et al*., 1999, 2002). Furthermore, chronic caffeine consumption has the ability to attenuate CNS injury, namely preventing cognitive impairment associated with Alzheimer's disease (*e.g.* Arendash *et al*., 2006; Dall'Igna *et al*., 2007; Maia and de Mendonça, 2002). On the other hand, habitual caffeine consumption has been suggested to reduce the risk of diabetes, since it is inversely associated with a reduction of glucose tolerance, possibly due to increased resting metabolic rate, peripheral energy expenditure and weight loss (*e.g.* Greenberg *et al*., 2006; Higdon and Frei, 2006; van Dame and Hu, 2005).

The molecular targets of caffeine in non-toxic concentrations are the adenosine A_1 and A_{2A} receptors (Fredholm *et al*., 1999), and chronic brain insults, including STZ-induced diabetes, modify their density in the hippocampus (reviewed in Cunha, 2005). Given that diabetes can lead to up-regulation of adenosine A_{2A} receptors in the CNS, it was hypothesized that chronic caffeine treatment could prevent diabetes-induced alterations in the hippocampus by both antagonizing hippocampal A_{2A} receptors and reducing the severity of uncontrolled diabetic condition through the control of peripheral glucose homeostasis.

4.4.1. Chronic caffeine consumption prevents diabetes-induced alterations in the hippocampus of NONcNZO10/LtJ mice

The question of whether caffeine consumption could prevent diabetes-induced hippocampal alterations was addressed using the diabetic mouse strain NONcNZO10/LtJ (Cho *et al.*, 2007), where it was investigated if chronic caffeine consumption could prevent the molecular and morphological alterations induced by diabetes in the hippocampus.

4.4.1.1. Caffeine intake reduced body weight and glycaemia

To evaluate whether caffeine is able to prevent hippocampal alterations induced by diabetes, NONcNZO10/LtJ diabetic mice and respective control mice were allowed to access caffeine at 1 g/L in the drinking water during 4 months, starting at 7 months of age. As shown in Table 4.12, the average caffeine intake was similar in both control and diabetic groups through out the treatment period, and achieved similar serum caffeine concentrations as measured after four months of

Table 4.12. Characteristics of the mice involved in the study, during and/or after caffeine treatment. The study included 10 mice in the control, diabetic and caffeine groups, and 9 diabetic mice treated with caffeine (1 g/L in drinking water). * P<0.05, ** P<0.01, *** P<0.001 compared to control; # P<0.05, ### P<0.001 compared to diabetic; $ P<0.05 compared to caffeine.

	Control mice	Diabetic mice	Diabetic mice + Caffeine	Control mice + Caffeine
Caffeine intake (mg/day/kg)				
month 1			101±12	91±8
month 2			104±5	92±5
month 3			91±5	87±5
month 4			86±5	85±4
Serum caffeine (µM)			50.1±13.8	54.8±10.4
Body weight (g)				
before	43.6±1.5	46.1±1.0	47.0±1.4 $	41.4±0.7
month 1	44.9±1.4	50.1±0.9	45.7±1.5	43.7±0.9 #
month 2	48.7±1.4	51.1±1.3	46.8±1.2	46.7±1.9
month 3	50.4±1.7	52.5±1.6	47.9±1.2	46.6±1.6 #
month 4	52.9±2.3	53.5±2.2	47.5±1.2 #	47.7±1.9 #
Glycaemia (mg/dL)				
month 1	138.7±3.6	375.0±57.9 ***	249.6±47.4 #	138.4±7.7 ###
month 2	165.6±6.0	396.9±55.2 ***	259.9±41.7 #	181.2±17.8 ###
month 3	153.4±11.9	357.9±58.2 ***	261.4±34.1 #	150.0±7.3 ###
month 4	162.67±23.8	426.1±61.9 ***	282.3±22.9 #. $	139.4±11.2 ###
Serum insulin (µg/L)	6.2±1.2	33.4±12.0 *	38.9±7.9 **	13.2±3.9

caffeine consumption. Both body weight and pre-prandial glycaemia were monitored through the study, and the serum insulin concentration was quantified at the end of the treatment period. Long-term caffeine consumption reduced the weight gain and pre-prandial glycaemia in obese and diabetic mice but failed to prevent diabetes-associated hyper-insulinemia (Table 4.12).

4.4.1.2. Caffeine prevents diabetes-induced memory deficits

The behavioural study was performed before and after the caffeine treatment period, at 7 and 11 months of age respectively. Since the Y-maze test is dependent on the exploratory behaviour of the mice, this was observed in an open-field arena immediately before the evaluation of Y-maze spontaneous alternation. Neither diabetes nor prolonged caffeine consumption affected significantly the locomotor activity or exploratory behaviour, as suggested by similar number of crossing (Figure 4.34A) and rearing (Figure 4.34B) events in the open-field arena test and similar number of explorations in the Y-maze arms (Figure 4.34C). However, the age factor consistently affected exploratory activity of the mice in the four animal groups, indicated by significant reduction of crossing and reading events ($P<0.001$, n=8-10) and entries in the Y-maze arms ($P<0.001$, n=8-10). The spontaneous alternation in the Y-maze task revealed that diabetes caused a reduction of the performance of hippocampal-dependent spatial memory at 11 months of age, in comparison

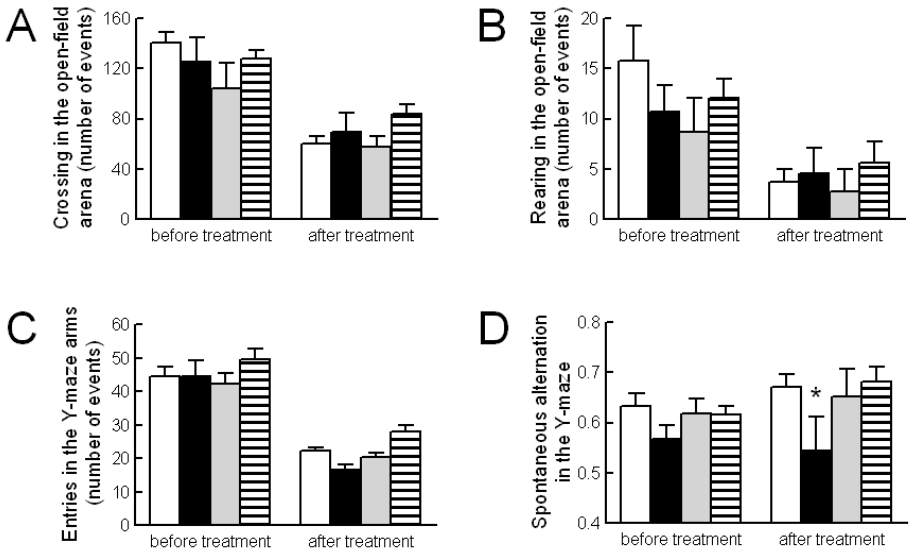

Figure 4.34. Behavioural tasks showed that caffeine consumption prevents spatial working memory deficits induced by diabetes. Number of crossings in the open-field arena was unaltered by diabetes or caffeine consumption (A), as well as the number of rearing events (B). The amount of entries in the Y-maze arms was similar in the four animal groups (C). Diabetic mice (black bars) displayed reduced spontaneous alternation in the Y-maze at 11 months of age, when compared to controls (white bars), but not if treated with caffeine (gray bars) for four months (D). Control mice consuming caffeine (striped bars) did not present significant behavioural alterations. Data is presented as mean±SEM and was compared with two-way ANOVA followed by Bonferroni's post-test (* $P < 0.05$ compared to control).

to the control mice (P<0.05, n=8-10); this was prevented by 4 months of caffeine consumption (Figure 4.34D), supporting the potential role of long-term caffeine consumption in the prevention of memory impairment caused by a diabetic condition.

4.4.1.3. Lack of neuronal degeneration in the hippocampus

Hippocampal cellular organization and degeneration were evaluated on brain sections stained with cresyl violet and FluoroJade-C, respectively. These histological analysis revealed qualitatively similar cresyl vilet staining of the Nissl bodies (Figure 4.35A) and lack of FluoroJade-C stained cells (data not shown) in the hippocampal formation among the four animal groups, supporting the lack of neuronal damage caused by diabetes. This was corroborated by the absence of modification of MAP2 immunoreactivity in the hippocampus, as observed in either immuno-histochemistry of brain sections (Figure 4.35B) or Western blot analysis of hippocampal membranes (Figure 4.35C).

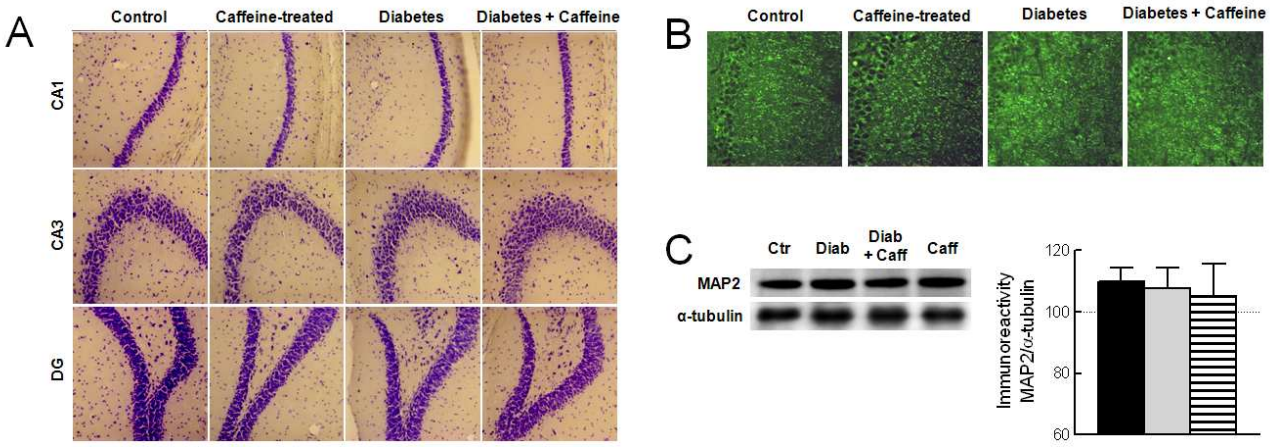

Figure 4.35. Diabetic NONcNZO10/LtJ mice did not present structural alterations in the hippocampus when evaluating Nissl bodies stained with cresyl violet (A) in dentate gyrus (DG), CA1 and CA3 regions. Neither diabetes nor caffeine consumption affected MAP2 immunoreactivity in the hippocampus as evaluated by qualitative immuno-histochemisty (B) and Western blot analysis (C). Panel B presents photographs of MAP2 immuno-histochemisty in the CA1 region of the hippocampus as example. Panel C shows Western blots representative of 6 similar experiments for the analysis of MAP2 density in hippocampal membranes; the bar graph displays the average immunoreactivity data normalised to α-tubulin immunoreactivity and calculated as percentage of control in the same Western blot experiment. Black, gray and striped bars represent diabetes, diabetes plus caffeine and caffeine groups, respectively.

4.4.1.4. Caffeine attenuates synaptic degeneration

We further evaluated whether NONcNZO10/LtJ diabetic mice displayed alterations on synaptic proteins, integrating the vesicular machinery at the nerve terminal, which could be related

to decreased hippocampal-dependent Y-maze spontaneous alternation. Western blot analysis of synaptic proteins (Figure 4.36A and B) showed a reduction in the immunoreactivity of synaptophysin (-23.3+4.9%, n=6, P<0.001) and SNAP25 (-28.6+6.5%, n=6, P<0.05) in membranes prepared from the hippocampus, indicating the occurrence of synaptic degeneration, previously shown to occur in STZ-induced diabetes (section 4.2.1.3). Caffeine consumption for four months was able to prevent diabetes-induced alteration of SNAP25 immunoreactivity (Figure 4.36B) and to attenuate synaptophysin decrease (Figure 4.36A) in the hippocampus of diabetic mice. These results suggest that caffeine may have a certain protective effect on the synaptic deterioration that occurs upon a diabetic condition. The synaptophysin immuno-histochemistry on brain sections (Figure 4.36C) was not sensitive enough to find the localization of this reduction in synaptophysin density within the hippocampal structure. Nevertheless, the quantification of the immunoreactivity in hippocampal regions showed a tendency for reduction of synaptopysin in the CA1, CA3 and dentate gyrus of the diabetic mice when compared to control mice or the other animal groups (Figure 4.36D).

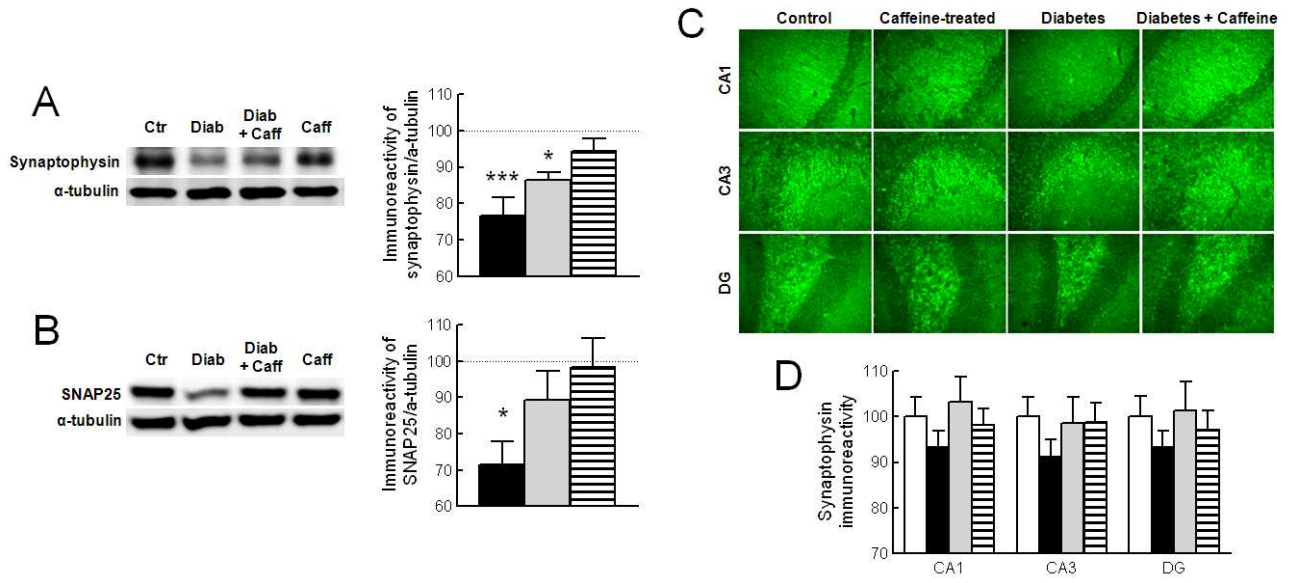

Figure 4.36. Caffeine consumption attenuated diabetes-induced synaptic degeneration. Western blot analysis revealed that diabetic mice displayed reduced immunoreactivity of both synaptophysin (A) and SNAP25 (B) in hippocampal membranes, when compared to controls. Caffeine consumption prevented this diabetes-induced reduction of SNAP25 and attenuated diabetes-induced reduction of synaptophysin. The graphs in panels A and B show the average immunoreactivity of synaptic proteins normalised to α-tubulin immunoreactivity and calculated as percentage of control in the same Western blot experiment. In the graphs, black, gray and striped bars represent diabetes, diabetes plus caffeine and caffeine groups, respectively. Immuno-histochemisty to synaptophysin (C and D) showed a non-significant reduction of immunoreactivity in the 3 regions of the hippocampus in the diabetes group compared to control. Data is shown as mean±SEM and was compared with ANOVA followed by Bonferroni's post-test (* P<0.05, *** P<0.001 compared to control).

4.4.1.5. Caffeine prevents diabetes-induced astrocytosis

Qualitative immuno-histochemistry of the astrocytic protein GFAP in brain sections revealed an increased number of GFAP-positive cells in the hippocampus of diabetic mice, when compared to controls (Figure 4.37A). Accordingly, western blot analysis of hippocampal membranes showed a 54.7+18.8% increase in the intensity of GFAP immunoreactivity (n=6, P<0.01) in the hippocampus of diabetic mice compared to controls (Figure 4.37B). As shown in Figure 4.37, caffeine consumption was able to prevent this diabetes-induced astrocytosis, as suggested by the reduction to control levels of GFAP immunoreactivity in hippocampal membranes and the number of GFAP-positive cells in the hippocampus.

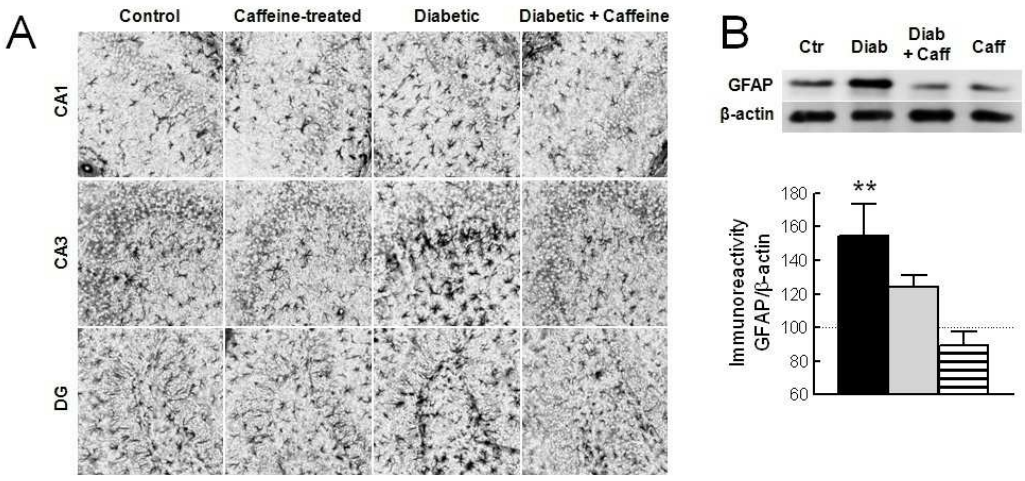

Figure 4.37. Caffeine consumption prevented astrocytosis caused by diabetes. Panel A shows representative photographs of CA1, CA3 and dentate gyrus (DG) of immuno-histochemistry for GFAP in mouse brain sections. When compared to controls, diabetic mice displayed increased number of GFAP-positive cells in the hippocampus, but not when allowed to consume caffeine. Panel B presents a Western blot representative of 6 similar experiments for the analysis of GFAP density in hippocampal membranes, showing increased of GFAP immunoreactivity in diabetes. Hippocampal membranes were applied in equal amounts to the SDS-PAGE gel, which was confirmed by β-actin immunoreactivity. In the graph bellow, GFAP immunoreactivity was normalised to β-actin and calculated as percentage of control in the same Western blot experiment. Black, gray and striped bars represent diabetes, diabetes plus caffeine and caffeine groups, respectively. Data is mean±SEM and was compared with ANOVA followed by Bonferroni's post-test (** P<0.01 compared to control).

4.4.1.6. Density of adenosine A_1 receptors

For the evaluation of A_1 receptor density, Western blot analysis was performed using hippocampal membranes. When compared to controls, diabetic mice displayed a significant reduction of A_1 receptor immunoreactivity (-29.6+6.7%, n=6, P<0.05) in hippocampal membranes, which was prevented by long term caffeine consumption (Figure 4.38).

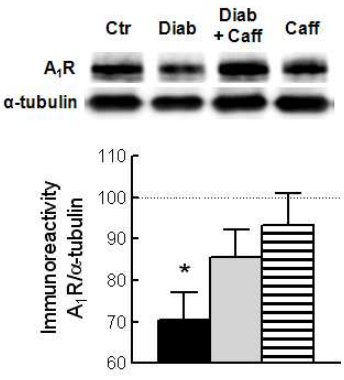

Figure 4.38. Diabetes-induced alteration of the density of hippocampal adenosine A_1 receptors is prevented by caffeine consumption. Western blot analysis (representative of 6 similar blots from different groups of rats) comparing the A_1 receptor immunoreactivity, corresponding to the 37 kDa band, in total membranes from the hippocampus of control and diabetic mice treated or not with caffeine, applied to the SDS-PAGE gel in equal amounts. A re-probing of the membranes to α-tubulin is shown below each gel, and confirmed that similar amounts of protein were added to the lanes. The graph below the gel shows the average immunoreactivity of A_1 receptors in total hippocampal membranes, normalized to α-tubulin and expressed as percentage of control immunoreactivity. Black, gray and striped bars represent diabetes, diabetes plus caffeine and caffeine groups, respectively. Data is mean±SEM and was compared with ANOVA followed by Bonferroni's post-test (* P<0.05 compared to control).

4.4.1.7. Synaptic distribution of adenosine A_1 and A_{2A} receptors

The distribution of adenosine A_1 and A_{2A} receptors within glutamatergic and GABAergic nerve terminals was evaluated by quantifying the co-localization of A_1 and A_{2A} receptors in synaptosomes purified from the hippocampus, as illustrated in Figure 4.39A. The fraction of co-localization of glutamatergic (vGluT1/2) and GABAergic (vGAT) markers with synaptophysin was not affected by either diabetes or caffeine consumption (Figure 4.39B), suggesting a preservation of the ratio of glutamatergic and GABAergic synapses in the hippocampus. The immunoreactivity of A_1 receptor and A_{2A} receptor detected in glutamatergic nerve terminals (identified by vGluT1/2) was similar in the four experimental groups (Figures 4.39C). As shown in Figure 4.39D, diabetes

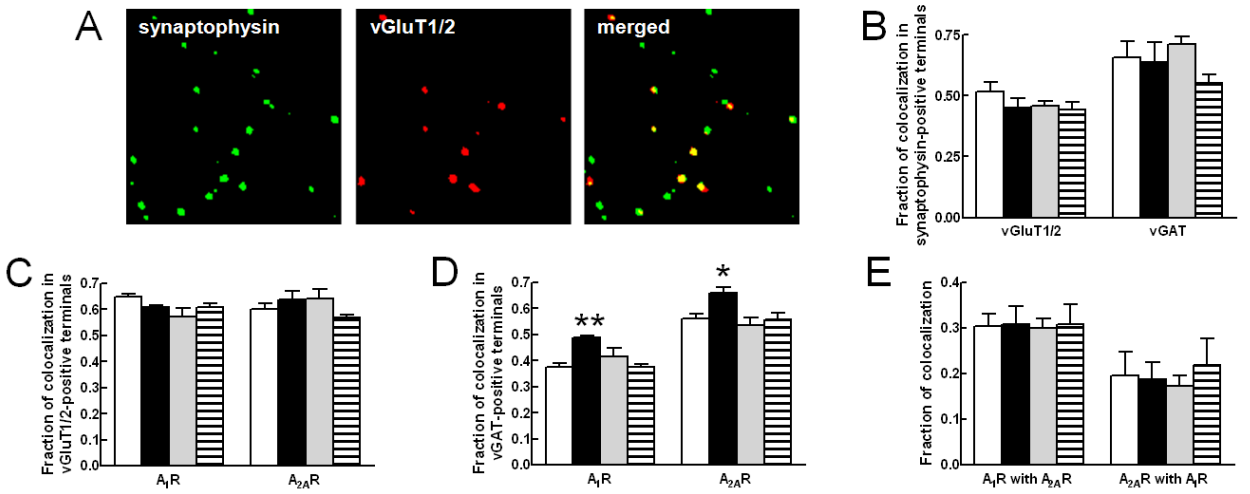

Figure 4.39. Co-localization analysis of A_1 and A_{2A} adenosine receptors in glutamatergic and GABAergic nerve terminals purified from the hippocampus. Panel A exemplifies the double immunostaining performed in this analysis, in this case to determine the fraction of glutamatergic (vGluT1/2-positive) nerve terminals (synaptophysin immunoreactivity). The fraction of glutamatergic and GABAergic nerve terminals in the hippocampus was similar in the four experimental groups (B). The amount of glutamatergic nerve terminals containing A_1 or A_{2A} receptors was not altered (C) but, compared to controls, diabetic mice displayed increased number of GABAergic nerve terminals endowed with A_1 or A_{2A} receptors (D). The fraction of nerve terminals immunoreactive for both A_1 and A_{2A} receptors was similar in the four animal groups. White, black, gray and striped bars represent control, diabetes, diabetes plus caffeine and caffeine groups, respectively. * P<0.05, ** P<0.01 compared to control (n=5 for each co-localization analysis).

increased the fraction of vGAT positive nerve terminals endowed with either A_1 receptor or A_{2A} receptor immunoreactivity by 30.7+1.3% ($P<0.05$, n=4) and 17.9+3.9% ($P<0.05$, n=4), respectively. This diabetes-induced increase in the fraction of GABAergic nerve terminals equipped with adenosine receptors was prevented by long-term consumption of caffeine (Figures 4.39D). Furthermore, the co-localization of A_1 receptor and A_{2A} receptor in hippocampal nerve terminals was investigated by double labelling of purified synatosomes with antibodies against each receptor; it was observed that there was neither modification of the fraction of A_1 receptor-positive nerve terminals containing A_{2A} receptors, nor vice versa (Figure 4.39E). Taken together, these results indicate that the balance between nerve terminals equipped with A_1 receptors and A_{2A} receptors is maintained upon a diabetic condition, but there is an alteration on adenosinergic signalling, occurring in GABAergic rather than glutamatergic nerve terminals.

4.4.1.8. Discussion

The main finding of the present work is that long-term caffeine consumption attenuates the deleterious effects of diabetes on the hippocampal tissue, associated with the prevention of diabetes-associated learning and memory impairments. Our results showed that NONcNZO10/LtJ diabetic mice neither display alterations on cellular organization nor present neuronal degeneration in the hippocampal structure. However, when compared to NON/LtJ controls, diabetic mice had reduced density of synaptic proteins in the hippocampus, indicating the occurrence of synaptic degeneration, which likely contributes to the diabetes-induced memory impairment. Likewise, streptozotocin-induced diabetic rats displayed a reduction of the density of synaptic proteins when compared to control animals (Nitta *et al*., 2002; see also section 4.2.1.3), which could be related to the observed spatial memory deficits in the Y-maze (Nitta *et al*., 2002) or the Morris water maze (*e.g.* Biessels *et al*., 1996).

Furthermore, synaptic alterations in the hippocampus were accompanied by astrocytosis, suggested by increased GFAP immunoreactivity and number of GFAP-positive cells in the diabetic hippocampus, when compared to controls. In the central nervous system, neurons and surrounding glial cells compose a highly specialized functional unit, where neurons form a network through synaptic contacts and the adjacent astrocytes provide a structural, metabolic and trophic support to neurons, and modulate neuronal excitability and neurotransmission (*e.g.* Dong and Benveniste, 2001). Upon neuronal damage, astrocytes can become reactive by altering their morphology and proliferating, and the hippocampus of diabetic mice displayed hypertrophic cell bodies and

increased processes with augmented density of GFAP. Similar to the observed astrocytosis in the aged brain (Pilegaard *et al*., 1996; Rozovsky *et al*., 1998; Wagner *et al*., 1993), these astrocytic changes may occur due to primary neuronal damage, and this altered glial function may negatively affect synaptic activity and neuronal survival for example due to the specific downregulation of glutamate transporters, which was observed in several pathologies such as amyotrophic lateral sclerosis (Barbeito *et al*., 2004), Alzheimer's disease (Lauderback *et al*., 2001) and Lewy-body dementia (Honig *et al*., 2000), or in result of the contribution for the formation of free radicals through the induction of iNOS (*e.g*. Chao *et al*., 1996), or even by the astrocytic production of apoptotic factors that was suggested to occur in several neurodegenerative pathologies (*e.g*. Crutcher *et al*., 1993; Fahnestock *et al*., 1996; Ferrer *et al*., 2000, 2001).

As shown to occur in STZ-induced diabetes (section 4.2.1), NONcNZO10/LtJ diabetic mice showed an alteration on the adenosinergic modulation system in the hippocampus. In particular, there was a global down-regulation of inhibitory A_1 receptors, and an increase in the fraction of GABAergic nerve terminals equipped with A_1 and/or A_{2A} adenosine receptors. The action of caffeine on synaptic A_{2A} receptors that are upregulated neurodegenerative disorders, in particular in the diabetic hippocampus, may cause a reduction of glutamate release into the synaptic cleft (Lopes *et al*., 2002), and eventually prevent glutamate excitotoxicity induced by hyperglycaemia. In addition, A_{2A} receptor blockade by caffeine on the glial compartment may inhibit glutamate outflow (Nishizaki *et al*., 2002; Pintor *et al*., 2004). Adenosine was already suggested to have a homeostatic role in the CNS, which could be related to direct control of intermediary metabolism (Hammer *et al*., 2001; Håberg *et al*., 2000). Because diabetes induces modification of extra-synaptic adenosine receptors, in particular increasing the density of A_{2A} receptors, neuroprotective effects of caffeine could be related to this ability of controlling brain metabolism, also suggested by its effects on glucose transport, namely in the hippocampus (Nehlig *et al*., 1984, 1986).

In the present experiments, long-term caffeine consumption attenuated diabetes-induced synaptic degeneration and prevented astrocytosis in the hippocampus. This beneficial effect of caffeine intake was reflected in the prevention of diabetes-associated memory impairment, as evaluated by the spontaneous alternation in the Y-maze. It was investigated the density of two synaptic markers with different locations: synaptophysin that is located in synaptic vesicles and SNAP25 that is a membrane protein at the active zone of nerve terminals (Pinheiro *et al*., 2003, and references therein). The density of both proteins decreased in the hippocampus of diabetic mice when compared to controls, and long-term caffeine intake prevented SNAP25 reduction and attenuated synaptophysin alteration. Also the alterations induced by diabetes on the adenosinergic modulation system were prevented by caffeine intake and interestingly, in this particular mouse

strain, it was not observed alteration of distribution of synaptic adenosine receptors caused by four months of caffeine consumption.

Astrocytes are the main glial cells involved in the metabolic support to neurons, and their glycogen storing capacity can be used to buffer fluctuations on glucose concentration (Gruetter, 2003). Moreover, adenosine receptors can control intermediary metabolism in the hippocampus (in both neurons and astrocytes; see section 4.1.3) and modulate astrocytic glycogen synthesis (Allaman *et al*., 2003; Magistretti *et al*., 1986). Thus there is the possibility of caffeine controlling glucose availability to neurons through actions on the metabolism of astrocytes.

The present work studied the global effect of caffeine intake on the prevention of the development of diabetic encephalopathy. Together with the action of caffeine on A_{2A} receptors located at the CNS, caffeine administered in the drinking water can activate peripheral adenosine receptors, leading to increased metabolic rates and elevated energy expenditure, which contribute for the management of the diabetic condition (*e.g.* Greenberg *et al*., 2006; Higdon and Frei, 2006; van Dame and Hu, 2005). In fact, adenosine was suggested to be involved in regulating glucose homeostasis in peripheral organs like the heart (*e.g.* Finegan *et al*., 1996; Fraser *et al*., 1999; Gao *et al*., 1997; Wyatt *et al*., 1989), liver (*e.g.* Buxton *et al*., 1986; Vanstapel *et al*., 1991) or muscle (*e.g.* Derave and Hespel, 1999; Hespel and Richter, 1998; Vergauwen *et al*., 1994). Moreover, caffeine can regulate the secretion of insulin by blocking adenosine receptors at the pancreatic islet cells (Johansson *et al*., 2007). Accordingly, diabetic mice that consumed caffeine displayed glycaemia lower than untreated diabetic mice, but circulating levels of insulin remained unaltered by caffeine intake. One can not exclude that the reduction of glycaemia may contribute to the beneficial effects of long-term caffeine intake in diabetic animals. However, since blood glucose levels of diabetic mice consuming caffeine was sustained above 250 mg/dL during 4 months (twice than in control mice), the observed neuroprotective effects of caffeine are likely due to blockade of central adenosine receptors.

In conclusion, the present animal model of diabetes displays spatial memory impairment, hippocampal synaptic degeneration without neuronal loss and astrocytosis. The results now obtained provide evidences to support the hypothesis that long-term caffeine consumption attenuates synaptic degeneration in hippocampal neurons and the extent of astrocytosis, leading to a prevention of diabetes-induced memory impairment. These are pioneering results suggesting that caffeine, or eventually other adenosine (A_{2A}) receptor antagonists, may be used for the prevention of diabetic encephalopathy.

4.4.2. Glucose transport and neurochemical profile in the hippocampus of streptozotocin-induced diabetic rats - effect of caffeine consumption

Glucose is the main source of energy for brain function, but the brain may eventually be able to adapt to a new metabolic condition (Pelligrino *et al*., 1992). In peripheral tissues, inadequate glucose utilization is the hallmark of a diabetic condition. However, published studies inconsistently report the effects of diabetes on substrate transport into the brain. In particular, glucose transport into the brain was suggested to be reduced (McCall *et al*., 1982), augmented (Duelli *et al*., 2000) or unaffected (Kainulainen *et al*., 1993; Simpson *et al*., 1999) by hyperglycaemia.

The recent developments in the resolution of *in vivo* ^{1}H NMR spectroscopy prompt re-evaluating the impact of diabetes on glucose uptake. Thus, the aim of the present work was to determine the effect of a diabetic condition characterized by chronic hyperglycaemia on the transport of glucose across the BBB and on the neurochemical profile in the hippocampus, and to test the potential protective role of chronic caffeine consumption on the observed hippocampal alterations. This was evaluated taking advantage of *in vivo* ^{1}H NMR spectra measured in the hippocampus of STZ-induced diabetic rats and age-matched controls that consumed or not caffeine. The technical and methodological developments in high-field *in vivo* NMR spectroscopy increased localization performance and sensitivity gain leading to high spectral quality and improved reliability of the metabolite concentrations achievable from *in vivo* ^{1}H NMR spectra (*e.g.* Mlynárik *et al*., 2006; Tkáč *et al*., 1999). This approach allowed revealing alterations in the neurochemical profile of the hippocampus caused by chronic hyperglycaemia, as well as to study hippocampal glucose transport kinetics.

Type 1 diabetes *mellitus* was induced with STZ in male Sprague-Dawley rats, resulting in blood glucose levels above 300 mg/dL after 3 days as in previous studies. Sham-treated age-matched control rats received vehicle injection and were maintained in the same conditions. Half of the animals were allowed to consume caffeine (1 g/L) that was provided for 6 weeks starting 2 weeks before STZ injection. Rats were maintained for 4 weeks with food and water *ad libitum*, and the NMR study was carried out 30 days after STZ-treatment.

During the period when the rats had free access to caffeine solution, both before and after STZ-treatment, body weight and pre-prandial glycaemia were monitored. As shown in Figures 4.40A and B, after STZ injection, there was a reduction of weight gain and a significant sustained increase in pre-prandial glycaemia of the diabetic rats when compared to controls, whether the animals consumed caffeine or not. Caffeine consumption was similar in control and STZ-treated

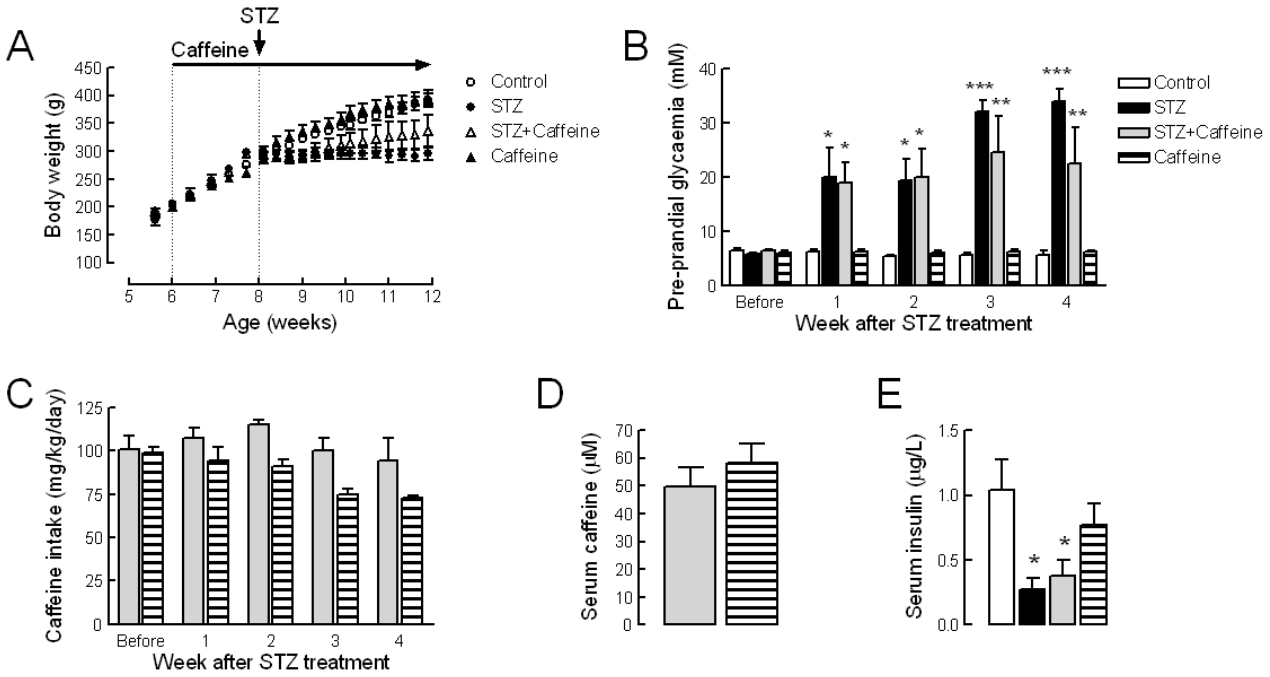

Figure 4.40. Characteristics of the animals used in the study, including body weight (A), pre-prandial glycaemia (B) and caffeine intake (C) measured across the housing period, and caffeine (D) and insulin (E) concentrations in the serum determined at the end of the treatment. Caffeine was available in the drinking water from 6 weeks old onwards and STZ was administered at 8 weeks of age (A), being the animals maintained under hyperglycaemia (B) and hypo-insulinemia (E) for 4 weeks. White, dark, grey and striped bars the graphs represent control (n=8), STZ-treated (n=6), STZ plus caffeine-treated (n=6), and caffeine-treated control (n=6) rats, respectively. Values are mean±SEM and significant differences on glycaemia (B) and serum insulin (E) were estimated with the ANOVA and are noted as follows: * P<0.05, ** P<0.01, *** P<0.001, relative to control.

rats (P>0.05, Figure 4.40C), and achieved similar serum caffeine levels (P>0.05, Figure 4.40D). Insulin concentration was reduced in STZ-treated rats when compared to controls (P<0.05), and caffeine consumption did not affect significantly circulating insulin levels (Figure 4.40E), suggesting that caffeine treatment did not interfere with STZ action.

4.4.2.1. Streptozotocin-induced diabetes affects neurochemical profile but not glucose transport in the hippocampus

Physiologic parameters measured during the period of NMR data acquisition were similar in the four experimental groups (Table 4.12). In healthy rats, plasma lactate concentration increased with the increase of plasma glucose concentrations. This did not occur in STZ-treated rats, suggesting reduced glucose uptake due to hypo-insulinemia, and consequent reduced glucose metabolism.

Table 4.12. Physiologic parameters measured at 5 different ranges of plasma glucose concentration during the NMR experiment. Values are shown as mean±SEM of n experiments for the different groups: control (n=8), caffeine-treated (n=6), STZ-treated (n=6) and STZ and caffeine-treated (n=6) rats. Significant differences in plasma lactate were determined with ANOVA and Bonferroni's post test, and are noted as follows: * P<0.05, ** P<0.01, *** P<0.001, relative to normoglycaemia (< 8 mM of plasma glucose).

Plasma glucose range (mM)		< 8	8 to 12	12 to 18	18 to 26	> 26
Body Temperature (°C)	Control	37.8±0.1	37.3±0.2	37.3±0.2	37.5±0.1	37.7±0.1
	Caffeine	37.2±0.2	37.6±0.1	37.4±0.1	37.4±0.1	37.7±0.1
	STZ	37.4±0.1	37.4±0.1	37.3±0.2	37.3±0.3	37.5±0.1
	STZ+Caff	37.2±0.1	37.5±0.1	37.6±0.1	37.6±0.2	37.4±0.2
Arterial pH	Control	7.36±0.02	7.35±0.01	7.31±0.02	7.36±0.01	7.35±0.04
	Caffeine	7.37±0.02	7.32±0.04	7.35±0.04	7.33±0.02	7.36±0.04
	STZ	7.32±0.04	7.40±0.01	7.37±0.01	7.38±0.02	7.39±0.01
	STZ+Caff	7.42±0.01	7.44±0.01	7.43±0.01	7.40±0.01	7.37±0.03
P_aCO_2 (mm Hg)	Control	41.0±1.1	40.6±1.7	44.0±1.5	44.4±0.9	46.0±2.1
	Caffeine	46.4±4.3	40.8±3.9	44.5±7.2	45.2±7.1	48.6±3.6
	STZ	47.5±4.8	41.6±3.9	37.6±0.7	38.2±1.6	42.6±2.0
	STZ+Caff	39.7±1.1	40.8±1.7	40.5±0.8	43.1±0.5	41.6±0.8
Plasma glucose (mM)	Control	5.6±0.4	10.2±0.5	14.5±0.6	22.3±0.5	32.8±1.2
	Caffeine	6.2±0.3	10.4±0.2	14.7±0.6	22.2±0.5	31.7±1.0
	STZ	5.7±0.5	10.4±0.5	15.7±0.5	20.4±0.8	32.6±1.2
	STZ+Caff	5.9±0.5	10.3±0.3	15.4±0.6	22.0±0.8	32.1±1.3
Plasma lactate (mM)	Control	0.8±0.1	1.5±0.1 **	2.2±0.3 ***	2.8±0.1 ***	3.2±0.1 ***
	Caffeine	1.1±0.2	1.6±0.2	1.8±0.2 *	2.2±0.2 ***	2.9±0.1 ***
	STZ	1.3±0.1	1.2±0.1	1.5±0.1	1.4±0.3	1.0±0.1
	STZ+Caff	1.5±0.2	1.9±0.2	1.8±0.2	1.7±0.2	2.0±0.2

A detailed investigation of diabetes-induced alterations in the hippocampal metabolite concentrations under hyper- and normo-glycaemia was then carried out. Figure 4.41 shows typical ^{1}H NMR spectra from the hippocampus obtained in the present study, which illustrates the spectral quality achieved at high field, *i.e.* high spectral resolution and signal to noise ratio in a volume as small as 18 µL localised in the hippocampus.

When compared to controls at euglycaemia (plasma glucose of 5.6±0.5 mM, n=8), STZ-induced diabetic rats under hyperglycaemia (plasma glucose of 33.3±3.4 mM, n=6) displayed significant alterations on the neurochemical profile of the hippocampus (Figure 4.42). Namely, there was an increase on the concentration of βHB, GPC, *myo*-inositol, NAA, taurine and total creatine, as well as a reduction of the concentration of GSH and NAAG. When glycaemia of STZ-treated rats was reduced by means of insulin infusion, the majority of the metabolic alterations in the hippocampus were normalised to control levels (Figure 4.42), suggesting that the metabolic alterations in the diabetic hippocampus result from deregulated osmolarity. In comparison to controls, STZ-treated rats under euglycaemia (plasma glucose of 7.9±1.7 mM, n=6) presented a significant increase of *myo*-inositol concentration in the hippocampus (36±5%, n=6, P<0.001).

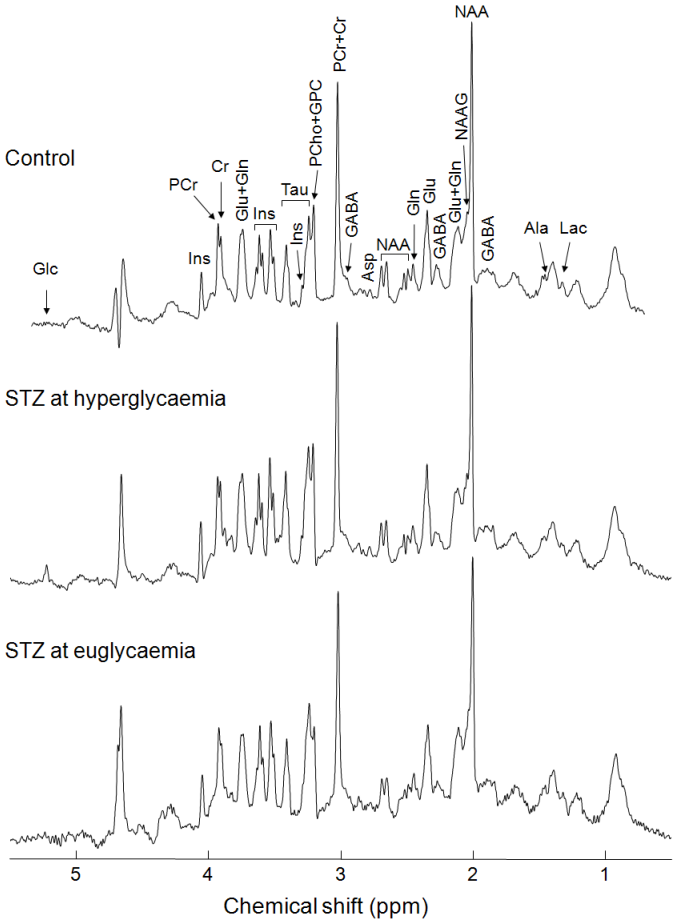

Figure 4.41. Representative *in vivo* ^{1}H NMR spectra of the rat hippocampus expanded from 0.5 to 5.5 ppm. The top spectrum was acquired from the hippocampus of a 12 week old healthy rat, while the spectra bellow were acquired from a STZ-induced diabetic rat of the same age either at hyper- or euglycaemia. The spectra were measured by the SPECIAL sequence with echo time of 2.8 ms, repetition time of 4 s, 640 scans and VOI of 18 µl. For resolution enhancement, a shifted Gaussian function (gf = 0.12 and gsf = 0.05) was applied before Fourrier transformation. Zero-phase but not baseline was corrected.

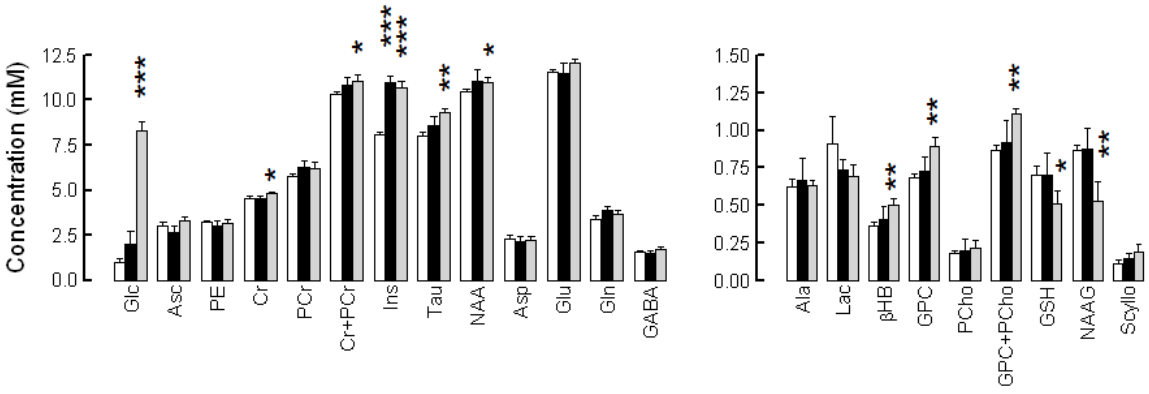

Figure 4.42. Effect of STZ-induced diabetes on the neurochemical profile of the hippocampus. The histograms show metabolite concentrations in the hippocampus of STZ-treated rats at hyperglycaemia (grey bars, n=6) and at euglycaemia (dark bars, n=6), and age matched healthy rats (white bars, n=8), determined by ^{1}H NMR spectroscopy. Values are presented as mean±SEM and statistically significant differences achieved with the Student's *t* test are noted for comparison with the control group: * P<0.05, ** P<0.01, *** P<0.001.

Chronic caffeine consumption had a distinct effect on the neurochemical profile at normoglycaemia (Figure 4.43). In fact, diabetes-induced increase of *myo*-inositol concentration in the hippocampus was attenuated by caffeine consumption to 15±5% increase (n=6, P<0.01) compared to controls. However, while the high taurine content in the hippocampus of STZ-treated rats was normalized at euglycaemia, it remained increased in the hippocampus of STZ-treated rats that consumed caffeine (23±6%, n=6, P<0.001, compared to controls). Interestingly, chronic caffeine consumption resulted in a slight reduction of total creatine (P<0.05 compared to controls) in the hippocampus of control rats (Figures 4.43 and 4.44). Control rats under hyperglycaemia did not exhibit significant alterations on the neurochemical profile of the hippocampus, when compared to euglycaemia (data not shown).

Regarding the group of rats treated with both STZ and caffeine, the neurochemical profile shown in Figure 4.43 was determined at euglycaemia (plasma glucose of 6.1±1.0 mM, n=6) and it

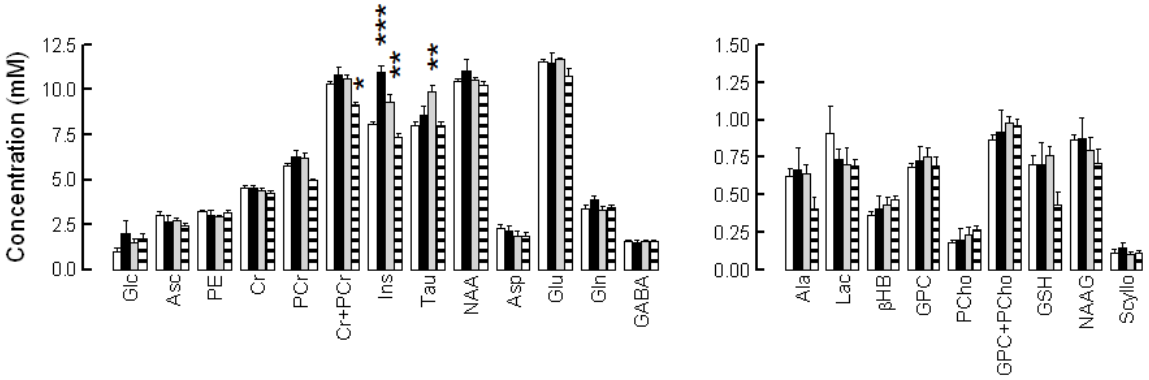

Figure 4.43. Metabolite concentrations in the hippocampus of control (white bars, n=8), STZ-treated (dark bars, n=6), STZ plus caffeine-treated (grey bars, n=6), and simply caffeine-treated (striped bars, n=6) rats, determined by ^{1}H NMR spectroscopy. Values are mean±SEM and significant differences determined in comparison with the control group by the ANOVA are noted as follows: * P<0.05, ** P<0.01, *** P<0.001.

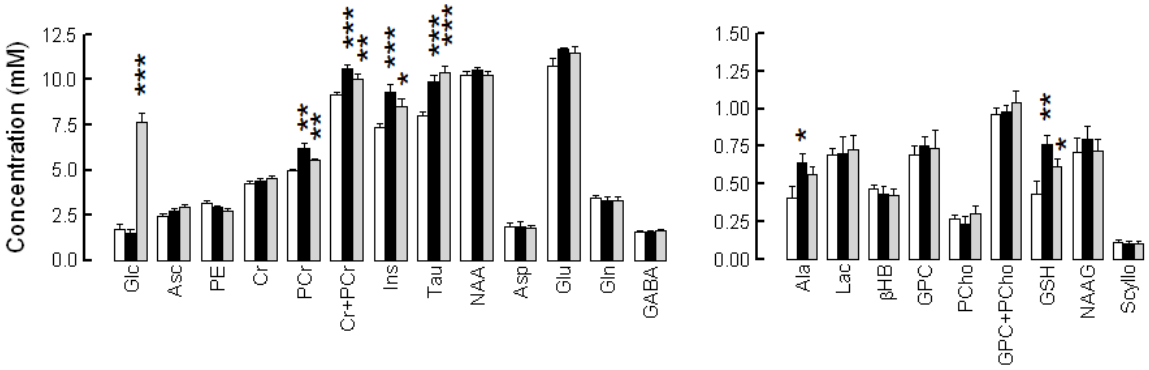

Figure 4.44. Neurochemical profile in the hippocampus of caffeine-treated STZ-induced diabetic rats at hyperglycaemia (grey bars, n=6) and at euglycaemia (dark bars, n=6), and age matched healthy caffeine-treated rats (white bars, n=6), determined by ^{1}H NMR spectroscopy. Values are presented as mean±SEM and statistically significant differences achieved with the Student's *t* test are noted for comparison with the control group: * P<0.05, ** P<0.01, *** P<0.001.

was similar to that found upon hyperglycaemia (plasma glucose of 31.6±2.7 mM, n=6) (Figure 4.44). Figures 4.43 and 4.44 illustrate the differences in the hippocampal neurochemical profile from diabetic and control rats, both treated with caffeine. Compared to the caffeine-treated group, the STZ-induced diabetic animals consuming caffeine had higher concentration of *myo*-inositol, PCr, taurine, alanine and GSH, and these concentrations were similar at hyper- and euglycaemia. In summary, from the analysis of the neurochemical profile in the hippocampus of the animals used, there are robust modifications in *myo*-inositol and taurine concentrations caused by STZ-induced diabetes. Compared to healthy rats, diabetic rats under hyperglycaemia displayed increased *myo*-inositol and taurine concentrations, being taurine levels restored at euglycaemia. However, diabetic rats that were allowed to consume caffeine, showed smaller increase of *myo*-inositol content, and did not normalise diabetes-induced increment of taurine levels at euglycaemia.

Glucose concentration was significantly increased in the hippocampus of the diabetic rat, as visible in the glucose signal at 5.23 ppm in ^{1}H NMR spectra, but returns to control levels upon normalization of glycaemia (Figure 4.41). However, as shown in Figure 4.45, the dependence of

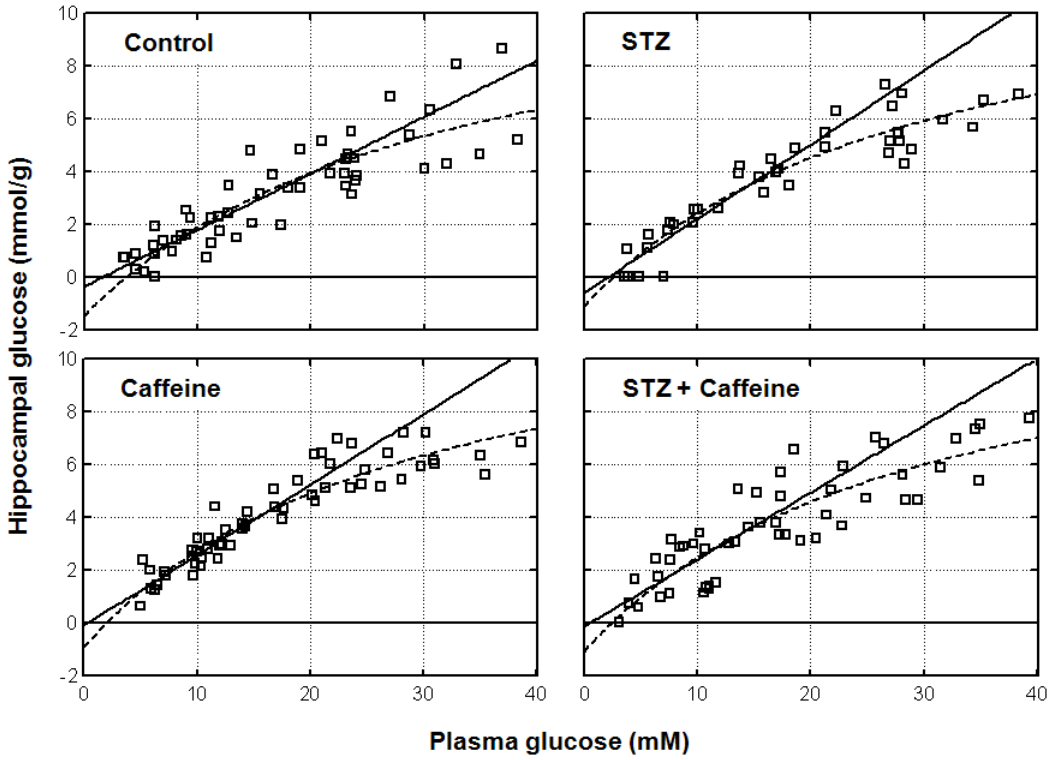

Figure 4.45. Relationship between hippocampal and plasma glucose concentrations in control, STZ-treated, STZ plus caffeine-treated, and caffeine-treated control rats. Open squares represent hippocampal glucose determined from ^{1}H NMR spectra measured (during about 40 minutes) after plasma glucose was stable for at least 15 minutes. The solid line is the best fit of the reversible Michaelis-Menten model to hippocampal glucose concentrations, up to 20 mM of plasma glucose. The dashed line represents the best fit of the standard Michaelis-Menten model to hippocampal glucose, over the entire range of plasma glucose concentrations measured. The kinetic parameters estimated from these fittings are presented in table 4.13 for each experimental group and each kinetic model.

hippocampal glucose on plasma glucose was not significantly different between controls and STZ-induced diabetic rats, suggesting that the rate of glucose transport across the BBB was not altered in the hippocampus in chronic hyperglycaemia. This was further supported by similar kinetic parameters for glucose transport estimated with either the standard or reversible Michaelis-Menten models (Table 4.13). Likewise, caffeine consumption did not significantly affect glucose transport in the hippocampus (Figure 4.45, Table 4.13).

Table 4.13. Apparent Michaelis-Menten constant K_t and ratio of T_{max} to CMR_{gluc} for the glucose transport across the BBB, estimated with the reversible and standard Michaelis-Menten models from the relationship between hippocampal and plasma glucose concentrations in control, STZ-treated, STZ and caffeine-treated, and caffeine-treated rats (data in Figure 4.45). While the standard model was fitted to the whole range of plasma glucose concentrations, the reversible model was applied up to 20 mM. Values are mean (95% confidence interval). Units of K_t are mM and T_{max}/CMR_{gluc} is adimensional.

	Reversible model		**Standard model**	
	K_t	T_{max}/CMR_{gluc}	K_t	T_{max}/CMR_{gluc}
Control	1.23 (0.00 - 3.79)	1.77 (1.48 - 2.07)	7.77 (5.68 - 9.86)	3.11 (2.91 - 3.31)
STZ-treated	2.44 (0.00 - 5.41)	2.15 (1.82 - 2.51)	6.53 (4.91 - 8.26)	3.57 (3.27 - 3.86)
STZ and Caffeine-treated	0.49 (0.00 - 4.39)	1.98 (1.53 - 2.45)	6.41 (4.25 - 8.61)	3.64 (3.25 - 4.01)
Caffeine-treated	0.34 (0.00 - 1.58)	2.06 (1.77 - 2.34)	5.83 (4.41 - 7.25)	3.98 (3.64 - 4.31)

4.4.2.2. Discussion

In the present study it was evaluated the effect of chronic hyperglycaemia, induced by STZ administration, in the neurochemical profile of the hippocampus. When compared to controls, STZ-induced diabetic rats under hyperglycaemia displayed a plethora of metabolic alterations in the hippocampus, most of which were normalised upon restoration of euglycaemia, suggesting that such alterations may be related to acute regulation of osmolarity. The observed modifications included increased concentration of glucose, βHB, GPC, *myo*-inositol, NAA, taurine and total creatine, as well as reduced concentration of GSH and NAAG. Being the hippocampus subjected to osmolarity deregulation upon hyperglycaemia, osmolites such as *myo*-inositol, taurine and creatine may be playing a role on osmotic adaptation (Lien *et al*., 1990, 1991). High concentration of *myo*-inositol was also reported in the hippocampus of Zucker diabetic fatty rats compared to controls (van der Graaf *et al*., 2004), and in the brain of diabetic patients relatively to healthy subjects (Geissler *et al*., 2003; Kreis and Ross, 1992).

Under hyperglycaemia, increased βHB concentration in the hippocampus of STZ-induced diabetic rats indicated ketoacidosis. However, upon glycaemia normalization, βHB concentration recovered to control levels, suggesting that inhibition of glucose metabolism by βHB with concomitant glucose accumulation (Lapidot and Haber, 2001) may occur only at hyperglycaemia.

The brain mainly requires glucose as the primary fuel to generate energy for cellular homeostasis and synaptic transmission. In the present study, the rate of glucose transport across the BBB was not altered in the rat hippocampus submitted to chronic hyperglycaemia for one month (Figure 4.44). Likewise, previous works in humans reported that poorly controlled diabetes did not affect brain glucose concentration (Seaquist *et al*., 2005) or glucose transport and metabolism (Fanelli *et al*., 1998). This reflects a preservation of the capacity of the BBB to transport glucose relative to the glucose metabolic rate and could thus be affected by alterations in glucose metabolic rate. However, [^{14}C]glucose uptake in the hippocampus and brain GLUT1 density were not altered in STZ-treated rats (Simpson *et al*., 1999), supporting the unaltered glucose transport through the BBB in diabetes. Other studies reported that diabetes increased 2-[^{14}C]deoxyglucose uptake in the dentate gyrus of the hippocampus without modification of GLUT1 or GLUT3 density (Duelli *et al*., 2000) or that glucose metabolism is reduced by chronic hyperglycaemia (Garcia-Espinosa *et al*., 2003), which could eventually result in altered neurotransmitter synthesis (Trudeau *et al*., 2004), or even altered synaptic connectivity and neuronal loss (Sima *et al*., 2004). To what extent glucose metabolic rates are specifically altered at high plasma glucose concentrations, or in chronic caffeine consumption, or in chronic hyperglycaemia (Pelligrino *et al*., 1992) remain to be determined. For example, acute but not chronic caffeine administration has been reported to increase the uptake of 2-[^{14}C]deoxyglucose in the hippocampus (Nehlig *et al*., 1984, 1986).

Disruption of the BBB was suggested to occur upon diabetic conditions, and particularly in STZ-induced diabetes (Huber *et al*., 2006). Such a disruption of the BBB is expected to lead to substantial increases in the glucose content of the brain approaching that in plasma. However, the presence of a sustained glucose concentration gradient into the hippocampus in this study suggests that leakage through a disrupted BBB did not occur for glucose. In the present modelling of hippocampal glucose transport, glucose consumption rate was considered invariable at euglycaemia and above. Thus, the present data suggest that chronic hyperglycaemia does not affect glucose transport across the BBB, contrary to what was reported in chronic hypoglycaemia (Lei and Gruetter, 2006), and suggests a differential regulation of GLUT1 gene expression at the BBB in response to alterations in glycaemia.

Habitual caffeine consumption has been reported to have peripheral effects that may aid in the control of glucose homeostasis (*e.g.* Greenberg *et al*., 2006; Higdon and Frei, 2006; van Dame and Hu, 2005). Moreover, caffeine is a non-selective adenosine receptor antagonist mostly acting as an A_{2A} receptor antagonist when consumed chronically (see Quarta *et al*., 2004), and thus should mainly block the up-regulated adenosine A_{2A} receptors in the hippocampus of STZ-induced diabetic rats. It is expected that caffeine would counteract hippocampal deterioration associated with

diabetes and aging process. In the present study, chronic caffeine intake attenuated diabetes-induced increase of *myo*-inositol concentration, and furthermore caused an increase in hippocampal taurine levels. Since taurine is a cerebral osmolyte whose intracellular content hippocampal changes in parallel with plasma osmolality, STZ-induced diabetes was suggested to increase brain taurine transport (Trachtman *et al*., 1992) and concentration (Rose *et al*., 2000). It is interesting that caffeine had an effect on the regulation of taurine homeostasis in the hippocampus of diabetic rats, and such effect could result from blockade of adenosine A_{2A} receptors and thus would antagonise adenosine modulation of taurine release from both neurons and glia (Corsi *et al*., 1997; Hada *et al*., 1998; Saransaari and Oja, 2000). Furthermore, taurine may have a role on neurotransmission, interacting with inhibitory $GABA_A$, $GABA_B$ and glycine receptors (reviewed in Albrecht and Schousboe, 2005), and modulating synaptic plasticity in the hippocampus (*e.g.* del Olmo *et al*., 2000). However, the presently used *in vivo* NMR spectroscopy does not allow revealing whether the observed changes in taurine levels are intra- or extracellular. Finally, taurine and its antioxidant effect may also contribute to reduction of oxidative stress (*e.g.* Di Leo *et al*., 2004) caused by glucose neurotoxicity that occurs in diabetes (*e.g.* Tomlinson and Gardiner, 2008), and was implicated in possible prevention of defects in nerve blood flow, motor nerve conduction velocity, and nerve sensory thresholds in experimental diabetic neuropathic rats (Li *et al*., 2006; Pop-Busui *et al*., 2001). Thus, one can speculate that an eventual neuroprotective role of caffeine upon diabetes may be linked to regulation of taurine homeostasis.

In summary, it was found that glucose content and thus glucose transport were unaltered by chronic hyperglycaemia. Thus, metabolic alterations in the hippocampus caused by STZ-induced diabetes are not related to changes in glucose transport through the BBB or alteration of the energy status. Otherwise, chronic hyperglycaemia induced a number of changes in the neurochemical profile, possibly linked to osmolarity regulation that is essential for the maintenance of cellular homeostasis. Habitual caffeine consumption was able to prevent metabolic alterations in the diabetic hippocampus under chronic hyperglycaemia, and that it has a potential effect on the mechanisms of osmolarity regulation, modulating *myo*-inositol and taurine metabolism.

4.4.3. Glucose transport and neurochemical profile in the hippocampus of Goto-Kakizaki diabetic rats - effect of caffeine consumption

In the previous study, it was not observed alteration of glucose transport in the hippocampus of STZ-induced diabetic rats, which are insulin-dependent. Since there are

inconsistent reports regarding the effects of a diabetic condition on glucose uptake into the brain, which was found to be reduced (McCall *et al*., 1982), augmented (Duelli *et al*., 2000) or to unaffected (Kainulainen *et al*., 1993; Simpson *et al*., 1999) by hyperglycaemia, it was now tested if glucose transport is affected by mild hyperglycaemia associated with hyper-insulinemia in a model of type 2 diabetes. Thus the previous study was repeated but now using GK rats to determine the effect of type 2 diabetes on the transport of glucose across the BBB and on the neurochemical profile in the hippocampus. Furthermore, it was also tested the potential protective role of chronic caffeine consumption on the observed hippocampal alterations. Again, *in vivo* ^{1}H NMR spectroscopy was used to achieve these goals (Mlynárik *et al*., 2006).

The experiments were performed in GK rats and age-matched controls at 6 months of age. Half of the animals were allowed to consume caffeine for 4 months, starting at 2 months of age. During the period when the rats had free to access caffeine solution, body weight and pre-prandial glycaemia were monitored, and insulin plasma levels were quantified two months after starting caffeine intake and at the end of the experiment. When compared to controls, GK rats showed reduced body weight (Figure 4.46A), significantly increased pre-prandial glycaemia ($P<0.05$, Figure 4.46B), and a significant augmentation of insulin concentration in plasma ($P<0.05$, Figure 4.46C). Caffeine consumption was similar in control and GK rats ($P>0.05$, Figure 4.46D), and achieved

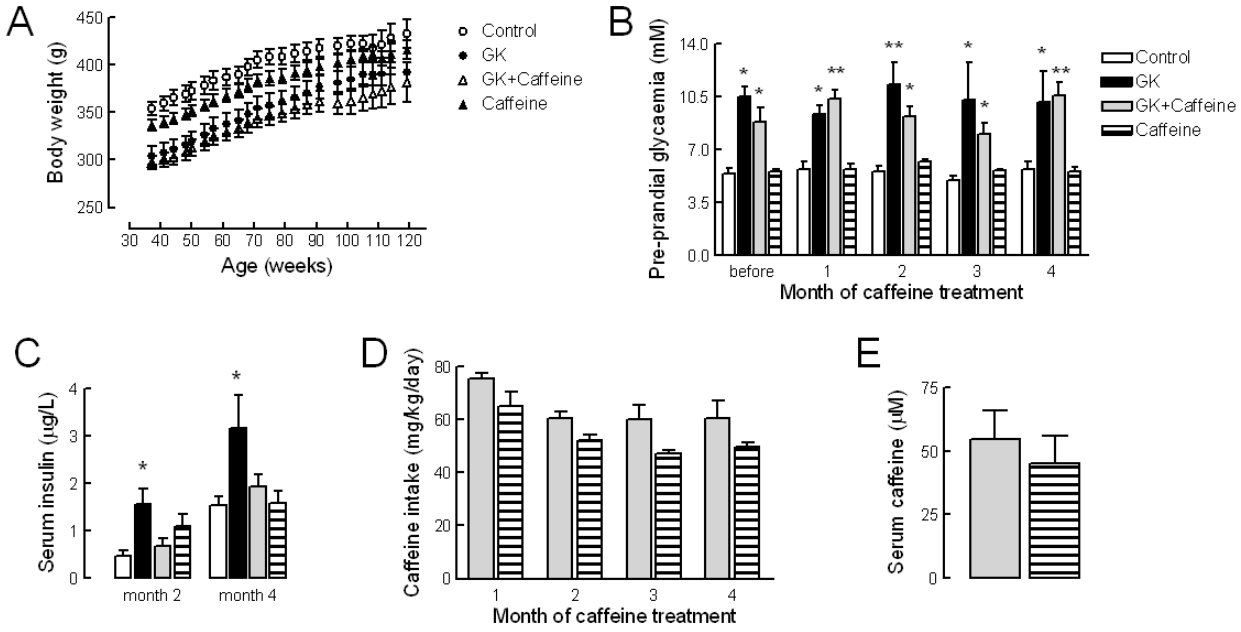

Figure 4.46. Characteristics of the GK rats and controls used in the study, including body weight (A), pre-prandial glycaemia (B) and caffeine intake (C) measured across the housing period, and caffeine (D) and insulin (E) concentrations in the serum determined after 2 months of treatment and/or at the end of the treatment. Caffeine was available in the drinking water for 4 months, starting from 2 months of age. White, black, grey and striped bars in the graphs represent control, GK, GK treated with caffeine, and caffeine-treated control rats, respectively. Values are mean±SEM of 8 rats and significant differences were estimated with the ANOVA followed by Bonferroni test and are noted as follows: * $P<0.05$, ** $P<0.01$, relative to controls.

similar serum caffeine levels (P>0.05, Figure 4.46E). Caffeine restored plasma insulin concentration of GK rats to control levels (Figure 4.46C) but did not affect blood glucose concentration (Figure 4.46B).

Physiologic parameters measured during the period of NMR data acquisition were similar in the four experimental groups (Table 4.14).

Table 4.14. Physiologic parameters measured at 5 different ranges of plasma glucose concentration during the NMR experiment. Values are shown as mean±SEM of 6 to 8 experiments for the different groups. Significant differences in plasma lactate were determined with ANOVA followed by Bonferroni's test and are noted as follows: * P<0.05, ** P<0.01, *** P<0.001, relative to normoglycaemia (< 8 mM of plasma glucose).

Plasma glucose range (mM)		**< 8**	**8 to 12**	**12 to 18**	**18 to 26**	**> 26**
Body Temperature (°C)	Control	37.5±0.2	37.4±0.1	37.5±0.1	37.2±0.2	37.3±0.1
	Caffeine	37.5±0.2	37.2±0.2	37.3±0.1	37.1±0.1	37.4±0.1
	GK	37.0±0.1	37.3±0.2	37.2±0.3	37.4±0.2	37.0±0.1
	GK+Caff	37.5±0.1	37.3±0.2	37.5±0.2	37.6±0.1	37.2±0.1
Arterial pH	Control	7.34±0.01	7.34±0.01	7.34±0.01	7.31±0.02	7.33±0.03
	Caffeine	7.42±0.02	7.38±0.01	7.35±0.01	7.35±0.01	7.33±0.02
	GK	7.41±0.02	7.40±0.02	7.42±0.02	7.40±0.01	7.39±0.01
	GK+Caff	7.44±0.01	7.45±0.01	7.39±0.02	7.39±0.02	7.38±0.02
P_aCO_2 (mm Hg)	Control	44.7±2.0	44.7±1.6	46.8±1.3	44.9±1.9	42.1±2.0
	Caffeine	39.9±2.9	41.5±2.7	45.7±3.9	41.7±2.7	41.4±2.9
	GK	39.0±3.4	38.6±2.0	37.2±2.7	40.3±2.6	43.2±2.3
	GK+Caff	35.7±1.7	39.5±4.7	38.9±3.0	40.7±3.0	40.1±1.3
Plasma glucose (mM)	Control	6.0±0.3	10.2±0.3	14.5±0.7	20.1±0.4	30.0±0.9
	Caffeine	6.4±0.4	10.5±0.6	15.2±0.4	21.3±0.8	31.9±1.6
	GK	6.4±0.5	10.4±0.4	14.1±0.6	21.0±0.7	31.7±1.7
	GK+Caff	7.1±0.2	10.2±0.5	14.5±0.6	21.5±1.0	29.6±1.0
Plasma lactate (mM)	Control	0.8±0.1	1.5±0.1 *	2.2±0.3 **	2.8±0.1 **	3.2±0.1 **
	Caffeine	1.3±0.1	1.8±0.1	2.6±0.2 **	2.7±0.2 **	2.9±0.4 **
	GK	1.9±0.2	2.0±0.2	2.2±0.2	2.7±0.2 *	2.7±0.5 *
	GK+Caff	1.7±0.1	2.0±0.1	2.3±0.2 *	2.4±0.2 **	2.8±0.1 ***

4.4.3.1. Neurochemical profile is altered in the hippocampus of GK rats

Typical ^{1}H NMR spectra from the hippocampus of GK and of control rats obtained, in the present study, were similar to the spectra shown for control and STZ-treated rats in the previous experiments (Figure 4.41). When compared to controls at euglycaemia (plasma glucose of 6.9±0.4 mM, n=6), GK diabetic rats under hyperglycaemia (plasma glucose of 13.5±1.6 mM, n=8) displayed significant alterations on the neurochemical profile of the hippocampus. Namely, there was a significant increase on the concentration of glucose, NAA, taurine and ascorbate, as well as a reduction of the concentration of choline-containing compounds and PE (Figure 4.47). From these, the most prominent alteration was the diabetes-induced increase in hippocampal taurine levels of

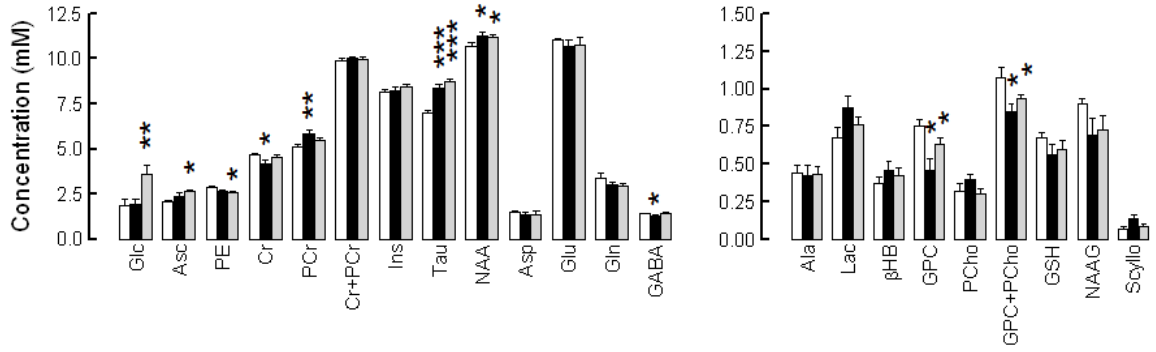

Figure 4.47. Effect of insulin-resistant diabetes on the neurochemical profile of the hippocampus. The histogram shows metabolite concentrations in the hippocampus of GK rats at hyperglycaemia (grey bars, n=8) and at euglycaemia (dark bars, n=8), and age matched healthy rats (white bars, n=6), determined by ^{1}H NMR spectroscopy. Values are presented as mean±SEM and statistically significant differences achieved with the Student's *t* test are noted for comparison with the control group: * P<0.05, ** P<0.01, *** P<0.001.

24±2% (P<0.001, n=8) compared to controls. The reduction of blood glucose of GK rats to approach normoglycaemia levels (plasma glucose of 7.6±0.8 mM, n=8) reduced hippocampal glucose content but did not affect the neurochemical profile to a great extent, relatively to hyperglycaemia. When compared to control rats, GK rats at euglycaemia showed the same metabolic alterations, and furthermore there was a reduction on the concentration of GABA and creatine, with increase of phosphocreatine, resulting in increased PCr/Cr of 28±2% (P<0.001, n=8), relative to control rats. These results suggest that the hippocampus of GK rats is adapted to the metabolic condition of mild hyperglycaemia.

While caffeine intake prevented most of the alterations in the hippocampus of STZ-induced diabetic rats, caffeine consumption for 4 months did not cause major modifications on diabetes-induced alterations in the neurochemical profile of GK rats, as shown in Figures 4.48 and 4.49. At euglycaemia (plasma glucose of 7.4±0.4 mM, n=8), GK rats consuming caffeine showed increased taurine, *scyllo*-inositol and ascorbate levels, and decreased GPC, GSH and NAAG levels (Figure 4.48). As shown in Figure 4.49, this neurochemical profile of GK rats treated with caffeine, determined at euglycaemia, was similar to that found at hyperglycaemia (plasma glucose of 12.5±1.0 mM, n=8). In addition to the referred metabolic alterations, caffeine-treated GK rats displayed increased *myo*-inositol content in the hippocampus, either at normoglycaemia (+6.8±2.1%, P<0.05) or hyperglycaemia (+6.5±0.7%, P<0.01) , when compared to caffeine consuming controls (Figure 4.49).

Chronic caffeine consumption resulted in alteration of the neurochemical profile in the hippocampus of control rats, namely a there was a significant reduction of total *myo*-inositol of 9.8±1.4% (P<0.05 compared to controls, Figure 4.48 and 4.49). Finally, it should be noted that control

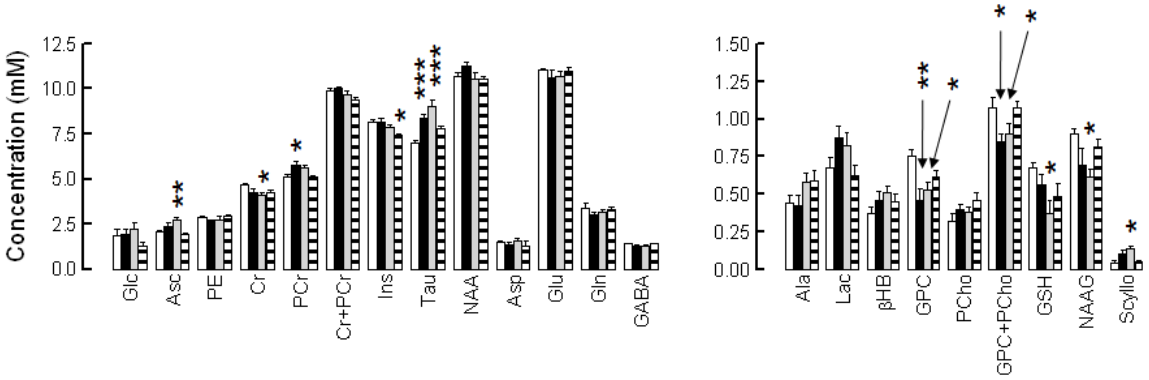

Figure 4.48. Metabolite concentrations in the hippocampus of control (white bars, n=6), GK (dark bars, n=8), caffeine-treated GK (grey bars, n=8), and caffeine-treated (striped bars, n=7) rats, determined by ^{1}H NMR spectroscopy. Values are mean±SEM and significant differences determined in comparison with the control group by the ANOVA are noted as follows: * P<0.05, ** P<0.01, *** P<0.001.

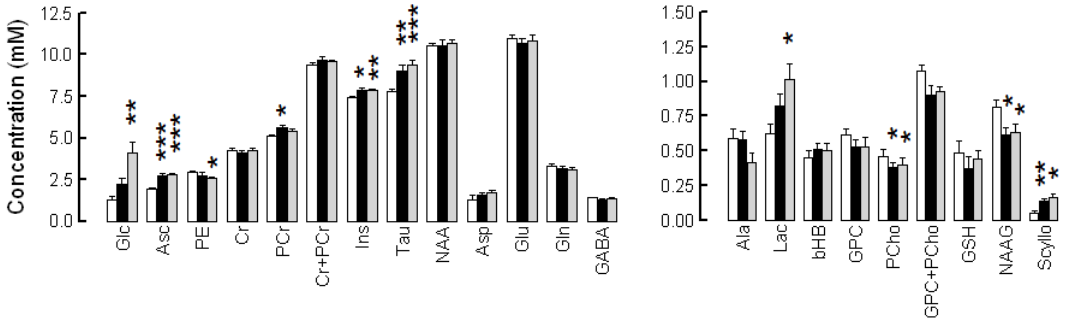

Figure 4.49. Neurochemical profile in the hippocampus of caffeine-treated GK rats at hyperglycaemia (grey bars, n=8) and at euglycaemia (dark bars, n=8), and age matched healthy caffeine-treated rats (white bars, n=7), determined by ^{1}H NMR spectroscopy. Values are presented as mean±SEM and statistically significant differences achieved with the Student's *t* test are noted for comparison with the control group: * P<0.05, ** P<0.01, *** P<0.001.

rats treated or not with caffeine did not show modifications of the neurochemical profile of the hippocampus under hyperglycaemia, when compared to euglycaemia (data not shown).

4.4.3.2. Diabetes does not affect glucose transport in the hippocampus

Glucose concentration in the hippocampus was dependent on glucose levels in the blood stream, and this dependence was similar in GK and control rats (Figure 5.50). This suggests that glucose transport rate across the BBB was not altered in the hippocampus in insulin-resistant rats, characterized by chronic mild hyperglycaemia (see Figure 4.46B).

Also chronic caffeine consumption failed to modify glucose transport rate in the hippocampus (Figure 4.50). Similar kinetic parameters for glucose transport were estimated with either the standard or reversible Michaelis-Menten models (Table 4.15). This reinforces the

conclusion that neither chronic hyperglycaemia nor chronic caffeine intake affect the transference of glucose from the blood stream to the hippocampus.

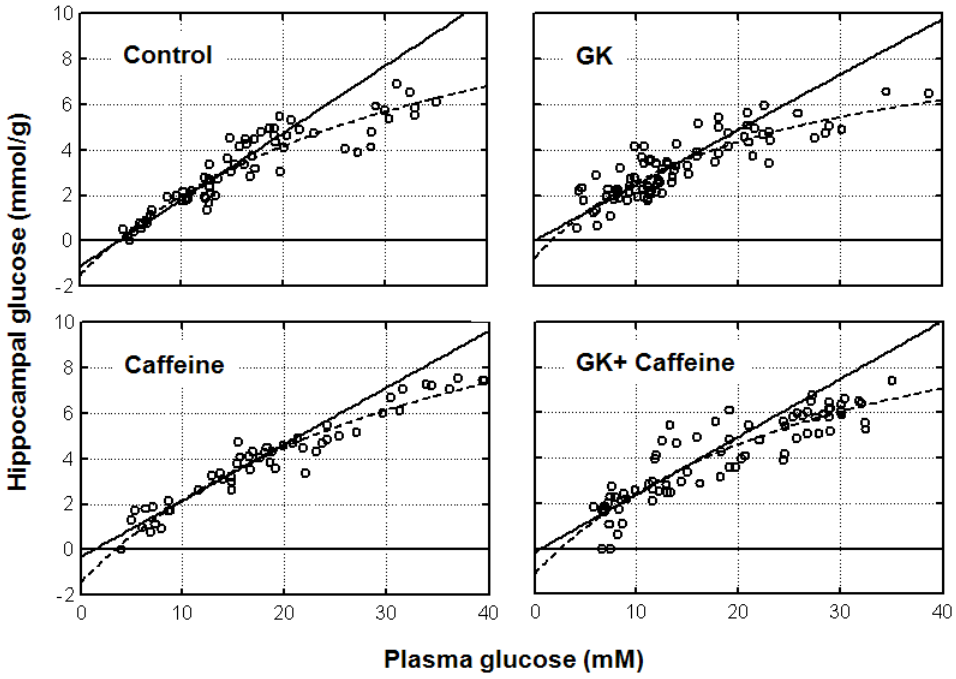

Figure 4.50. Relationship between hippocampal and plasma glucose concentrations in control and GK rats treated or not with caffeine (1 g/L). Open circles represent hippocampal glucose levels determined from ^{1}H NMR spectra measured (during 40 minutes) after plasma glucose was stable for at least 15 minutes. The solid line is the best fit of the reversible Michaelis-Menten model to hippocampal glucose concentrations, up to 20 mM of plasma glucose. The dashed line represents the best fit of the standard Michaelis-Menten model to hippocampal glucose, over the entire range of plasma glucose concentrations measured. The kinetic parameters estimated from these fittings are presented in Table 4.15 for each experimental group and each kinetic model.

Table 4.15. Apparent Michaelis-Menten constant K_t and ratio of T_{max} to CMR_{gluc} for the glucose transport across the BBB, estimated with the reversible and standard Michaelis-Menten models from the relationship between hippocampal and plasma glucose concentrations in control, GK, caffeine-treated GK, and caffeine-treated control rats (data in Figure 4.50). While the standard model was fitted to the whole range of plasma glucose concentrations, the reversible model was applied up to 20 mM. Values are mean (95% confidence interval).Units of K_t are mM and T_{max}/CMR_{gluc} is adimensional.

	Reversible model		**Standard model**	
	K_t	T_{max}/CMR_{gluc}	K_t	T_{max}/CMR_{gluc}
Control	4.78 (2.30 - 7.26)	2.24 (1.98 - 2.49)	8.18 (6.73 - 9.63)	3.21 (3.10 - 3.33)
GK	0.00	1.93 (1.67 - 2.18)	4.67 (3.46 - 5.87)	3.80 (3.47 - 4.13)
Caffeine-treated GK	0.57 (0.00 - 3.83)	1.99 (1.60 - 2.37)	6.58 (5.11 - 8.03)	3.63 (3.38 - 3.87)
Caffeine-treated control	1.22 (0.00 - 3.15)	1.95 (1.75 - 2.15)	8.21 (7.01 - 9.39)	3.42 (3.30 - 3.54)

4.4.3.3. Discussion

The present study evaluated the neurochemical profile in the hippocampus of GK rats, an animal model of insulin-resistant diabetes without obesity, in comparison to healthy age-matched

controls. Like STZ-induced diabetic rats (see previous study), when compared to controls, GK rats under mild hyperglycaemia (its normal pre-prandial glycaemia levels) displayed a plethora of metabolic modifications in the hippocampus. Thus, GK rats displayed alterations of the neurochemical profile that included an increase on the concentrations of NAA, taurine and ascorbate, as well as a reduction of choline-containing compounds and PE levels. Surprisingly, the concentration of *myo*-inositol was not significantly altered in the hippocampus of GK rats, as observed in STZ-induced diabetic rats (previously shown results) or in Zucker diabetic fat rats (van der Graaf *et al*., 2004). These last animal models of diabetes displayed sustained hyperglycaemia ranging 25 to 30 mM of blood glucose (see Figure 4.40B and *e.g.* Wilkes *et al*., 2005), while GK rats are characterised by sustained but mild hyperglycaemia (around 11 mM blood glucose, see Figure 4.46B). This suggests that *myo*-inositol levels may be related to the levels of glucose or the degree of hyper-osmolarity. Instead, GK rats showed a marked increased in taurine concentration in the hippocampus, relative to the control rats. As discussed above, taurine may have a role on modulating inhibitory receptors (reviewed in Albrecht and Schousboe, 2005) and synaptic plasticity in the hippocampus (*e.g.* del Olmo *et al*., 2000), may act as antioxidant contributing to reduction of oxidative stress (*e.g.* Di Leo *et al*., 2004), and can eventually prevent defects in nerve blood flow, motor nerve conduction velocity, and nerve sensory thresholds in experimental diabetic neuropathic rats (Li *et al*., 2006; Pop-Busui *et al*., 2001). These functions of taurine in the CNS, in particular upon a diabetic condition, link this metabolite to a possible neuroprotective role. Supporting a need of the diabetic hippocampus to scavenge reactive oxygen or nitrogen species and prevent oxidative stress, there was also an increase in hippocampal ascorbate (vitamine C) concentration in GK rats, compared to controls. The reduction on the concentrations of choline-containing compounds and PE in the hippocampus, together with an increased concentration of NAA, suggest that a reduction of membrane mielination and lipid synthesis, which relies on oligodendrocyte activity (see Moffett *et al*., 2007). Usually reduced NAA concentration would be expected upon neurodegeneration associated with neuronal loss (Moffett *et al*., 2007), but as shown for NONcNZO10/LtJ mice, neuronal dead may not occur upon diabetes.

Compared to controls, GK rats at euglycaemia displayed augmented PCr/Cr ratio, suggesting that metabolic alterations observed in the hippocampus of GK rats may result from cellular adaptation and be devoid of deleterious effects, so that when glycaemia is restored to normal values there is a higher metabolic performance that results in increased storage of high energy phosphate bounds on creatine.

Like for STZ-induced diabetes, insulin-resistant diabetic GK rats did not show altered glucose transport rate across the BBB that leads to hippocampal glucose concentrations similar to

controls. Caffeine-treatment failed to prevent or attenuate diabetes-induced alterations of neurochemical profile in the hippocampus of GK rats, in opposition to what occurred in STZ-induced diabetes. Once again, chronic caffeine intake for four months did not affect hippocampal glucose transport rate in healthy rats.

Chronic caffeine-treatment prevented hyper-insulinemia without affecting circulating blood glucose level of GK rats. In fact, by modulating adenosine receptors at the pancreatic islet cells, caffeine can regulate the secretion of insulin (Johansson *et al*., 2007). Since caffeine consumption prevented hyperglycaemia and failed to prevent hippocampal metabolite alterations in GK rats, it can be inferred that hyperglycaemia and not hyper-insulinemia must by related to diabetes-induced modification of the neurochemical profile in the hippocampus.

The most relevant observation of this study is that GK rats show increased taurine concentration in the hippocampus, relative to controls, either at hyper- and normoglycaemia, treated or not with caffeine. The roles in the CNS of taurine as neuromodulator, antioxidant or osmolyte must be clarified, in order to understand its function on diabetic encephalopathy.

This and the previous study showed that diabetes does not affect glucose transport into the hippocampus, and this structure will be subjected to glucose neurotoxicity that will possibly lead to learning and memory impairment.

4.4.4. Chronic caffeine intake prevents alterations caused by diabetes in the hippocampus of streptozotocin-treated and Goto-Kakizaki rats

As observed in the studies described above, diabetic conditions affect the CNS, namely the hippocampus, causing several metabolic and molecular alterations, as well as spatial memory impairment. Furthermore, the results obtained with NONcNZO10/LtJ diabetic mice (described in section 4.4.1) suggested a neuroprotective role of caffeine, in particular in the prevention of astrogliosis, synaptic degeneration, and memory impairment. Thus, behavioral tests in the open-field arena and in the Y-maze were carried out with the GK rats treated or not with caffeine (and respective controls), two days before the *in vivo* ^{1}H NMR experiments. After the each NMR study, the hippocampus of the animals (STZ-treated, GK and respective control rats, treated or not with caffeine) was dissected and stored at -80 °C. A Western blot analysis was then carried out with particular interest in accessing synaptic degeneration and astrogliosis. For physiological characteristics of these rats refer to Figures 4.40 and 4.46.

4.4.4.1. Caffeine prevents spatial memory impairment in Goto-kakizaki rats

As explained before, the Y-maze test is dependent on the exploratory behaviour of the rats, which was observed in an open-field arena immediately before testing Y-maze spontaneous alternation. Control and GK rats showed similar locomotor activity or exploratory behaviour, as suggested by similar number of crossing (Figure 4.51A) and rearing (Figure 4.51B) events in the open-field arena test, and similar number of explorations in the Y-maze arms (Figure 4.51C). Caffeine consumption reduced the number of rearing events in both controls and GK rats ($P<0.05$; Figure 4.51B). The spontaneous alternation in the Y-maze task revealed that diabetes caused a reduction on the performance of hippocampal-dependent spatial memory, in comparison to control rats ($P<0.05$), which was prevented by 4 months of caffeine consumption (Figure 4.51D), supporting again a role of chronic caffeine consumption in preventing diabetes-induced memory impairment.

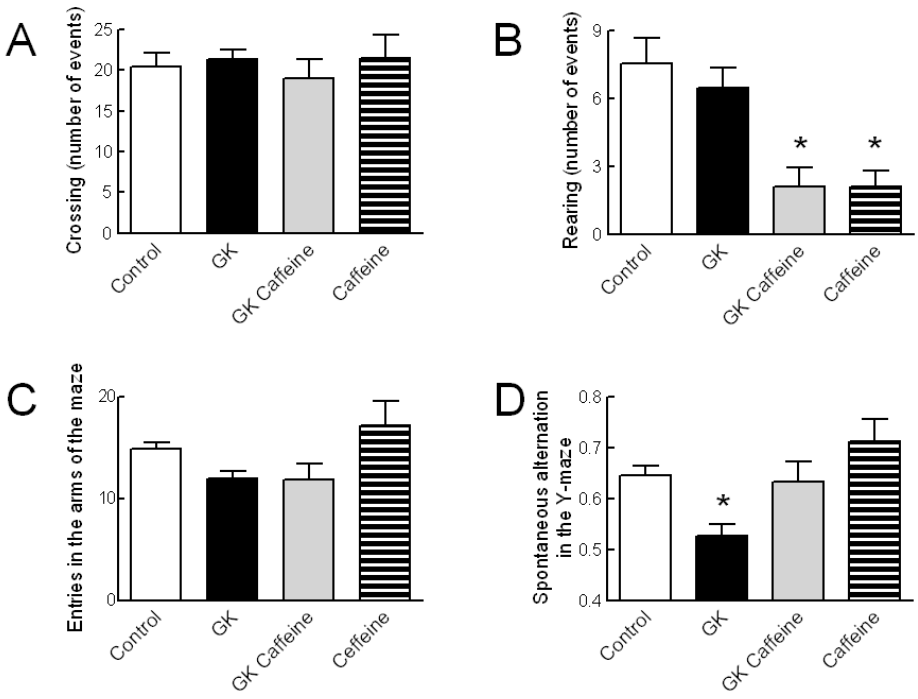

Figure 4.51. Caffeine consumption prevents spatial working memory deficits in diabetic GK rats. The number of crossings in the open-field arena was unaltered by diabetes or caffeine consumption (panel A), but the number of rearing events was reduced upon chronic caffeine consumption (panel B). The number of entries in the Y-maze arms was similar in the four animal groups (panel C). GK rats (black bars) displayed reduced spontaneous alternation in the Y-maze at 6 months of age, when compared to controls (white bars), but not if treated with caffeine (gray bars) for four months (panel D). GK rats from *in vivo* studies with [1-^{13}C]glucose infusion were included in these behavioural experiments. Results are presented as mean±SEM of 23 animals (for control and GK) or 8 animals (for caffeine and GK plus caffeine), and were compared with one-way ANOVA followed by Bonferroni's post-test (* $P < 0.05$ compared to control).

4.4.4.2. Synaptic alterations in the hippocampus of GK rats are prevented by caffeine consumption

As shown before for STZ-induced diabetic rats and NONcNZO10/Ltj diabetic mice, the hippocampus of insulin-resistant GK rats displayed synaptic degeneration, as suggested by reduced immunoreactivity for SNAP25 (-22.7±5.4%, P<0.05, n=8) and synaptophysin (-18.5±2.6%, P<0.05, n=5) in synaptosomal membranes, when compared to control rats (Figure 4.52A and B). In order to evaluate if diabetes also affected the post-synaptic zone, it was quantified the immunoreactivity of postsynaptic density-95 (PSD95), a standard postsynaptic marker. As described in Figure 4.52C, the immunoreactivity of PSD95 was not significantly altered in nerve terminal membranes of GK rats when compared to controls (P>0.05, n=5). Chronic caffeine consumption for 4 months prevented diabetes-induced reduction on immunoreactivity for SNAP25 but not synaptophysin. In control rats, caffeine treatment did not affect significantly the immunoreactivity for any of these synaptic markers.

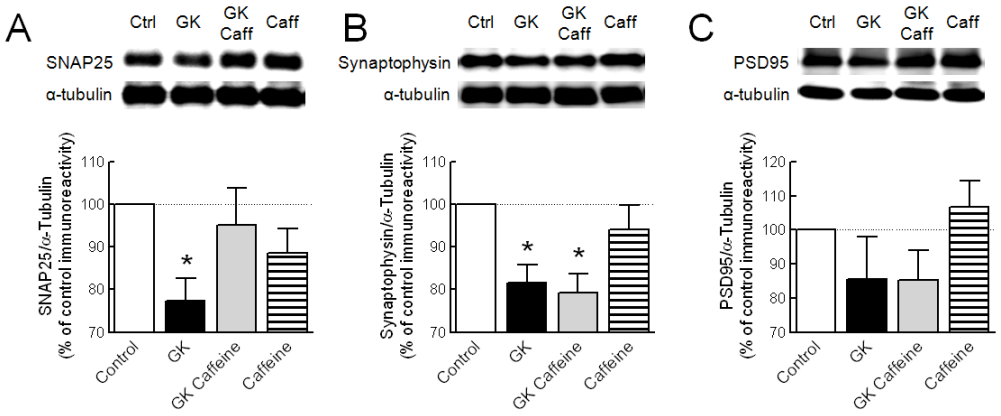

Figure 4.52. Caffeine consumption had a beneficial effect on diabetes-induced synaptic degeneration. Western blot analysis revealed that nerve-terminal membranes from diabetic GK rats displayed reduced immunoreactivity of both SNAP25 (panel A) and synaptophysin (panel B) but not PSD95 (panel C) in hippocampal membranes, when compared to controls. Caffeine consumption prevented diabetes-induced reduction of SNAP25 but not synaptophysin. Immunoreactivity of synaptic proteins was normalised to α-tubulin and calculated as percentage of control (open bar) in the same Western blot experiment. In the graphs, black, gray and striped bars represent GK, caffeine-treated GK, and caffeine-treated control rats, respectively. Results are shown as mean±SEM of 5-8 experiments with membranes from different animals, and were compared with ANOVA followed by Bonferroni's post-test (* P<0.05 compared to control).

4.4.4.3. Synaptic alterations in the hippocampus of STZ-treated rats are prevented by caffeine consumption

Previous studies suggested the occurrence of synaptic degeneration upon a diabetic condition (Figures 4.15 and 4.36). The hippocampus of STZ-induced diabetic rats displayed synaptic

degeneration, as suggested by reduced immunoreactivity for SNAP25 (-19.4±2.7%, P<0.05, n=7), synaptophysin (-17.4±2.2%, P<0.05, n=5) and syntaxin (-18.3±2.8%, P<0.05, n=7) in synaptosomal membranes, when compared to control rats (Figures 4.53A B and C). Furthermore, immunoreactivity of PSD95 was determined to evaluate the post-synaptic zone and was not significantly altered in nerve terminal membranes of STZ-treated rats when compared to controls (P>0.05, n=4, Figure 4.52D). Caffeine treatment prevented diabetes-induced reduction of synaptophysin and syntaxin, but failed to prevent the decrease of SNAP25 immunoreactivity. Again, one month of caffeine treatment did not affect significantly the immunoreactivity for any of these synaptic markers.

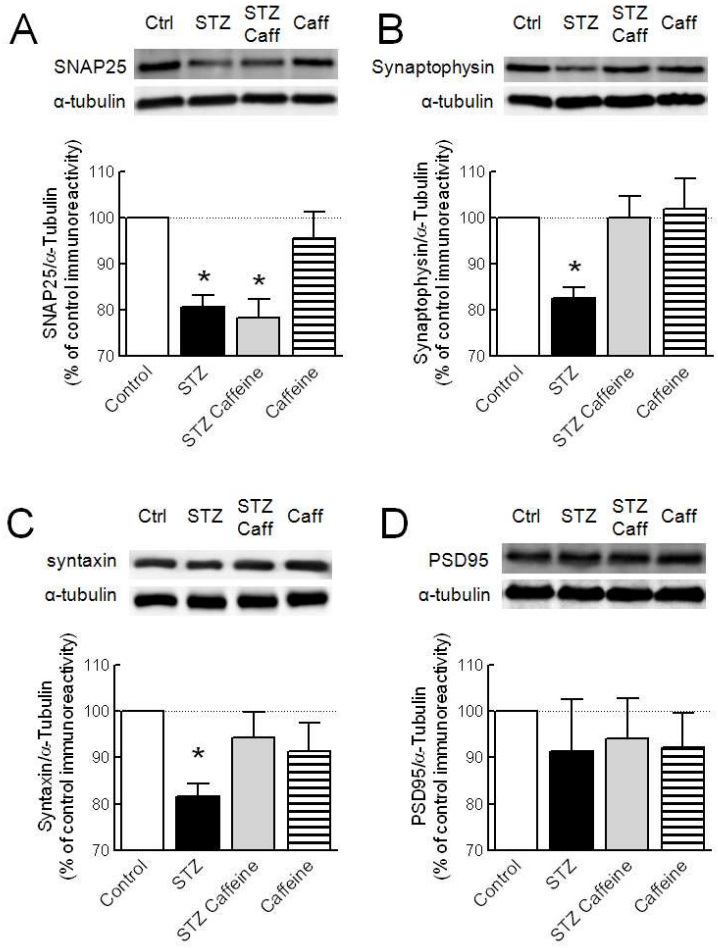

Figure 4.53. Caffeine consumption had a beneficial effect on diabetes-induced synaptic degeneration. Western blot analysis revealed that nerve-terminal membranes from STZ-induced diabetic rats displayed reduced immunoreactivity of SNAP25 (panel A), synaptophysin (panel B) and syntaxin (panel C) but not PSD95 (panel D) in hippocampal membranes, when compared to controls. Caffeine consumption prevented diabetes-induced reduction of synaptophysin and syntaxin but not SNAP25. Immunoreactivity of synaptic proteins was normalised to α-tubulin and calculated as percentage of control (open bar) in the same western blot experiment. In the graphs, black, gray and striped bars represent STZ-treated, STZ plus caffeine-treated, and caffeine-treated control rats, respectively. Results are shown as mean±SEM of 5 or 7 experiments with membranes from different animals, and were compared with ANOVA followed by Bonferroni's post-test (* P<0.05 compared to control).

4.4.4.4. Chronic caffeine intake prevents diabetes-induced astrogliosis in GK and STZ-induced diabetic rats

Astrogliosis occurs upon several neurodegenerative diseases, which was also found in the hippocampus of NONcNZO10/LtJ diabetic mice (see above). It was now found that both GK and STZ-induced diabetic rats displayed hippocampal astrogliosis, as suggested by increased GFAP or vimentin immunoreactivity in the hippocampus (figure 4.54). In fact, when compared to membranes from controls, total hippocampal membranes prepared from GK rats showed a increase in GFAP (+31.5±13.4%, P<0.05, n=8) and vimentin (+65.3±27.9%, P<0.05, n=8) immunoreactivity. Hippocampal membranes from STZ-treated rats also displayed increased immunoreactivity of GFAP relative to control rats (+19.6±4.7%, P<0.05, n=8). Caffeine consumption prevented diabetes-induced increase in GFAP and vimentin immunoreactivity, indicating prevention of astrogliosis, without effect on control rats.

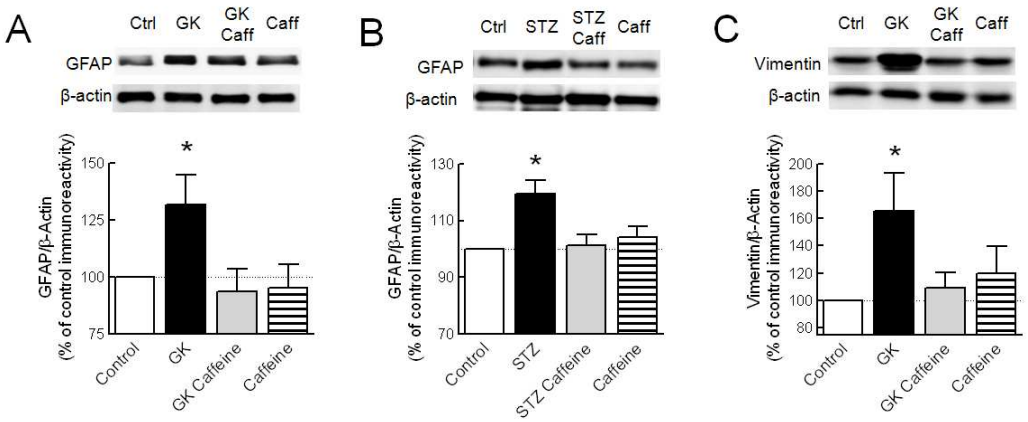

Figure 4.54. Caffeine consumption prevented diabetes-induced astrogliosis, as suggested by Western blot analysis revealing that GFAP immunoreactivity was increased in total hippocampal membranes from GK (panel A) and STZ-induced diabetic (panel B) rats, relative to the respective control rats. Panel C shows vimentin immunoreactivity in total membranes from the hippocampus of GK rats that corroborates occurrence of astrogliosis, when compared to controls. Caffeine consumption prevented diabetes-induced increase of GFAP and/or vimentin immunoreactivity. Immunoreactivity of GFAP and vimentin was normalised to β-actin and calculated as percentage of control (open bar) in the same Western blot experiment. In the graphs, black, gray and striped bars represent diabetic, caffeine-treated diabetic, and caffeine-treated control rats, respectively. Results are shown as mean±SEM of 8 experiments with membranes from different animals, and were compared with ANOVA followed by Bonferroni's post-test (* P<0.05 compared to control).

4.4.4.5. Modification of the density of adenosine A_1 receptor in the hippocampus of GK and STZ-induced diabetic rats

Previously it was demonstrated that STZ-induced diabetes affected the adenosinergic system in the hippocampus (see section 4.2.1). It was now observed that the density of adenosine A_1

receptors is reduced in the hippocampus not only of STZ-induced diabetic rats but also of GK rats. As shown in Figure 4.55A, synaptosomal membranes prepared from the hippocampus of GK rats displayed reduced immunoreactivity for A_1 receptor (-27.8±7.0%, P<0.05, n=8), which was reversed by caffeine consumption for four months. It was repeated this test in synaptosomal membranes from STZ-induced diabetic rats Figure 4.55B and it was not observed significant alterations on A_1 receptor immunoreactivity either on STZ-treated or caffeine-treated rats. Total hippocampal membranes from GK rats showed 52.8±8.3% reduction of A_1 receptor immunoreactivity (P<0.05, n=8, compared to controls), which was prevented by chronic caffeine intake (Figure 4.55C). Also total hippocampal membranes from STZ-induced diabetic rats showed a decrease of 29.0±10.4% in A_1 receptor immunoreactivity (P<0.05, n=8, compared to respective controls), which was prevented by caffeine intake (Figure 4.55D). Like before, the present results suggest that a diabetic condition result on decreased density of adenosine A_1 receptors, which is more evident in total membranes rather than nerve terminal-enriched membranes from the hippocampus. This reduction on A_1 receptors was prevented or even reversed (in the case of nerve terminals from GK rats) by log-term caffeine consumption.

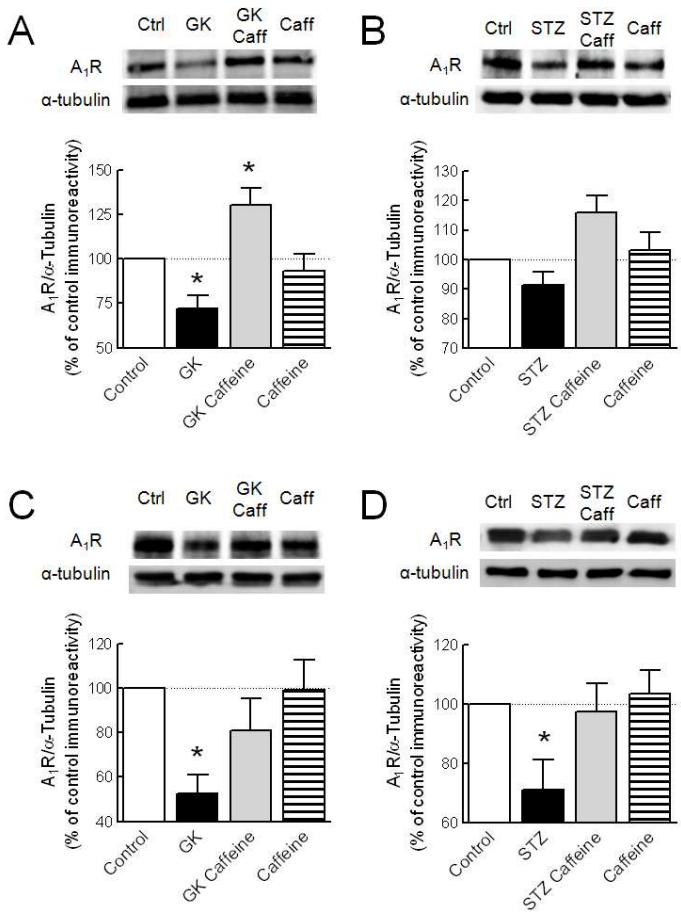

Figure 4.55. Western blot analysis revealed that diabetes reduced A_1 receptor density immunoreactivity in the hippocampus, which was prevented by caffeine consumption. Nerve-terminal membranes from the hippocampus of GK rats (panel A) showed reduced A_1 receptor immunoreactivity reversed by caffeine intake. Nerve terminal membranes from STZ-induced diabetic rats did not show alteration of A_1 receptor immunoreactivity (panel B). Total membranes from the hippocampus of GK (panel C) or STZ-induced diabetic rats (panel D) displayed reduced A_1 receptor immunoreactivity ehich was prevented by caffeine consumption. A_1 receptor immunoreactivity was normalised to α-tubulin and calculated as percentage of control (open bar) in the same western blot experiment. In the graphs, black, gray and striped bars represent diabetic, caffeine-treated diabetic, and caffeine-treated control rats, respectively. Results are shown as mean±SEM of 8 experiments with membranes from different animals, and were compared with ANOVA followed by Bonferroni's post-test (* P<0.05 compared to control).

4.4.4.6. Discussion

The main finding of this work is that long-term caffeine consumption prevents deleterious effects of diabetes on the hippocampus of GK and STZ-induced diabetic rats, as showed before for NONcNZO10/LtJ diabetic mice. These results show that GK and STZ-treated rats present neurodegeneration that is not in the entire neuron, as suggested by unaltered MAP2 immunoreactivity (data not shown), but instead at the nerve terminal level. Supporting this synaptic degeneration, it was observed a diabetes-induced reduction of the density of synaptic proteins in the hippocampus, namely syntaxin, SNAP25 and synaptophysin. The density of the postsynaptic protein PSD95 was not significantly altered in the hippocampus of GK and STZ-treated rats, when compared to the respective control rats, suggesting that diabetes mainly affects the pre-synaptic component of the nerve terminal. These synaptic modifications eventually induce cognitive impairment, which was confirmed by observation of a reduction in the Y-maze spontaneous alternation of GK rats.

Furthermore, astrocytosis occur in the diabetic hippocampus suggested by increased GFAP and/or vimentin immunoreactivity in hippocampal membranes of GK and STZ-induced diabetic rats, when compared to controls. This astrocyte proliferation might result from neuronal damage, as observed in other situations of neurodegeneration such as amyotrophic lateral sclerosis (Barbeito *et al*., 2004), Alzheimer's disease (Lauderback *et al*., 2001) and Lewy-body dementia (Honig *et al*., 2000). On the other hand, astrocyte proliferation can contribute for the formation of free radicals (*e.g.* Chao *et al*., 1996) or production of apoptotic factors (*e.g.* Crutcher *et al*., 1993; Fahnestock *et al*., 1996; Ferrer *et al*., 2000, 2001), accentuating neuronal damage.

As shown to occur in STZ-induced diabetes and NONcNZO10/LtJ diabetic mice, also GK rats showed down-regulation of inhibitory adenosine A_1 receptors, which occur mainly in total membranes and to a less extent in the nerve terminal membranes. This down-regulation of adenosine A_1 receptors was prevented by caffeine intake, and even reversed in the hippocampal nerve terminals from GK rats. Since A_{2A} receptors are the main target of chronically consumed caffeine (see Quarta *et al*., 2004), it would be interesting to perform further binding studies to test whether the hippocampal facilitatory A_{2A} receptors are up-regulated, like previously observed in other models of diabetes.

Chronic caffeine intake was again tested on the prevention of the development of diabetic encephalopathy, not only by acting on A_{2A} receptors located at the CNS, but also by regulating peripheral metabolic rates and energy expenditure, which contribute for the management of a diabetic situation. It was now found that long-term caffeine consumption prevented some diabetes-

induced alterations at the synapse and astrocytosis in the hippocampus. This beneficial effect of caffeine intake was reflected in the prevention of diabetes-associated memory impairment, as evaluated by the spontaneous alternation in the Y-maze. It was investigated the density of synaptic proteins with different locations: synaptophysin that is located in synaptic vesicles, and syntaxin and SNAP-25 both in the membrane of nerve terminals (Pinheiro *et al*., 2003, and references therein). The density of the three proteins decreased in the hippocampus of diabetic GK and STZ-induced diabetic rats, when compared to controls. Like occurring in NONcNZO10/LtJ mice, long-term caffeine intake prevented SNAP25 but not synaptophysin alteration, in the hippocampus of GK rats. However, in STZ-induced diabetic rats caffeine treatment prevented the reduction of synaptophysin but not SNAP25 caused by diabetes. Because the prevention of the decrease of syntaxin by caffeine intake was observed in nerve terminals from STZ-induced diabetic rats, it can be inferred that this effect is not revealing an alteration on the synaptic membrane, but suggests specific alteration on particular synaptic proteins. In fact, the density of synaptic proteins may depend on insulin receptor signalling, since both NONcNZO10/LtJ mice and GK rats present hyper-insulinemia, and STZ-induced diabetic rats are characterised by hypo-insulinemia. Furthermore, insulin receptor was suggested to have a role on learning and memory by controlling synaptic function (reviewed in Zhao and Alkon, 2001) and, in particular, to be involved in the regulation of the number of synapses (Chiu *et al*., 2008).

In conclusion, the present results reinforce the neuroprotective role of caffeine in diabetic encephalopathy, since chronic caffeine consumption may help preventing synaptic degeneration, astrogliosis, and memory deficits caused by uncontrolled diabetes. Caffeine consumption was successful in ameliorating diabetes-induced hippocampal alterations in both insulin-dependent (STZ-treated rats) and insulin-resistant (GK rats) diabetes, indicating that caffeine effects are unrelated to insulin availability.

5. Concluding Remarks

The main goal of the present research was to reveal the existence of important molecular and metabolic alterations in the hippocampus of animal models of diabetes that could contribute to the diabetes-induced memory deficits, and to test if such alterations could be prevented or corrected by manipulating neuromodulation systems. The major conclusion is that a diabetic condition affects the hippocampal structure causing degeneration of the nerve terminals (without neuronal loss), astrocyte reactivity and proliferation, adaptation of the metabolic network, modification of neuromodulation systems that are able to control neuronal and glial metabolism, and leading to spatial memory deficits. Moreover, this thesis provides the first evidences supporting the value of long-term caffeine intake for the prevention or amelioration of diabetes-induced hippocampal alterations, therefore preventing diabetes-associated memory decline.

It was implemented and validated the use of acutely dissociated hippocampal slices superfused with specific ^{13}C enriched substrates to simultaneously investigate metabolism in different brain compartments, namely astrocytes, glutamatergic and GABAergic neurons. This methodology was then used to demonstrate that neuromodulation systems like those operated by adenosine and endocanabinnoids may directly control intermediary metabolism in neuronal and glial compartments. In particular, it was found that the tonic activation of adenosine A_1 receptors in the hippocampal slices controls the metabolic recovery from a metabolic insult like hypoxia. It was also shown that CB1 cannabinoid receptors directly control the flow of the TCA cycle flux in neurons and astrocytes, in superfused hippocampal slices under stimulation.

Since diabetes is a metabolic disease and affects learning and memory processes that result from synaptic events (*e.g.* Biessels *et al*., 2002; Trudeau *et al*., 2004), it was investigated the effect of a diabetic condition on neuromodulation systems in synaptic and extra-synaptic compartments of the hippocampus. In the particular model of STZ-induced diabetes characterised by sustained chronic hyperglycaemia, it was observed that hippocampal modulation systems operated by adenosine, ATP and endocannabinoids are modified in membranes from the synapse, where such systems modulate neurotransmission processes, and principally in extra-synaptic membranes, from compartments where they would be typically involved in the control of events in the neuronal body and glial cells, such as metabolism, cellular homeosthasis, glial proliferation, neuroinflamation. The adenosinergic and endocannabinoid modulation systems were found altered in the cortex of STZ-induced and GK diabetic rats, suggesting that these alterations are not restricted to the hippocampal structure.

The *in vivo* metabolism of [1-^{13}C]glucose in the hippocampus of Goto-Kakizaki (GK) diabetic rats was studied by ^{13}C NMR spectroscopy and suggested that intermediary metabolic pathways in

the diabetic hippocampus are rearranged, namely becoming more flexible in the use of other substrates in alternative to glucose, possibly in order to counteract alterations of glucose transport and utilization. However, *in vivo* studies of the kinetics of glucose transport in to the hippocampus revealed that the transport of glucose across the BBB is not altered in STZ-induced and GK diabetic rats. Thus, these observations suggest that the glucose-buffering effect of glycogen (Gruetter, 2003) may have an important role upon a diabetic condition. Furthermore, *in vivo* ^{1}H NMR spectroscopy showed that STZ-induced and GK diabetic rats have alterations of the neurochemical profile of the hippocampus, mainly related to osmolarity regulation rather than energy metabolism. In conclusion, upon chronic hyperglycaemia (observed in both STZ-induced and GK diabetic rats), glucose transport kinetics at the BBB is not altered and thus the hippocampus is subjected to high glucose concentrations, which trigger mechanisms of osmotic compensation and induce an adaptation of intermediary metabolic pathways, likely in the astrocytic compartment. However, the high glucose concentration (considered glucose toxicity) in the hippocampus induces primarily and typically the formation reactive oxygen species, leading to oxidative stress and then degeneration (Tomlinson and Gardiner, 2008). Moreover, in hippocampal slices prepared from STZ-induced diabetic rats, which were suggested to display altered synaptic plasticity compares to controls (e.g. Biessels *et al*., 2002), did not show significant modifications of relative fluxes of intermediary metabolism, indicating that synaptic alterations rather than metabolic stress may be responsible for the observed spatial memory deficits (*e.g.* Gispen and Biessels, 2000).

In different animal models of either insulin-dependent or insulin-resistant diabetes, which display spatial memory impairment evaluated in the Y-maze, it was shown that diabetes causes the degeneration of nerve terminals that is characterized by decreased density of synaptic proteins including syntaxin, synaptophysin and SNAP25. In general, the density of the postsynaptic protein PSD95 was not altered in the hippocampus of diabetic rats, suggesting that mainly the pre-synaptic button, involved in neurotransmitter release, is affected by diabetes. In fact, synaptic transmission was suggested to be affected by diabetes (*e.g.* Biessels *et al*., 2002). The general morphological structure of the hippocampus was similar between control and diabetic rats, as well as the density of the neuronal marker MAP2. Thus, it is concluded that diabetes causes a synaptic degeneration without occurring neuronal dead. The present results do not support the occurrence of neuronal loss caused by diabetes, but it can eventually occur in latter stages of diabetes, as suggested by other authors (De Jong, 1977; Jakobsen *et al*., 1987; Li *et al*., 2002a). Furthermore, when compared to controls, the hippocampus of diabetic animals displayed elevated number of astrocytes and/or higher density of astrocyte-associated proteins, namely GFAP and vimentin, suggesting the occurrence of astrocyte reactivity and proliferation.

Finally, caffeine, which is an antagonist of adenosine mainly acting on A_{2A} receptors that was now found up-regulated in chronic hyperglycaemia, was tested as a neuroprotective strategy for the prevention of diabetes-induced hippocampal alterations. In fact, long-term caffeine intake was shown to prevent diabetes-induced memory impairment, and to counteract synaptic degeneration, astrocytosis and some metabolic alterations caused by diabetes in the hippocampus. Caffeine exerts effects not only in the CNS, but also in peripheral tissues in particular controlling glucose metabolism in the heart (*e.g.* Finegan *et al*., 1996; Fraser *et al*., 1999), liver (*e.g.* Buxton *et al*., 1986; Vanstapel *et al*., 1991) or muscle (*e.g.* Hespel and Richter, 1998; Vergauwen *et al*., 1994), and regulating the secretion of insulin (Johansson *et al*., 2007). However, the study of three animal models of diabetes characterized by sustained hyperglycaemia but with different diabetes phenotypes, namely insulin-dependent (STZ-treated rats), insulin-resistant (GK rats) and obesity-associated (NONcNZO10/LtJ mice) diabetes, consistently revealed attenuation or prevention of the diabetes-induced hippocampal alterations, strongly supporting the beneficial effect of habitual caffeine intake that successfully prevented cognitive decline on diabetic animals.

The *in vivo* NMR study of the neurochemical profile of the hippocampus of diabetic rats showed that in general, alterations of metabolite levels observed under hyperglycaemia were normalised upon acute glycaemia restoration to control levels. In line with these results, hippocampal slices prepared from STZ-treated rats that were superfused in the same conditions as controls did not show altered glial or neuronal metabolism. Observing the effect of caffeine consumption, in general it did not restore diabetes-induced metabolic modifications but, on the other hand, long-term caffeine intake prevented diabetes-associated spatial memory impairment as well as synaptic alterations. Thus, from the present studies, it can be concluded that hippocampal metabolism is flexible and adapts to the metabolic challenge upon diabetes, and that synaptic degeneration caused by hyperglycaemia is possibly the major cause for the diabetes-induced memory decline.

In summary, the work in the present thesis identified several hippocampal alterations induced by diabetes *mellitus*, and assigned synaptic degeneration as the major event contributing to the observed diabetes-associated cognitive decline. Furthermore, long-term caffeine consumption was shown to be successful in the amelioration of such hippocampal alterations, thus preventing diabetes-induced memory impairment.

References

Abbracchio MP, Burnstock G, Boeynaems JM, Barnard EA, Boyer JL, Kennedy C, Knight GE, Fumagalli M, Gachet C, Jacobson KA, Weisman GA (2006) International Union of Pharmacology LVIII: update on the P2Y G protein-coupled nucleotide receptors: from molecular mechanisms and pathophysiology to therapy. Pharmacol Rev 58, 281-341.

Abbracchio MP, Rainaldi G, Giammarioli AM, Ceruti S, Brambilla R, Cattabeni F, Barbieri D, Franceschi C, Jacobson KA, Malorni W (1997) The A_3 adenosine receptor mediates cell spreading, reorganization of actin cytoskeleton, and distribution of Bcl-XL: studies in human astroglioma cells. Biochem Biophys Res Commun 241, 297-304.

Abbracchio MP, Verderio C (2006) Pathophysiological roles of P2 receptors in glial cells. Novartis Found Symp 276, 91-103.

Abdipranoto A, Liu GJ, Werry EL, Bennett MR (2003) Mechanisms of secretion of ATP from cortical astrocytes triggered by uridine triphosphate. Neuroreport, 14, 2177-2181.

Agranoff BW, Cotman CW, Uhler MD (1999) Learning and Memory. In: Siegel GJ, Agranoff BW, Albers RW, Fisher SK, Uhler MD "Basic Neurochemistry: Molecular, Cellular, and Medical Aspects", Lippincott Williams & Wilkins, Philadelphia, pp. 1027-1052.

Agteresch HJ, Dagnelie PC, van den Berg JW, Wilson JH (1999) Adenosine triphosphate: established and potential clinical applications. Drugs 58, 211-232.

Aihara H, Fujiwara S, Mizuta I, Tada H, Kanno T, Tozaki H, Nagai K, Yajima Y, Inoue K, Kondoh T, Motooka Y, Nishizaki T (2002) Adenosine triphosphate accelerates recovery from hypoxic/hypoglycemic perturbation of guinea pig hippocampal neurotransmission via a P2 receptor. Brain Res 952, 31-37.

Albrecht J, Schousboe A (2005) Taurine interaction with neurotransmitter receptors in the CNS: an update. Neurochem Res 30, 1615-1621.

Allaman I, Lengacher S, Magistretti PJ, Pellerin L (2003) A_{2B} receptor activation promotes glycogen synthesis in astrocytes through modulation of gene expression. Am J Physiol 284, C696-C704.

Alloisio S, Cugnoli C, Ferroni S, Nobile M (2004) Differential modulation of ATP-induced calcium signalling by A_1 and A_2 adenosine receptors in cultured cortical astrocytes. Br J Pharmacol 141, 935-942.

Almeida T, Rodrigues RJ, de Mendonça A, Ribeiro JA, Cunha RA (2003) Purinergic P2 receptors trigger adenosine release leading to adenosine A_{2A} receptor activation and facilitation of long-term potentiation in rat hippocampal slices. Neuroscience 122, 111-121.

Ambrósio AF, Malva JO, Carvalho AP, Carvalho CM (1997) Modulation of Ca^{2+} channels by activation of adenosine A_1 receptors in rat striatal glutamatergic nerve terminals. Neurosci Lett 220, 163-166.

Anchors JM, Karnovsky ML (1975) Purification of cerebral glucose-6-phosphatase. An enzyme involved in sleep. J Biol Chem 250, 6408-6416.

Andiné P, Rudolphi KA, Fredholm BB, Hagberg H (1990) Effect of propentofylline (HWA 285) on extracellular purines and excitatory amino acids in CA1 of rat hippocampus during transient ischaemia. Br J Pharmacol 100, 814-818.

Angelucci ME, Cesário C, Hiroi RH, Rosalen PL, Da Cunha C (2002) Effects of caffeine on learning and memory in rats tested in the Morris water maze. Braz J Med Biol Res 35, 1201-1208.

Angelucci ME, Vital MA, Cesário C, Zadusky CR, Rosalen PL, Da Cunha C (1999) The effect of caffeine in animal models of learning and memory. Eur J Pharmacol 373, 135-140.

Appel E, Kazimirsky G, Ashkenazi E, Kim SG, Jacobson KA, Brodie C (2001) Roles of BCL-2 and caspase 3 in the adenosine A_3 receptor-induced apoptosis. J Mol Neurosci 17, 285-292.

Araki Y, Nomura M, Tanaka H, Yamamoto H, Yamamoto T, Tsukaguchi I, Nakamura H (1994) MRI of the brain in diabetes *mellitus*. Neuroradiology 36, 101-103.

Arendash GW, Schleif W, Rezai-Zadeh K, Jackson EK, Zacharia LC, Cracchiolo JR, Shippy D, Tan J (2006) Caffeine protects Alzheimer's mice against cognitive impairment and reduces brain β-amyloid production. Neuroscience 142, 941-952.

Armstrong JN, Brust TB, Lewis RG, MacVicar BA (2002) Activation of presynaptic $P2X_7$-like receptors depresses mossy fiber-CA3 synaptic transmission through p38 mitogen-activated protein kinase. J Neurosci 22, 5938-5945.

Arrigoni E, Crocker AJ, Saper CB, Greene RW, Scammell TE (2005) Deletion of presynaptic adenosine A_1 receptors impairs the recovery of synaptic transmission after hypoxia. Neuroscience 132:575-580.

Artola A, Kamal A, Ramakers GM, Gardoni F, Di Luca M, Biessels GJ, Cattabeni F, Gispen WH (2002) Synaptic plasticity in the diabetic brain: advanced aging? Prog Brain Res 138, 305-314.

Ates O, Cayli SR, Altinoz E, Yucel N, Kocak A, Tarim O, Durak A, Turkoz Y, Yologlu S (2006a) Neuroprotective effect of mexiletine in the central nervous system of diabetic rats. Mol Cell Biochem 286, 125-131.

Ates O, Yucel N, Cayli SR, Altinoz E, Yologlu S, Kocak A, Cakir CO, Turkoz Y (2006b) Neuroprotective effect of etomidate in the central nervous system of streptozotocin-induced diabetic rats. Neurochem Res 31, 777-783.

Atkinson DE (1968) The energy charge of the adenylate pool as a regulatory parameter. Interaction with feedback modifiers. Biochemistry 7:4030-4034.

Austin EJ, Deary IJ (1999) Effects of repeated hypoglycaemia on cognitive function. A psychometrically validated reanalysis of the Diabetes Control and Complications Trial data. Diabetes Care 22, 1273-1277.

Badar-Goffer RS, Bachelard HS, Morris PG (1990) Cerebral metabolism of acetate and glucose studied by ^{13}C-n.m.r. spectroscopy - A technique for investigating metabolic compartmentation in the brain. Biochem J 266, 133-139.

Bahr BA, Kessler M, Rivera S, Vanderklish PW, Hall RA, Mutneja MS, Gall C, Hoffman KB (1995) Stable maintenance of glutamate receptors and other synaptic components in long-term hippocampal slices. Hippocampus 5, 425-439.

Baker D, Jackson SJ, Pryce G (2007) Cannabinoid control of neuroinflammation related to multiple sclerosis.Br J Pharmacol 152, 649-654.

Bakken IJ, Sonnewald U, Clark JB, Bates TE (1997) [U-^{13}C]glutamate metabolism in rat brain mitochondria reveals malic enzyme activity. Neuroreport 8, 1567-1570.

Balázs R, Machiyama Y, Hammond BJ, Julian T, Richter D (1970) The operation of the gamma-aminobutyrate bypath of the tricarboxylic acid cycle in brain tissue *in vitro*. Biochem J 116, 445-461.

Balestrino M, Lensman M, Parodi M, Perasso L, Rebaudo R, Melani R, Polenov S, Cupello A (2002) Role of creatine and phosphocreatine in neuronal protection from anoxic and ischemic damage. Amino Acids 23:221-229.

Ballerini P, Di Iorio P, Ciccarelli R, Nargi E, D'Alimonte I, Traversa U, Rathbone MP, Caciagli F (2002) Glial cells express multiple ATP binding cassette proteins which are involved in ATP release. Neuroreport 13, 1789-1792.

Barbeito LH, Pehar M, Cassina P, Vargas MR, Peluffo H, Viera L, Estévez AG, Beckman JS (2004) A role for astrocytes in motor neuron loss in amyotrophic lateral sclerosis. Brain Res Brain Res Rev 47, 263-274.

Barber M, Kasturi BS, Austin ME, Patel KP, MohanKumar SM, MohanKumar PS (2003) Diabetes-induced neuroendocrine changes in rats: role of brain monoamines, insulin and leptin. Brain Res 964, 128-135.

Barrington WW, Jacobson KA, Hutchison AJ, Williams M, Stiles GL (1989) Identification of the A_2 adenosine receptor binding subunit by photoaffinity crosslinking. Proc Natl Acad Sci USA 86, 6572-6576.

Barsotti C, Pesi R, Felice F, Ipata PL (2003) The purine nucleoside cycle in cell-free extracts of rat brain: evidence for the occurrence of an inosine and a guanosine cycle with distinct metabolic roles. Cell Mol Life Sci 60, 786-793.

Baslow MH (2003) *N*-Acetylaspartate in the vertebrate brain: metabolism and function. Neurochem Res 28:941-953.

Baydas G, Nedzvetskii VS, Tuzcu M, Yasar A, Kirichenko SV (2003) Increase of glial fibrillary acidic protein and S-100B in hippocampus and cortex of diabetic rats: effects of vitamin E. Eur J Pharmacol 462, 67-71.

Beauquis J, Roig P, Homo-Delarche F, De Nicola A, Saravia F (2006) Reduced hippocampal neurogenesis and number of hilar neurones in streptozotocin-induced diabetic mice: reversion by antidepressant treatment. Eur J Neurosci 23, 1539-1546.

Beauquis J, Saravia F, Coulaud J, Roig P, Dardenne M, Homo-Delarche F, De Nicola A (2008) Prominently decreased hippocampal neurogenesis in a spontaneous model of type 1 diabetes, the nonobese diabetic mouse. Exp Neurol 210, 359-367.

Behar KL, Petroff OA, Prichard JW, Alger JR, Shulman RG (1986) Detection of metabolites in rabbit brain by ^{13}C NMR spectroscopy following administration of [1-^{13}C]glucose. Magn Reson Med 3:911-920.

Ben-Yoseph O, Badar-Goffer RS, Morris PG, Bachelard HS (1993) Glycerol 3-phosphate and lactate as indicators of the cerebral cytoplasmic redox state in severe and mild hypoxia respectively: a ^{13}C- and ^{31}P-n.m.r. study. Biochem J 291, 915-919.

Berghuis P, Dobszay MB, Wang X, Spano S, Ledda F, Sousa KM, Schulte G, Ernfors P, Mackie K, Paratcha G, Hurd YL, Harkány T (2005) Endocannabinoids regulate interneuron migration and morphogenesis by transactivating the TrkB receptor. Proc Natl Acad Sci USA 102, 19115-19120.

Bernard-Hélary K, Ardourel M, Magistretti P, Hévor T, Cloix JF (2002) Stable transfection of cDNAs targeting specific steps of glycogen metabolism supports the existence of active gluconeogenesis in mouse cultured astrocytes. Glia 37, 379-382.

Bernstine EG, Koh C, Lovelace CC (1979) Regulation of mitochondrial malic enzyme synthesis in mouse brain. Proc Natl Acad Sci USA 76, 6539-6541.

Bhardwaj SK, Sharma P, Kaur G (1998) Alterations in free radical scavenger system profile of type I diabetic rat brain. Mol Chem Neuropathol 35, 187-202.

Biber K, Klotz KN, Berger M, Gebicke-Härter PJ, van Calker D (1997) Adenosine A_1 receptor-mediated activation of phospholipase C in cultured astrocytes depends on the level of receptor expression. J Neurosci 17, 4956-4964.

Biessels GJ, Braun KP, de Graaf RA, van Eijsden P, Gispen WH, Nicolay K (2001) Cerebral metabolism in streptozotocin-diabetic rats: an *in vivo* magnetic resonance spectroscopy study. Diabetologia 44, 346-353.

Biessels GJ, Cristino NA, Rutten GJ, Hamers FP, Erkelens DW, Gispen WH (1999) Neurophysiological changes in the central and peripheral nervous system of streptozotocin-diabetic rats. Course of development and effects of insulin treatment. Brain 122 Pt 4, 757-768.

Biessels GJ, Kamal A, Ramakers GM, Urban IJ, Spruijt BM, Erkelens DW, Gispen WH (1996) Place learning and hippocampal synaptic plasticity in streptozotocin-induced diabetic rats. Diabetes 45, 1259-1266.

Biessels GJ, Kamal A, Urban IJ, Spruijt BM, Erkelens DW, Gispen WH (1998) Water maze learning and hippocampal synaptic plasticity in streptozotocin-diabetic rats: effects of insulin treatment. Brain Res 800, 125-135.

Biessels GJ, Kappelle LJ; Utrecht Diabetic Encephalopathy Study Group (2006b) Increased risk of Alzheimer's disease in Type II diabetes: insulin resistance of the brain or insulin-induced amyloid pathology? Biochem Soc Trans 33(Pt 5), 1041-1044.

Biessels GJ, Staekenborg S, Brunner E, Brayne C, Scheltens P (2006a) Risk of dementia in diabetes *mellitus*: a systematic review. Lancet Neurol 5, 64-74.

Biessels GJ, van der Heide LP, Kamal A, Bleys RL, Gispen WH (2002) Ageing and diabetes: implications for brain function. Eur J Pharmacol 441, 1-14.

Blood AB, Hunter CJ, Power GG (2003) Adenosine mediates decreased cerebral metabolic rate and increased cerebral blood flow during acute moderate hypoxia in the near-term fetal sheep. J Physiol 553:935-945.

Bloom AS, Tershner S, Fuller SA, Stein EA (1997) Cannabinoid-induced alterations in regional cerebral blood flow in the rat. Pharmacol Biochem Behav 57, 625-631.

Blum D, Gall D, Galas MC, d'Alcantara P, Bantubungi K, Schiffmann SN (2002) The adenosine A_1 receptor agonist adenosine amine congener exerts a neuroprotective effect against the development of striatal lesions and motor impairments in the 3-nitropropionic acid model of neurotoxicity. J Neurosci 22, 9122-9133.

Bouaboula M, Perrachon S, Milligan L, Canat X, Rinaldi-Carmona M, Portier M, Barth F, Calandra B, Pecceu F, Lupker J, Maffrand JP, Le Fur G, Casellas P (1997) A selective inverse agonist for central cannabinoid receptor inhibits mitogen-activated protein kinase activation stimulated by insulin or insulin-like growth factor 1. Evidence for a new model of receptor/ligand interactions. J Biol Chem 272, 22330-22239.

Boué-Grabot E, Barajas-López C, Chakfe Y, Blais D, Bélanger D, Emerit MB, Séguéla P (2003) Intracellular cross talk and physical interaction between two classes of neurotransmitter-gated channels. J Neurosci 23, 1246-1253.

Boué-Grabot E, Toulmé E, Emerit MB, Garret M (2004) Subunit-specific coupling between γ-aminobutyric acid type A and $P2X_2$ receptor channels. J Biol Chem 279, 52517-52525.

Bouzier A, Thiaudiere E, Biran M, Rouland R, Canioni P, Merle M (2000) The metabolism of [3-^{13}C]lactate in the rat brain is specific of a pyruvate carboxylase-deprived compartment. J Neurochem 75, 480-486.

Bouzier-Sore AK, Voisin P, Canioni P, Magistretti PJ, Pellerin L (2003) Lactate is a preferential oxidative energy substrate over glucose for neurons in culture. J Cereb Blood Flow Metab 23:1298-1306.

Bowser DN, Khakh BS (2004) ATP excites interneurons and astrocytes to increase synaptic inhibition in neuronal networks. J Neurosci 24, 8606-8620.

Bradler JE, Barrionuevo G, Panchalingam K, McKeag D, Pettegrew JW (1991) Actions of phosphomonoesters on CA1 hippocampal neurons as revealed by a combined electrophysiological and nuclear magnetic resonance study. Synapse 9, 7-13.

Brambilla D, Chapman D, Greene R (2005) Adenosine mediation of presynaptic feedback inhibition of glutamate release. Neuron 46, 275-283.

Brambilla R, Cottini L, Fumagalli M, Ceruti S, Abbracchio MP (2003) Blockade of A_{2A} adenosine receptors prevents basic fibroblast growth factor-induced reactive astrogliosis in rat striatal primary astrocytes. Glia 43, 190-194.

Brand A, Vissiennon Z, Eschke D, Nieber K (2001) Adenosine A_1 and A_3 receptors mediate inhibition of synaptic transmission in rat cortical neurons. Neuropharmacology 40, 85-95.

Brands AMA, Biessels GJ, de Haan EHF, Kappelle LJ, Kessels RPC (2005) The effects of type 1 diabetes on cognitive performance. Diabetes Care 28:726-735.

Brayne C, Gao L, Matthews F, MRC Cognitive Function and Ageing Study (2005) Challenges in the epidemiological investigation of the relationships between physical activity, obesity, diabetes, dementia and depression. Neurobiol Aging 26 Suppl 1, 6-10.

Brooks KJ, Porteous R, Bachelard HS (1989) Effects of hypoglycaemia and hypoxia on the intracellular pH of cerebral tissue as measured by ^{31}P nuclear magnetic resonance. J Neurochem 52:604-610.

Brown SG, Townsend-Nicholson A, Jacobson KA, Burnstock G, King BF (2002) Heteromultimeric $P2X_{1/2}$ receptors show a novel sensitivity to extracelullar pH. J Pharmacol Exp Ther 300, 673-680.

Burnstock G (2006) Purinergic signalling. Br J Pharmacol 147, 172-181.

Buxton DB, Robertson SM, Olson MS (1986) Stimulation of glycogenolysis by adenine nucleotides in the perfused rat liver. Biochem J 237, 773-780.

Caciagli F, Ciccarelli R, Di Iorio P, Ballerini P, Tacconelli L (1988) Cultures of glial cells release purines under field electrical stimulation: the possible ionic mechanisms. Pharmacol Res Commun 20, 935-947.

Campbell VA, Downer EJ (2008) Cannabinoids and Neuroprotection. In: Köfalvi A, "Cannabinoids and the Brain", Springer, New York, pp. 317-330.

Campbell VA, Gowran A (2007) Alzheimer's disease; taking the edge off with cannabinoids? Br J Pharmacol 152, 655-662.

Carlson G, Wang Y, Alger BE (2002) Endocannabinoids facilitate the induction of LTP in the hippocampus. Nat Neurosci 5, 723-724.

Carriba P, Ortiz O, Patkar K, Justinova Z, Stroik J, Themann A, Müller C, Woods AS, Hope BT, Ciruela F, Casadó V, Canela EI, Lluis C, Goldberg SR, Moratalla R, Franco R, Ferré S (2007) Striatal adenosine A_{2A} and cannabinoid CB1 receptors form functional heteromeric complexes that mediate the motor effects of cannabinoids. Neuropsychopharmacology 32, 2249-2259.

Cass CE, Young JD, Baldwin SA (1998) Recent advances in the molecular biology of nucleoside transporters of mammalian cells, Biochem. Cell Biol 76, 761-770.

Cavaliere F, D'Ambrosi N, Ciotti MT, Mancino G, Sancesario G, Bernardi G, Volonté C (2001a) Glucose deprivation and chemical hypoxia: neuroprotection by P2 receptor antagonists. Neurochem Int 38, 189-197.

Cavaliere F, D'Ambrosi N, Sancesario G, Bernardi G, Volonte C (2001b) Hypoglycaemia-induced cell death: features of neuroprotection by the P2 receptor antagonist basilen blue. Neurochem Int 38, 199-207.

Cerdán S, Künnecke B, Seelig J (1990) Cerebral metabolism of [1,2-$^{13}C_2$]acetate as detected by *in vivo* and *in vitro* ^{13}C NMR. J Biol Chem 265, 12916-12926.

Chabot C, Massicotte G, Milot M, Trudeau F, Gagne J (1997) Impaired modulation of AMPA receptors by calcium-dependent processes in streptozotocin-induced diabetic rats. Brain Res 768, 249-256.

Chakrabarti S, Zhang WX, Sima AAF (1991) Optic neuropathy in the diabetic BB-rat. Adv Exp Med Biol 291, 257-264.

Chance B (2004) Mitochondrial NADH redox state, monitoring discovery and deployment in tissue. Methods Enzymol 385, 361-370.

Chang L, Ernst T, Poland RE, Jenden DJ (1996) *In vivo* proton magnetic resonance spectroscopy of the normal aging human brain. Life Sci 58:2049-2056.

Chao CC, Hu S, Sheng WS, Bu D, Bukrinsky MI, Peterson PK (1996) Cytokine-stimulated astrocytes damage human neurons via a nitric oxide mechanism. Glia 16, 276-284.

Chateil J, Biran M, Thiaudiere E, Canioni P, Merle M (2001) Metabolism of [1-^{13}C]glucose and [2-^{13}C]acetate in the hypoxic rat brain, Neurochem Int 38, 399-407.

Chen GJ, Harvey BK, Shen H, Chou J, Victor A, Wang Y (2006) Activation of adenosine A_3 receptors reduces ischemic brain injury in rodents. J Neurosci Res 84, 1848-1855.

Chen JF, Huang Z, Ma J, Zhu J, Moratalla R, Standaert D, Moskowitz MA, Fink JS, Schwarzschild MA (1999) A_{2A} adenosine receptor deficiency attenuates brain injury induced by transient focal ischemia in mice. J Neurosci 19, 9192-9200.

Chen JF, Xu K, Petzer JP, Staal R, Xu YH, Beilstein M, Sonsalla PK, Castagnoli K, Castagnoli N Jr, Schwarzschild MA (2001) Neuroprotection by caffeine and A_{2A} adenosine receptor inactivation in a model of Parkinson's disease. J Neurosci 21, RC143.

Chen S, Atkins CM, Liu CL, Alonso OF, Dietrich WD, Hu BR (2007) Alterations in mammalian target of rapamycin signaling pathways after traumatic brain injury. J Cereb Blood Flow Metab 27, 939-949.

Cheng SC, Cheng RH (1972) A mitochondrial phosphoenolpyruvate carboxykinase from rat brain. Arch Biochem Biophys 151, 501-511.

Chiu SL, Chen CM, Cline HT (2008) Insulin receptor signaling regulates synapse number, dendritic plasticity, and circuit function in vivo. Neuron 58, 708-719.

Cho YR, Kim HJ, Park SY, Ko HJ, Hong EG, Higashimori T, Zhang Z, Jung DY, Ola MS, Lanoue KF, Leiter EH, Kim JK (2007) Hyperglycemia, maturity-onset obesity, and insulin resistance in NONcNZO10/LtJ males, a new mouse model of type 2 diabetes. Am J Physiol Endocrinol Metab 293, E327-336.

Choi HB, Ryu JK, Kim SU, McLarnon JG (2007) Modulation of the purinergic $P2X_7$ receptor attenuates lipopolysaccharide-mediated microglial activation and neuronal damage in inflamed brain. J Neurosci 27, 4957-4968.

Choi IY, Tkác I, Ugurbil K, Gruetter R (1999) Noninvasive measurements of [1-^{13}C]glycogen concentrations and metabolism in rat brain *in vivo*. J Neurochem 73, 1300-1308.

Ciruela F, Casadó V, Rodrigues RJ, Luján R, Burgueño J, Canals M, Borycz J, Rebola N, Goldberg SR, Mallol J, Cortés A, Canela EI, López-Giménez JF, Milligan G, Lluis C, Cunha RA, Ferré S, Franco R (2006) Presynaptic control of striatal glutamatergic neurotransmission by adenosine A_1-A_{2A} receptor heteromers. J Neurosci 26, 2080-2087.

Ciruela F, Escriche M, Burgueno J, Angulo E, Casado V, Soloviev MM, Canela EI, Mallol J, Chan WY, Lluis C, McIlhinney RA, Franco R (2001) Metabotropic glutamate 1α and adenosine A_1 receptors assemble into functionally interacting complexes. J Biol Chem 276, 18345-18351.

Clodfelder-Miller B, De Sarno P, Zmijewska AA, Song L, Jope RS (2005) Physiological and pathological changes in glucose regulate brain Akt and glycogen synthase kinase-3. J Biol Chem 280, 39723-39731.

Cloix JF, Beaulieu E, Hevor T (1997) Various fructose-1,6-bisphosphatase mRNAs in mouse brain, liver, kidney and heart. Neuroreport 8, 617-622.

Coco S, Calegari F, Pravettoni E, Pozzi D, Taverna E, Rosa P, Matteoli M, Verderio C (2003) Storage and release of ATP from astrocytes in culture. J Biol Chem 278, 1354-1362.

Cohen MM, Pettegrew JW, Kopp SJ, Minshew N, Glonek T (1984) P-31 nuclear magnetic resonance analysis of brain: normoxic and anoxic brain slices. Neurochem Res 9, 785-801.

Convit A (2005) Links between cognitive impairment in insulin resistance: an explanatory model. Neurobiol Aging 26 Suppl 1, 31-35.

Convit A, De Leon MJ, Tarshish C, De Santi S, Tsui W, Rusinek H, George A (1997) Specific hippocampal volume reductions in individuals at risk for Alzheimer's disease. Neurobiol Aging 18, 131-138.

Convit A, Wolf OT, Tarshish C, de Leon MJ (2003) Reduced glucose tolerance is associated with poor memory performance and hippocampal atrophy among normal elderly. Proc Natl Acad Sci USA 100, 2019-2022.

Cormier RJ, Mennerick S, Melbostad H, Zorumski CF (2001) Basal levels of adenosine modulate mGluR5 on rat hippocampal astrocytes. Glia 33, 24-35.

Correia-de-Sá P, Ribeiro JA (1994) Potentiation by tonic A_{2a}-adenosine receptor activation of CGRP-facilitated [^{3}H]-ACh release from rat motor nerve endings. Br J Pharmacol 111, 582-588.

Corsi C, Pazzagli M, Bianchi L, Della Corte L, Pepeu G, Pedata F (1997) *In vivo* amino acid release from the striatum of aging rats: adenosine modulation. Neurobiol Aging 18, 243-50.

Costenla AR, Lopes LV, de Mendonça A, Ribeiro JA (2001) A functional role for adenosine A_3 receptors: modulation of synaptic plasticity in the rat hippocampus. Neurosci Lett 302, 53-57.

Cota D, Marsicano G, Tschop M, Grubler Y, Flachskamm C, Schubert M, Auer D, Yassouridis A, Thone-Reineke C, Ortmann S, Tomassoni F, Cervino C, Nisoli E, Linthorst AC, Pasquali R, Lutz B, Stalla GK, Pagotto U (2003) The endogenous cannabinoid system affects energy balance via central orexigenic drive and peripheral lipogenesis. J Clin Invest 112, 423-431.

Cotrina ML, Lin JH, López-García JC, Naus CC, Nedergaard M (2000) ATP-mediated glia signaling. J Neurosci 20, 2835-2844.

Coutinho-Silva R, Parsons M, Robson T, Lincoln J, Burnstock G (2003) P2X and P2Y purinoceptor expression in pancreas from streptozotocin-diabetic rats. Mol Cell Endocrinol 204, 141-154.

Cox DJ, Gonder-Frederick LA, Schroeder DB, Cryer PE, Clarke WL (1993) Disruptive effects of acute hypoglycemia on speed of cognitive and motor performance. Diabetes Care 16, 1391-1393.

Cox DJ, Kovatchev BP, Gonder-Frederick LA, Summers KH, McCall A, Grimm KJ, Clarke WL (2005) Relationships between hyperglycemia and cognitive performance among adults with type 1 and type 2 diabetes. Diabetes Care 28, 71-77.

Criego AB, Tkac I, Kumar A, Thomas W, Gruetter R, Seaquist ER (2005a) Brain glucose concentrations in patients with type 1 diabetes and hypoglycemia unawareness. J Neurosci Res 79, 42-47.

Criego AB, Tkac I, Kumar A, Thomas W, Gruetter R, Seaquist ER (2005b) Brain glucose concentrations in healthy humans subjected to recurrent hypoglycemia. J Neurosci Res 82, 525-530.

Crutcher KA, Scott SA, Liang S, Everson WV, Weingartner J (1993) Detection of NGF-like activity in human brain tissue: increased levels in Alzheimer's disease. J Neurosci 13, 2540-2550.

Cruz F, Cerdán S (1999) Quantitative ^{13}C NMR studies of metabolic compartmentation in the adult mammalian brain. NMR Biomed 12, 451-462.

Cruz F, Scott SR, Barroso I, Santisteban P, Cerdán S (1998) Ontogeny and cellular localization of the pyruvate recycling system in rat brain. J Neurochem 70, 2613-2619.

Cunha GM, Canas PM, Oliveira CR, Cunha RA (2006) Increased density and synapto-protective effect of adenosine A_{2A} receptors upon sub-chronic restraint stress. Neuroscience 141, 1775-1781.

Cunha RA (1998) On slices, synaptosomes and dissociated neurones to study *in vitro* ageing physiology, Trends Neurosci 21, 286-287.

Cunha RA (2001) Adenosine as a neuromodulator and as a homeostatic regulator in the nervous system: different roles, different sources and different receptors. Neurochem Int 38, 107-125.

Cunha RA (2001a) Regulation of the ecto-nucleotidase pathway in rat hippocampal nerve terminals. Neurochem Res 26, 979-991.

Cunha RA (2005) Neuroprotection by adenosine in the brain: from A_1 receptor activation to A_{2A} receptor blockade. Purinergic Signal 1, 111-134.

Cunha RA, Almeida T, Ribeiro JA (2001) Parallel modification of adenosine extracellular metabolism and modulatory action in the hippocampus of aged rats. J Neurochem 76, 372-382.

Cunha RA, Constantino MD, Ribeiro JA (1997) ZM241385 is an antagonist of the facilitatory responses produced by the A_{2A} adenosine receptor agonists CGS21680 and HENECA in the rat hippocampus. Br J Pharmacol 122, 1279-1284.

Cunha RA, Constantino MD, Ribeiro JA (1999) G protein coupling of CGS 21680 binding sites in the rat hippocampus and cortex is different from that of adenosine A_1 and striatal A_{2A} receptors. Naunyn Schmiedebergs Arch Pharmacol 359, 295-302.

Cunha RA, Johansson B, van der Ploeg I, Sebastião AM, Ribeiro JA, Fredholm BB (1994) Evidence for functionally important adenosine A_{2a} receptors in the rat hippocampus. Brain Res 649, 208-216.

Cunha RA, Porciuncula LO, Rodrigues RJ, Canas PM, Oliveira CR (2006a) Blockade of synaptic P2Y1 (ATP) receptors prevents neurotoxicity in cultured hippocampal neurons. FENS Abstr vol.3, A236.4.

Cunha RA, Ribeiro JA (2000) ATP as a presynaptic modulator. Life Sci 68, 119-137.

Cunha RA, Ribeiro JA (2000b) Adenosine A_{2A} receptor facilitation of synaptic transmission in the CA1 area of the rat hippocampus requires protein kinase C but not protein kinase A activation. Neurosci Lett 289, 127-130.

Cunha RA, Ribeiro JA (2000c) Purinergic modulation of [^{3}H]GABA release from rat hippocampal nerve terminals. Neuropharmacology 39, 1156-1167.

Cunha RA, Vizi ES, Ribeiro JA, Sebastião AM (1996) Preferential release of ATP and its extracellular catabolism as a source of adenosine upon high- but not low-frequency stimulation of rat hippocampal slices. J Neurochem 67, 2180-2187.

d'Alcantara P, Ledent C, Swillens S, Schiffmann SN (2001) Inactivation of adenosine A_{2A} receptor impairs long term potentiation in the accumbens nucleus without altering basal synaptic transmission. Neuroscience 107, 455-464.

Dall'Igna OP, Fett P, Gomes MW, Souza DO, Cunha RA, Lara DR (2007) Caffeine and adenosine A_{2A} receptor antagonists prevent β-amyloid (25-35)-induced cognitive deficits in mice. Exp Neurol 203, 241-245.

Darby M, Kuzmiski JB, Panenka W, Feighan D, MacVicar BA (2003) ATP released from astrocytes during swelling activates chloride channels. J Neurophysiol 89, 1870-1877.

de Graaf RA (1998) *In vivo* NMR spectroscopy: principles and techniques, Willey, England.

de la Monte SM (1989) Quantitation of cerebral atrophy in preclinical and end-stage Alzheimer's disease. Ann Neurol 25, 450-459.

De Leon MJ, George AE, Golomb J, Tarshish C, Convit A, Kluger A, De Santi S, McRae T, Ferris SH, Reisberg B, Ince C, Rusinek H, Bobinski M, Quinn B, Miller DC, Wisniewski HM (1997) Frequency of hippocampal formation atrophy in normal aging and Alzheimer's disease. Neurobiol Aging 18, 1-11.

de Mendonça A, Ribeiro JA (1994) Endogenous adenosine modulates long-term potentiation in the hippocampus. Neuroscience 62, 385-390.

de Mendonça A, Sebastião AM, Ribeiro JA (1995) Inhibition of NMDA receptor-mediated currents in isolated rat hippocampal neurones by adenosine A_1 receptor activation. Neuroreport 6, 1097-1100.

de Mendonça A, Sebastião AM, Ribeiro JA (2000) Adenosine: Does it have a neuroprotective role after all?. Brain Res Rev 33:258-274.

Deary IJ, Crawford JR, Hepburn DA, Langan SJ, Blackmore LM, Frier BM (1993) Severe hypoglycemia and intelligence in adult patients with insulin-treated diabetes. Diabetes 42, 341-344.

Deary IJ, Frier BM (1996) Severe hypoglycemia and cognitive impairment in diabetes: link not proven. Br Med J 313, 767-780.

Deary IJ, Sommerfield AJ, McAulay V, Frier BM (2003) Moderate hypoglycaemia obliterates working memory in humans with and without insulin treated diabetes. J Neurol Neurosurg Psychiatry 74, 278-279.

Debrah K, Sherwin RS, Murphy J, Kerr D (1996) Effect of caffeine on recognition of and physiological responses to hypoglycaemia in insulin-dependent diabetes. Lancet 347, 19-24.

Decking UKM, Schlieper G, Kroll K, Schrader J (1997) Hypoxia-induced inhibition of adenosine kinase potentiates cardiac adenosine release. Circ Res 81, 154-164.

Degroot A, Köfalvi A, Wade MR, Davis RJ, Rodrigues RJ, Rebola N, Cunha RA, Nomikos GG (2006) CB1 receptor antagonism increases hippocampal acetylcholine release: site and mechanism of action. Mol Pharmacol 70, 1236-1245.

DeJong RN (1950) The nervous system complications in diabetes *mellitus* with special reference to cerebrovascular changes. J Nerv Ment Dis 111, 181-206.

DeJong RN (1977) CNS manifestations of diabetes *mellitus*. Postgrad Med 61, 101-107.

del Olmo N, Galarreta M, Bustamante J, Martín del Rio R, Solís JM (2000) Taurine-induced synaptic potentiation: role of calcium and interaction with LTP. Neuropharmacology 39, 40-54.

Derave W, Hespel P (1999) Role of adenosine in regulating glucose uptake during contractions and hypoxia in rat skeletal muscle. J Physiol 515 (Pt 1), 255-263.

Devlin MG, Christopoulos A (2002) Modulation of cannabinoid agonist binding by 5-HT in the rat cerebellum. J Neurochem 80, 1095-1102.

DeYoe EA, Bandettini P, Neitz J, Miller D, Winans P (1994) Functional magnetic resonance imaging (FMRI) of the human brain. J Neurosci Methods 54, 171-187.

Di Leo MA, Santini SA, Silveri NG, Giardina B, Franconi F, Ghirlanda G (2004) Long-term taurine supplementation reduces mortality rate in streptozotocin-induced diabetic rats. Amino Acids 27, 187-191.

di Virgilio F (2000) Dr. Jekyll/Mr. Hyde: the dual role of extracellular ATP. J Auton Nerv Syst 81, 59-63.

Díaz-Cabiale Z, Hurd Y, Guidolin D, Finnman UB, Zoli M, Agnati LF, Vanderhaeghen JJ, Fuxe K, Ferré S (2001) Adenosine A_{2A} agonist CGS 21680 decreases the affinity of dopamine D2 receptors for dopamine in human striatum. Neuroreport 12, 1831-1834.

Diógenes MJ, Fernandes CC, Sebastião AM, Ribeiro JA (2004) Activation of adenosine A_{2A} receptor facilitates brain-derived neurotrophic factor modulation of synaptic transmission in hippocampal slices. J Neurosci 24, 2905-2913.

Dixon AK, Gubitz AK, Sirinathsinghji DJ, Richardson PJ, Freeman TC (1996) Tissue distribution of adenosine receptor mRNAs in the rat. Br J Pharmacol 118, 1461-1468.

Dodd PR (2002) Excited to death: different ways to lose your neurones. Biogerontology 3, 51-56.

Dodd PR, Bradford HF, Chain EB (1971) The metabolism of glucose 6-phosphate by mammalian cerebral cortex in vitro. Biochem J 125, 1027-1038.

Dodd PR, Bradford HF, Chain EB (1972) Formation of glucose from glucose 6-phosphate by rat brain slices. Biochem J 127, 20P-21P.

Dong Y, Benveniste EN (2001) Immune function of astrocytes. Glia 36, 180-190.

Doolette DJ (1997) Mechanism of adenosine accumulation in the hippocampal slice during energy deprivation. Neurochem Int 30, 211-223.

Draelos MT, Jacobson AM, Weinger K, Widom B, Ryan CM, Finkelstein DM, Simonson DC (1995) Cognitive function in patients with insulin-dependent diabetes *mellitus* during hyperglycemia and hypoglycaemia. Am J Med 98 , 135-144.

Dringen R, Schmoll D, Cesar M, Hamprecht B (1993) Incorporation of radioactivity from [^{14}C]lactate into the glycogen of cultured mouse astroglial cells. Evidence for gluconeogenesis in brain cells. Biol Chem Hoppe Seyler 374, 343-347.

Duan S, Anderson CM, Keung EC, Chen Y, Chen Y, Swanson RA (2003) $P2X_7$ receptor-mediated release of excitatory amino acids from astrocytes. J Neurosci 23, 1320-1328.

Duelli R, Maurer MH, Staudt R, Heiland S, Duembgen L, Kuschinsky W (2000) Increased cerebral glucose utilization and decreased glucose transporter Glut1 during chronic hyperglycemia in rat brain. Brain Res 858, 338-347.

Dunkley PR, Heath JW, Harrison SM, Jarvie PE, Glenfield PJ, Rostas JAP (1988) A rapid Percoll gradient procedure for isolation of sinaptosomes directly from an S1 fraction: homogeneity and morphology of subcellular fractions. Brain Res 441, 59-71.

Dunwiddie TV, Masino SA (2001) The role and regulation of adenosine in the central nervous system. Annu Rev Neurosci 24, 31-55.

Ebert D, Haller RG, Walton ME (2003) Energy contribution of octanoate to intact rat brain metabolism measured by ^{13}C nuclear magnetic resonance spectroscopy. J Neurosci 23, 5928-5935.

El-Falougy H, Benuska J (2006) History, anatomical nomenclature, comparative anatomy and functions of the hippocampal formation. Bratisl Lek Listy 107, 103-106.

Elliott JI, Higgins CF (2004) Major histocompatibility complex class I shedding and programmed cell death stimulated through the proinflammatory $P2X_7$ receptor: a candidate susceptibility gene for NOD diabetes. Diabetes 53, 2012-2017.

Eurostat (2007) Europe in figures – Eurostat yearbook 2006-07. Luxembourg: Office for Official Publications of the European Communities

Fahnestock M, Scott SA, Jetté N, Weingartner JA, Crutcher KA (1996) Nerve growth factor mRNA and protein levels measured in the same tissue from normal and Alzheimer's disease parietal cortex. Brain Res Mol Brain Res 42, 175-178.

Fanelli CG, Dence CS, Markham J, Videen TO, Paramore DS, Cryer PE, Powers WJ (1998b) Blood-to-brain glucose transport and cerebral glucose metabolism are not reduced in poorly controlled type 1 diabetes. Diabetes 47, 1444-1450.

Fanelli CG, Paramore DS, Hershey T, Terkamp C, Ovalle F, Craft S, Cryer PE (1998a) Impact of nocturnal hypoglycemia on hypoglycemic cognitive dysfunction in type 1 diabetes. Diabetes 47, 1920-1927.

Färber K, Kettenmann H (2006) Purinergic signaling and microglia. Pflugers Arch 452, 615-621.

Fedorova IM, Jacobson MA, Basile A, Jacobson KA (2003) Behavioral characterization of mice lacking the A_3 adenosine receptor: sensitivity to hypoxic neurodegeneration. Cell Mol Neurobiol 23, 431-447.

Fernandez M, Svenningsson P, Fredholm BB (1996) Adaptative changes in adenosine receptors following long-term treatment with the adenosine receptor agonist R-phenylisopropyl adenosine. Life Sci 58, 769-776.

Ferré S, Karcz-Kubicha M, Hope BT, Popoli P, Burgueño J, Gutiérrez MA, Casadó V, Fuxe K, Goldberg SR, Lluis C, Franco R, Ciruela F (2002) Synergistic interaction between adenosine A_{2A} and glutamate mGlu5 receptors: implications for striatal neuronal function. Proc Natl Acad Sci USA 99, 11940-11945.

Ferre S, von Euler G, Johansson B, Fredholm BB, Fuxe K (1991) Stimulation of high-affinity adenosine A_2 receptors decreases the affinity of dopamine D2 receptors in rat striatal membranes. Proc Natl Acad Sci USA 88, 7238-7241.

Ferrer I, Blanco R, Carmona M (2001) Differential expression of active, phosphorylation-dependent MAP kinases, MAPK/ERK, SAPK/JNK and p38, and specific transcription factor substrates following quinolinic acid excitotoxicity in the rat. Brain Res Mol Brain Res 94, 48-58.

Ferrer I, Blanco R, Cutillas B, Ambrosio S (2000) Fas and Fas-L expression in Huntington's disease and Parkinson's disease. Neuropathol Appl Neurobiol 26, 424-433.

Fiebich BL, Biber K, Gyufko K, Berger M, Bauer J, van Calker D (1996) Adenosine A_{2b} receptors mediate an increase in interleukin (IL)-6 mRNA and IL-6 protein synthesis in human astroglioma cells. J Neurochem 66, 1426-1431.

Fiebich BL, Biber K, Lieb K, van Calker D, Berger M, Bauer J, Gebicke-Haerter PJ (1996b) Cyclooxygenase-2 expression in rat microglia is induced by adenosine A_{2a}-receptors. Glia 18, 152-160.

Fields RD, Burnstock G (2006) Purinergic signalling in neuron-glia interactions. Nat Rev Neurosci 7, 423-436.

Finegan BA, Lopaschuk GD, Gandhi M, Clanachan AS (1996) Inhibition of glycolysis and enhanced mechanical function of working rat hearts as a result of adenosine A1 receptor stimulation during reperfusion following ischaemia. Br J Pharmacol 118:355-363.

Fischer Y, Becker C, Löken C (1999) Purinergic inhibition of glucose transport in cardiomyocytes. J Biol Chem 274, 755-761.

Flood JF, Mooradian AD, Morley JE (1990) Characteristics of learning and memory in streptozocin-induced diabetic mice. Diabetes 39, 1391-1398.

Fonseca CP, Jones JG, Carvalho RA, Jeffrey FMH, Montezinho LP, Geraldes CFGC, Castro MMCA (2005) Tricarboxylic acid cycle inhibition by Li^+ in the human neuroblastoma SH-SY5Y cell line: a ^{13}C NMR isotopomer analysis. Neurochem Int 47, 385-393.

Fowler JC (1989) Adenosine antagonists delay hypoxia-induced depression of neuronal activity in hippocampal brain slice. Brain Res 490:378-384.

Fowler JC (1993) Purine release and inhibition of synaptic transmission during hypoxia and hypoglycemia in rat hippocampal slices. Neurosci Lett 157:83-86.

Franco R, Casado V, Ciruela F, Saura C, Mallol J, Canela EI, Lluis C (1997) Cell surface adenosine deaminase: much more than an ectoenzyme. Prog Neurobiol 52, 283-294.

Franke H, Krugel U, Illes P (2006) P2 receptors and neuronal injury. Pflugers Arch Eur J Physiol 452, 622-644.

Fraser H, Lopaschuk GD, Clanachan AS (1999) Cardioprotection by adenosine A1-receptor stimulation alters glycogen and glucose metabolism. Br J Pharmacol 128:197-205.

Fredholm BB, Bättig K, Holmén J, Nehlig A, Zvartau EE (1999) Actions of caffeine in the brain with special reference to factors that contribute to its widespread use. Pharmacol Rev 51, 83-133.

Fredholm BB, Chen JF, Cunha RA, Svenningsson P, Vaugeois JM (2005) Adenosine and brain function. Int Rev Neurobiol 63, 191-270.

Fredholm BB, Cunha RA, Svenningsson P (2003) Pharmacology of adenosine A_{2A} receptors and therapeutic applications. Curr Top Med Chem 3, 413-26.

Fredholm BB, Dunwiddie TV, Bergman B, Lindström K (1984) Levels of adenosine and adenine nucleotides in slices of rat hippocampus. Brain Res 295, 127-136.

Fredholm BB, Ijzerman AP, Jacobson KA, Klotz KN, Linden J (2001) International Union of Pharmacology. XXV. Nomenclature and classification of adenosine receptors. Pharmacol Rev 53, 527-552.

Freedland CS, Whitlow CT, Miller MD, Porrino LJ (2002) Dose-dependent effects of Delta9-tetrahydrocannabinol on rates of local cerebral glucose utilization in rat. Synapse 45, 134-142.

Freedland CS, Whitlow CT, Smith HR, Porrino LJ (2003) Functional consequences of the acute administration of the cannabinoid receptor antagonist, SR141716A, in cannabinoid-naive and -tolerant animals: a quantitative 2-[^{14}C]deoxyglucose study. Brain Res 962, 169-179.

Frenguelli BG, Llaudet E, Dale N (2003) High-resolution real-time recording with microelectrode biosensors reveals novel aspects of adenosine release during hypoxia in rat hippocampal slices. J Neurochem 86:1506-1515.

Freund TF, Katona I, Piomelli D (2003) Role of endogenous cannabinoids in synaptic signaling. Physiol Rev 83, 1017-1066.

Fujii S, Kato H, Ito K, Itoh S, Yamazaki Y, Sasaki H, Kuroda Y (2000) Effects of A_1 and A_2 adenosine receptor antagonists on the induction and reversal of long-term potentiation in guinea pig hippocampal slices of CA1 neurons. Cell Mol Neurobiol 20, 331-350.

Gagné J, Milot M, Gélinas S, Lahsaïni A, Trudeau F, Martinoli MG, Massicotte G (1997) Binding properties of glutamate receptors in streptozotocin-induced diabetes in rats. Diabetes 46, 841-846.

Gamberino WC, Berkich DA, Lynch CJ, Xu B, LaNoue KF (1997) Role of pyruvate carboxylase in facilitation of synthesis of glutamate and glutamine in cultured astrocytes. J Neurochem 69, 2312-2325.

Gao Z, Downey HF, Sun J, He M, Mallet RT (1997) Adenosine receptor blockade enhances glycolysis in hypoperfused guinea-pig myocardium. Cardiovasc Res 33:31-44.

García-Espinosa MA, García-Martín ML, Cerdán S (2003) Role of glial metabolism in diabetic encephalopathy as detected by high resolution ^{13}C NMR. NMR Biomed 16, 440-449.

García-Espinosa MA, Rodrigues TB, Sierra A, Benito M, Fonseca C, Gray HL, Bartnik BL, García-Martín ML, Ballesteros P, Cerdán S (2004) Cerebral glucose metabolism and the glutamine cycle as detected by *in vivo* and *in vitro* ^{13}C NMR spectroscopy. Neurochem Int 45, 297-303.

Geissler A, Frund R, Scholmerich J, Feuerbach S, Zietz B (2003) Alterations of cerebral metabolism in patients with diabetes *mellitus* studied by proton magnetic resonance spectroscopy. Exp Clin Endocrinol Diabetes 111, 421-427.

Gelfand EV, Cannon CP (2006) Rimonabant: a cannabinoid receptor type 1 blocker for management of multiple cardiometabolic risk factors. J Am Coll Cardiol 47, 1919-1926.

Gerdeman GL, Lovinger DM (2003) Emerging roles for endocannabinoids in long-term synaptic plasticity. Br J Pharmacol 140, 781-789.

Gessi S, Merighi S, Varani K, Leung E, Mac Lennan S, Borea PA (2008) The A_3 adenosine receptor: an enigmatic player in cell biology. Pharmacol Ther 117, 123-140.

Ghosh A, Cheung YY, Mansfield BC, Chou JY (2005) Brain contains a functional glucose-6-phosphatase complex capable of endogenous glucose production. J Biol Chem 280, 11114-11119.

Gibbs ME, Hutchinson D, Hertz L (2008) Astrocytic involvement in learning and memory consolidation. Neurosci Biobehav Rev 32, 927-944.

Ginés S, Hillion J, Torvinen M, Le Crom S, Casadó V, Canela EI, Rondin S, Lew JY, Watson S, Zoli M, Agnati LF, Verniera P, Lluis C, Ferré S, Fuxe K, Franco R (2000) Dopamine D1 and adenosine A_1 receptors form functionally interacting heteromeric complexes. Proc Natl Acad Sci USA 97, 8606-8611.

Gispen WH, Biessels GJ (2000) Cognition and synaptic plasticity in diabetes *mellitus*. Trends Neurosci 23, 542-549.

Gjedde A (1980) Rapid steady-state analysis of blood-brain glucose transfer in rat. Acta Physiol Scand 108, 331-339.

Gold AE, Deary IJ, Jones RW, O'Hare JP, Reckless JP, Frier BM (1994) Severe deterioration in cognitive function and personality in five patients with long-standing diabetes: a complication of diabetes or a consequence of treatment? Diabet Med 11, 499-505.

Gold AE, Deary IJ, MacLeod KM, Thomson KJ, Frier BM (1995) Cognitive function during insulin-induced hypoglycemia in humans: short-term cerebral adaptation does not occur. Psychopharmacology (Berl) 119, 325-333.

Gold SM, Dziobek I, Sweat V, Tirsi A, Rogers K, Bruehl H, Tsui W, Richardson S, Javier E, Convit A (2007) Hippocampal damage and memory impairments as possible early brain complications of type 2 diabetes. Diabetologia 50, 711-719.

Gómez del Pulgar T, De Ceballos ML, Guzmán M, Velasco G (2002) Cannabinoids protect astrocytes from ceramide-induced apoptosis through the phosphatidylinositol 3-kinase/protein kinase B pathway. J Biol Chem 277, 36527-36533.

Gonçalves ML, Cunha RA, Ribeiro JA (1997) Adenosine A_{2A} receptors facilitate $^{45}Ca^{2+}$ uptake through class A calcium channels in rat hippocampal CA3 but not CA1 synaptosomes. Neurosci Lett 238, 73-77.

Goto Y, Kakizaki M (1981) The spontaneous diabetic rat: A model of noninsulin dependent diabetes *mellitus*. Proc Jpn Acad 57, 381-384.

Govindaraju V, Young K, Maudsley AA (2000) Proton NMR chemical shifts and coupling constants for brain metabolites. NMR Biomed 13, 129-153.

Gradman TJ, Laws A, Thompson LW, Reaven GM (1993) Verbal learning and/or memory improves with glycemic control in older subjects with non-insulin-dependent diabetes *mellitus*. J Am Geriatr Soc 41, 1305-1312.

Gray EG, Whittaker VP (1962) The isolation of nerve endings from brain: an electron microscopic study of cell fragments derived by homogeneization and centrifugation. J Anatomy 96, 79-88.

Greenberg JA, Boozer CN, Geliebter A (2006) Coffee, diabetes, and weight control. Am J Clin Nutr 84, 682-693.

Grenz A, Baier D, Petroktistis F, Wehrmann M, Köhle C, Schenk M, Sessler M, Gleiter CH, Fandrich F, Osswald H (2006) Theophylline improves early allograft function in rat kidney transplantation. J Pharmacol Exp Ther 317, 473-479.

Gribkoff VK, Bauman LA, VanderMaelen CP (1990) The adenosine antagonist 8-cyclopentyltheophylline reduces the depression of hippocampal neuronal responses during hypoxia. Brain Res 512:353-357.

Grillo CA, Piroli GG, Wood GE, Reznikov LR, McEwen BS, Reagan LP (2005) Immunocytochemical analysis of synaptic proteins provides new insights into diabetes-mediated plasticity in the rat hippocampus. Neuroscience 136, 477-486.

Gruetter R (1993) Automatic, localized *in vivo* adjustment of all first- and second-order shim coils. Magn Reson Med 29, 804-811.

Gruetter R (2002) *In vivo* ^{13}C NMR studies of compartmentalized cerebral carbohydrate metabolism. Neurochem Int 41, 143-154.

Gruetter R (2003) Glycogen: the forgotten cerebral energy store. J Neurosci Res 74, 179-183.

Gruetter R, Adriany G, Choi IY, Henry PG, Lei H, Oz G (2003) Localized in vivo ^{13}C NMR spectroscopy of the brain. NMR Biomed 16, 313-338.

Gruetter R, Seaquist ER, Ugurbil K (2001) A mathematical model of compartmentalized neurotransmitter metabolism in the human brain. Am J Physiol Endocrinol Metab 281, E100-E112.

Gruetter R, Tkáč I (2000) Field mapping without reference scan using asymmetric echo-planar techniques. Magn Reson Med 43, 319-323.

Gruetter R, Ugurbil K, Seaquist ER (1998) Steady-state cerebral glucose concentrations and transport in the human brain. J Neurochem 70, 397-408.

Gubitz AK, Widdowson L, Kurokawa M, Kirkpatrick KA, Richardson PJ (1996) Dual signalling by the adenosine A_{2a} receptor involves activation of both N- and P-type calcium channels by different G proteins and protein kinases in the same striatal nerve terminals. J Neurochem 67, 374-381.

Gundlfinger A, Bischofberger J, Johenning FW, Torvinen M, Schmitz D, Breustedt J (1997) Adenosine modulates transmission at the hippocampal mossy fibre synapse via direct inhibition of presynaptic calcium channels. J Physiol 582 (Pt 1), 263-277.

Guyot LL, Diaz FG, O'Regan MH, Song D, Phillis JW (2001) The effect of streptozotocin-induced diabetes on the release of excitotoxic and other amino acids from the ischemic rat cerebral cortex. Neurosurgery 48, 385-390.

Guzmán M, Sánchez C (1999) Effects of cannabinoids on energy metabolism. Life Sci 65, 657-664.

Håberg A, Qu H, Haraldseth O, Unsgård G, Sonnewald U (2000) *In vivo* effects of adenosine A_1 receptor agonist and antagonist on neuronal and astrocytic intermediary metabolism studied with *ex vivo* ^{13}C NMR spectroscopy. J Neurochem 74(1):327-333.

Hada J, Kaku T, Morimoto K, Hayashi Y, Nagai K (1998) Activation of adenosine A_2 receptors enhances high K^+-evoked taurine release from rat hippocampus: a microdialysis study. Amino Acids 15, 43-52.

Hammann M, Attwell D (1996) Non-synaptic release of ATP by electrical stimulation in slices of rat hippocampus, cerebellum and habenula. Eur J Neurosci 8, 1510-1515.

Hammarberg C, Schulte G, Fredholm BB (2003) Evidence for functional adenosine A_3 receptors in microglia cells. J Neurochem 86, 1051-1054.

Hammer J, Qu H, Håberg A, Sonnewald U (2001) *In vivo* effects of adenosine A_2 receptor agonist and antagonist on neuronal and astrocytic intermediary metabolism studied with *ex vivo* ^{13}C MR spectroscopy. J Neurochem 79(4):885-892.

Hampson RE, Deadwyler SA (1999) Cannabinoids, hippocampal function and memory. Life Sci 65, 715-723.

Hansson AC, Bermúdez-Silva FJ, Malinen H, Hyytia P, Sanchez-Vera I, Rimondini R, Rodriguez de Fonseca F, Kunos G, Sommer WH, Heilig M (2006) Genetic Impairment of Frontocortical Endocannabinoid Degradation and High Alcohol Preference. Neuropsychopharmacology 32, 117-126.

Hassel B (2000) Carboxylation and anaplerosis in neurons and glia. Mol Neurobiol 22, 21-40.

Hassel B, Brathe A (2000) Cerebral metabolism of lactate *in vivo*: evidence for neuronal pyruvate carboxylation. J Cereb Blood Flow Metab 20, 327-336.

Hatazawa J, Fujita H, Kanno I, Satoh T, Iida H, Miura S, Murakami M, Okudera T, Inugami A, Ogawa T, *et al*. (1995) Regional cerebral blood flow, blood volume, oxygen extraction fraction, and oxygen utilization rate in normal volunteers measured by the autoradiographic technique and the single breath inhalation method. Ann Nucl Med 9, 15-21.

Haussinger D, Stehle T, Gerok W (1987) Actions of extracellular UTP and ATP in perfused rat liver. A comparative study. Eur J Biochem 167, 65-71.

Haydon PG, Carmignoto G (2006) Astrocyte control of synaptic transmission and neurovascular coupling. Physiol Rev 86, 1009-1031.

Heeger DJ, Ress D (2002) What does fMRI tell us about neuronal activity? Nat Rev Neurosci 3, 142-151.

Henry PG, Tkác I, Gruetter R (2003) ^{1}H-localized broadband ^{13}C NMR spectroscopy of the rat brain *in vivo* at 9.4 T. Magn Reson Med 50, 684-692.

Hentschel S, Lewerenz A, Nieber K (2003) Activation of A_3 receptors by endogenous adenosine inhibits synaptic transmission during hypoxia in rat cortical neurons. Restor Neurol Neurosci 21, 55-63.

Herholz K, Heiss WD (2004) Positron emission tomography in clinical neurology. Mol Imaging Biol 6, 239-269.

Hertz L (2004) Intercellular metabolic compartmentation in the brain: past, present and future. Neurochem Int 45, 285-296.

Hertz L, Dienel GA (2002) Energy metabolism in the brain. Int Rev Neurobiol 51, 1-102.

Hertz L, Dringen R, Schousboe A, Robinson SR (1999) Astrocytes: glutamate producers for neurons. J Neurosci Res 57, 417-428.

Hertz L, Hertz E (2003) Cataplerotic TCA cycle flux determined as glutamate-sustained oxygen consumption in primary cultures of astrocytes. Neurochem Int 43, 355-61.

Hespel P, Richter EA (1998) Role of adenosine in regulation of carbohydrate metabolism in contracting muscle. Adv Exp Med Biol 441, 97-106.

Hettinger BD, Leid M, Murray TF (1998) Cyclopentyladenosine-induced homologous down-regulation of A_1 adenosine receptors (A_1AR) in intact neurons is accompanied by receptor sequestration but not a reduction in A_1AR mRNA or G-protein alpha-subunit content. J. Neurochem. 71, 221-230.

Higdon JV, Frei B (2006) Coffee and health: a review of recent human research. Crit Rev Food Sci Nutr 46, 101-123.

Hilairet S, Bouaboula M, Carrière D, Le Fur G, Casellas P (2003) Hypersensitization of the Orexin 1 receptor by the CB1 receptor: evidence for cross-talk blocked by the specific CB1 antagonist, SR141716. J Biol Chem 278, 23731-23737.

Holmes CS, Richman LC (1985) Cognitive profiles of children with insulin-dependent diabetes. J Dev Behav Pediatr 6, 323-326.

Honig LS, Chambliss DD, Bigio EH, Carroll SL, Elliott JL (2000) Glutamate transporter EAAT2 splice variants occur not only in ALS, but also in AD and controls. Neurology 55, 1082-1088.

Huang CC, Yang PC, Lin HJ, Hsu KS (2007) Repeated cocaine administration impairs group II metabotropic glutamate receptor-mediated long-term depression in rat medial prefrontal cortex. J Neurosci 27, 2958-2968.

Huber JD, VanGilder RL, Houser KA (2006) Streptozotocin-induced diabetes progressively increases blood-brain barrier permeability in specific brain regions in rats. Am J Physiol Heart Circ Physiol. 291, H2660-H2668.

Hussl S, Boehm S (2006) Functions of neuronal P2Y receptors. Pflugers Arch 452, 538-551.

Ikeda K, Kurokawa M, Aoyama S, Kuwana Y (2002) Neuroprotection by adenosine A_{2A} receptor blockade in experimental models of Parkinson's disease. J Neurochem 80, 262-270.

Ikeda M, Busto R, Yoshida S, Santiso M, Martinez E, Ginsberg MD (1988) Cerebral phosphoinositide, triacylglycerol and energy metabolism during severe hypoxia and recovery. Brain Res 459:344-350.

Illes P, Ribeiro JA (2004) Neuronal P2 receptors of the central nervous system. Curr Top Med Chem 4, 831-838.

Inoue K, Koizumi S, Nakazawa K (1995) Glutamate-evoked release of adenosine 5'-triphosphate causing an increase in intracellular calcium in hippocampal neurones. Neuroreport 6, 437-440.

Instituto Nacional de Estatística (2007) Estatísticas Demográficas 2005, Instituto Nacional de Estatística, Lisboa.

International Diabetes Federation (2006) Diabetes Atlas, 3rd ed., International Diabetes Federation, Brussels, Belgium.

Irving AJ, McDonald NA, Harkany T (2008) CB1 Cannabinoid Receptors: Molecular Biology, Second Messenger Coupling and Polarized Trafficking in Neurons. In: Köfalvi A, "Cannabinoids and the Brain", Springer, New York, pp. 59-74.

Ito T, Quastel JH (1970) Acetoacetate metabolism in infant and adult rat brain *in vitro*. Biochem J 116, 641-655.

Jackson SJ, Diemel LT, Pryce G, Baker D (2005) Cannabinoids and neuroprotection in CNS inflammatory disease. J Neurol Sci 233, 21-25.

Jakobsen J, Sidenius P, Gundersen HJ, Østerby R (1987) Quantitative changes of cerebral neocortical structure in insulin-treated long-term streptozocin-induced diabetes in rats. Diabetes 36, 597-601.

Jeong HJ, Jang IS, Nabekura J, Akaike N (2003) Adenosine A_1 receptor-mediated presynaptic inhibition of GABAergic transmission in immature rat hippocampal CA1 neurons. J Neurophysiol 89, 1214-1222.

Jiang W, Zhang Y, Xiao L, Van Cleemput J, Ji SP, Bai G, Zhang X (2005) Cannabinoids promote embryonic and adult hippocampus neurogenesis and produce anxiolytic- and antidepressant-like effects. J Clin Invest 115, 3104–3116.

Jiménez AI, Castro E, Mirabet M, Franco R, Delicado EG, Miras-Portugal MT (1999) Potentiation of ATP calcium responses by A_{2B} receptor stimulation and other signals coupled to G_s proteins in type-1 cerebellar astrocytes. Glia 26, 119-128.

Johansson SM, Salehi A, Sandström ME, Westerblad H, Lundquist I, Carlsson PO, Fredholm BB, Katz A (2007) A_1 receptor deficiency causes increased insulin and glucagon secretion in mice. Biochem Pharmacol 74, 1628-1635.

Johnson-Kozlow M, Kritz-Silverstein D, Barrett-Connor E, Morton D (2002) Coffee consumption and cognitive function among older adults. Am J Epidemiol, 156, 842-850.

Jones TW, Davis EA (2003) Hypoglycemia in children with type 1 diabetes: current issues and controversies. Pediatr Diabetes 4, 143-150.

Joost HG, Bell GI, Best JD, Birnbaum MJ, Charron MJ, Chen YT, Doege H, James DE, Lodish HF, Moley KH, Moley JF, Mueckler M, Rogers S, Schürmann A, Seino S, Thorens B (2002) Nomenclature of the GLUT/SLC2A family of sugar/polyol transport facilitators. Am J Physiol Endocrinol Metab 282, E974-E976.

Juan-Picó P, Fuentes E, Bermúdez-Silva FJ, Javier Díaz-Molina F, Ripoll C, Rodríguez de Fonseca F, Nadal A (2006) Cannabinoid receptors regulate Ca^{2+} signals and insulin secretion in pancreatic beta-cell. Cell Calcium 39, 155-162.

Junod A, Lambert AE, Stauffacher W, Renold AE (1969) Diabetogenic action of streptozotocin: relationship of dose to metabolic response. J Clin Invest 48, 2129-2139.

Juranyi Z, Sperlagh B, Vizi ES (1999) Involvement of P2 purinoceptors and the nitric oxide pathway in [^{3}H]purine outflow evoked by short-term hypoxia and hypoglycemia in rat hippocampal slices. Brain Res 823, 183-190.

Kacsoh B (2000) Endocrine physiology, McGraw-Hill, New York.

Kainulainen H, Schürmann A, Vilja P, Joost HG (1993) *In-vivo* glucose uptake and glucose transporter proteins GLUT1 and GLUT3 in brain tissue from streptozotocin-diabetic rats. Acta Physiol Scand, 149, 221-225.

Kalkman HO (2006) The role of the phosphatidylinositide 3-kinase-protein kinase B pathway in schizophrenia. Pharmacol Ther 110, 117-134.

Kamal A, Biessels GJ, Duis SE, Gispen WH (2000) Learning and hippocampal synaptic plasticity in streptozotocin-diabetic rats: interaction of diabetes and ageing. Diabetologia 43, 500-506.

Kamal A, Biessels GJ, Urban IJ, Gispen WH (1999) Hippocampal synaptic plasticity in streptozotocin-diabetic rats: impairment of long-term potentiation and facilitation of long-term depression. Neuroscience 90, 737-745.

Katona I, Sperlagh B, Magloczky Z, Santha E, Köfalvi A, Czirjak S, Mackie K, Vizi ES, Freund TF (2000) GABAergic interneurons are the targets of cannabinoid actions in the human hippocampus. Neuroscience 100, 797-804.

Katona I, Sperlágh B, Sík A, Käfalvi A, Vizi ES, Mackie K, Freund TF (1999) Presynaptically located CB1 cannabinoid receptors regulate GABA release from axon terminals of specific hippocampal interneurons. J Neurosci 19, 4544-4558.

Kauppinen RA, Williams SR (1990) Cerebral energy metabolism and intracellular pH during severe hypoxia and recovery: a study using ^{1}H, ^{31}P, and ^{1}H[^{13}C] nuclear magnetic resonance spectroscopy in the guinea pig cerebral cortex *in vitro*. J Neurosci Res 26:356-369.

Kawamura Y, Fukaya M, Maejima T, Yoshida T, Miura E, Watanabe M, Ohno-Shosaku T, Kano M (2006) The CB1 cannabinoid receptor is the major cannabinoid receptor at excitatory presynaptic sites in the hippocampus and cerebellum. J Neurosci 26, 2991-3001.

Kearn CS, Blake-Palmer K, Daniel E, Mackie K, Glass M (2005) Concurrent stimulation of cannabinoid CB1 and dopamine D2 receptors enhances heterodimer formation: a mechanism for receptor cross-talk? Mol Pharmacol 67, 1697-1704.

Keller JN (2006) Age-related neuropathology, cognitive decline, and Alzheimer's disease. Ageing Res Rev 5, 1-13.

Khakh BS (2001) Molecular physiology of P2X receptors and ATP signalling at synapses. Nat Rev 2, 165-173.

Khakh BS, Gittermann D, Cockayne DA, Jones A (2003) ATP modulation of excitatory synapses onto interneurons. J Neurosci 23, 7426-7437.

Khakh BS, Henderson G (1998) ATP receptor-mediated enhancement of fast excitatory neurotransmitter release in the brain. Mol Pharmacol 54, 372-378.

Khakh BS, North RA (2006) P2X receptors as cell-surface ATP sensors in health and disease. Nature 442, 527-532.

Kim MS, Lee J, Ha J, Kim SS, Kong Y, Cho YH, Baik HH, Kanga I (2002) ATP stimulates glucose transport through activation of P2 purinergic receptors in C2C12 skeletal muscle cells. Arch Biochem Biophys 401, 205-214.

King BF, Townsend-Nicholson A, Wildman SS, Thomas T, Spyer KM, Burnstock G (2000) Coexpression of rat $P2X_2$ and rat $P2X_6$ subunits in Xenopus oocytes. J Neurosci 20, 4871-4877.

Kloda A, Clements JD, Lewis RJ, Adams DJ (2004) Adenosine triphosphate acts as both a competitive antagonist and a positive allosteric modulator at recombinant *N*-methyl-D-aspartate receptors. Mol Pharmacol 65, 1386-1396.

Klunk WE, Panchalingam K, Moossy J, McClure RJ, Pettegrew JW (1992) *N*-acetyl-L-aspartate and other amino acid metabolites in Alzheimer's disease brain: a preliminary proton nuclear magnetic resonance study. Neurology 42, 1578-1585.

Kobayashi S, Millhorn DE (1999) Stimulation of expression for the adenosine A_{2A} receptor gene by hypoxia in PC12 cells. A potential role in cell protection. J Biol Chem 274, 20358-20365.

Köfalvi A (2008) Alternative interacting sites and novel receptors for cannabinoid ligands. In: Köfalvi A, "Cannabinoids and the Brain", Springer, New York, pp. 131-160.

Kopf SR, Melani A, Pedata F, Pepeu G (1999) Adenosine and memory storage: effects of A_1 and A_2 receptor antagonists. Psychopharmacol 146, 214-219.

Kramer L, Fasching P, Madl C, Schneider B, Damjancic P, Waldhäusl W, Irsigler K, Grimm G (1998) Previous episodes of hypoglycemic coma are not associated with permanent cognitive brain dysfunction in IDDM patients on intensive insulin treatment. Diabetes 47, 1909-1914.

Kreis R, Ross BD (1992) Cerebral metabolic disturbances in patients with subacute and chronic diabetes *mellitus*: detection with proton MR spectroscopy. Radiology 184, 123-130.

Kroll K, Decking UK, Dreikorn K, Schrader J (1993) Rapid turnover of the AMP-adenosine metabolic cycle in the guinea pig heart. Circ Res 73, 846-856.

Kuge Y, Hikosaka K, Seki K, Ohkura K, Nishijima K, Tsukamoto E, Tamaki N (2002) *In vitro* uptake of [1-^{14}C]Octanoate in brain slices of rats: basic studies for assessing [1-^{11}C]Octanoate as a PET tracer of glial functions. Nucl Med Biol 29, 303-306.

Kuge Y, Yajima K, Kawashima H, Yamazaki H, Hashimoto N, Miyake Y (1995) Brain uptake and metabolism of [1-^{11}C]octanoate in rats: pharmacokinetic basis for its application as a radiopharmaceutical for studying brain fatty acid metabolism. Ann Nucl Med 9, 137-142.

Kulikov AV, Arkhipova LV, Tretyak TM, Bragin AG (1986) Serotonin and norepinephrine content in brain structures of rats with experimental and transplantation-compensated diabetes. J Hirnforsch 27, 495-499.

Kull B, Svenningsson P, Fredholm BB (2000) Adenosine A_{2A} receptors are colocalized with and activate g(olf) in rat striatum. Mol Pharmacol 58, 771-777.

Künnecke B, Cerdán S, Seelig J (1993) Cerebral metabolism of [1,2-$^{13}C_2$]glucose and [U-$^{13}C_4$]3-hydroxybutyrate in rat brain as detected by ^{13}C NMR spectroscopy. NMR Biomed 6, 264-277.

Lalonde R (2002) The neurobiological basis of spontaneous alternation. Neurosci Biobehav Rev 26, 91-104.

Lammer A, Gunther A, Beck A, Krugel U, Kittner H, Schneider D, Illes P, Franke H (2006) Neuroprotective effects of the P2 receptor antagonist PPADS on focal cerebral ischaemia-induced injury in rats. Eur J Neurosci 23, 2824-2828.

Langan SJ, Deary IJ, Hepburn DA, Frier BM (1991) Cumulative cognitive impairment following recurrent severe hypoglycaemia in adult patients with insulin-treated diabetes *mellitus*. Diabetologia 34, 337-344.

Lapidot A, Haber S (2001) Effect of endogenous beta-hydroxybutyrate on glucose metabolism in the diabetic rabbit brain: a ^{13}C-magnetic resonance spectroscopy study of [U-^{13}C]glucose metabolites. J Neurosci Res 64, 207-216.

Lastres-Becker I, De Miguel R, Fernández-Ruiz JJ (2003) The endocannabinoid system and Huntington's disease. Curr Drug Targets CNS Neurol Disord 2, 335-347.

Latini S, Corsi C, Pedata F, Pepeu G (1996) The source of brain adenosine outflow during ischemia and electrical stimulation. Neurochem Int 28, 113-118.

Latini S, Pedata F (2001) Adenosine in the central nervous system: release mechanisms and extracellular concentrations. J Neurochem 79, 463-484.

Lauderback CM, Hackett JM, Huang FF, Keller JN, Szweda LI, Markesbery WR, Butterfield DA (2001) The glial glutamate transporter, GLT-1, is oxidatively modified by 4-hydroxy-2-nonenal in the Alzheimer's disease brain: the role of Aβ1-42. J Neurochem 78, 413-416.

Lazarowski ER, Boucher RC, Harden TK (2003) Mechanisms of release of nucleotides and integration of their action as P2X- and P2Y-receptor activating molecules. Mol Pharmacol 64, 785-795.

Lê KT, Babinski K, Séguela P (1998) Central $P2X_4$ and $P2X_6$ channel subunits coassemble into a novel heteromeric ATP receptor. J Neurosci 18, 7152-7159.

Lê KT, Boué-Grabot E, Archambault V, Séguela P (1999) Functional and biochemical evidence for heteromeric ATP-gated channels composed of $P2X_1$ and $P2X_5$. J Biol Chemistry 274, 15415-15419.

Lee JY, Jhun BS, Oh YT, Lee JH, Choe W, Baik HH, Ha J, Yoon KS, Kim SS, Kang I (2006) Activation of adenosine A_3 receptor suppresses lipopolysaccharide-induced TNF-alpha production through inhibition of PI 3-kinase/Akt and NF-kappaB activation in murine BV2 microglial cells. Neurosci Lett 396, 1-6.

Lee KS, Tetzlaff W, Kreutzberg GW (1986) Rapid down regulation of hippocampal adenosine receptors following brief anoxia. Brain Res 380, 155-158.

Lei H, Gruetter R (2006) Effect of chronic hypoglycaemia on glucose concentration and glycogen content in rat brain: A localized ^{13}C NMR study. J Neurochem 99, 260-268.

Léon C, Freund M, Latchoumanin O, Farret A, Petit P, Cazenave JP, Gachet C (2005) The $P2Y_1$ receptor is involved in the maintenance of glucose homeostasis and in insulin secretion in mice. Purinergic Signal 1, 145-151.

Lester-Coll N, Rivera EJ, Soscia SJ, Doiron K, Wands JR, de la Monte SM (2006) Intracerebral streptozotocin model of type 3 diabetes: relevance to sporadic Alzheimer's disease. J Alzheimer's Dis 9, 13-33.

Li F, Abatan OI, Kim H, Burnett D, Larkin D, Obrosova IG, Stevens MJ (2006) Taurine reverses neurological and neurovascular deficits in Zucker diabetic fatty rats. Neurobiol Disease 22, 669-676.

Li X, Aou S, Hori T, Oomura Y (2002b) Spatial memory deficit and emotional abnormality in OLETF rats. Physiol Behav 75, 15-23.

Li ZG, Zhang W, Grunberger G, Sima AAF (2002a) Hippocampal neuronal apoptosis in type 1 diabetes. Brain Res 946, 221-231.

Lien YH, Shapiro JI, Chan L (1990) Effects of hypernatremia on organic brain osmoles, J Clin Invest 85, 1427-1435.

Lien YH, Shapiro JI, Chan L (1991) Study of brain electrolytes and organic osmolytes during correction of chronic hyponatremia. Implications for the pathogenesis of central pontine myelinolysis, J Clin Invest 88, 303-309.

Lincoln NB, Faleiro RM, Kelly C, Kirk BA, Jeffcoate WJ (1996) Effect of long-term glycemic control on cognitive function. Diabetes Care 19, 656-658.

Löffler T, Al-Robaiy S, Bigl M, Eschrich K, Schliebs R (2001) Expression of fructose-1,6-bisphosphatase mRNA isoforms in normal and basal forebrain cholinergic lesioned rat brain. Int J Dev Neurosci 19, 279-285.

Lopes da Silva FH, Arnolds DE (1978) Physiology of the hippocampus and related structures. Annu Rev Physiol 40, 185-216.

Lopes LV, Cunha RA, Kull B, Fredholm BB, Ribeiro JA (2002) Adenosine A_{2A} receptor facilitation of hippocampal synaptic transmission is dependent on tonic A_1 receptor inhibition. Neuroscience 112, 319-329.

Lopes LV, Halldner L, Rebola N, Johansson B, Ledent C, Chen JF, Fredholm BB, Cunha RA (2004) Binding of the prototypical adenosine A_{2A} receptor agonist CGS 21680 to the cerebral cortex of adenosine A_1 and A_{2A} receptor knockout mice. Br J Pharmacol 141, 1006-1014.

Louw DF, Yang FW, Sutherland GR (2000) The effect of Δ^9-tetrahydrocannabinol on forebrain ischemia in rat. Brain Res 857, 183-187.

Lucchi R, Latini S, de Mendonça A, Sebastião AM, Ribeiro JA (1996) Adenosine by activating A_1 receptors prevents $GABA_A$-mediated actions during hypoxia in the rat hippocampus. Brain Res 732, 261-266.

Luesse HG, Schiefer J, Spruenken A, Puls C, Block F, Kosinski CM (2001) Evaluation of R6/2 HD transgenic mice for therapeutic studies in Huntington's disease: behavioral testing and impact of diabetes *mellitus*. Behav Brain Res 126, 185-195.

Lund-Andersen H (1979) Transport of glucose from blood to brain. Physiol Rev 59, 305-352.

Lunetta M, Damanti AR, Fabbri G, Lombardo M, Di Mauro M, Mughini L (1994) Evidence by magnetic resonance imaging of cerebral alterations of atrophy type in young insulin-dependent diabetic patients. J Endocrinol Invest 17, 241-245.

Lupien SJ, de Leon M, de Santi S, Convit A, Tarshish C, Nair NPV, Thakur M, McEwen BS, Hauger RL, Meaney MJ (1998) Cortisol levels during human aging predict hippocampal atrophy and memory deficits. Nature Neurosci 1, 69-73.

Luse SA (1970) The ultrastructure of the brain in the diabetic Chinese hamster with special reference to synaptic abnormalities. Electroencephalogr Clin Neurophysiol 29, 410.

Lynch MA (2004) Long-term potentiation and memory. Physiol Rev 84, 87-136.

Macek TA, Schaffhauser H, Conn PJ (1998) Protein kinase C and A_3 adenosine receptor activation inhibit presynaptic metabotropic glutamate receptor (mGluR) function and uncouple mGluRs from GTP-binding proteins. J Neurosci 18, 6138-6146.

MacGregor DG, Graham DI, Stone TW (1997) The attenuation of kainate-induced neurotoxicity by chlormethiazole and its enhancement by dizocilpine, muscimol, and adenosine receptor agonists. Exp Neurol 148, 110-123.

MacGregor DG, Miller WJ, Stone TW (1993) Mediation of the neuroprotective action of R-phenylisopropyl-adenosine through a centrally located adenosine A_1 receptor. Br J Pharmacol 110, 470-476.

Mackie K (2006) Cannabinoid receptors as therapeutic targets. Annu Rev Pharmacol Toxicol 46, 101-122.

Magistretti PJ, Hof PR, Martin JL (1986) Adenosine stimulates glycogenolysis in mouse cerebral cortex: a possible coupling mechanism between neuronal activity and energy metabolism. J Neurosci 6:2558-2562.

Magistretti PJ, Pellerin L (1999) Astrocytes couple synaptic activity to glucose utilization in the brain. News Physiol Sci 14:177-182.

Maher F, Davies-Hill TM, Simpson IA (1996) Substrate specificity and kinetic parameters of GLUT3 in rat cerebellar granule neurons. Biochem J 315, 827-831.

Maher F, Vannucci S, Takeda J, Simpson IA (1992) Expression of mouse-GLUT3 and human-GLUT3 glucose transporter proteins in brain. Biochem Biophys Res Commun 182, 703-711.

Maher F, Vannucci SJ, Simpson IA (1994) Glucose transporter proteins in brain. FASEB J 8, 1003-1011.

Maia L, de Mendonça A (2002) Does caffeine intake protect from Alzheimer's disease? Eur J Neurol 9, 377-382.

Majumder AL, Eisenberg F Jr (1977) Unequivocal demonstration of fructose-1,6-bisphosphatase in mammalian brain. Proc Natl Acad Sci USA 74, 3222-3225.

Majumder P, Trujillo CA, Lopes CG, Resende RR, Gomes KN, Yuahasi KK, Britto LR, Ulrich H (2007) New insights into purinergic receptor signaling in neuronal differentiation, neuroprotection, and brain disorders. Purinergic Signal 3, 317-331.

Malecki MT (2004) Type 2 Diabetes *mellitus* and its complications: from the molecular biology to the clinical practice. Rev Diabet Stud 1, 5-8.

Malloy CR, Sherry AD, Jeffrey FM (1988) Evaluation of carbon flux and substrate selection through alternate pathways involving the citric acid cycle of the heart by ^{13}C NMR spectroscopy. J Biol Chem 263, 6964-6971.

Malloy CR, Thompson JR, Jeffrey FM, Sherry AD (1990) Contribution of exogenous substrates to acetyl coenzyme A: measurement by ^{13}C NMR under non-steady-state conditions. Biochemistry 29, 6756-6761.

Malone JI, Hanna SK, Saporta S (2006) Hyperglycemic brain injury in the rat. Brain Res 1076, 9-15.

Manschot SM, Biessels GJ, de Valk H, Algra A, Rutten GE, van der Grond J, Kappelle LJ; on behalf of the Utrecht Diabetic Encephalopathy Study Group (2007) Metabolic and vascular determinants of impaired cognitive performance

and abnormalities on brain magnetic resonance imaging in patients with type 2 diabetes. Diabetologia 50, 2388-2397.

Manschot SM, Brands AM, van der Grond J, Kessels RP, Algra A, Kappelle LJ, Biessels GJ; Utrecht Diabetic Encephalopathy Study Group (2006) Brain magnetic resonance imaging correlates of impaired cognition in patients with type 2 diabetes. Diabetes 55, 1106-1113.

Marala RB, Mustafa SJ (1993) Direct evidence for the coupling of A_2-adenosine receptor to stimulatory guanine nucleotide-binding-protein in bovine brain striatum. J Pharmacol Exp Ther 266, 294-300.

Maran A, Lomas J, Macdonald IA, Amiel SA (1995) Lack of preservation of higher brain function during hypoglycaemia in patients with intensively-treated IDDM. Diabetologia 38, 1412-1418.

Marchbanks RM (1967) The osmotically sensitive potassium and sodium compartments of synaptossomes. Biochem J 104, 148-157.

Margulies JE, Hammer RP Jr (1991) Δ^9-tetrahydrocannabinol alters cerebral metabolism in a biphasic, dose-dependent manner in rat brain. Eur J Pharmacol 202, 373-378.

Marsicano G, Goodenough S, Monory K, Hermann H, Eder M, Cannich A, Azad SC, Cascio MG, Gutiérrez SO, van der Stelt M, López-Rodriguez ML, Casanova E, Schütz G, Zieglgänsberger W, Di Marzo V, Behl C, Lutz B (2003) CB1 cannabinoid receptors and on-demand defense against excitotoxicity. Science 302, 84-88.

Marsicano G, Kuner R (2007) Anatomical Distribution of Receptors, Ligands and Enzymes in the Brain and in the Spinal Cord: Circuitries and Neurochemistry. In: Köfalvi A, "Cannabinoids and the Brain", Springer, New York, pp. 161-201.

Marsicano G, Lutz B (2006) Neuromodulatory functions of the endocannabinoid system. J Endocrinol Invest 29, 27-46.

Marsicano G, Moosmann B, Hermann H, Lutz B, Behl C (2002b) Neuroprotective properties of cannabinoids against oxidative stress: role of the cannabinoid receptor CB1. J Neurochem 80, 448-456.

Marsicano G, Wotjak CT, Azad SC, Bisogno T, Rammes G, Cascio MG, Hermann H, Tang J, Hofmann C, Zieglgänsberger W, Di Marzo V, Lutz B (2002a) The endogenous cannabinoid system controls extinction of aversive memories. Nature 418, 530-434.

Martin DL, Rimvall K (1993) Regulation of gamma-aminobutyric acid synthesis in the brain. J Neurochem 60, 395-407.

Martin ED, Fernandez M, Perea G, Pascual O, Haydon PG, Araque A, Cena V (2007) Adenosine released by astrocytes contributes to hypoxia-induced modulation of synaptic transmission. Glia 55:36-45.

Martin RL, Lloyd HGE, Cowan AI (1994) The early events of oxygen and glucose deprivation: setting the scene for neuronal death? Trends Neurosci 17:251-257.

Mason GF, Petersen KF, Lebon V, Rothman DL, Shulman GI (2006) Increased brain monocarboxylic acid transport and utilization in type 1 diabetes. Diabetes 55, 929-934.

Matias I, Gonthier MP, Orlando P, Martiadis V, De Petrocellis L, Cervino C, Petrosino S, Hoareau L, Festy F, Pasquali R, Roche R, Maj M, Pagotto U, Monteleone P, Di Marzo V (2006) Regulation, function, and dysregulation of endocannabinoids in models of adipose and β-pancreatic cells and in obesity and hyperglycemia. J Clin Endocrinol Metab 91, 3171-3180.

Matsuda LA, Lolait SJ, Brownstein MJ, Young AC, Bonner TI (1990) Structure of a cannabinoid receptor and functional expression of the cloned cDNA. Nature 346, 561-564.

McAulay V, Deary IJ, Ferguson SC, Frier BM (2001) Acute hypoglycemia in humans causes attentional dysfunction while nonverbal intelligence is preserved. Diabetes Care 24, 1745-1750.

McCall AL (2004) Cerebral glucose metabolism in diabetes *mellitus*. Eur J Pharmacol 490, 147-158.

McCall AL, Millington WR, Wurtman RJ (1982) Metabolic fuel and amino acid transport into the brain in experimental diabetes *mellitus*. Proc Natl Acad Sci USA 79, 5406-5410.

McCall AL, Van Bueren AM, Moholt-Siebert M, Cherry NJ, Woodward WR (1994) Immunohistochemical localization of the neuron-specific glucose transporter (GLUT3) to neuropil in adult rat brain. Brain Res 659, 292-297

McCorry D, Nicolson A, Smith D, Marson A, Feltbower RG, Chadwick DW (2006) An association between type 1 diabetes and idiopathic generalized epilepsy. Ann Neurol 59, 204-206.

McNay EC, Fries TM, Gold PE (2000) Decreases in rat extracellular hippocampal glucose concentration associated with cognitive demand during a spatial task. Proc Natl Acad Sci USA 97, 2881-2885.

Melani A, Amadio S, Gianfriddo M, Vannucchi MG, Volontè C, Bernardi G, Pedata F, Sancesario G (2006) $P2X_7$ receptor modulation on microglial cells and reduction of brain infarct caused by middle cerebral artery occlusion in rat. J Cereb Blood Flow Metab 26, 974-982.

Melo TM, Nehlig A, Sonnewald U (2006) Neuronal-glial interactions in rats fed a ketogenic diet. Neurochem Int 48, 498-507.

Miles WR, Root HF (1922) Psychologic tests applied to diabetic patients. Arch Int Med 30, 767-777.

Miras-Portugal MT, Gualix J, Mateo J, Díaz-Hernández M, Gómez-Villafuertes R, Castro E, Pintor J (1999) Diadenosine polyphosphates, extracellular function and catabolism. Prog Brain Res 120, 397-409.

Mlynárik V, Gambarota G, Frenkel H, Gruetter R (2006) Localized short-echo-time proton MR spectroscopy with full signal-intensity acquisition. Magn Reson Med 56, 965-970.

Moffett JR, Ross B, Arun P, Madhavarao CN, Namboodiri AM (2007) *N*-Acetylaspartate in the CNS: from neurodiagnostics to neurobiology. Prog Neurobiol 81, 89-131.

Mogul DJ, Adams ME, Fox AP (1993) Differential activation of adenosine receptors decreases N-type but potentiates P-type Ca^{2+} current in hippocampal CA3 neurons. Neuron 10, 327-334.

Molina-Holgado F, Molina-Holgado E, Guaza C, Rothwell NJ (2002) Role of CB1 and CB2 receptors in the inhibitory effects of cannabinoids on lipopolysaccharide-induced nitric oxide release in astrocyte cultures. J Neurosci Res 67, 829-836.

Monopoli A, Lozza G, Forlani A, Mattavelli A, Ongini E (1998) Blockade of adenosine A_{2A} receptors by SCH 58261 results in neuroprotective effects in cerebral ischaemia in rats. Neuroreport 9, 3955-3959.

Mooradian AD (1997) Central nervous system complications of diabetes *mellitus* - a perspective from the blood-brain barrier. Brain Res Brain Res Rev 23, 210-218.

Mori A, Shindou T, Ichimura M, Nonaka H, Kase H (1996) The role of adenosine A_{2a} receptors in regulating GABAergic synaptic transmission in striatal medium spiny neurons. J Neurosci 16, 605-611.

Moriwaki Y, Yamamoto T, Suda M, Nasako Y, Takahashi S, Agbedana OE, Hada T, Higashino K (1993) Purification and immunohistochemical tissue localization of human xanthine oxidase. Biochim Biophys Acta 1164, 327-330.

Morrison PD, Mackinnon MWB, Bartrup JT, Skett PG, Stone TW (1992) Changes in adenosine sensitivity in the hippocampus of rats with streptozotocin-induced diabetes. Br J Pharmacol 105, 1004-1008.

Motaghedi R, McGraw TE (2008) The CB1 Endocannabinoid System Modulates Adipocyte Insulin Sensitivity. Obesity (Silver Spring) In press.

Müller TB, Sonnewald U, Westergaard N, Schousboe A, Petersen SB, Unsgard G (1994) ^{13}C NMR spectroscopy study of cortical nerve cell cultures exposed to hypoxia, J Neurosci Res 38, 319-326.

Munro S, Thomas KL, Abu-Shaar M (1993) Molecular characterization of a peripheral receptor for cannabinoids. Nature 365, 61-65.

Myhrer T (2003) Neurotransmitter systems involved in learning and memory in the rat: a meta-analysis based on studies of four behavioral tasks. Brain Res Brain Res Rev 41, 268-287.

Nagamatsu S, Sawa H, Kamada K, Nakamichi Y, Yoshimoto K, Hoshino T (1993) Neuron-specific glucose transporter (NSGT): CNS distribution of GLUT3 rat glucose transporter (RGT3) in rat central neurons. FEBS Lett 334, 289-295.

Nagasawa H, Araki T, Kogure K (1994) Alteration of adenosine A_1 receptor binding in the post-ischaemic rat brain. Neuroreport 5, 1453-1456.

Nakata H (1992) Biochemical and immunological characterization of A_1 adenosine receptors purified from human brain membranes. Eur J Biochem 206, 171-177.

Nanoff C, Mitterauer T, Roka F, Hohenegger M, Freissmuth M (1995) Species differences in A_1 adenosine receptor/G protein coupling: identification of a membrane protein that stabilizes the association of the receptor/G protein complex. Mol Pharmacol 48, 806-817.

Neary JT, Kang Y (2005) Signaling from P2 nucleotide receptors to protein kinase cascades induced by CNS injury: implications for reactive gliosis and neurodegeneration. Mol Neurobiol 31, 95-103.

Neary JT, Kang Y, Shi YF, Tran MD, Wanner IB (2006) P2 receptor signalling, proliferation of astrocytes, and expression of molecules involved in cell-cell interactions. Novartis Found Symp 276, 131-143.

Nehlig A, Daval JL, Boyet S, Vert P (1986) Comparative effects of acute and chronic administration of caffeine on local cerebral glucose utilization in the conscious rat. Eur J Pharmacol 129, 93-103.

Nehlig A, Lucignani G, Kadekaro M, Porrino LJ, Sokoloff L (1984) Effects of acute administration of caffeine on local cerebral glucose utilization in the rat. Eur J Pharmacol 101, 91-100.

Nicholls DG (2003) Bioenergetics and transmitter release in the isolated nerve terminal. Neurochem Res 28:1433-1441.

Nicke A, Kerschensteiner D, Soto F (2005) Biochemical evidence for heteromeric assembly of $P2X_1$ and $P2X_4$ subunits. J Neurochem 92, 925-933.

Nishizaki T, Nagai K, Nomura T, Tada H, Kanno T, Tozaki H, Li XX, Kondoh T, Kodama N, Takahashi E, Sakai N, Tanaka K, Saito N (2002) A new neuromodulatory pathway with a glial contribution mediated via A_{2A} adenosine receptors. Glia 39, 133-147.

Nitta A, Murai R, Suzuki N, Ito H, Nomoto H, Katoh G, Furukawa Y, Furukawa S (2002) Diabetic neuropathies in brain are induced by deficiency of BDNF. Neurotoxicol Teratol 24, 695-701.

Nörenberg W, Wirkner K, Assmann H, Richter M, Illes P (1998) Adenosine A_{2A} receptors inhibit the conductance of NMDA receptor channels in rat neostriatal neurons. Amino Acids 14, 33-39.

North RA (2002) Molecular physiology of P2X receptors. Physiol Rev 82, 1013-1067.

North RA, Surprenant A (2000) Pharmacology of cloned P2X receptors. Annu Rev Pharmacol Toxicol 40, 563-580.

North RA, Verkhratsky A (2006) Purinergic transmission in the central nervous system. Pflugers Arch Eur J Physiol 452, 479-485.

Ochiishi T, Chen L, Yukawa A, Saitoh Y, Sekino Y, Arai T, Nakata H, Miyamoto H (1999) Cellular localization of adenosine A_1 receptors in rat forebrain: immunohistochemical analysis using adenosine A_1 receptor-specific monoclonal antibody. J Comp Neurol 411, 301-316.

Offermanns S, Simon MI (1995) G alpha 15 and G alpha 16 couple a wide variety of receptors to phospholipase C. J Biol Chem 270, 15175-15180.

Okada M, Nutt DJ, Murakami T, Zhu G, Kamata A, Kawata Y, Kaneko S (2001) Adenosine receptor subtypes modulate two major functional pathways for hippocampal serotonin release. J Neurosci 21, 628-640.

Olah ME (1997) Identification of A_{2a} adenosine receptor domains involved in selective coupling to Gs. Analysis of chimeric A_1/A_{2a} adenosine receptors. J Biol Chem 272, 337-344.

Olstad E, Olsen GM, Qu H, Sonnewald U (2007) Pyruvate recycling in cultured neurons from cerebellum. J Neurosci Res 85, 3318-3325.

Ortinau S, Laube B, Zimmermann H (2003) ATP inhibits NMDA receptors after heterologous expression and in cultured hippocampal neurons and attenuates NMDA-mediated neurotoxicity. J Neurosci 23, 4996-5003.

Othman T, Yan H, Rivkees SA (2003) Oligodendrocytes express functional A_1 adenosine receptors that stimulate cellular migration. Glia 44, 166-172.

Pagotto U, Marsicano G, Cota D, Lutz B, Pasquali R (2006) The emerging role of the endocannabinoid system in endocrine regulation and energy balance. Endocr Rev 27, 73-100.

Panikashvili D, Mechoulam R, Beni SM, Alexandrovich A, Shohami E (2005) CB1 cannabinoid receptors are involved in neuroprotection via NF-kappa B inhibition. J Cereb Blood Flow Metab 25, 477-484.

Panikashvili D, Simeonidou C, Ben-Shabat S, Hanus L, Breuer A, Mechoulam R, Shohami E (2001) An endogenous cannabinoid (2-AG) is neuroprotective after brain injury. Nature 413, 527-531.

Pankratov Y, Lalo U, Verkhratsky A, North RA (2006) Vesicular release of ATP at central synapses. Pflugers Arch 452, 589-597.

Pankratov YV, Lalo UV, Krishtal OA (2002) Role for P2X receptors in long-term potentiation. J Neurosci 22, 8363-8369.

Park CK, Rudolphi KA (1994) Antiischemic effects of propentofylline (HWA 285) against focal cerebral infarction in rats. Neurosci Lett 178, 235-238.

Pascual O, Casper KB, Kubera C, Zhang J, Revilla-Sanchez R, Sul JY, Takano H, Moss SJ, McCarthy K, Haydon PG (2005) Astrocytic purinergic signaling coordinates synaptic networks. Science 310, 113-116.

Patel AB, de Graaf RA, Mason GF, Rothman DL, Shulman RG, Behar KL (2005) The contribution of GABA to glutamate/glutamine cycling and energy metabolism in the rat cortex *in vivo*. Proc Natl Acad Sci USA 102, 5588-5593.

Patel MS, Korotchkina LG (2001) Regulation of mammalian pyruvate dehydrogenase complex by phosphorylation: complexity of multiple phosphorylation sites and kinases. Exp Mol Med 33, 191-197.

Pawelczyk T, Grden M, Rzepko R, Sakowicz M, Szutowicz A (2005) Region-specific alterations of adenosine receptors expression level in kidney of diabetic rat. Am J Pathol 167, 315-325.

Peakman MC, Hill SJ (1994) Adenosine A_{2B}-receptor-mediated cyclic AMP accumulation in primary rat astrocytes. Br J Pharmacol 111, 191-198.

Peinnequin A, Mouret C, Birot O, Alonso A, Mathieu J, Clarençon D, Agay D, Chancerelle Y, Multon E (2004) Rat pro-inflammatory cytokine and cytokine related mRNA quantification by real-time polymerase chain reaction using SYBR green. BMC Immunol 5, 3.

Pellerin L (2003) Lactate as a pivotal element in neuron-glia metabolic cooperation. Neurochem Int 43:331-338.

Pellerin L, Bouzier-Sore AK, Aubert A, Serres S, Merle M, Costalat R, Magistretti PJ (2007) Activity-dependent regulation of energy metabolism by astrocytes: an update. Glia 55, 1251-1262.

Pellerin L, Magistretti PJ (1994) Glutamate uptake into astrocytes stimulates aerobic glycolysis: a mechanism coupling neuronal activity to glucose utilization. Proc Natl Acad Sci USA 91, 10625-10629.

Pellerin L, Magistretti PJ (2004) Neuroenergetics: calling upon astrocytes to satisfy hungry neurons. Neuroscientist 10, 53-62.

Pellerin L, Pellegri G, Bittar PG, Charnay Y, Bouras C, Martin JL, Stella N, Magistretti PJ (1998) Evidence supporting the existence of an activity-dependent astrocyte-neuron lactate shuttle, Dev Neurosci 20, 291-299.

Pelligrino DA, LaManna JC, Duckrow RB, Bryan RM Jr, Harik SI (1992) Hyperglycemia and blood-brain barrier glucose transport. J Cereb Blood Flow Metab 12, 887-899.

Pennanen C, Kivipelto M, Tuomainen S, Hartikainen P, Hänninen T, Laakso MP, Hallikainen M, Vanhanen M, Nissinen A, Helkala EL, Vainio P, Vanninen R, Partanen K, Soininen H (2004) Hippocampus and entorhinal cortex in mild cognitive impairment and early AD. Neurobiol Aging 25, 303-310.

Peoples RW, Li C (1998) Inhibition of NMDA-gated ion channels by the P2 purinoceptor antagonists suramin and reactive blue 2 in mouse hippocampal neurones. Br J Pharmacol 124, 400-408.

Perlmuter LC, Hakami MK, Hodgson-Harrington C, Ginsberg J, Katz J, Singer DE, Nathan DM (1984) Decreased cognitive function in aging non-insulin-dependent diabetic patients. Am J Med 77, 1043-1048.

Perros P, Deary IJ, Sellar RJ, Best JJ, Frier BM (1997) Brain abnormalities demonstrated by magnetic resonance imaging in adult IDDM patients with and without a history of recurrent severe hypoglycemia. Diabetes Care 20, 1013-1018.

Peterfreund RA, MacCollin M, Gusella J, Fink JS (1996) Characterization and expression of the human A_{2a} adenosine receptor gene. J Neurochem 66, 362-368.

Phelps ME, Mazziotta JC, Huang SC (1982) Study of cerebral function with positron computed tomography. J Cereb Blood Flow Metab 2, 113-162.

Phillips ME, Coxon RV (1975) Incorporation of isotopic carbon into cerebral glycogen from non-glucose substrates. Biochem J 146, 185-189.

Pignataro G, Simon RP, Boison D (2007) Transgenic overexpression of adenosine kinase aggravates cell death in ischemia. J Cereb Blood Flow Metab 27, 1-5.

Pilegaard K, Ladefoged O (1996) Total number of astrocytes in the molecular layer of the dentate gyrus of rats at different ages. Anal Quant Cytol Histol 18, 279-285.

Pinheiro PS, Rodrigues RJ, Silva AP, Cunha RA, Oliveira CR, Malva JO (2003) Solubilization and immunological identification of presynaptic α-amino-3-hydroxy-5-methyl-4-isoxazolepropionic acid receptors in the rat hippocampus. Neurosci Lett 336, 97-100.

Pintor A, Galluzzo M, Grieco R, Pèzzola A, Reggio R, Popoli P (2004) Adenosine A_{2A} receptor antagonists prevent the increase in striatal glutamate levels induced by glutamate uptake inhibitors. J Neurochem 89, 152-156.

Piomelli D (2003) The molecular logic of endocannabinoid signalling. Nat Rev Neurosci 4, 873-884.

Pitkänen A, Sutula TP (2002) Is epilepsy a progressive disorder? Prospects for new therapeutic approaches in temporal-lobe epilepsy. Lancet Neurol 1, 173-181.

Plum L, Belgardt BF, Brüning JC (2006) Central insulin action in energy and glucose homeostasis. J Clin Invest 116, 1761-1766.

Pontieri FE, Conti G, Zocchi A, Fieschi C, Orzi F (1999) Metabolic mapping of the effects of WIN 55212-2 intravenous administration in the rat. Neuropsychopharmacology 21, 773-776.

Pop-Busui R, Sullivan KA, Van Huysen C, Bayer L, Cao X, Towns R, Stevens MJ (2001) Depletion of taurine in experimental diabetic neuropathy: implications for nerve metabolic, vascular, and functional deficits. Exp Neurol 168, 259-272.

Popoli P, Pintor A, Domenici MR, Frank C, Tebano MT, Pèzzola A, Scarchilli L, Quarta D, Reggio R, Malchiodi-Albedi F, Falchi M, Massotti M (2002) Blockade of striatal adenosine A_{2A} receptor reduces, through a presynaptic mechanism, quinolinic acid-induced excitotoxicity: possible relevance to neuroprotective interventions in neurodegenerative diseases of the striatum. J Neurosci 22, 1967-1975.

Prediger RD, Batista LC, Takahashi RN (2005) Caffeine reverses age-related deficits in olfactory discrimination and social recognition memory in rats. Involvement of adenosine A_1 and A_{2A} receptors. Neurobiol. Aging 26, 957-964.

Proctor WR, Dunwiddie TV (1987) Pre- and postsynaptic actions of adenosine in the in vitro rat hippocampus. Brain Res 426, 187-190.

Provencher SW (1993) Estimation of metabolite concentrations from localized *in vivo* proton NMR spectra. Magn Reson Med 30, 672-679.

Purves D, Augustine GJ, Fitzpatrick D, Hall WC, LaMantia AS, McNamara JO, Williams SM (2004) Neuroscience 3rd ed., Sinauer Associates, Sunderland.

Quarta D, Ferré S, Solinas M, You ZB, Hockemeyer J, Popoli P, Goldberg SR (2004). Opposite modulatory roles for adenosine A_1 and A_{2A} receptors on glutamate and dopamine release in the shell of the nucleus accumbens. Effects of chronic caffeine exposure. J. Neurochem. 88, 1151-1158.

Queiroz G, Gebicke-Haerter PJ, Schobert A, Starke K, von Kügelgen I (1997) Release of ATP from cultured rat astrocytes elicited by glutamate receptor activation. Neuroscience 78, 1203-1208.

Queiroz G, Talaia C, Gonçalves J (2003) Adenosine A_{2A} receptor-mediated facilitation of noradrenaline release involves protein kinase C activation and attenuation of presynaptic inhibitory receptor-mediated effects in the rat vas deferens. J Neurochem 85, 740-748.

Qutub AA, Hunt CA (2005) Glucose transport to the brain: a systems model. Brain Res Brain Res Rev 49, 595-617.

Radford KM, Virginio C, Surprenant A, North RA, Kawashima E (1997) Baculovirus expression provides direct evidence for heteromeric assembly of $P2X_2$ and $P2X_3$ receptors. J Neurosci 17, 6529-6533.

Ralevic V, Burnstock G (1998) Receptors for purines and pyrimidines. Pharmacol Rev 50, 413-492.

Ramírez BG, Blázquez C, Gómez del Pulgar T, Guzmán M, de Ceballos ML (2005) Prevention of Alzheimer's disease pathology by cannabinoids: neuroprotection mediated by blockade of microglial activation. J Neurosci 25, 1904-1913.

Reaven GM, Thomson LW, Nahum P, Haskins E (1990) Relationship between hyperglycemia and cognitive junction in older NIDDM patients. Diabetes Care 13, 16-21.

Rebola N, Canas PM, Oliveira CR, Cunha RA (2005a) Different synaptic and subsynaptic localization of adenosine A_{2A} receptors in the hippocampus and striatum of the rat. Neuroscience 132, 893-903

Rebola N, Lujan R, Cunha RA, Mulle C (2008) Adenosine A_{2A} receptors are essential for long-term potentiation of NMDA-EPSCs at hippocampal mossy fiber synapses. Neuron 57, 121-134.

Rebola N, Oliveira CR, Cunha RA (2002) Transducing system operated by adenosine A_{2A} receptors to facilitate acetylcholine release in the rat hippocampus. Eur J Pharmacol 454, 31-38.

Rebola N, Pinheiro PC, Oliveira CR, Malva JO, Cunha RA (2003a). Subcellular localization of adenosine A_1 receptors in nerve terminals and synapses of the rat hippocampus. Brain Res. 987, 49-58.

Rebola N, Porciuncula LO, Lopes LV, Oliveira CR, Soares-da-Silva P, Cunha RA (2005b). Long-term effect of convulsive behavior on the density of adenosine A_1 and A_{2A} receptors in the rat cerebral cortex. Epilepsia 46 (Suppl 5), 159-165.

Rebola N, Rodrigues RJ, Oliveira CR, Cunha RA (2005c) Different roles of adenosine A_1, A_{2A} and A_3 receptors in controlling kainate-induced toxicity in cortical cultured neurons. Neurochem Int 47, 317-325.

Rebola N, Sebastião AM, de Mendonça A, Oliveira CR Ribeiro JA, Cunha RA (2003b) Enhanced adenosine A_{2A} receptor facilitation of synaptic transmission in the hippocampus of aged rats. J. Neurophysiol. 90, 1295-1303.

Rees DA, Alcolado JC (2005) Animal models of diabetes *mellitus*. Diabetic Med 22, 359-370.

Revsin Y, Saravia F, Roig P, Lima A, de Kloet ER, Homo-Delarche F, De Nicola AF (2005) Neuronal and astroglial alterations in the hippocampus of a mouse model for type 1 diabetes. Brain Res 1038, 22-31.

Richardson PJ, Brown SJ (1987) ATP release from affinity-purified rat cholinergic nerve terminals. J Neurochem 48, 622-630.

Robinson AM, Williamson DH (1980) Physiological roles of ketone bodies as substrates and signals in mammalian tissues. Physiol Rev 60, 143-187.

Rodrigues RJ, Almeida T, de Mendonça A, Cunha RA (2006) Interaction between P2X and nicotinic acetylcholine receptors in glutamate nerve terminals of the rat hippocampus. J Mol Neurosci 30, 173-176.

Rodrigues RJ, Almeida T, Richardson PJ, Oliveira CR, Cunha RA (2005a) Dual presynaptic control by ATP of glutamate release via facilitatory $P2X_1$, $P2X_{2/3}$, and $P2X_3$ and inhibitory $P2Y_1$, $P2Y_2$, and/or $P2Y_4$ receptors in the rat hippocampus. J Neurosci 25, 6286-6295.

Rose SJ, Bushi M, Nagra I, Davies WE (2000) Taurine fluxes in insulin dependent diabetes *mellitus* and rehydration in streptozotocin treated rats. Adv Exp Med Biol 483:497-501.

Rosin DL, Robeva A, Woodard RL, Guyenet PG, Linden J (1998) Immunohistochemical localization of adenosine A_{2A} receptors in the rat central nervous system. J Comp Neurol 401, 163-186.

Ross AJ, Sachdev PS (2004) Magnetic resonance spectroscopy in cognitive research. Brain Res Brain Res Rev 44, 83-102.

Rozovsky I, Finch CE, Morgan TE (1998) Age-related activation of microglia and astrocytes: *in vitro* studies show persistent phenotypes of aging, increased proliferation, and resistance to down-regulation. Neurobiol Aging 19, 97-103.

Rubini R, Biasiolo F, Fogarolo F, Magnavita V, Martini A, Fiori MG (1992) Brainstem auditory evoked potentials in rats with streptozotocin-induced diabetes. Diabetes Res Clin Pract 16, 19-25.

Rubio ME, Soto F (2001) Distinct Localization of P2X receptors at excitatory postsynaptic specializations. J Neurosci 21, 641-653.

Rudolphi KA, Schubert P, Parkinson FE, Fredholm BB (1992a) Adenosine and brain ischemia. Cerebrovasc Brain Metab Rev 4, 346-369.

Rudolphi KA, Schubert P, Parkinson FE, Fredholm BB (1992b) Neuroprotective role of adenosine in cerebral ischaemia. Trends Pharmacol Sci 13, 439-445.

Rusakov DA, Harrison E, Stewart MG (1998) Synapses in the hippocampus occupy only 1-2% of cell membranes and are spaced less than half-micron apart: a quantitative ultrastructural analysis with discussion of physiological implications. Neuropharmacol 37, 513-521.

Ryan CM (1988) Neurobehavioral complications of type I diabetes. Examination of possible risk factors. Diabetes Care 11, 86-93.

Ryan CM, Geckle M (2000) Why is learning and memory dysfunction in Type 2 diabetes limited to older adults?. Diabetes Metab Res Rev 16, 308-315.

Ryan CM, Williams TM (1993) Effects of insulin-dependent diabetes on learning and memory efficiency in adults. J Clin Exp Neuropsychol 15, 685-700.

Ryan CM, Williams TM, Finegold DN, Orchard TJ (1993) Cognitive dysfunction in adults with type 1 insulin-dependent diabetes *mellitus* of long duration: effects of recurrent hypoglycaemia and other chronic complications. Diabetologia 36, 329-334.

Sager TN, Laursen H, Hansen AJ (1995) Changes in *N*-acetyl-aspartate content during focal and global brain ischemia of the rat. J Cereb Blood Flow Metab 15, 639-646.

Salazar-Martinez E, Willett WC, Ascherio A, Manson JE, Leitzmann MF, Stampfer MJ, Hu FB (2004) Coffee consumption and risk for type 2 diabetes *mellitus*. Ann Intern Med 140, 1-8.

Sanchez C, Galve-Roperh I, Rueda D, Guzman M (1998) Involvement of sphingomyelin hydrolysis and the mitogen-activated protein kinase cascade in the Δ^9-tetrahydrocannabinol-induced stimulation of glucose metabolism in primary astrocytes. Mol Pharmacol 54, 834-843.

Sanchez C, Velasco G, Guzman M (1997) Δ^9-tetrahydrocannabinol stimulates glucose utilization in C6 glioma cells. Brain Res 767, 64-71.

Saransaari P, Oja SS (2000) Modulation of the ischemia-induced taurine release by adenosine receptors in the developing and adult mouse hippocampus. Neuroscience 97:425-430.

Saravia FE, Revsin Y, Gonzalez Deniselle MC, Gonzalez SL, Roig P, Lima A, Homo-Delarche F, De Nicola AF (2002) Increased astrocyte reactivity in the hippocampus of murine models of type 1 diabetes: the nonobese diabetic (NOD) and streptozotocin-treated mice. Brain Res 957, 345-353.

Saura J, Angulo E, Ejarque A, Casadó V, Tusell JM, Moratalla R, Chen JF, Schwarzschild MA, Lluis C, Franco R, Serratosa J (2005) Adenosine A_{2A} receptor stimulation potentiates nitric oxide release by activated microglia. J Neurochem 95, 919-929.

Schmoll D, Cesar M, Führmann E, Hamprecht B (1995b) Colocalization of fructose-1,6-bisphosphatase and glial fibrillary acidic protein in rat brain. Brain Res 677, 341-344.

Schmoll D, Führmann E, Gebhardt R, Hamprecht B (1995a) Significant amounts of glycogen are synthesized from 3-carbon compounds in astroglial primary cultures from mice with participation of the mitochondrial phosphoenolpyruvate carboxykinase isoenzyme. Eur J Biochem 227, 308-315.

Schmued LC, Stowers CC, Scallet AC, Xu L (2005) Fluoro-Jade C results in ultra high resolution and contrast labeling of degenerating neurons. Brain Res 1035, 24-31.

Schoenle EJ, Schoenle D, Molinari L, Largo RH (2002) Impaired intellectual development in children with Type I diabetes: association with HbA_{1c}, age at diagnosis and sex. Diabetologia 45, 108-114.

Schulte G, Fredholm BB (2003) The G_s-coupled adenosine A_{2B} receptor recruits divergent pathways to regulate ERK1/2 and p38. Exp Cell Res 290, 168-176.

Schurr A, Payne RS, Miller JJ, Rigor BM (1999) Study of cerebral energy metabolism using the rat hippocampal slice preparation. Methods 18, 117-126.

Schwaninger M, Neher M, Viegas E, Schneider A, Spranger M (1997) Stimulation of interleukin-6 secretion and gene transcription in primary astrocytes by adenosine. J Neurochem 69, 1145-1150.

Schwartz WJ, Smith CB, Davidsen L, Savaki H, Sokoloff L (1979) Metabolic mapping of functional activity in the hypothalamo-neurohypophysial system of the rat. Science 205, 723-725.

Schwiebert EM (1999) ABC transporter-facilitated ATP conductive transport. Am J Physiol 276, (1 Pt 1), C1-C8.

Schwiebert EM (2000) Extracellular ATP-mediated propagation of Ca^{2+} waves. Focus on "mechanical strain-induced Ca^{2+} waves are propagated via ATP release and purinergic receptor activation". Am J Physiol Cell Physiol 279, C281-C283.

Scott ID, Nicholls DG (1980) Energy transduction in intact synaptosomes. Influence of plasma membrane depolarizations on the respiration and membrane potential of internal mitochondria determined *in situ*. Biochem J 186, 21-33.

Seaquist ER, Tkac I, Damberg G, Thomas W, Gruetter R (2005) Brain glucose concentrations in poorly controlled diabetes *mellitus* as measured by high-field magnetic resonance spectroscopy. Metabolism 54, 1008-1013.

Sebastião AM, Cunha RA, de Mendonça A, Ribeiro JA (2000) Modification of adenosine modulation of synaptic transmission in the hippocampus of aged rats. Br J Pharmacol 131:1629-1634.

Sebastião AM, de Mendonça A, Moreira T, Ribeiro JA (2001) Activation of synaptic NMDA receptors by action potential-dependent release of transmitter during hypoxia impairs recovery of synaptic transmission on reoxygenation. J Neurosci 21:8564-8571.

Sebastião AM, Ribeiro JA (1992) Evidence for the presence of excitatory A_2 adenosine receptors in the rat hippocampus. Neurosci Lett 138, 41-44.

Sexl V, Mancusi G, Höller C, Gloria-Maercker E, Schütz W, Freissmuth M (1997) Stimulation of the mitogen-activated protein kinase via the A_{2A}-adenosine receptor in primary human endothelial cells. J Biol Chem 272, 5792-5799.

Sharma R, Patnaik SK (1983) Induction of phosphoenolpyruvate carboxykinase by hydrocortisone in rat liver and brain as a function of age. Biochem Int 7, 535-540.

Shen J, Petersen KF, Behar KL, Brown P, Nixon TW, Mason GF, Petroff OA, Shulman GI, Shulman RG, Rothman DL (1999) Determination of the rate of the glutamate/glutamine cycle in the human brain by *in vivo* ^{13}C NMR. Proc Natl Acad Sci USA 96, 8235-8240.

Shindou T, Nonaka H, Richardson PJ, Mori A, Kase H, Ichimura M (2002) Presynaptic adenosine A_{2A} receptors enhance GABAergic synaptic transmission via a cyclic AMP dependent mechanism in the rat globus pallidus. Br J Pharmacol 136, 296-302.

Shinohara M, Dollinger B, Brown G, Rapoport S, Sokoloff L (1979) Cerebral glucose utilization: local changes during and after recovery from spreading cortical depression. Science 203, 188-190.

Shinozaki Y, Koizumi S, Ishida S, Sawada J, Ohno Y, Inoue K (2005) Cytoprotection against oxidative stress-induced damage of astrocytes by extracellular ATP via $P2Y_1$ receptors. Glia 49, 288-300.

Shulman RG, Rothman DL, Behar KL, Hyder F (2004) Energetic basis of brain activity: implications for neuroimaging. Trends Neurosci 27, 489-495.

Sibson NR, Mason GF, Shen J, Cline GW, Herskovits AZ, Wall JE, Behar KL, Rothman DL, Shulman RG (2001) *In vivo* ^{13}C NMR measurement of neurotransmitter glutamate cycling, anaplerosis and TCA cycle flux in rat brain during. J Neurochem 76, 975-989.

Sibson NR, Shen J, Mason GF, Rothman DL, Behar KL, Shulman RG (1998) Functional energy metabolism: *in vivo* ^{13}C-NMR spectroscopy evidence for coupling of cerebral glucose consumption and glutamatergic neuronalactivity. Dev Neurosci 20, 321-330.

Siesjö BK (1982) Lactic acidosis in the brain: occurrence, triggering mechanisms and pathophysiological importance. Ciba Found Symp 87, 77-100.

Sima AA, Kamiya H, Li ZG (2004) Insulin, C-peptide, hyperglycemia, and central nervous system complications in diabetes. Eur J Pharmacol 490, 187-197.

Sima AAF, Zhang WX, Cherian PV, Chakrabarti S (1992) Impaired visual evoked potential and primary axonopathy of the optic nerve in the diabetic BB/W-rat. Diabetologia 35, 602-607.

Simpson IA, Appel NM, Hokari M, Oki J, Holman GD, Maher F, Koehler-Stec EM, Vannucci SJ, Smith QR (1999) Blood-brain barrier glucose transporter: effects of hypo- and hyperglycemia revisited. J Neurochem 72, 238-247.

Simpson IA, Carruthers A, Vannucci SJ (2007) Supply and demand in cerebral energy metabolism: the role of nutrient transporters. J Cereb Blood Flow Metab 27, 1766-1791.

Sinclair AJ, Girling AJ, Bayer AJ (2000) Cognitive dysfunction in older subjects with diabetes *mellitus*: impact on diabetes self-management and use of care services. All Wales Research into Elderly AWARE Study. Diabetes Res Clin Pract 50, 203-212.

Slanina KA, Roberto M, Schweitzer P (2005) Endocannabinoids restrict hippocampal long-term potentiation via CB1. Neuropharmacology 49, 660-668.

Smith PK, Krohn RI, Hermanson GT, Mallia AK, Gartner FH, Provenzano MD, Fujimoto EK, Goeke NM, Olson BJ, Klenk DC (1985) Measurement of protein using bicinchoninic acid. Anal Biochem 150:76-85.

Sokoloff L (1989) Circulation and energy metabolism in the brain. In: Siegel G, Agranoff B, Albers RW, Molinoff P, "Basic Neurochemistry", Raven Press, New York, pp. 565-590.

Sokoloff L (2004) Energy metabolism in neural tissues *in vivo* at rest and in functionally altered states. In: Shulman RG, Rothman DL, "Brain energetics and neuronal activity", Wiley, England, pp. 11-30.

Sokoloff L, Reivich M, Kennedy C, Des Rosiers MH, Patlak, CS, Pettigrew KD, Sakurada O, Shinohara M (1977) The [^{14}C]deoxyglucose method for the measurement of local cerebral glucose utilization: theory, procedure, and normal values in the conscious and anesthetized albino rat. J Neurochem 28, 897-916.

Sokolova E, Nistri A, Giniatullin R (2001) Negative cross talk between anionic $GABA_A$ and cationic P2X ionotropic receptors of rat dorsal root ganglion neurons. J Neurosci 21, 4958-4968.

Solini A, Chiozzi P, Morelli A, Adinolfi E, Rizzo R, Baricordi OR, di Virgilio F (2004) Enhanced $P2X_7$ activity in human fibroblasts from diabetic patients: a possible pathogenetic mechanism for vascular damage in diabetes. Arterioscler Thromb Vasc Biol 24, 1240-1245.

Solini A, Chiozzi P, Morelli A, Passaro A, Fellin R, di Virgilio F (2003) Defective P2Y Purinergic Receptor Function: A Possible Novel Mechanism for Impaired Glucose Transport. J Cell Physiol 197, 435-444.

Sommerfield AJ, Deary IJ, McAulay V, Frier BM (2003) Short-term, delayed, and working memory are impaired during hypoglycemia in individuals with type 1 diabetes. Diabetes Care 26, 390-396.

Sonnewald U, Müller TB, Westergaard N, Unsgard G, Petersen SB, Schousboe A (1994) NMR spectroscopic study of cell cultures of astrocytes and neurons exposed to hypoxia: compartmentation of astrocyte metabolism. Neurochem Int 24:473-483.

Sonnewald U, Westergaard N, Jones P, Taylor A, Bachelard HS, Schousboe A (1996) Metabolism of [U-$^{13}C_5$] glutamine in cultured astrocytes studied by NMR spectroscopy: first evidence of astrocytic pyruvate recycling. J Neurochem 67, 2566-2572.

Sperlágh B, Köfalvi A, Deuchars J, Atkinson L, Milligan CJ, Buckley NJ, Vizi ES (2002) Involvement of $P2X_7$ receptors in the regulation of neurotransmitter release in the rat hippocampus. J Neurochem 81, 1196-1211.

Sperlágh B, Vizi ES (1996) Neuronal synthesis, storage and release of ATP. Sem Neurosci 8, 175-186.

Squire LR, Stark CE, Clark RE (2004) The medial temporal lobe. Annu Rev Neurosci 27, 279-306.

Starr JM, Wardlaw J, Ferguson K, MacLullich A, Deary IJ, Marshall I (2003) Increased blood-brain barrier permeability in type II diabetes demonstrated by gadolinium magnetic resonance imaging. J Neurol Neurosurg Psychiatry 74, 70-76.

Stein EA, Fuller SA, Edgemond WS, Campbell WB (1998) Selective effects of the endogenous cannabinoid arachidonylethanolamide (anandamide) on regional cerebral blood flow in the rat. Neuropsychopharmacology 19, 481-491.

Stella N, Schweitzer P, Piomelli D (1997) A second endogenous cannabinoid that modulates long-term potentiation. Nature 388, 773-778.

Stewart VC, Land JM, Clark JB, Heales SJ (1998) Comparison of mitochondrial respiratory chain enzyme activities in rodent astrocytes and neurones and a human astrocytoma cell line. Neurosci Lett 247, 201-203.

Stiles GL, Daly DT, Olsson RA (1985) The A_1 adenosine receptor. Identification of the binding subunit by photoaffinity cross-linking. J Biol Chem 260, 10806-10811.

Strachan MW, Deary IJ, Ewing FM, Frier BM (1997) Is type II diabetes associated with an increased risk of cognitive dysfunction? A critical review of published studies. Diabetes Care 20, 438-445.

Stranahan AM, Arumugam TV, Cutler RG, Lee K, Egan JM, Mattson MP (2008) Diabetes impairs hippocampal function through glucocorticoid-mediated effects on new and mature neurons. Nat Neurosci 11, 309-317.

Stumpe T, Schrader J (1997) Phosphorylation potential, adenosine formation, and critical PO_2 in stimulated rat cardiomyocytes, Am J Physiol 273(2 Pt 2), H756- H766.

Sugiyama T, Kobayashi M, Kawamura H, Li Q, Puro DG (2004) Enhancement of $P2X_7$-induced pore formation and apoptosis: an early effect of diabetes on the retinal microvasculature. Invest Ophthalmol Vis Sci 45, 1026-1032.

Summers SA, Birnbaum MJ (1997) A role for the serine/threonine kinase, Akt, in insulin-stimulated glucose uptake. Biochem Soc Trans 25, 981-988.

Svenningsson P, Le Moine C, Fisone G, Fredholm BB (1999) Distribution, biochemistry and function of striatal adenosine A_{2A} receptors. Prog Neurobiol 59, 355-396.

Szkudelski T (2001) The mechanism of alloxan and streptozotocin action in B cells of the rat pancreas. Physiol Res 50, 537-546.

Takahashi S, Driscoll BF, Law MJ, Sokoloff L (1995) Role of sodium and potassium ions in regulation of glucose metabolism in cultured astroglia. Proc Natl Acad Sci USA 92, 4616-4620.

Tatlisumak T, Takano K, Carano RA, Miller LP, Foster AC, Fisher M (1998) Delayed treatment with an adenosine kinase inhibitor, GP683, attenuates infarct size in rats with temporary middle cerebral artery occlusion. Stroke 29, 1952-1958.

Tetzlaff W, Schubert P, Kreutzberg GW (1987) Synaptic and extrasynaptic localization of adenosine binding sites in the rat hippocampus. Neuroscience 21, 869-875.

Thomas BF, Gilliam AF, Burch DF, Roche MJ, Seltzman HH (1998) Comparative receptor binding analyses of cannabinoid agonists and antagonists. J Pharmacol Exp Ther 285, 285-292.

Tibbs GR, Barrie AP, van Mieghem FJ, McMahon HT, Nicholls DG (1989) Repetitive action potentials in isolated nerve terminals in the presence of 4-aminopyridine: effects on cytosolic free Ca^{2+} and glutamate release. J Neurochem 53, 1693-9.

Tkáč I, Starcuk Z, Choi IY, Gruetter R (1999) *In vivo* ^{1}H NMR spectroscopy of rat brain at 1 ms echo time. Magn Reson Med 41, 649-656.

Tomlinson DR, Gardiner NJ (2008) Glucose neurotoxicity. Nat Rev Neurosci 9, 36-45.

Tonazzini I, Trincavelli ML, Storm-Mathisen J, Martini C, Bergersen LH (2007) Co-localization and functional cross-talk between A_1 and $P2Y_1$ purine receptors in rat hippocampus. Eur J Neurosci 26, 890-902.

Trachtman H, Futterweit S, Sturman JA (1992) Cerebral taurine transport is increased during streptozocin-induced diabetes in rats. Diabetes 41, 1130-1140.

Tretter L, Adam-Vizi V (2004) Generation of reactive oxygen species in the reaction catalyzed by α-ketoglutarate dehydrogenase. J Neurosci 24, 7771-7778.

Trudeau F, Gagnon S, Massicotte G (2004) Hippocampal synaptic plasticity and glutamate receptor regulation: influences of diabetes *mellitus*. Eur J Pharmacol 490, 177-186.

Trulson ME, Jacoby JH, MacKenzie RG (1986) Streptozotocin-induced diabetes reduces brain serotonin synthesis in rats. J Neurochem 46, 1068-1072.

Tsutsui S, Schnermann J, Noorbakhsh F, Henry S, Yong VW, Winston BW, Warren K, Power C (2004) A_1 adenosine receptor upregulation and activation attenuates neuroinflammation and demyelination in a model of multiple sclerosis. J Neurosci 24, 1521-1529.

Tsutsui S, Vergote D, Shariat N, Warren K, Ferguson SS, Power C (2008) Glucocorticoids regulate innate immunity in a model of multiple sclerosis: reciprocal interactions between the A_1 adenosine receptor and beta-arrestin-1 in monocytoid cells. FASEB J 22, 786-796.

Tun PA, Nathan DM, Perlmuter LC (1990) Cognitive and affective disorders in elderly diabetics. Clin Geriatr Med 6, 731-746.

Tuomilehto J, Tuomilehto-Wolf E, Virtala E, LaPorte R (1990) Coffee consumption as trigger for insulin dependent diabetes *mellitus* in childhood. Br Med J 300, 642-643.

Tyson RL, Gallagher C, Sutherland GR (2003) ^{13}C-Labeled substrates and the cerebral metabolic compartmentalization of acetate and lactate. Brain Res 992, 43-52.

Valastro B, Cossette J, Lavoie N, Gagnon S, Trudeau F, Massicotte G (2002) Up-regulation of glutamate receptors is associated with LTP defects in the early stages of diabetes *mellitus*. Diabetologia 45, 642-650.

van Dam RM, Hu FB (2005) Coffee consumption and risk of type 2 diabetes: a systematic review. JAMA 294, 97-104.

van der Graaf M, Janssen SW, van Asten JJ, Hermus AR, Sweep CG, Pikkemaat JA, Martens GJ, Heerschap A (2004) Metabolic profile of the hippocampus of Zucker Diabetic Fatty rats assessed by *in vivo* ^{1}H magnetic resonance spectroscopy. NMR Biomed 17, 405-410.

Van Sickle MD, Duncan M, Kingsley PJ, Mouihate A, Urbani P, Mackie K, Stella N, Makriyannis A, Piomelli D, Davison JS, Marnett LJ, Di Marzo V, Pittman QJ, Patel KD, Sharkey KA (2005) Identification and functional characterization of brainstem cannabinoid CB2 receptors. Science 310, 329-332.

Vanstapel F, Waebens M, Van Hecke P, Decanniere C, Stalmans W (1991) Modulation of maximal glycogenolysis in perfused rat liver by adenosine and ATP. Biochem J 277 (Pt 3), 597-602.

Varvel SA, Lichtman AH (2002) Evaluation of CB1 receptor knockout mice in the Morris water maze. J Pharmacol Exp Ther 301, 915-924.

Vergauwen L, Hespel P, Richter EA (1994) Adenosine receptors mediate synergistic stimulation of glucose uptake and transport by insulin and by contractions in rat skeletal muscle. J Clin Invest 93, 974-981.

Vergé V, Hevor TK (1995) Regulation of fructose-1,6-bisphosphatase activity in primary cultured astrocytes. Neurochem Res 20, 1049-1056.

Voet D, Voet GJ (1995) Biochemistry, 2nd ed., John Willey and Sons, New York.

Volonté C, Amadio S, Cavaliere F, D'Ambrosi N, Vacca F, Bernardi G (2003) Extracellular ATP and neurodegeneration. Curr Drug Targets CNS Neurol Disord 6, 403-412.

Volterra A, Steinhauser C (2004) Glial modulation of synaptic transmission in the hippocampus. Glia 47, 249-257.

Von Lubitz DK, Kim J, Beenhakker M, Carter MF, Lin RC, Meshulam Y, Daly JW, Shi D, Zhou LM, Jacobson KA (1995) Chronic NMDA receptor stimulation: therapeutic implications of its effect on adenosine A_1 receptors. Eur J Pharmacol 283, 185-192.

Von Lubitz DK, Lin RC, Melman N, Ji XD, Carter MF, Jacobson KA (1994a) Chronic administration of selective adenosine A_1 receptor agonist or antagonist in cerebral ischemia. Eur J Pharmacol 256, 161-167.

Von Lubitz DK, Lin RC, Popik P, Carter MF, Jacobson KA (1994c) Adenosine A_3 receptor stimulation and cerebral ischemia. Eur J Pharmacol 263, 59-67.

Von Lubitz DK, Paul IA, Ji XD, Carter M, Jacobson KA (1994b) Chronic adenosine A_1 receptor agonist and antagonist: effect on receptor density and *N*-methyl-D-aspartate induced seizures in mice. Eur J Pharmacol 253, 95-99.

Waagepetersen HS, Qu H, Hertz L, Sonnewald U, Schousboe A (2002) Demonstration of pyruvate recycling in primary cultures of neocortical astrocytes but not in neurons. Neurochem Res 27, 1431-1437.

Waagepetersen HS, Qu H, Schousboe A, Sonnewald U (2001) Elucidation of the quantitative significance of pyruvate carboxylation in cultured cerebellar neurons and astrocytes. J Neurosci Res 66, 763-770.

Wagner AP, Reck G, Platt D (1993) Evidence that V^+ fibronectin, GFAP and S100 beta mRNAs are increased in the hippocampus of aged rats. Exp Gerontol 28, 135-143.

Wajner M, Harkness RA (1989) Distribution of xanthine dehydrogenase and oxidase activities in human and rabbit tissues. Biochim Biophys Acta 991, 79-84.

Waniewski RA, Martin DL (1998) Preferential utilization of acetate by astrocytes is attributable to transport. J Neurosci 18, 5225-5233.

Westergaard N, Sonnewald U, Schousboe A (1995) Metabolic trafficking between neurons and astrocytes: the glutamate/glutamine cycle revisited. Dev Neurosci 17:203-211.

Whitlow CT, Freedland CS, Porrino LJ (2002) Metabolic mapping of the time-dependent effects of Δ^9-tetrahydrocannabinol administration in the rat. Psychopharmacology (Berl) 161, 129-136.

Whitlow CT, Freedland CS, Porrino LJ (2003) Functional consequences of the repeated administration of Δ^9-tetrahydrocannabinol in the rat. Drug Alcohol Depend 71, 169-177.

Whittingham TS, Lust WD, Christakis DA, Passonneau JV (1984) Metabolic stability of hippocampal slice preparations during prolonged incubation. J Neurochem 43, 689-696.

Wienhard K (2002) Measurement of glucose consumption using [^{18}F]fluorodeoxyglucose. Methods 27, 218-225.

Wieraszko A, Enrlich YH (1994) On the role of extracellular ATP in the induction of long-term potentiation in the hippocampus. J Neurochemistry 63, 1731-1738.

Wieraszko A, Goldsmith G, Seyfried TN (1989) Stimulation-dependent release of adenosine triphosphate from hippocampal slices. Brain Res 485, 244-250.

Wilkes JJ, Nelson E, Osborne M, Demarest KT, Olefsky JM (2005) Topiramate is an insulin-sensitizing compound *in vivo* with direct effects on adipocytes in female ZDF rats. Am J Physiol Endocrinol Metab 288, E617-E624.

World Health Organization (1999) Definition, diagnosis and classification of diabetes *mellitus* and its complications: report of a WHO consultation. World Health Organization, Geneva

Worrall G, Moulton N, Briffett E (1993) Effect of type II diabetes *mellitus* on cognitive function. J Fam Pract 36, 639-643.

Wotjak CT (2005) Role of endogenous cannabinoids in cognition and emotionality. Mini Rev Med Chem 5, 659-670.

Wredling R, Levander S, Adamson U, Lins PE (1990) Permanent neuropsychological impairment after recurrent episodes of severe hypoglycaemia in man. Diabetologia 33, 152-157.

Wyatt DA, Edmunds MC, Rubio R, Berne RM, Lasley RD, Mentzer RM Jr (1989) Adenosine stimulates glycolytic flux in isolated perfused rat hearts by A_1-adenosine receptors. Am J Physiol 257, H1952-H1957.

Yamato T, Misumi Y, Yamasaki S, Kino M, Aomine M (2004) Diabetes *mellitus* decreases hippocampal release of neurotransmitters: an *in vivo* microdialysis study of awake, freely moving rats. Diabetes Nutr Metab 17, 128-136.

Yanagisawa D, Kitamura Y, Takata K, Hide I, Nakata Y, Taniguchi T (2008) Possible involvement of $P2X_7$ receptor activation in microglial neuroprotection against focal cerebral ischemia in rats. Biol Pharm Bull 31, 1121-1130.

Yang K, Fujita T, Kumamoto E (2004) Adenosine inhibits GABAergic and glycinergic transmission in adult rat substantia gelatinosa neurons. J Neurophysiol 92m 2867-2877.

Yoshioka K, Saitoh O, Nakata H (2001) Heteromeric association creates a P2Y-like adenosine receptor. Proc Natl Acad Sci USA 98, 7617-7622.

Zhang JM, Wang HK, Ye CQ, Ge W, Chen Y, Jiang ZL, Wu CP, Poo MM, Duan S (2003) ATP released by astrocytes mediates glutamatergic activity-dependent heterosynaptic suppression. Neuron 40, 971-982.

Zhao WQ, Alkon DL (2001) Role of insulin and insulin receptor in learning and memory. Mol Cell Endocrinol 177, 125-134.

Zimmermann H (1996) Biochemistry, localization and functional roles of ecto-nucleotidases in the nervous system. Prog Neurobiol 49, 589-618.

Zimmermann H (2000) Extracellular metabolism of ATP and other nucleotides. Naunyn Schmiedberg's Arch Pharmacol 362, 299-309.

Zona C, Marchetti C, Volontè C, Mercuri NB, Bernardi G (2000) Effect of P2 purinoceptor antagonists on kainate-induced currents in rat cultured neurons. Brain Res 882, 26-35.

Zwingmann C, Leibfritz D (2003) Regulation of glial metabolism studied by ^{13}C-NMR. NMR Biomed 16, 370-399.

Zwingmann C, Richter-Landsberg C, Brand A, Leibfritz D (2000) NMR spectroscopic study on the metabolic fate of [3-^{13}C]alanine in astrocytes, neurons, and cocultures: implications for glia-neuron interactions in neurotransmitter metabolism. Glia 32, 286-303.

Zwingmann C, Richter-Landsberg C, Leibfritz D (2001) ^{13}C isotopomer analysis of glucose and alanine metabolism reveals cytosolic pyruvate compartmentation as part of energy metabolism in astrocytes. Glia 34, 200-212.